EFFECTS OF NOISE EXPOSURE ON COCHLEAR ANATOMY, AUDITORY PHYSIOLOGY, AND HEARING-IN-NOISE IN NONHUMAN PRIMATES

By

Jane Ann Mondul, Au.D.

Dissertation

Submitted to the Faculty of the

Graduate School of Vanderbilt University

in partial fulfillment of the requirements

for the degree of

DOCTOR OF PHILOSOPHY

in

Neuroscience

June 30, 2022

Nashville, Tennessee

Approved:

Mark Wallace, Ph.D.

Ramnarayan Ramachandran, Ph.D.

Troy Hackett, Ph.D.

Michael Heinz, Ph.D.

M. Charles Liberman, Ph.D.

Acknowledgments

I was born a psychologist; fascinated by people, always watching and interpreting behaviors around me. This interest in how people navigate and react to their world propelled me to pursue studies of psychology in college, and ultimately led me to discover my love of the sensory systems. Although I pursued clinical training to live out these passions, I always had a strong desire to learn more and conduct research. This led me to working in the Ramachandran Lab, digging into the neurophysiological bases of perceptual phenomena such as frequency selectivity. But my clinical training forged a persistent interest in auditory disorders, and some that may be overlooked or poorly characterized in the clinic. Ultimately, my work led me to not only better appreciate but truly demonstrate that we hear with our brains, not our ears. Hidden hearing loss is only hidden if you're looking in the wrong place. And, as someone once told me, the brain is the final frontier, and may remain that for quite some time. Though I entered the PhD program as a psychologist and audiologist, I truly feel that I am leaving as a neuroscientist. This would not have been possible without the mentoring, guidance, and support from so many individuals, some of whom I will briefly acknowledge here.

First, to my family and friends, thank you for your continuous love and support. You made this long journey possible through your patience and understanding of my crazy lifestyle and the healthy distractions from my work.

And now, a brief look back on my academic journey. To my first research mentor, Jeremy Loebach, Ph.D., and my dear friends in the SCog lab (Sarah Phillips, Ph.D., Carly Stork, and Kelsey Klein, Au.D., Ph.D.), thank you for igniting my love for hearing research and guiding me toward a career as a clinician scientist. To Doug Sladen, Ph.D. and everyone at Mayo Clinic Audiology, my summer research experience in 2012 was one of the defining moments in choosing my path forward in audiology and hearing research. This gave me an inside view of how fulfilling clinical audiology can be. I am so grateful for the opportunity to explore this fulfilling career.

After being exposed to cochlear implant research at St. Olaf College and Mayo Clinic, I was especially excited to come to Vanderbilt for my audiology training and to have the opportunity to work with the leading expert in CI research, René Gifford, Ph.D. René, thank you for advising me along the way, and especially for always reminding me of how my passion for

research is a unique gift that is worth pursuing. To another of my Au.D. mentors, Linda Hood, Ph.D., thank you also for identifying and supporting my love of research, and for introducing me to Ram eight years ago.

It was through my NIH T35 traineeship in the summer of 2014 that I first met Ram and began my translational research journey. I will be forever grateful for this opportunity to fully immerse in the research world during my clinical training and test the waters of a research career. I was also blessed with a wonderful and supportive cohort of fellow trainees (John Lee, Au.D., Ph.D., Lauren (Charles) Alexander, Au.D., Sadie (Schwarz) Cramer, Au.D., Sarah Kate Fisher, Au.D.).

To my audiology classmates (Vanderbilt Au.D. class of 2017), many of you have become lifelong friends and I thank you for your support during our Au.D. training, especially when I was splitting my time across campus for research. We truly capitalized on our varied educational backgrounds and clinical interests to make for an enriching training experience that I hold with me today.

Thank you to my clinical supervisors at the Medical University of South Carolina for training me to be an autonomous and confident clinical audiologist during my clinical externship year in 2016-2017. I could not have imagined a better experience for my clinical externship, from comprehensive clinical diagnostics and treatments, to the passionate and devoted patient care, and the incredible relationships among the providers. This training truly shaped who I am as a clinician scientist today. A special thank you to Meredith Holcomb, Au.D. and Teddy McRackan, M.D. for providing me with the opportunity to conduct two clinical research studies during my externship.

I then returned to Vanderbilt to begin my Ph.D. journey. First, I want to acknowledge my cohort (Alisa Zoltowski, Jen Quinde) and other friends made along the way (Anna Kasdan, Kacie Dunham, Sarah Naguib, Ph.D.). Thank you for not being afraid to talk about the hard things, and always being there to celebrate the great things! Next, thank you to the Vanderbilt Brain Institute and Neuroscience Graduate Program leadership, Lisa Monteggia, Ph.D. and Bruce Carter, Ph.D., as well as Roz Johnson, Pamela Doss, and Darlene Pope for their administrative support. It was a pleasure working with this team of individuals in my term serving as the Vanderbilt Brain Institute retreat coordinator and the Neuroscience Student

Organization president. Also, a special and hearty thank you to Allison Leich Hilbun, Ph.D., for her assistance with statistical analyses throughout my Ph.D. research.

To the Vanderbilt University Graduate School, the Biomedical Research Education and Training office, and associated resources. The seminars that I attended through ASPIRE and the Graduate Leadership Institute helped me cultivate a strong professional identity at each stage of my training. The Certificate in College Teaching program nurtured my passion for teaching and mentorship, and improved my ability to present challenging material in an effective and engaging way.

Next, to our sister lab, the Wallace Lab. Many members of this lab were senior graduate students that I looked up to early in my training (Aaron Nidiffer, Ph.D., Jean-Paul Noel, Ph.D., David Simon, Ph.D.), so thank you for inspiring my intellectual journey. And especially to David Tovar, M.D., Ph.D., you were always there to provide deep intellectual conversations about science and life, and you continue to challenge me to think in new ways.

To my dissertation committee: First, Charlie Liberman, Ph.D. and Mike Heinz, Ph.D. Having you as external committee members has been an exceptional gift to me. Thank you for your willingness to serve on my committee. Your expertise and support was essential and invaluable in the success of my dissertation research. To Mark Wallace, Ph.D., thank you for being a part of this journey. Even though you don't normally spend much time thinking about the inner ear, your big picture perspectives were the perfect complement to this committee and helped me contextualize my work more broadly. And to Troy Hackett, Ph.D. (a.k.a. Uncle Troy), my unofficial co-mentor, thank you for always providing a healthy dose of skepticism along with genuine enthusiasm when it is deserved. Your discernment and honesty are what make you such a wonderful mentor, and I respect few people's opinions as much as yours.

To some of my closest peers turned colleagues: John Lee, Au.D., Ph.D. and Kelly Jahn, Au.D., Ph.D., thank you for paving the way in this dual degree journey. I'm so glad our paths crossed during our Au.D. training and I look forward to continuing our research careers together.

To Jordan Racca, Au.D., Ph.D., you are one of those rare friends that not only cares but also inspires. Your work ethic and passion for science and education are somehow exceeded by your ability to actively listen and provide insight and compassion. I have been so lucky to go through the second half of the Au.D. Ph.D. journey with you, and I can't wait to see what you do in the future.

To Samantha Hauser, Au.D., we both took the plunge in the Ram lab and look where we are today. The Purdue University Ph.D. program is lucky to have you, and I hope that the Burton (well now Mondul) – Hauser enterprises comes to fruition one day!

Next, I would like to acknowledge the 45 monkeys that I have had the pleasure of working with and that truly made this research possible. I would also like to thank the Animal Care Staff, the veterinary staff, and especially acknowledge Mary Feurtado, our veterinary anesthetist for her assistance with our countless sedated procedures.

Finally, the Ram Lab: my family for the past 8 years. When I started in the lab, there was one postdoctoral fellow, two research assistants, and two undergraduate students. Since then, I have had the pleasure of working with 11 research assistants, 6 Au.D. students, 10 undergraduate students, and 3 graduate students. It's been amazing to see the lab grow and change as new perspectives and skills came and went. We've had a lot of fun in the lab, and outside the lab at restaurants or traveling for conferences. We've celebrated successful qualifying exams, birthdays, paper acceptances, and grant awards. And we've made other incredible friends along the way with collaborating labs. At times, we epitomized the meaning of "work hard, play hard". And beyond the normal work relationships, we have grown deep friendships that I am confident will withstand the test of time.

To Namrata Temghare, Alex Tarabillo, and Katy Alek, this research would not have been possible with your contributions as dedicated research assistants. These studies are hard and time consuming. It was a pleasure to work with each of you and to see you grow as scientists, and to develop great friendships too.

To Amy Stahl, Au.D., it's been a joy watching your Au.D. Ph.D. journey from the beginning. From the early days when I was the teaching assistant in your first year Au.D. neuroscience course to now working alongside you to develop new measures in the lab and having intellectual conversations about data and career paths, you're an incredible colleague and I'm excited for to see where your research journey takes you.

To Chase Mackey, you are my academic brother and that is a bond that many people can't understand. Thank you for always being there to talk about new and exciting (or weird) data, help me with stats and coding, and just being an open ear to all things academic and not.

I've enjoyed watching you cultivate your own scientific identity and I know that your future in science is bright.

Taking it back to May 2014, there were three very important things happened to me: I began my NIH T35 traineeship in the Ramachandran lab, I got my first dog (Lena), and just three weeks after starting in the lab, I was asked to train a new summer undergraduate research student. We became instant friends and bonded over our love of huskies and Rascal Flatts. I used to plan lab outings just to have an excuse to spend time with him, and I attended almost every home football game just to see him doing those fancy sousaphone dances out on the field at half time. Although it was a long and winding road to get here, I now get to call that summer undergraduate my best friend forever.

To my husband, Corey Mondul: It's been a joy to be by your side through our academic journeys and our growth as human beings over the past 8 years. It's not often that one's personal life is so interwoven with their professional life, but our relationship would not have been without our experiences in this lab and the love and support of our Ram lab colleagues turned friends. And so, to Corey, I love you, I appreciate you more than anything, and I can't wait to see what God has in store for us.

And last but certainly not least, to my mentor, Ramnarayan Ramachandran, Ph.D., a man of exquisite style and many words. I have worked with Ram for 8 years almost to the day. I still vividly remember the first time we met. Linda Hood walked me over from the medical campus. It was raining, your office lights were off (as always), and you asked, "Do you know what an RZ6 is?" I thought I was a goner for sure, but you've proven me wrong ever since. We have both experienced huge professional and personal milestones in the past 8 years. You were awarded tenure and became a father. I earned my Au.D., was awarded my first grant, and got married. We've changed for the better and together. Anyone who knows Ram knows that his office door is always open and he's there to talk about anything - science, code, monkey antics, ethics, food, books, movies - and probably for a lot longer than you planned on. But it's a testament to how deeply he cares for the people who he trains. Ram is invested in fostering your scientific and intellectual development as much as your personal growth. Ram has given me so many opportunities to grow as a scientist (meetings, grants, talking to collaborators) and it has cultivated my own professional independence. So Ram, thank you for taking me on as your first then audiology student, and now graduate student. It's been an honor.

TABLE OF CONTENTS

Page

LIST OF TABLES

LIST OF FIGURES

CHAPTER 1

The use of nonhuman primates in studies of noise injury and treatment

Chapter 1 is reproduced from an original article with the permission of AIP Publishing. The version of record can be found at: https://asa.scitation.org/doi/full/10.1121/1.5132709

Burton, J. A., Valero, M. D., Hackett, T. A., & Ramachandran, R. (2019). The use of nonhuman primates in studies of noise injury and treatment. *J Acoust Soc Am*, *146*(5), 3770. https://doi.org/10.1121/1.5132709

1.1 ABSTRACT

Exposure to prolonged and high intensity noise increases the risk for permanent hearing impairment. Over several decades, researchers characterized the nature of harmful noise exposures and worked to establish guidelines for effective protection. Recent laboratory studies, primarily conducted in rodent models, indicate that the auditory system may be more vulnerable to noise-induced hearing loss (NIHL) than previously thought, driving renewed inquiries into the harmful effects of noise in humans. To bridge the translational gaps between rodents and humans, nonhuman primates (NHPs) may serve as key animal models. Their phylogenetic proximity to humans underlies tremendous similarity in many features of the auditory system (genomic, anatomical, physiological, behavioral), all of which are important considerations in the assessment and treatment of NIHL. This review summarizes the literature pertaining to NHPs as models of hearing and noise-induced hearing loss. It also discusses factors relevant to the translation of diagnostics and therapeutics from animals to humans. The article concludes with some of the practical considerations involved in conducting NHP research.

1.2 INTRODUCTION

Auditory research has greatly benefitted from basic and applied research involving a broad range of species. At every level of analysis, from molecular to cellular to systems, the vast majority of what we know about the structure and function of the auditory system has been gleaned from studies conducted in selected animal models. Each model offers inherent

advantages for the exploration of particular features, but may have limited utility for the study of others. The tremendous depth and breadth of our understanding, both current and future, is the product of this diverse collective.

With respect to the harmful effects of noise on hearing, it is well-established that single or multiple exposures to loud noise can elevate auditory thresholds, and is hypothesized to induce hypersensitivity and tinnitus. Noise-induced threshold shifts can be temporary (temporary threshold shift, TTS) or permanent (permanent threshold shift, PTS). Early research indicated that PTS is caused primarily by outer (OHC) hair cell loss, and that nerve fiber loss was secondary to the loss of inner hair cells (IHCs), whereas TTS was not associated with permanent cochlear pathology (Liberman & Dodds, 1984; Moody et al., 1978); reviewed in McGill & Schuknecht, 1976; Saunders et al., 1985). These conclusions have been augmented by recent studies in rodents showing that IHC ribbon synapses and afferent nerve fibers are more sensitive to acoustic trauma than previously thought (Kujawa & Liberman, 2009). Ribbon synapses are rapidly and permanently lost following exposure to noise sufficiently loud to induce TTS, followed by delayed loss of spiral ganglion cells (Fernandez et al., 2015). Furthermore, exposures sufficient to kill OHCs are accompanied by significant losses of afferent nerve fibers on IHCs that survive the exposure (Valero et al., 2017).

As these discoveries expand our understanding of NIHL, they also raise issues relevant to human health and lifestyle. First, the vulnerability of humans to all forms of NIHL is uncertain. Most of the recent discoveries were derived from studies in rodents, where histological verification of cochlear pathology is easily achieved. Comparable studies in humans are limited by practical and ethical concerns. Second, susceptibility to NIHL appears to vary widely between individuals and species. TTS and PTS are induced at lower sound pressure levels in rodents, compared to humans and nonhuman primates. Dose-response assessments of the risk for developing NIHL are incompletely defined along the TTS-PTS continuum, as are related variables such as age, sex, circadian rhythms, and type of noise (see Topics 1 and 2, this issue). Third, reliable and sensitive diagnostic metrics are needed to identify synaptopathy and other types of peripheral and central pathology associated with noise exposure. The pure tone audiogram and other classic audiologic assessment tools are generally insensitive to the presence of synaptopathy in TTS. Finally, the treatment of NIHL by emerging pharmacologic and

genomic techniques under development in rodent models raise questions about translation to humans (see Cousins, this issue).

Nonhuman primates (NHPs) may be a key translational model to help address many of these issues. Non-human primates occupy a unique niche in biomedical research due to their phylogenetic proximity to humans, and because the physiological processes and phenotypic outcomes associated with human disorders are often closely mirrored in monkey models. Old-world monkeys, such as rhesus macaques, cynomolgus macaques, and baboons, as well as New-World monkeys, such as marmosets and squirrel monkeys, have served as invaluable models in a wide array of biomedical studies, including within the auditory research field. These model systems may be the key to better defining regulations for workplace noise exposure and for translating therapeutics to the clinic.

In this review, we summarize literature pertaining to the use of NHPs as models of hearing and noise-induced hearing loss. Because macaque monkeys are currently the most thoroughly studied NHP with respect to noise trauma, studies of this species are emphasized. We also discuss factors relevant to the translation of therapeutic strategies from animals to humans, including potential advantages of NHPs as an intermediate model. The article concludes with some of the practical considerations involved in conducting NHP research.

1.3 NONHUMAN PRIMATES AS A MODEL OF AUDITION

1.3.1 Phylogeny

The primary rationale for the inclusion of NHPs in basic and applied biomedical research is their phylogenetic proximity to humans, and Old-World monkeys are more closely related to humans than are New-World monkeys. Macaque monkeys, for example, diverged from humans approximately 25 million years ago and share 93.5% genetic sequence similarity with humans. By comparison, rodents diverged from humans about 70 million years ago, and retain about 85% sequence homology (Kumar & Hedges, 1998; Rhesus Macaque Genome Sequencing and Analysis Consortium, 2007). Consequently, NHPs exhibit greater similarity to human physiology, neurobiology, and susceptibility to infectious and metabolic diseases. These features support the inclusion of NHPs in biomedical research, where the goal is to maximize success and minimize risk in a wide array of human applications (e.g., cardiology, cognition, genetics, HIV/AIDS, immunology, neurology, pharmacology, reproduction, respiratory disease,

movement disorders, and vaccines against Ebola and Zika viruses) (Phillips et al., 2014; Wichmann et al., 2018; Espeland et al., 2018; Heppner et al., 2017).

Within the auditory system, patterns of gene expression and regulation will likely be important factors with respect to individual vulnerability to acoustic trauma (e.g., (Barden et al., 2012; Burns et al., 2015; Cai et al., 2015; Lavinsky et al., 2016; Mutai et al., 2018), age-related hearing loss (Bowl & Brown, 2018; Hoffmann et al., 2016), as well as one's responsivity to therapeutics. The high genomic conservation between humans and macaques supports similarities in structure and function. While genomic studies of NHP and human cochleas are emerging (Mutai et al., 2018; Schrauwen et al., 2016), comparable studies of the central auditory system are lacking.

1.3.2 Behavioral training and psychoacoustic testing

One of the most notable advantages of the NHP model is its ability to quickly learn complex tasks and perform these tasks with great accuracy for long durations of time. Within a few weeks to months of training, primates can perform behavioral tasks in daily sessions lasting up to several hours. Various training methods have been employed with great success, including positive reinforcement with fluid or food rewards or shock avoidance paradigms. Because primates are highly motivated by positive reinforcement, this more ethically favorable technique is most commonly used today. Furthermore, technological advances that allow for cage-side subject training and testing (depending on the study constraints) increase subject comfort (Berger et al., 2018; Calapai et al., 2017). Behavioral studies considerably strengthen the translational power of the primate model, as the same tasks can be utilized in both human and nonhuman studies, allowing for direct cross-species comparisons. Here, we describe behavioral studies of NHP hearing across the hierarchy of auditory perception, including investigations of auditory detection, discrimination, identification, and comprehension.

The first behavioral investigations of NHP auditory function characterized hearing sensitivity by assessing tone detection in quiet. Audiograms have been measured in NHPs under a variety of pathologic states, including noise-induced hearing loss (as discussed in detail below) and age-related hearing loss (Bennett et al., 1983). Previously published reviews have extensively discussed normative behavioral audiograms in nearly 30 different nonhuman primate species, including Coleman (2009) and Coleman & Colbert (2010), as well as more recent additions by Osmanski & Wang (2011) and Dylla et al. (2013).

Briefly, primates have varying audible frequency ranges, but generally cover frequencies between 40 to 40,000 Hz (Coleman, 2009), approximately one octave higher than the 20 to 20,000 Hz range of humans (Hawkins & Stevens, 1950; Sivian & White, 1933; further species comparisons in Heffner & Heffner, 2007). NHP audiograms generally resemble those of humans, though with slightly poorer low frequency hearing and an extended high frequency hearing range (see Heffner, 2004). Humans and macaques have a U-shaped audiogram with an area of greatest sensitivity that approaches values of 0 dB SPL (humans: 500-4000 Hz, e.g. Hawkins & Stevens, 1950; Sivian & White, 1933; rhesus macaques: 1000-16000 Hz, Figure 1.1; Pfingst et al., 1978; Dylla et al., 2013), surrounded by a shallow low frequency tail and a steep high frequency tail. Several species of New-World primates, including marmosets, owl monkeys, and squirrel monkeys, have W-shaped audiograms, in which a less sensitive frequency region is flanked by a lower- and higher-frequency region of increased sensitivity (marmosets: Seiden, 1957; Osmanski & Wang, 2011; owl monkeys: Beecher, 1974a; squirrel monkeys: Beecher, 1974b). However, this should not be mistaken as a phenomenon specific to New-World primates, as W-shaped audiograms have also been observed in baboons (Hienz et al., 1982) and chimpanzees (Kojima, 1990).

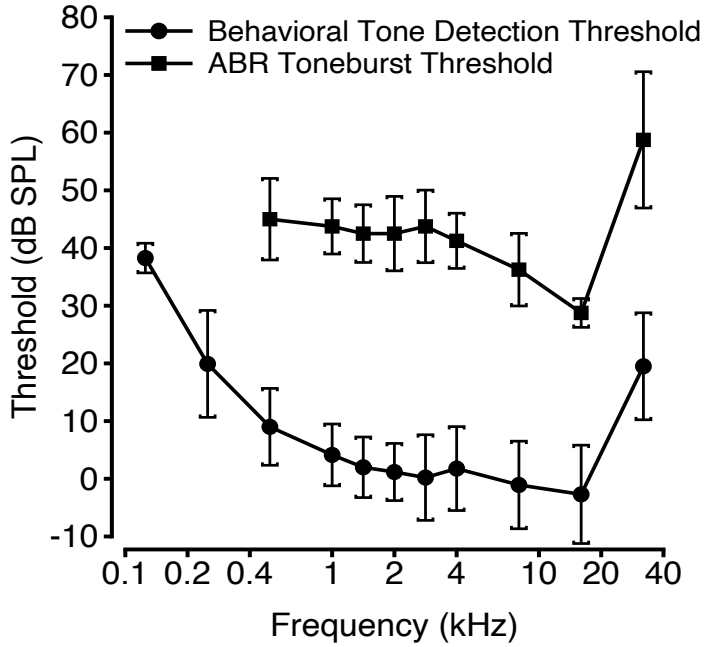

Figure 1.1 Mean behavioral (n = 10 rhesus macaques) and auditory brainstem response (ABR; n = 8 ears from 4 rhesus macaques) thresholds as a function of stimulus frequency. Error bars illustrate one standard deviation from the mean.

In addition to tone detection in quiet, the macaque psychoacoustics literature is rich with iterations of tone detection experiments in quiet and in background noise to probe more complex auditory processing (e.g. Dylla et al., 2013; Gourevitch, 1970). While these assays have been used to further our understanding of basic auditory processing, many of these can inform the consequences of acoustic trauma on auditory perception. For example, researchers have attempted to estimate loudness perception in NHPs by examining the relationship between reaction time latency and signal intensity (Gates et al., 1963; Stebbins, 1966; Stebbins & Miller, 1964). Following noise exposure, NHPs experience loudness recruitment during temporary and permanent hearing loss (see Studies of Auditory Dysfunction section for further details), consistent with reports in humans (Moore, 1996).

Primate frequency selectivity has been measured behaviorally via psychophysical tuning curves (Serafin et al., 1982) and tone detection in narrowband noise (Gourevitch, 1970) or notched-noise (Burton et al., 2018). These behavioral studies, as well as a pair of studies using otoacoustic emissions (OAEs) to probe frequency selectivity (Joris et al., 2011; Verschooten, Desloovere, & Joris, 2018), have demonstrated slightly broader frequency selectivity in macaques relative to humans.

Amplitude-modulation detection (Moody, 1994; O'Connor et al., 2011), tone detection in amplitude-modulated noise (Bohlen et al., 2014; Dylla et al., 2013), and tone detection in gated and inversely-gated noise (Rocchi et al., 2017) have been used to assess primate temporal resolution. While some studies have suggested that temporal resolution in macaques is poorer than in humans (O'Connor et al., 1999; O'Connor et al., 2011), data from the authors' laboratory show comparable temporal resolution (Dylla et al., 2013). Furthermore, spatial release from masking in macaques appears to be similar to humans (Rocchi et al., 2017).

Nonhuman primates are also able to perform a variety of auditory discrimination tasks that may inform the consequences of acoustic trauma but are too extensive to review thoroughly here. Acoustic parameters to discriminate include: tone frequency (Moody et al., 1971; Osmanski et al., 2016; Pfingst, 1993; Prosen et al., 1990; Recanzone et al., 1991; Sinnott et al., 1985; Stebbins, 1973; Wienicke et al., 2001), tone intensity (Pfingst, 1993; Sinnott & Brown, 1993a, 1993b; Sinnott et al., 1985; Stebbins, 1973), amplitude-modulation frequency (Moody, 1994), monaural phase (Moody et al., 1998), stimulus rise time (Prosen & Moody, 1995), stimulus location (Brown et al., 1978; Brown et al., 1978, 1980; Heffner & Heffner, 1990;

Heffner & Masterton, 1975; May et al., 1986), and harmonic complex composition (Le Prell et al., 2001; Tomlinson & Schwarz, 1988). Monkeys have also been trained to discriminate conspecific vocalizations (Heffner & Heffner, 1984; Hopp et al., 1992; Le Prell & Moody, 1997; May et al., 1989; Petersen et al., 1978; Zoloth et al., 1979) as well as human speech sounds (Sinnott et al., 1976; Sinnott, 1989; Sinnott et al., 2006; Sommers et al., 1992).

Auditory stimulus identification and comprehension are more challenging to probe in nonhuman animals. In perhaps one of the first studies of its kind in the auditory domain, Hocherman et al. (1976) trained rhesus monkeys to perform an audiovisual selective attention task, where subjects moved the lever to the left or right according to the type of auditory or visual stimulus presented. Researchers continue to push the envelope with regards to task complexity. In recent studies, NHPs have been trained to perform tasks such as a 'delayed match to sample' task to assess auditory working memory (Ng et al., 2014; Scott et al., 2012). Another task assesses short-term memory, as well as decision-making, by asking subjects to discriminate acoustic flutter stimuli with long inter-stimulus intervals (Lemus et al., 2009). Even more complex behaviors include the discrimination of auditory illusory percepts to investigate auditory feature-ground grouping (Petkov et al., 2003), stream segregation (Christison-Lagay & Cohen, 2014; Lakatos et al., 2013) or feature-specific discrimination (Downer et al., 2017) to probe selective auditory attention, and sequence content identification (i.e. does the sequence contain more high or low frequency tones) to investigate perceptual decision-making (Tsunada et al., 2016).

While it is not trivial to train primates on behavioral tasks, the data provide an invaluable link to the following complementary approaches for studying auditory function in primates as well as illuminate the translatability of the NHP model to humans.

1.3.3 Noninvasive electrophysiology

Behavioral assessments of hearing and hearing loss may be augmented by a number of noninvasive techniques to probe the integrity of specific structures in the auditory pathway. Several clinical audiology measures have been modified for use in animals, including the auditory brainstem response (ABR), electrocochleography (ECochG), OAEs, and immittance testing. These noninvasive diagnostic tests can be performed identically in well-trained or anesthetized animal models and human patient populations, linking invasive observations in animal models, such as histology and/or invasive physiology, to the noninvasive metrics in

humans. In particular, these metrics are essential for the differential diagnosis of auditory pathologies, especially when behavioral data are difficult to obtain, as in children and some animal species.

ABRs are evoked potentials measured at the scalp in response to short-duration stimuli. This test evaluates the integrity and synchrony of the auditory system from cochlea to brainstem. The electrical responses are averaged over many signal presentations at multiple signal intensities and frequencies. Attempts to compare ABR thresholds and behavioral thresholds in nonhuman primates have been made (Lasky et al., 1999), though it is of utmost importance to establish normative correction factors in order to use ABR data in this way. The need for correction factors is demonstrated by the difference in behavioral pure tone thresholds and ABR toneburst thresholds, illustrated for macaques in Figure 1.1.

The ABR waveform is characterized by four to five peaks that are time-locked to the stimulus onset and represent the summed response of progressively more central generators in the auditory periphery and brainstem. The generator of Wave I is clearly the auditory nerve, regardless of species, but macaque ABRs have prominent Waves I, II, and IV, which are likely homologous to the classical human Waves I, III, and V (Allen & Starr, 1978; Kraus et al., 1985; Lasky et al., 1995; Alegre et al., 2001). Similar waveform discrepancies have been noted in squirrel monkeys (Pineda et al., 1989) and marmosets (Harada & Tokuriki, 1997).

ABRs have been used in macaques to assess hearing status and auditory system integrity in the normal aging process (Torre & Fowler, 2000; Fowler et al., 2002; Fowler et al., 2010; Ng et al., 2015), to assess the effects of caloric restriction on aging of the auditory system (Fowler et al., 2002, 2010), to assess the effects of AIDS (Raymond et al., 1998; Riazi et al., 2009), prosthetic implantation (Dai et al., 2011), lead exposure (Lasky et al., 2001), ototoxic drug administration (Shepherd et al., 1994), or acoustic trauma (Hauser et al., 2018; Valero et al., 2017) on hearing status, and following intracochlear injections of saline (Dai et al., 2017). Most of these studies have used ABRs to estimate hearing thresholds (as illustrated for rhesus macaques in Figure 1.1), but the suprathreshold ABR may be more informative for identifying the loss of IHC synapses (see below).

ECochG is conceptually similar to the ABR, except the recording electrode is placed on or near the tympanic membrane instead of the ear lobe or mastoid. This nearer-field electrode placement improves the isolation of the summating potential (SP) and Wave I. ECochG is

primarily used clinically in the diagnosis of Meniere's disease. However, it has recently regained popularity as a possible diagnostic for synaptopathy (Liberman et al., 2016). ECochG has been reliably obtained in macaques, showing similar morphology to humans (see Figure 1.2; also Pugh et al., 1973).

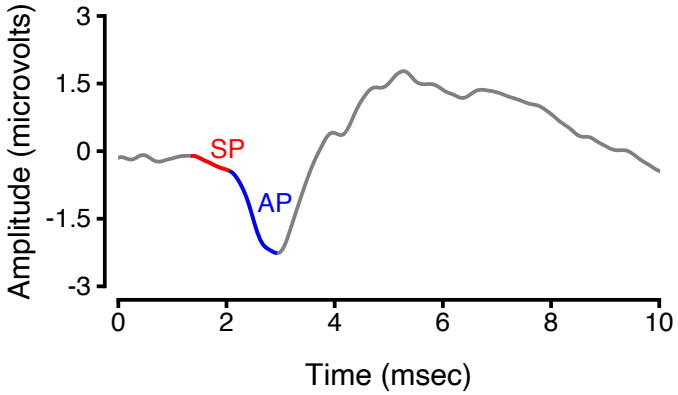

Figure 1.2 Electrocochleography tracing measured from a rhesus macaque monkey using a TM-trode. SP = summating potential. AP = action potential.

Otoacoustic emissions (OAEs), which are spontaneous or sound-evoked sounds originating from nonlinearities in OHC electromotility, can be measured non-invasively from the external auditory canal. As such, OAEs are used to evaluate OHC health, and this metric is an important differential diagnostic tool when paired with ABRs, particularly in cases of auditory neuropathy, in which ears with normal OAEs have grossly abnormal ABR waveform morphology (Starr et al., 1996). Several varieties of OAEs have been reported for macaques, including: spontaneous (SOAEs: Martin et al., 1985, 1988; Lonsbury-Martin et al., 1988; Lonsbury-Martin & Martin, 1988), stimulus-frequency (SFOAEs: Martin et al., 1988; Lonsbury-Martin & Martin, 1988; Joris et al., 2011), transient-evoked (TEOAEs: Martin et al., 1988; Lasky, Beach, & Laughlin, 2000), and distortion product (DPOAEs: Martin et al., 1988; Lasky et al., 1995; Park et al., 1995; Lasky et al., 1999; McFadden et al., 2006; Dai et al., 2011, 2017; Valero et al., 2017). The prevalence of SOAEs is lower in macaques than humans, though much higher than other laboratory species (Lonsbury-Martin & Martin, 1988). DPOAEs amplitudes are similar to those observed for humans using similar stimulus parameters, suggesting similar peripheral generation mechanisms (Martin et al., 1988; Lasky et al., 1995; Park et al., 1995; Lasky et al., 2000).

Acoustic immittance testing can be used to evaluate patency of the middle ear (tympanometry) and integrity of the acoustic reflex pathways (middle ear muscle reflex, medial olivocochlear reflex). Tympanometry has been evaluated in normal hearing and pathologic macaques and squirrel monkeys (Igarashi et al., 1979; Jerger et al., 1978b, 1978a; Lasky et al., 2000; Bachmann, 1996). Macaques have smaller ear canal volumes and reduced compliance compared to humans (Bachmann, 1996; Lasky et al., 2000). Stapedius reflexes have been evaluated in squirrel monkeys (Igarashi et al., 1979; Jerger et al., 1978b, 1978a; Thompson et al., 1984) and macaques (Mangham & Miller, 1976). Immittance testing is a reliable diagnostic tool for differentiating between conductive and sensorineural hearing losses (Jerger et al., 1978b, 1978a), and is a promising metric for the diagnosis of synaptopathy (Valero et al., 2016; Valero et al. 2018; Wojtczak et al., 2017; Bharadwaj et al., 2019).

1.4 AUDITORY DYSFUNCTION FOLLOWING NOISE EXPOSURE

1.4.1 Background

Historically, the primary motivations for studies of noise-induced hearing loss have been to establish safety standards and damage-risk criteria for industrial workers and military personnel and, more recently, to identify potential therapeutics for prevention or recovery from acoustic trauma. As is the case for all human pathologies, humans are the most relevant model system for assessing vulnerability to noise-induced hearing loss. However, the availability of post-mortem cochlear tissue is necessarily opportunistic in human research, and the likelihood of a concomitant audiogram and noise-exposure history being available is low.

Controlled noise exposure studies carried out on young adult humans in the mid-20th century helped to characterize the relationship between signal duration and intensity to the severity of TTS and rate of TTS recovery (e.g. Davis et al., 1950; Ward et al., 1959; Ward, 1960; Klein & Mills, 1981; Mills et al., 1981) and the results of such studies are reviewed elsewhere (Dobie & Humes, 2017). These studies were informative for setting damage-risk criteria, but the lack of structure-function correlations in this experimental design, due to the inability to non-invasively biopsy or image cochleas, was limiting. Furthermore, ethical considerations caused these studies to quickly fall out of favor due to the potential for permanent cochlear damage. In more recent years, human noise exposure studies have re-emerged in the context of drug development (Grinn et al., 2017; Le Prell et al., 2012; Spankovich et al., 2014), but exposures are

carefully designed to minimize the risk for permanent damage and to maintain ethical standards (Maison & Rauch, 2017).

As human noise-exposure studies declined, researchers turned to laboratory animals, such as rats and chinchillas, to address the persistent questions concerning noise-induced hearing loss. In particular, chinchillas share a similar hearing range and cochlear length to humans and have a docile nature, permitting awake non-invasive procedures and operant conditioning behavioral paradigms. However, concerns were raised regarding species-specific differences in susceptibility to damage by acoustic overexposure (e.g., Drescher & Eldredge, 1974; Hunter-Duvar & Bredberg, 1974; Luz & Lipscomb, 1973), suggesting limited translatability for establishing damage-risk criteria. This instigated the onset of several series of experiments in nonhuman primates.

These studies aimed to describe the relationships between:

1. Noise exposure stimulus parameters and cochlear pathology at the gross anatomical level, in terms of both severity and location of cochlear damage.
2. Noise exposure stimulus parameters and the magnitude of TTS and PTS, as assessed by behavioral audiograms.
3. Initial severity, growth, and recovery rate of TTS and any eventual PTS.

What follows is a detailed review of the existing literature on nonhuman primates and noise-induced hearing loss. While many aspects of the experimental design varied across studies, this review will be divided into sections based on the type of exposure stimulus: octave band and broadband noise, pure tones, and impulse noise. Studies of noise-induced hearing loss in NHPs are listed with experimental details in Table 1.1. This review is intended to be comprehensive to the best knowledge of the authors. The relative paucity of nonhuman primate studies should be apparent from the table.

Table 1.1 Nonhuman primate studies of noise exposures, hearing impairment, and cochlear pathology. Studies are listed chronologically.

Citation	Species	Exposure Stimulus	Exposure Level	Exposure Duration	Multiple Exposures?	Behavioral Audiogram?	ABR/DPOAE/ Immittance?	Cochlear Histology?	Additional Details
Martin, Romba, & Gates (1963)	Rhesus macaques	Machine gun impulse	165 dB SPL	1x	No	Yes	No	No	Single subject; mild TTS in mid/high frequencies only; full recovery within 72 hr
Romba & Gates (1964)	Rhesus macaques	Machine gun impulses	154-166 dB SPL	1x	Yes (8-12)	Yes	No	No	TTS recovery and PTS accumulation varies extensively across subjects and exposures
Harris (1967)	Rhesus macaques	Pure tones (2-kHz)	90-120 dB SPL	30-60 min	Yes (4<)	Yes	No	No	TTS and PTS accumulate across exposures
Luz & Hodge (1971)	Rhesus macaques	Impulse noise Tank noise	168 dB SPL 110 dB SPL	2x 12 min	Yes (2) Yes (3)	Yes	No	No	TTS severity and recovery
Hunter-Duvar & Elliott (1972)	Squirrel monkeys	Pure tones (1- or 2-kHz)	120 dB SPL	5-15 min, 20 min-12 hr	Yes (1-7)	Yes	No	Yes	TTS and PTS do not correlate with OHC or IHC loss
Hunter-Duvar & Elliott (1973)	Squirrel monkeys	Pure tones (1- or 2-kHz)	130 or 140 dB SPL	3 or 4 hr	No	Yes	No	Yes	PTS does not correlate with OHC or IHC loss
Luz et al. (1973) Jordan et al. (1973) Pinheiro et al. (1973)	Rhesus macaques	Impulse noise Tank noise	168 dB SPL 110 dB SPL	2x 12 min	Yes (3-18) Yes (2)	Yes	No	Yes	TTS and PTS accumulation across exposures; OHC & IHC counts; improved LF sensitivity in some subjects
Pugh, Horwitz, & Anderson (1974)	Pigtail macaques,	OBN (8-kHz CF)	114 dB SPL	30 min	Yes (not specified)	Yes	Yes	No	Simultaneously recorded AP from chronically implanted

	squirrel monkeys								electrode; smaller neural TTS than behavioral TTS
Scheib, Stebbins, & Moody (1975)	Rhesus macaques	OBN (2-kHz CF)	90 dB SPL	36 days	No	Yes	No	No	TTS growth over duration of exposure
Scheib et al. (1975)	Rhesus macaques	OBN (2-kHz CF)	90 dB SPL	90 days	No	Yes	No	Yes	TTS growth and accumulation to PTS; no relation to OHC/IHC loss
Hawkins et al. (1976)	Rhesus, pigtail, & crab-eating macaques, baboon	OBN (0.5-, 2-, 4-, or 8-kHz CF) or BBN (100-Hz to 10-kHz)	120 dB SPL	8 hr	Yes (20)	Yes	No	Yes	TTS and PTS accumulation over time; weakly correlated with OHC and IHC loss; BBN causes more damage than OBN
Citation	**Species**	**Exposure Stimulus**	**Exposure Level**	**Exposure Duration**	**Multiple Exposures?**	**Behavioral Audiogram?**	**ABR/DPOAE/ Immittance?**	**Cochlear Histology?**	**Additional Details**
Jerger, Maudlin, & Igarashi (1978)	Squirrel monkey	BBN	108-118 dB SPL	1-2 hr	Yes (1-5)	No	Yes	Yes	Tympanometry and acoustic reflexes pre- and post-noise exposure; reflexes predict severity and extent of cochlear damage
Nielsen et al. (1978)	Squirrel monkeys	NBN (375-750-Hz)	95 or 105 dB SPL	1, 2, 4, 8, 16, 24, or 48 hr	Yes (7<)	Yes	No	No	TTS growth increases with longer exposure times; TTS recovery is biphasic
Moody et al. (1978)	Rhesus, pigtail, and crab-eating	OBN (0.5-, 2-, 4-, or 8-kHz CF) or BBN	120 dB SPL	8 hr	Yes (20)	Yes	No	Yes	Extension of Hawkins et al. (1976); TTS does not increase with continued exposure; weak correlation

	macaques, baboon	(100-Hz to 10-kHz) OBN (2-kHz CF)	120 dB SPL	40 hr	No	Yes		Yes	between PTS and OHC/IHC loss; Stebbins et al. (1979) references this data in species comparison
Nielsen et al. (1978)	Squirrel monkeys	NBN (375-750-Hz)	95 or 105 dB SPL	1, 2, 4, 8, 16, 24, or 48 hr	Yes (7<)	Yes	No	No	TTS growth increases with longer exposure times; TTS recovery is biphasic
Pugh, Moody, & Anderson (1979)	Pigtail macaques	OBN (8-kHz CF) OBN (8-kHz CF)	108 dB SPL 118 dB SPL	1 hr 8 hr	No Yes (20)	Yes	Yes	Yes	Loudness recruitment during TTS and PTS; similar estimates via reaction time task and chronic electrocochleography
Moody et al. (1980)	Rhesus macaques	OBN (2-kHz CF)	100 dB SPL	1 or 2 hr	No	Yes	No	No	Response latency as a function of tone intensity during TTS recovery; compared to effects of ethanol administration
Lonsbury-Martin & Martin (1981)	Rhesus macaques	Pure tones (many different CFs)	100 dB SPL	3 min	Yes (not specified)	Yes	No	No	TTS and neuronal adaptation recovery times; recorded neurons in cochlear nucleus and inferior colliculus
Nielsen et al. (1984)	Squirrel monkeys	OBN (500-Hz CF)	95 dB SPL	2, 4, 8, 12, 16, 24, 36, 48, 60, 72, or 96 hr	Yes (7<)	Yes	No	No	Continuous vs. interrupted exposures; TTS growth is faster for continuous than interrupted noise

Citation	Species	Exposure Stimulus	Exposure Level	Exposure Duration	Multiple Exposures?	Behavioral Audiogram?	ABR/DPOAE/ Immittance?	Cochlear Histology?	Additional Details
Lonsbury-Martin et al. (1987)	Rhesus macaques	Pure tones (many different CFs)	100 dB SPL	3 min	Yes (not specified; 5.5-14.4 hrs total)	Yes	No	Yes	Total of 5-14 hr of exposure; mild PTS accumulation from TTS; no relationship between PTS and OHC/IHC loss
Valero et al. (2017)	Rhesus macaques	NBN (2-kHz CF, 50-Hz BW)	108, 120, 140, 146 dB SPL	4 hours	Yes (1-5)	No	Yes	Yes	ABR and DPOAE characterization of TTS & PTS; OHC, IHC, and IHC ribbon synapse counts
Hauser et al. (2018)	Rhesus and bonnet macaques	NBN (2-kHz CF, 50-Hz BW)	140, 146 dB SPL	4 hours	No	Yes	Yes	Yes	Tone detection in quiet, steady state noise, and amplitude modulated noise following PTS; correlated with OHC/IHC/synapse loss

NBN = narrowband noise; OBN = octave band noise; BBN = broadband noise; CF = center frequency; BW = bandwidth; ABR = auditory brainstem response; DPOAE = distortion product otoacoustic emission; OHC = outer hair cell; IHC = inner hair cell; LF = low frequency; AP = action potential from auditory nerve

Literature searches for this review were completed in PubMed using keywords such as: nonhuman primate, monkey, macaque, noise, exposure, impulse, hearing loss, cochlea, hair cell, sensorineural, threshold shift

1.4.2 Octave band and broadband noise exposures

Researchers at the University of Michigan were among the first to study cochlear pathology in NHPs. Their initial focus on antibiotic ototoxicity identified severe cochlear lesions characterized by complete IHC and OHC loss and the presence of phalangeal scars following aminoglycoside use (e.g. Stebbins et al., 1969). The lesions progressed from base to apex with increasing treatment duration. Behavioral pure-tone audiograms were correlated with the anatomical findings, with threshold shifts of 60+ dB resulting from the cochlear lesions. Steep cutoffs and a high degree of symmetry across ears were noted, both anatomically and behaviorally. Overall, these findings provided some of the first direct scientific evidence for the place theory of hearing, which was relatively new at the time (Davis, 1957).

Following this and other studies on ototoxicity, several groups took on investigations of noise-induced hearing loss, due to its broader relevance and greater prevalence. Modeling noise exposure conditions against typical work-related noise conditions, the Michigan group created permanent hearing loss with long, repeated exposures to 120 dB SPL noise (presented for 8 hours per day for 20 days). In these classical studies, the noise bands were either broadband or octave band with varying center frequencies (Hawkins et al., 1976; Moody et al., 1978). In agreement with the prior ototoxicity studies, the basal cochlea seemed uniquely vulnerable to damage. The basal-most hook region of the cochlea was particularly vulnerable, showing complete ablation in nearly all noise-exposed subjects (Hawkins et al., 1976). This extreme basal loss of all OHCs and IHCs was thus termed a juxtafenestral (*"near the window"*) lesion (Hawkins et al., 1976)

Beyond the base, noise-induced damage was observed tonotopically along the cochlear length, according to the frequency spectrum of noise to which the subject was exposed. These tonotopic lesions were broader and less severe than the juxtafenestral lesions. OHC loss was more severe than IHC loss, suggesting greater vulnerability of OHCs than IHCs to noise-induced damage. Higher center frequency noises (e.g. 2-, 4-, or 8-kHz) were more effective at generating noise-induced hearing loss than lower center frequency noises (e.g. 0.5- or 1-kHz). However, Hawkins et al. (1976) noted "a 'central tendency', reminiscent of the familiar 4-kHz dip in the audiograms of patients with noise-induced hearing loss". This suggests that the mid- to high-frequency region of the cochlea may be particularly vulnerable to noise damage, regardless of the spectrum of the noise exposure.

Behavioral audiograms in the same macaques revealed TTS up to 60-85 dB and PTS typically peaking around 40-55 dB. Both TTS and PTS were highly symmetric within a given subject. TTS did not increase throughout the course of exposure, but PTS accumulated over time, with greater losses observed after longer exposure durations (Hawkins et al., 1976; Moody et al., 1978; also demonstrated in chinchillas: Clark & Bohne, 1978). In addition, the authors found that the broadband noise caused more severe hearing loss and greater hair cell loss than any of the octave band noises.

While Moody et al. (1978) concluded that their data supported a strong relationship between cochlear pathology and audiometric threshold, again furnishing the place theory of hearing, a closer examination of the data suggest a weak relationship with several exceptions. Importantly, some subjects had significant PTS accompanied by minimal hair cell loss along the entire cochlear length (Moody et al., 1978). The authors suggested that some of the hair cells, though still present, must have experienced extensive damage without being lost. In a subsequent publication, Stebbins et al. (1979) argued that these data supported the notion of two distinct receptor cell types in the cochlea. Through investigations of behavioral thresholds and cochlear damage following ototoxic treatment in chinchillas, Ryan & Dallos (1975) concluded that OHCs were necessary for normal hearing detection and that OHCs facilitate normal IHC function. Still regarded today as largely true, Stebbins and colleagues (1979) provided the critical cross-species validation by comparing across datasets in chinchillas, guinea pigs, patas monkeys, and macaques.

The same researchers at University of Michigan also studied TTS in macaques using 2-kHz octave band noise continuously presented at 90 dB SPL for 36-90 days (Scheib et al., 1975a; Scheib et al., 1975b). The minimal descriptions available from these studies indicate that TTS accumulated to an initial plateau of approximately 20 dB over the first 7-12 hours of exposure (sometimes described as an “asymptotic threshold shift”; Clark & Bohne, 1978). Thresholds continued to increase, though much more slowly, over the next 5-7 days until leveling to a second plateau, approximately 10 dB higher than the initial TTS. Considerable inter-subject variability was noted. One subject had much larger threshold shifts (60 dB) than the other three, and when thresholds were measured 72 hours following termination of the noise exposure, sensitivity had fully recovered in two subjects and the remaining two had PTS of 15-25 dB. Thus, a stimulus that initially caused only a TTS eventually caused a PTS in 50% of the NHPs.

All subjects had scattered hair cell loss that was not predicted by the TTS or PTS. These studies demonstrate the extent to which susceptibility can vary, even in a small cohort of NHP subjects.

Pugh and colleagues, also at the University of Michigan, conducted chronic intracochlear recording in NHPs (Pugh et al., 1973) to investigate the relationship between noise-induced changes to the auditory nerve action potential (AP) and behavior (Pugh et al. 1974; Pugh et al., 1979). In their first study, a mild TTS was induced in pigtail macaques and squirrel monkeys following exposure to 8-kHz octave band noise at 114 dB SPL for 30 minutes (Pugh et al., 1974). Interestingly, the TTS magnitude was larger in behavioral than neural measures. The exposure also caused relatively small changes in suprathreshold AP amplitude, but an increase in input/output function slope.

In a later study, Pugh et al. (1979) used reaction times from behavioral audiograms, as well as AP latency, to assess loudness recruitment in subjects before and after noise exposure. Subjects were exposed to 8-kHz octave band noise at 108 dB SPL for 1 hour to induce TTS and were later exposed to the same noise at 118 dB SPL for 8 hours daily for 20 days to induce PTS. Both reaction times and AP latency were assessed as a function of stimulus intensity. During TTS and following PTS, reaction times for low-intensity sounds were much higher and reaction times decreased more rapidly with increasing stimulus level, and whereas reaction times for high intensity tones were unchanged. The AP latency vs. stimulus level functions showed comparable results. Histopathology revealed OHC loss in the PTS ears, suggesting that loudness recruitment may be related to OHC function.

In relation to their previous work investigating loudness recruitment in normal hearing macaques (Stebbins, 1966; Stebbins & Miller, 1964), Moody et al. (1980) used a more acute model of TTS to investigate changes in the latency-intensity function. Macaques were exposed to 1 or 2 hours of 2-kHz octave band noise at 100 dB SPL. As thresholds recovered over the next 48 hours, reaction times were recorded across tone levels. Consistent with the findings of Pugh et al. (1979), these results suggested that the subjects had loudness recruitment during TTS recovery, as evidenced by the increased slope of the latency-intensity functions. Once hearing sensitivity recovered to pre-exposure levels, the latency-intensity functions also returned to normal. These investigations of loudness recruitment were some of the only early nonhuman primate studies of noise-induced hearing loss (including TTS or PTS) to examine perceptual changes beyond basic hearing sensitivity.

Concurrently, researchers at Henry Ford Hospital in Detroit, Michigan began investigating the time course of TTS in squirrel monkeys exposed to 500-Hz octave band noise. The subjects underwent several exposures of varying durations across several days to weeks. Hearing sensitivity was assessed behaviorally at 750 Hz only. Nielsen et al. (1978) observed 5-10 dB of initial TTS growth during the first 1-8 hours of noise exposure, followed by a continuous increase in TTS severity with increasing exposure time (up to 48-hour duration). This lack of asymptotic threshold shift contrasts the findings described above (Hawkins et al., 1976; Moody et al., 1978; Scheib et al., 1975a; Scheib et al., 1975b). Following cessation of the noise exposure, TTS recovered in a biphasic manner: an initial fast phase (<15 min) followed by a slow phase (up to 48 hours). Higher intensity exposures caused more severe TTS and longer recovery times. The results of these studies were remarkably similar to human studies of TTS growth and recovery. In a follow-up study, Nielsen et al. (1984) observed faster TTS growth in subjects with continuous – as opposed to interrupted – noise exposures. Despite large variability in severity of TTS and TTS growth rate, all subjects recovered back to normal hearing sensitivity within a few days after exposure.

A separate group studied changes in middle ear acoustic immittance following PTS caused by broadband noise exposure in squirrel monkeys (Jerger et al., 1978b). Tympanometry and acoustic reflexes (elicited by 0.5, 1, 2, and 4 kHz tonebursts and broadband noise) were measured before and after exposure to 108-118 dB SPL noise for 1-2 hours over the course of multiple days. While tympanometry showed excellent middle ear compliance pre- and post-exposure, acoustic reflexes predicted the severity and extent of cochlear hair cell loss.

1.4.3 High intensity pure tone exposures

Pre-dating the use of noise as an exposure stimulus, researchers utilized high intensity pure tone exposure to examine TTS growth and recovery and the accumulation to PTS in macaques (Harris, 1967). Harris (1967) was particularly interested in predicting susceptibility to PTS from TTS, so he employed a cross-species approach of humans, rats, and macaques (though it is important to note that exposure stimuli and conditions were quite varied across experiments and species). Macaques were exposed to 2-kHz tones for 30-60 minutes, with tone levels increasing from 90 to 120 dB SPL over several sessions. Higher exposure levels caused greater TTS and a mild PTS (<30 dB) accumulated across several exposures for 75% of the macaques (Harris, 1967). The one NHP subject that did not develop PTS was also notably more resistant to

TTS than the others. No other obvious trends between TTS and PTS were observed for the remaining subjects. Humans and rats exhibited similarly weak TTS-PTS relationships (Harris, 1967).

In contrast to octave band or broadband noise, pure tones generate narrower activation patterns in the cochlea. Therefore, exposure to high intensity tones should lead to narrower cochlear lesions and a more limited spectrum of threshold elevation. In two seminal studies, Hunter-Duvar & Elliott (1972, 1973) exposed squirrel monkeys to 1- or 2-kHz pure tones monaurally at 120, 130, or 140 dB SPL. Behavioral audiograms were measured prior to obtaining cytocochleograms for the exposed and unexposed ears. Shorter duration exposures (5-15 minutes) elicited up to 30 dB TTS, with no differences in IHC or OHC counts between the exposed and unexposed ear. Longer duration (2-4 hours) and higher intensity exposures ultimately generated PTS. However, severity and extent of PTS varied extensively across subjects, ranging from 20-50 dB peak loss anywhere between 1- to 6-kHz.

The impact of these experiments, however, comes from the fact that Hunter-Duvar and Elliott did not observe any measurable relationship between hair cell loss and PTS. For example, one subject presented with a 50 dB PTS following a three-hour exposure to a 1-kHz tone at 140 dB SPL, but had normal hair cell counts bilaterally. Additionally, a different subject had less than 20 dB PTS following a four-hour exposure to a 140 dB SPL 1-kHz tone, but exhibited complete loss of OHCs and some IHC loss along the entire basal half of the overexposed cochlea. No subjects showed narrow, tonotopically localized cochlear lesions, as might be predicted by cochlear mechanics. Instead, either unilateral basal cochlear lesions of varying extent were observed or no observable damage was present at all. Pure juxtafenestral lesions were not observed in any of the subjects.

A few years later, Lonsbury-Martin & Martin (1981) used short (3 minute) 100 dB SPL pure tone exposures to create mild, quickly reversible monaural TTS in macaque monkeys. Behavioral thresholds typically recovered within 15-20 minutes post-exposure. High frequency tones elicited more severe TTS and longer recovery times than low frequency tones. Single unit recordings in the cochlear nucleus and inferior colliculus of the awake subjects revealed that neurons in the CN and IC typically exhibited larger threshold shifts and took longer to recover to baseline levels when compared with behavioral thresholds.

In a follow-up study, Lonsbury-Martin and colleagues (1987) conducted repeated monaural pure tone exposures over the course of 12-18 months, using similar stimulus conditions as the 1981 study. After 12 months of 100 dB SPL pure tone exposures accumulating to a total of 5.5 hours, one subject had a narrow cochlear lesion (complete loss of IHCs and OHCs) in the mid-basal cochlea, but did not have any measurable PTS. The two macaques that underwent 18 months of 100 dB SPL pure tone exposures accumulating to 13-14 hours had up to 10-15 dB PTS between 8-16 kHz. Cytocochleograms revealed a narrow cochlear lesion in one subject and normal cochlear anatomy in the other. Once again, these data suggest that sounds that initially only cause a TTS can accumulate to create PTS, but the underlying cochlear pathology is not well predicted by audiometric threshold shifts.

1.4.4 Impulse noise exposures

Due to the Department of Defense's vested interest in noise-induced hearing loss, many experimental paradigms are intended to model noise exposure conditions experienced by military personnel. High intensity impulse noises have been used in studies of humans and animals to probe the effect of blast exposures on hearing sensitivity. In fact, the earliest studies of noise-induced hearing loss in NHPs were completed in rhesus macaques by Romba and colleagues in the early 1960s using highly realistic military exposure conditions (Martin et al., 1962; Romba, 1962; Romba & Gates, 1964). Subjects were seated in a tank and exposed to machine gun blasts, which were approximately 165 dB SPL. Audiograms were obtained immediately following blast exposure and repeated over the course of 72 hours. TTS was greatest (up to 20 dB) at 2- and 4-kHz, less severe at 6-, 8-, and 12-kHz, and not present below 1-kHz. Following multiple exposures, some subjects acquired PTS while others did not. TTS recovery and PTS accumulation varied extensively across subjects (Romba & Gates, 1964), suggesting large individual differences in susceptibility to NIHL.

Luz & Hodge (1971) also undertook experiments to probe the effect of blast exposures on hearing sensitivity in rhesus macaques and humans, specifically inquiring about TTS recovery patterns following exposure to blasts and to continuous broadband tank noise (110 dB SPL, 12-minute duration). Following exposure to two 168 dB SPL impulses, subjects had TTS ranging from 5-40 dB that recovered to baseline sensitivity in as little as 20 minutes in some subjects or up to 32 hours in others. Recovery patterns suggested two independent pathophysiological processes with different time constants (consistent with the observations of Nielsen et al., 1978,

1984), resulting in five distinct TTS recovery pattern classifications. Subjects underwent several impulse noise exposures and several continuous noise exposures. Severity of TTS and recovery pattern varied extensively by subject, test frequency, exposure type, and exposure number. In comparison to young adults exposed to gun shots in the laboratory, macaques had more severe TTS and slower recovery times. However, monkey and human shared the same recovery patterns, suggesting similar pathophysiology across species (Luz & Hodge, 1971).

Following their initial study, Luz et al. (1973) continued exposing the macaques to the impulse and continuous noises in order to generate PTS, with four weeks between exposures in order to reach maximal hearing recovery. As seen in nearly all studies described thus far, the magnitude and recovery pattern of TTS, the magnitude and bandwidth of PTS, and overall individual susceptibility was highly variable across subjects. However, a few unique findings are worth mentioning in greater detail here. First, seven of the nine subjects showed less severe TTS following their second noise exposure than following their first noise exposure. This and similar findings have been posited as a 'toughening of the ears', or an increased resistance or tolerance of damage within the cochlea. Taken together with the notion that TTS-related noise damage can accumulate to generate PTS, one can certainly appreciate the complexity of noise-induced cochlear pathology. Second, the majority of subjects required many noise exposures to induce even a mild, high frequency PTS (e.g. a series of 10 or 20 impulse noises resulted in 10-25 dB PTS). Macaques seem quite robust to blast exposure, albeit more susceptible than humans. Third, most subjects exhibited improved low frequency hearing sensitivity following noise exposure in the presence of high frequency PTS. The reason for this improved sensitivity is unknown, but has been reported by others (Moody et al., 1978).

Jordan et al. (1973) completed cytocochleograms on the Luz et al. (1973) macaque cohort. The extent and severity of hair cell loss was highly variable across subjects, ranging from normal IHC counts with a few missing OHCs and auditory nerve fibers to large basal wipeouts to isolated mid-cochlear OHC losses. All subjects exhibited juxtafenestral lesions of differing extents. Furthermore, hair cell damage was not well predicted by the pure tone audiogram (Pinheiro et al., 1973). Jordan et al. noted that hair cells adjacent to areas of loss were often swollen or damaged, suggesting ultrastructural damage and possible malfunction. At the level of the hair-cell and audiogram, cochlear pathology resulting from impulse noise exposure does not seem to differ from the damage resulting from continuous noise or pure tone exposures in NHPs.

1.4.5 Recent nonhuman primate studies of noise-induced hearing loss

In the 30+ years since the last studies of NIHL in NHPs, many methodological improvements have emerged including advanced behavioral assays, novel histological preparations including immunohistochemistry, higher-resolution imaging methods, and improved electrophysiological measures. Due to these advances, it is appropriate to re-visit the classical studies of macaque noise-induced hearing loss in order to gain a more complete understanding of the relationship between noise exposure, cochlear pathology, auditory pathway integrity, and behavioral manifestations.

The first application of these comprehensive and updated methodological approaches in NHPs was completed by the present authors (Valero et al., 2017). In this study, cochlear function was assessed by ABRs and DPOAEs in macaques exposed to narrowband noise at sound pressure levels ranging from 108 – 146 dB SPL. Histopathological assessments of hair cell and synapse survival indicated that IHC ribbon synapse loss accompanies IHC and OHC loss in cases of PTS in macaque monkeys exposed to 146 dB SPL narrowband noise. Furthermore, macaques exhibited moderate IHC synapse loss in the absence of IHC or OHC loss following TTS induced by exposure to 108 dB SPL narrowband noise.

To follow up on the behavioral consequences of such noise exposures that cause NIHL, to draw parallels between the human literature and data from animal models, and to establish perceptual correlates of cochlear histopathology, we obtained behavioral metrics on a detection task. Macaques were trained to detect tones in quiet and in the presence of various background noises. The behavioral indices were obtained before and after a four hour narrowband noise exposure that caused PTS (Hauser et al., 2018). Subjects had 40-60 dB increase in audiometric threshold (PTS) across a narrow range of tone frequencies following exposure. These studies showed that macaques with PTS had slower increase in detection thresholds in increasing broadband background noise masker levels. Further, they also showed reduced release from masking when the broadband masker was modulated by low frequency sinusoids relative to pre-exposure values. These behavioral measures were also correlated with degree of PTS across test frequencies. Additionally, threshold shift rate was significantly correlated with IHC, OHC, and synapse loss observed in a cohort of NHPs that underwent an identical noise exposure (from Valero et al. 2017). We are continuing studies of these and other noise exposed animals in order to investigate changes in auditory perception following TTS and PTS. These data serve as one of

the first direct corroborations of complex auditory perception (beyond a behavioral audiogram) and cochlear histopathology following noise-induced hearing loss for any species.

1.4.6 Summary of NHP noise exposure studies

Despite the relative paucity of primate studies of noise-induced hearing loss, several noteworthy conclusions, including conspecific trends, can be gleaned from this literature:

1. Higher intensity and longer duration stimuli generate more severe cochlear damage, starting with OHC damage/loss, followed by IHC loss.
2. A stimulus that initially causes a TTS can, with repeated exposures, eventually cause a PTS.
3. The basal-most region of the cochlea is more susceptible to noise-induced damage than the apical regions, regardless of the characteristics of the exposure stimulus.
4. Severity of TTS can predict the likelihood, but not the severity, of PTS.
5. The relationship between severity of cochlear damage and the magnitude of TTS or PTS remains unclear.
6. The lack of relationship between severity of cochlear damage and degree of TTS or PTS may be due to ultrastructural damage that is not visible in light microscopy. These pathophysiological processes may also account for the different configurations of TTS recovery over time.
7. NHPs are more resistant to noise-induced damage than other laboratory species, but more susceptible than humans (Luz & Hodge, 1971; Luz & Lipscomb, 1973; Stebbins et al., 1979; Valero et al., 2017).

1.5 NONHUMAN PRIMATES AS A MODEL FOR DEVELOPMENT AND VALIDATION OF THERAPEUTICS FOR NOISE-INDUCED HEARING LOSS

1.5.1 Overview

The discovery and validation of therapeutic approaches to treat medical conditions, such as hearing loss, is an extremely long process fraught with numerous challenges. Only a tiny fraction of the promising therapeutics that reach clinical trials are effective, let alone ultimately approved, by the FDA (Garner, 2014). Long before the commencement of clinical trials, prospective treatments are developed and validated in small animal models, typically mice and other rodents.

Intermediate species (e.g., canines, felines, NHPs) are used when deemed appropriate. As a recent example, Voretigene became the first FDA-approved gene therapy for correction of a specific gene mutation in the U.S. (Petersen-Jones & Komáromy, 2015; Russell et al., 2017). In earlier stages of development, the procedure was refined and vetted in rodents, then applied to a large-animal canine model for further validation (Acland et al., 2001). This was a suitable choice as the mutation naturally occurs in some dogs. By virtue of their close phylogenetic relationship to humans, the use of NHPs as an intermediate animal model may be an appropriate choice to increase confidence in the application and translation of foundational discoveries made in other species. Indeed, as mentioned above, NHPs have been chosen for development of diagnostics and therapeutics where phylogenetic similarity was an important factor (e.g., cardiology, cognition, genetics, HIV/AIDS, immunology, pharmacology, reproduction, respiratory disease) (Phillips et al., 2014).

Ideally, species selected as models would provide information that translates directly to humans with high sensitivity and specificity in a manner that is cost-effective. Unfortunately, the path is rarely this direct. In theory, translational challenges from rodents to humans should be minimal for highly conserved biological targets (e.g., hair cells), and the necessity of a large-animal intermediate could potentially be minimal. In practice, unforeseen factors combine to impede progress (Perlman, 2016), as successful outcomes may also depend on interactions with other factors, such as body size, inflammatory response, metabolic rate, hormonal composition, biocompatibility, etc.

The development of pharmacologic and gene therapies for acquired and hereditary forms of hearing loss has rapidly progressed over the last decade, but most therapies remain at a relatively early stage. The vast majority involves rodent models, and none of the datasets derived from systematic testing in a large animal intermediate have been publicly disclosed. Here we consider a few of the many factors that may significantly impact the development of effective therapeutics, including species differences that may pose challenges to translation.

1.5.2 Species differences in susceptibility to NIHL

As briefly mentioned above, susceptibility to NIHL (PTS, TTS) and related conditions (e.g., hyperacusis, tinnitus) appears to differ significantly between individuals and species (Dobie & Humes, 2017; Henderson, Subramaniam, & Boettcher, 1993; Knipper et al., 2013; Luz & Hodge, 1971; Luz & Lipscomb, 1973; Sliwinska-Kowalska & Pawelczyk, 2013; Stebbins et

al., 1979; Valero et al., 2017), including strains of inbred mice used in research (Myint et al., 2016). Controlled studies in NHP and humans are relatively rare (or prohibited), and often have lower subject numbers, variable or unknown noise exposures, and less control of contributing factors such as exposure history, lifestyle, sex, age and genetics.

An important observation is that the exposures sufficient to generate TTS and PTS are lower overall in rodents than NHPs and humans (see Table 1.1; also discussed in Dobie & Humes, 2017; Valero et al., 2017; Yankaskas et al., 2017). The range of sound pressure levels (SPLs) that cause cochlear damage in mice, ranging from synaptopathy to hair cell loss, is relatively small when compared to NHPs and humans. In mice, a single exposure to octave-band noise of 97-98 dB SPL causes TTS, accompanied by a narrow-band synaptopathic lesion, while an increase to 116 dB SPL can rupture the reticular lamina, leading to large wipeout regions in the organ of Corti (Wang et al., 2002). In macaque monkeys, the range of exposures over which these effects have been observed spans 108 – 146 dB SPL (Valero et al., 2017). Cochlear synaptopathy of approximately 30% accompanied a single TTS-inducing 108-dB exposure to narrowband noise, whereas a single 146-dB exposure caused PTS, substantial synaptopathy (up to ~80% in a given region), and hair cell loss. Comparable PTS data and hair-cell counts have been reported in other NHP studies and humans (see Table 1.1).

1.5.3 Factors influencing therapeutic efficacy

The mouse model is invaluable for early-stage development and validation of potential therapeutics, particularly when a transgenic model can add value to mechanistic questions. However, mice and humans often respond differently to the same treatments (Perlman, 2016), and there are obvious anatomical differences that may limit the translation of a given approach (see sections 2 and 3 below). Therefore, an intermediate translational model will likely be essential when developing drugs and the delivery approach for humans. For some treatments, intermediate testing in NHPs may be an effective strategy to optimize effectiveness and reduce risk, with respect to the biological target, design of the therapeutic agent, delivery route, therapeutic window, and other (perhaps unforeseen) factors. A few of these are highlighted here.

1.5.3.1 Genetics. Similarities and differences in gene expression and regulation between species are certain to be important factors with respect to hearing and hearing loss. Several studies have linked genomic variations to significant differences in anatomy and physiology, as well as to hearing loss (Dou et al., 2003; Hosoya et al., 2016a; Hosoya et al., 2016b; Köppl et al., 2018;

Makishima et al., 2005; Matsuzaki et al., 2018; Plum et al., 2001; Suzuki et al., 2007; Van Laer et al., 2006, 2005; Wang et al., 2018). Transcriptome profiling has been productively applied to the cochlea and portions of the central pathways of humans and mice (Burns et al., 2015; Cai et al., 2015; Guo et al., 2016; Hackett et al., 2015; Schrauwen et al., 2016), while studies of the impact of NIHL on gene expression are beginning to emerge (Frenzilli et al., 2017; Lavinsky et al., 2016; Manohar et al., 2019; Manohar et al., 2016; Sun et al., 2008). To date, none include NHPs, although improved diagnostic and treatment efficacy could potentially be fostered by studies in species with closer phylogenetic and developmental similarity to humans. This may be especially relevant for applications involving gene therapy (Ahmed et al., 2017; Gao et al., 2018), where genomic and gestational differences between species are significant factors in treatment efficacy (Wang et al., 2018).

1.5.3.2 Inner ear anatomy. Fortunately, the major structures in the cochlea (hair cells, supporting cells, neuronal types) are highly conserved across species, implying relative uniformity with respect to biological targets. However, the dimensions of most structures and fluid filled compartments (i.e., hair cells, supporting cells, stereocilia, round window, oval window, scala tympani, scala media, scala vestibuli, cochlear aqueduct, endolymphatic duct, round window membrane, etc.) vary significantly between species and in a manner that could impact one or more aspects of drug delivery (Glueckert et al., 2018). For example, differences in fluid volume and flow in the perilymphatic or endolymphatic spaces may contribute to pharmacokinetic variability (Salt & Hirose, 2018). The volume of the macaque inner ear is about 24 times greater than mouse, and the human cochlea is about 3 times larger than macaques (Dai et al., 2017; Ekdale, 2013; Kirk & Gosselin-Ildari, 2009). Basilar membrane lengths range from a mean of 6.8mm in mice, 12.1 mm in rats, 20.5 mm in guinea pigs, 22.5 mm in cats, 27 mm in macaques, compared to a mean of 35 mm in humans (Kirk & Gosselin-Ildari, 2009). NHPs have one row of inner hair cells and three rows of outer hair cells, with ectopic or supernumerary hair cells frequently noted (Valero et al., 2017), consistent with reports in humans (Rask-Andersen et al., 2017).

An important feature related to labyrinthine volume concerns the patency and dimensions of the cochlear aqueduct, which is longer and narrower in NHPs and humans (Gopen et al., 1997). This channel links the scala tympani with the subarachnoid space in the brain and is a potential route by which drugs delivered to the scala tympani could exit the cochlea or mix with

incoming CSF. Rodents and primates appear to differ with respect to CSF influx and efflux through this channel. These and numerous other factors (not discussed here) can significantly alter the pharmacokinetics of drugs delivered to the perilymph, and differentially impact basal and apical regions (Salt & Hirose, 2018; Salt et al., 2016). Comparable principles impact pharmacokinetics in the middle ear, as well. Accordingly, species differences are important considerations, and while modeling may be a useful guide, direct testing in large animal models may be needed to validate predictions and/or refine the models.

1.5.3.3 Innervation of the cochlea. Afferent and efferent innervation appears to be fairly well conserved between species, although intensive studies in NHPs are lacking. Branching of Type 1 radial afferent fibers has been noted in NHPs (Kimura, 1975), as well as rats (Perkins & Morest, 1975), guinea pigs (Fernandez, 1951), cats (Liberman, 1982; Perkins & Morest, 1975), and humans (Nadol, 1983). Additionally, human spiral ganglion cell somata are primarily unmyelinated (Nadol, 1988; Ota & Kimura, 1980; Rattay et al., 2013), unlike most other laboratory species (Rattay et al., 2013). It is unknown whether NHP spiral ganglion cell somata are myelinated.

While there are very limited data on NHP auditory nerve fiber (ANF) physiology (Katsuki et al., 1962; Nomoto et al., 1964; Nomoto, 1980; Joris et al., 2011), all studies seem to stray from the properties observed in other laboratory species. For example, macaques do exhibit a bimodal population distribution of ANF spontaneous rates similar to that observed in other mammals (Nomoto et al., 1964; Joris et al., 2011). However, there is no evidence for a relationship between spontaneous rate and threshold at the ANF's characteristic frequency (CF; an ANF's most sensitive frequency; Joris et al., 2011; Nomoto et al., 1964). The relationship between CF threshold and spontaneous rates of auditory nerve fibers is one of the most important features of the findings in other mammalian species (e.g. Liberman, 1978). These results suggest that one of the primary organizational principles of the auditory periphery may be different in primates relative to other mammals, causing concern for translatability (Hickox et al., 2017). This is especially relevant to pathologies like synaptopathy, which preferentially affects low spontaneous rate ANFs in rodents (Furman et al., 2013; Song et al., 2016).

1.5.3.4 Delivery route. The effective delivery of therapeutic agents to the inner ear is an active area of exploration. Major factors include the route of delivery and composition of the therapeutic. Both factors may be significantly impacted by species specific features, with

implications for translation to humans. Promising delivery routes include transtympanic injection into the tympanum, injection into perilymphatic space through the round window, cochleostomy of the basal or apical turns, and injection into the posterior semicircular canal (Akil & Lustig, 2019; El Kechai et al., 2015; Isgrig & Chien, 2019; Lichtenhan et al., 2016; Suzuki et al., 2017). Each has advantages and disadvantages, including the risk of unintended middle or inner ear damage. In addition, efficacy appears to depend on interactions between the delivery route and the biological target (cell type), the therapeutic agent, and various subject characteristics (Salt & Plontke, 2018). A few examples follow.

1.5.3.5 Therapeutic window. Although afferent synapses on IHCs are immediately lost following acoustic overexposure, the terminal dendrites retract slowly and the neuronal cell bodies can remain in the spiral ganglion for months to years (Fernandez et al., 2015). This offers a long window during which a therapeutic agent might encourage the reinnervation of IHCs by cochlear nerve fibers. Treatments under evaluation for NIHL typically involve delivery of the therapeutic agent (viral vector, pharmacologic agent) within a window of hours to weeks after the exposure (Du et al., 2018; Sly et al., 2016; Suzuki, Corfas, & Liberman, 2016), or even prior to exposure (Chen et al., 2018). The optimal therapeutic window for humans is unknown, therefore preliminary studies in NHPs may improve predictions.

1.5.3.6 Properties of therapeutic agents. Unfortunately, a thorough discussion of the factors related to design of potential therapeutic agents is well beyond the scope of this review, however a few relevant observations are highlighted here.

For genetic and acquired hearing loss, viral mediated gene delivery for cell-type-specific targeting currently offers the most promise for effective treatments (Ahmed et al., 2017; Akil & Lustig, 2019; Chien et al., 2015; Fukui & Raphael, 2013; Géléoc & Holt, 2014; Holt & Vandenberghe, 2012; Zheng & Zuo, 2017). Adeno-associated viruses (AAV) are the most promising vectors for gene transfer. Scores of serotypes, identified from screens in NHP and human tissue (Gao et al., 2004; Gao et al., 2002), are now known, but transduction appears to vary by cell type (Kim et al., 2019). In addition, tropism patterns have not been determined for most serotypes, and could certainly vary by species and biological target. Fortunately, the conservation of cellular and molecular features between species appears to be quite high, suggesting that cell-type specific therapies vetted in rodents may also be effective in primates, including humans. However, differences in the expression and regulation of some genes and

proteins can be substantial, as discussed earlier (see Rationale section), with potential impact on outcomes. Expression profiling and direct testing in NHPs could be a useful step in the validation process for promising vectors.

For the treatment of NIHL or other conditions by pharmacologic agents (e.g., anti-inflammatories, neurotrophins, antibiotics), translational efficacy also depends on myriad factors, many of which remain incompletely defined. The resultant impact on pharmacokinetics appears to depend on interactions between the anatomical features briefly highlighted above and the delivery method, dosage, and physical properties of the compound (Salt & Plontke, 2018). Species differences are well characterized for very few of the compounds currently in clinical use, thus it remains to be determined how predictive these data will be for novel formulations.

1.5.3.7 Conclusion. Overall, the data highlighted in this section reveal that multiple interdependent factors contribute to treatment efficacy. The differences between species in this respect are not merely a matter of scaling, but involve complex interactions between factors that cannot be reliably predicted from modeling alone. Direct testing in animal models and humans will be needed to augment predictions, and given the sizable differences between mice and humans, we suggest that NHPs are an ideal intermediate species for improving the efficacy and safety of this process.

1.6 PRACTICAL CONSIDERATIONS

The paper thus far highlights the importance of the NHP model to investigate noise induced hearing loss, both the basic aspects as well as the clinical translational and therapeutic aspects. While there are many possible opportunities to important and fruitful research plans, there are a few practical matters to consider. As opposed to rats and mice, the care and use of NHPs is regulated by the United States Department of Agriculture (USDA), and are under much stricter oversight from the Institutional Animal Care and Use Committee and veterinary staff. The institutional laboratory animal veterinary staff then must include expertise in primate medicine to assure and provide adequate veterinary oversight of the animals in the research program. In addition, the program needs to ensure the provision of species-specific environmental enrichment to adhere to the USDA policies as expressed in their document, Guide for the Care and Use of Laboratory Animals. Making sure that such requirements are met requires additional staff with specialized training.

A second consideration is space. Macaques are larger than the traditional laboratory animal species used (mice, rats, gerbils, guinea pigs, cats, etc.), and this necessitates greater housing room. As with other species, the space requirement varies with the body weight of the animal; the smallest primates require the least space per animal. Minimum space requirements range from about 2.1 sq. ft /animal for the smallest animals (< 1.5 kg) to > 25 sq. ft. for animals over 30 kg. These are much larger compared to the range for mice (6 - >15 sq. in /animal), rats (17 – 70 sq. in.), and guinea pigs (60 – 100 sq. in./animal). The minimum space requirement for the smallest primates are about 4 times the space requirement for the largest rats and 3 times the caging size requirements for the largest guinea pigs. Further, the social nature of nonhuman primates requires that they are socially housed, in pairs or groups. Additionally, primates are required to have enough vertical space to permit standing vertically on two legs, to swing from the cage ceiling without hitting the floor, and to make brachiating movements. These constraints increase the space requirements to house and maintain these valuable animals.

The third consideration is the monetary costs for acquiring and maintaining primates. These costs include purchasing, shipping, and housing. A survey of nonhuman primate vendors revealed that the purchase costs were species dependent and far higher than that of common rodents. In comparison to the cost of a mouse or a rat, squirrel monkeys cost about 100 – 130 times as much, marmosets cost about 140 – 200 times, and macaques range from 200 to 300 times the cost. The shipping costs depend on the distance between the institutions and the vendor, ranging from $4000 to $12000 per batch of primates. Housing costs were extrapolated from the 2017 Yale University survey on housing costs, with information collected from 57 institutions, with an annual increase of about 3%. These costs depended on the primate species and institution (public vs. private, location within the United States of America). Housing or per-diem costs range from about 12 times the cost of a mouse cage (typically 3 – 5 mice) to 25 times the cost of a cage of mice, depending on the location. While it is true that most NHP labs utilize fewer subjects and maintain the same colony for many years, costs remain significantly greater than those incurred by rodent research programs. Such high costs necessarily constrain the funds that can be devoted to non-animal costs given the limited funds provided by funding agencies to perform the studies that have highly variable effects, as discussed above.

1.7 FUTURE DIRECTIONS

Given the relatively sparse literature on nonhuman primates and NIHL, the opportunities are vast, and the primate is an excellent candidate to fill the gaps in our knowledge. We propose some broad classes of studies that would be essential to further our understanding of the mechanisms of NIHL, their perceptual effects, and treatment option to ultimately reverse the effects of the noise exposures. In spite of the considerations discussed above, these essential experiments would advance our knowledge of basic mechanisms and enhance the translatability of the growing rodent and human literatures on noise-induced pathologies.

(1) Genomics. Although the human genome is more similar to NHPs than mice and other species (Breschi et al., 2017; Marques-Bonet et al., 2009), they are not identical, and the differences in structure and function can be significant in ways that limit translation (Bailey, 2005). For many genes, structural and functional conservation is quite high, suggesting a better prognosis for translation, while for others, species differences are substantial, even in homologous structures (Bernard et al., 2012; Chen et al., 2016; Konopka & Geschwind, 2010; Mashiko et al., 2012; Mitchell & Silver, 2018; Sousa et al., 2017; Zeng et al., 2012). For this reason, predictions about functional outcomes for a specific biological target (e.g., hair cells, auditory nerve) must be determined in a cell- or tissue-specific manner for each species. To improve predictions and outcomes, genomic and proteomic profiling of peripheral and central auditory structures should be pursued in NHPs and humans for comparison with other models.

(2) Inner ear anatomy and physiology. Descriptions of the structural and functional features of the inner ear and major cochlear structures have not been systematically carried out for NHPs, and existing data may lack essential details. Advanced understanding of key features (e.g., dimensions of fluid compartments, cell types, innervation, membrane permeability, fluid dynamics) could greatly enhance functional modeling and therapeutic design (i.e., pharmacological, gene therapy). Further, characterizing the physiological encoding schemes and their changes with the structural damage caused by noise exposure will also aid in identifying physiological and behavioral assays for differential diagnosis of specific cochlear pathologies.

(3) Clinically viable assessment tools. Development of sensitive new tools to augment routine audiological assessments are needed to identify different forms of auditory pathology caused by overexposure to noise (e.g., synaptopathy with and without hair cell loss), and perhaps distinguish those patterns from hearing loss caused by other factors (e.g., aging, hereditary factors, ototoxicity). The same tools could be used to assess recovery from NIHL, or other

pathology, as therapeutic tools move toward clinical trials in humans. Research involving NHPs will be invaluable in this regard, as assessment tools can be developed and subsequently validated by histological analyses of the cochlea, auditory nerve, and central pathways, with support from direct recordings from these structures (see Valero et al., 2017).

(4) Individual variability. It is often noted that two subjects with identical noise exposure histories can have very different cochlear pathology and performance in perceptual tasks. This difference in susceptibility to noise exposure has been attributed in the literature to "tough" and "tender" ears (Cody & Robertson, 1983; Maison & Liberman, 2000). It is not a big stretch to extend the individual variability to treatment effectiveness as well. Coupled with the large inter- and intra-species genetic variability that is observed in primates (including humans, reviewed briefly above), individual variability should be systematically investigated. These investigations may ultimately shed light on efficacious treatment options to combat NIHL.

1.8 ACKNOWLEDGMENTS

The authors would like to acknowledge the anonymous reviewers for their review of this manuscript, Amy Stahl for compiling the data for Figure 1.1, and Chase Mackey for comments on an earlier version of the manuscript. JB was supported by NIH T32 MH 064913-16 (PI: Danny Winder), and TAH and RR were partially supported by NIH R01 DC 015988 (MPI: R. Ramachandran & B. Shinn-Cunningham).

1.9 REFERENCES

Acland, G. M., Aguirre, G. D., Ray, J., Zhang, Q., Aleman, T. S., Cideciyan, A. V., … Bennett, J. (2001). Gene therapy restores vision in a canine model of childhood blindness. *Nature Genetics*, *28*(1), 92–95. https://doi.org/10.1038/ng0501-92

Ahmed, H., Shubina-Oleinik, O., & Holt, J. R. (2017). Emerging Gene Therapies for Genetic Hearing Loss. *JARO: Journal of the Association for Research in Otolaryngology*, *18*(5), 649–670. https://doi.org/10.1007/s10162-017-0634-8

Akil, O., & Lustig, L. (2019). AAV-Mediated Gene Delivery to the Inner Ear. In M. J. Castle (Ed.), *Adeno-Associated Virus Vectors: Design and Delivery* (pp. 271–282). https://doi.org/10.1007/978-1-4939-9139-6_16

Alegre, M., Gurtubay, I. G., Iriarte, J., Ciordia, E., Manrique, M., & Artieda, J. (2001). Brainstem auditory evoked potentials (BAEPs) in the cynomolgus macaque monkey Equivalence with human BAEPs and proposal of a new nomenclature. *Hearing Research*, *151*, 115–120.

Allen, A. R., & Starr, A. (1978). Auditory brain stem potentials in monkey (M. Mulatta) and man. *Electroencephalography and Clinical Neurophysiology*, *45*(1), 53–63. https://doi.org/10.1016/0013-4694(78)90341-3

Bachmann, K. R. (1996). *Dissertation- A study of the effect of clinical doses of furosemide on DPOAEs and ABRs in a non-human primate*.

Bailey, J. (2005). Non-human primates in medical research and drug development: A critical review. *Biogenic Amines*, *19*(4), 235–255. https://doi.org/10.1163/156939105774647385

Barden, E. K., Rellinger, E. A., Ortmann, A. J., & Ohlemiller, K. K. (2012). Inheritance patterns of noise vulnerability and “protectability” in (C57BL/6J × CBA/J) F1 hybrid mice. *Journal of the American Academy of Audiology*, *23*(5), 332–340. https://doi.org/10.3766/jaaa.23.5.4

Beecher, M. D. (1974a). Hearing in the owl monkey (Aotus trivirgatus): I. Auditory sensitivity. *Journal of Comparative and Physiological Psychology*, *86*(5), 898–901. https://doi.org/10.1037/h0036416

Beecher, M. D. (1974b). Pure-tone thresholds of the squirrel monkey (*Saimiri sciureus*). *The Journal of the Acoustical Society of America*, *55*(1), 196–198. https://doi.org/10.1121/1.1928152

Bennett, C. L., Davis, R. T., & Miller, J. M. (1983). Demonstration of Presbycusis Across Repeated Measures in a Nonhuman Primate Species. *Behavioral Neuroscience*, *97*(4), 602–607.

Berger, M., Calapai, A., Stephan, V., Niessing, M., Burchardt, L., Gail, A., & Treue, S. (2018). Standardized automated training of rhesus monkeys for neuroscience research in their housing environment. *Journal of Neurophysiology*, *119*(3), 796–807. https://doi.org/10.1152/jn.00614.2017

Bernard, A., Lubbers, L. S., Tanis, K. Q., Luo, R., Podtelezhnikov, A. A., Finney, E. M., … Lein, E. (2012). Transcriptional Architecture of the Primate Neocortex. *Neuron*, *73*(6), 1083–1099. https://doi.org/10.1016/j.neuron.2012.03.002

Bharadwaj, H. M., Mai, A. R., Simpson, J. M., Choi, I., Heinz, M. G., & Shinn-Cunningham, B. G. (2019). Non-Invasive Assays of Cochlear Synaptopathy -- Candidates and Considerations. *BioRxiv*. https://doi.org/10.1101/565655

Bohlen, P., Dylla, M., Timms, C., & Ramachandran, R. (2014). Detection of Modulated Tones in Modulated Noise by Non-human Primates. *Journal of the Association for Research in Otolaryngology*, *15*(5), 801–821. https://doi.org/10.1007/s10162-014-0467-7

Bowl, M. R., & Brown, S. D. M. (2018). Genetic landscape of auditory dysfunction. *Human Molecular Genetics*, *27*(R2), R130–R135. https://doi.org/10.1093/hmg/ddy158

Breschi, A., Gingeras, T. R., & Guigó, R. (2017). Comparative transcriptomics in human and mouse. *Nature Reviews Genetics*, *18*(7), 425–440. https://doi.org/10.1038/nrg.2017.19

Brown, C., Beecher, M., Moody, D., & Stebbins, W. (1978). Localization of primate calls by old world monkeys. *Science*, *201*(4357), 753–754. https://doi.org/10.1126/science.97785

Brown, C. H., Beecher, M. D., Moody, D. B., & Stebbins, W. C. (1978). Localization of pure tones by Old World monkeys. *The Journal of the Acoustical Society of America*, *63*(5), 1484–1492. https://doi.org/10.1121/1.381842

Brown, C. H., Beecher, M. D., Moody, D. B., & Stebbins, W. C. (1980). Localization of noise bands by Old World monkeys. *The Journal of the Acoustical Society of America*, *68*(1), 127–132. https://doi.org/10.1121/1.384638

Burns, J. C., Kelly, M. C., Hoa, M., Morell, R. J., & Kelley, M. W. (2015). Single-cell RNA-Seq resolves cellular complexity in sensory organs from the neonatal inner ear. *Nature Communications*, *6*, 8557. https://doi.org/10.1038/ncomms9557

Burton, J. A., Dylla, M. E., & Ramachandran, R. (2018). Frequency selectivity in macaque monkeys measured using a notched-noise method. *Hearing Research*, *357*, 73–80. https://doi.org/10.1016/j.heares.2017.11.012

Cai, T., Jen, H.-I., Kang, H., Klisch, T. J., Zoghbi, H. Y., & Groves, A. K. (2015). Characterization of the Transcriptome of Nascent Hair Cells and Identification of Direct Targets of the Atoh1 Transcription Factor. *Journal of Neuroscience*, *35*(14), 5870–5883. https://doi.org/10.1523/JNEUROSCI.5083-14.2015

Calapai, A., Berger, M., Niessing, M., Heisig, K., Brockhausen, R., Treue, S., & Gail, A. (2017). A cage-based training, cognitive testing and enrichment system optimized for rhesus macaques in neuroscience research. *Behavior Research Methods*, *49*(1), 35–45. https://doi.org/10.3758/s13428-016-0707-3

Chen, H., Xing, Y., Xia, L., Chen, Z., Yin, S., & Wang, J. (2018). AAV-mediated NT-3 overexpression protects cochleae against noise-induced synaptopathy. *Gene Therapy*, *25*(4), 251–259. https://doi.org/10.1038/s41434-018-0012-0

Chen, W., Xia, X., Song, N., Wang, Y., Zhu, H., Deng, W., … Qin, C. (2016). Cross-Species Analysis of Gene Expression and Function in Prefrontal Cortex, Hippocampus and Striatum. *PLOS ONE*, *11*(10), e0164295. https://doi.org/10.1371/journal.pone.0164295

Chien, W. W., Monzack, E. L., McDougald, D. S., & Cunningham, L. L. (2015). Gene Therapy for Sensorineural Hearing Loss: *Ear and Hearing*, *36*(1), 1–7. https://doi.org/10.1097/AUD.0000000000000088

Christison-Lagay, K. L., & Cohen, Y. E. (2014). Behavioral correlates of auditory streaming in rhesus macaques. *Hearing Research*, *309*, 17–25. https://doi.org/10.1016/j.heares.2013.11.001

Clark, W. W., & Bohne, B. A. (1978). Animal Model for the 4-kHz Tonal Dip. *Annals of Otology, Rhinology & Laryngology*, *87*(4_suppl), 1–16. https://doi.org/10.1177/00034894780870S401

Cody, A. R., & Robertson, D. (1983). Variability of noise-induced damage in the guinea pig cochlea: Electrophysiological and morphological correlates after strictly controlled exposures. *Hearing Research*, *9*, 55–70.

Coleman, M. N. (2009). What do primates hear? A meta-analysis of all known nonhuman primate behavioral audiograms. *Int J Primatol*, *30*, 55–91.

Coleman, M. N., & Colbert, M. W. (2010). Correlations between auditory structures and hearing sensitivity in non-human primates. *Journal of Morphology*, *271*, 511–532. https://doi.org/10.1002/jmor.10814

Dai, C., Fridman, G. Y., & Della Santina, C. C. (2011). Effects of vestibular prosthesis electrode implantation and stimulation on hearing in rhesus monkeys. *Hearing Research*, *277*(1–2), 204–210. https://doi.org/10.1016/j.heares.2010.12.021

Dai, C., Lehar, M., Sun, D. Q., Rvt, L. S., Carey, J. P., MacLachlan, T., … Della Santina, C. C. (2017). Rhesus Cochlear and Vestibular Functions Are Preserved After Inner Ear Injection of Saline Volume Sufficient for Gene Therapy Delivery. *Journal of the Association for Research in Otolaryngology*, *18*(4), 601–617. https://doi.org/10.1007/s10162-017-0628-6

Davis, H., Morgan, C. T., Hawkins, J. E., Galambos, R., & Smith, F. W. (1950). Temporary deafness following exposure to loud tones and noise. *Acta Oto-Laryngologica*, *88*(Suppl), 19–21.

Davis, Hallowell. (1957). Biophysics and Physiology of the Inner Ear. *Physiological Reviews*, *37*(1), 1–49. https://doi.org/10.1152/physrev.1957.37.1.1

Dobie, R. A., & Humes, L. E. (2017). Commentary on the regulatory implications of noise-induced cochlear neuropathy. *International Journal of Audiology*, *56*(sup1), 74–78. https://doi.org/10.1080/14992027.2016.1255359

Dou, H., Finberg, K., Cardell, E. L., Lifton, R., & Choo, D. (2003). Mice lacking the B1 subunit of H+-ATPase have normal hearing. *Hearing Research*, *180*(1–2), 76–84. https://doi.org/10.1016/S0378-5955(03)00108-4

Downer, J. D., Rapone, B., Verhein, J., O'Connor, K. N., & Sutter, M. L. (2017). Feature-Selective Attention Adaptively Shifts Noise Correlations in Primary Auditory Cortex. *The Journal of Neuroscience*, *37*(21), 5378–5392. https://doi.org/10.1523/JNEUROSCI.3169-16.2017

Drescher, D. G., & Eldredge, D. H. (1974). Species differences in cochlear fatigue related to acoustics of outer and middle ears of guinea pig and chinchilla. *The Journal of the Acoustical Society of America*, *56*(3), 929–934. https://doi.org/10.1121/1.1903350

Du, X., Cai, Q., West, M. B., Youm, I., Huang, X., Li, W., … Kopke, R. D. (2018). Regeneration of Cochlear Hair Cells and Hearing Recovery through Hes1 Modulation

with siRNA Nanoparticles in Adult Guinea Pigs. *Molecular Therapy*, *26*(5), 1313–1326. https://doi.org/10.1016/j.ymthe.2018.03.004

Dylla, M., Hrnicek, A., Rice, C., & Ramachandran, R. (2013). Detection of Tones and Their Modification by Noise in Nonhuman Primates. *Journal of the Association for Research in Otolaryngology*, *14*(4), 547–560. https://doi.org/10.1007/s10162-013-0384-1

Ekdale, E. G. (2013). Comparative Anatomy of the Bony Labyrinth (Inner Ear) of Placental Mammals. *PLOS ONE*, *8*(6), e66624. https://doi.org/10.1371/journal.pone.0066624

El Kechai, N., Agnely, F., Mamelle, E., Nguyen, Y., Ferrary, E., & Bochot, A. (2015). Recent advances in local drug delivery to the inner ear. *International Journal of Pharmaceutics*, *494*(1), 83–101. https://doi.org/10.1016/j.ijpharm.2015.08.015

Espeland, E. M., Tsai, C.-W., Larsen, J., & Disbrow, G. L. (2018). Safeguarding against Ebola: Vaccines and therapeutics to be stockpiled for future outbreaks. *PLoS Neglected Tropical Diseases*, *12*(4), e0006275. https://doi.org/10.1371/journal.pntd.0006275

Felix, H. (2002). Anatomical differences in the peripheral auditory system of mammals and man. *Advances in Oto-Rhino-Laryngology*, *59*, 1–10.

Fernandez, C. (1951). The innervation of the cochlea (guinea pig). *The Laryngoscope*, *61*(12), 1152–1172.

Fernandez, K. A., Jeffers, P. W. C., Lall, K., Liberman, M. C., & Kujawa, S. G. (2015). Aging after Noise Exposure: Acceleration of Cochlear Synaptopathy in "Recovered" Ears. *Journal of Neuroscience*, *35*(19), 7509–7520. https://doi.org/10.1523/JNEUROSCI.5138-14.2015

Fowler, C. G., Chiasson, K. B., Leslie, T. H., Thomas, D., Beasley, T. M., Kemnitz, J. W., & Weindruch, R. (2010). Auditory function in rhesus monkeys: Effects of aging and caloric restriction in the Wisconsin monkeys five years later. *Hearing Research*, *261*(1–2), 75–81. https://doi.org/10.1016/j.heares.2010.01.006

Fowler, C. G., Torre, P., & Kemnitz, J. W. (2002). Effects of caloric restriction and aging on the auditory function of rhesus monkeys (Macaca mulatta): The University of Wisconsin Study. *Hearing Research*, *169*, 24–35.

Frenzilli, G., Ryskalin, L., Ferrucci, M., Cantafora, E., Chelazzi, S., Giorgi, F. S., … Fornai, F. (2017). Loud Noise Exposure Produces DNA, Neurotransmitter and Morphological

Damage within Specific Brain Areas. *Frontiers in Neuroanatomy*, *11*. https://doi.org/10.3389/fnana.2017.00049

Fukui, H., & Raphael, Y. (2013). Gene therapy for the inner ear. *Hearing Research*, *297*, 99–105. https://doi.org/10.1016/j.heares.2012.11.017

Furman, A. C., Kujawa, S. G., & Liberman, M. C. (2013). Noise-induced cochlear neuropathy is selective for fibers with low spontaneous rates. *Journal of Neurophysiology*, *110*(3), 577–586. https://doi.org/10.1152/jn.00164.2013

Gao, G., Vandenberghe, L. H., Alvira, M. R., Lu, Y., Calcedo, R., Zhou, X., & Wilson, J. M. (2004). Clades of Adeno-Associated Viruses Are Widely Disseminated in Human Tissues. *Journal of Virology*, *78*(12), 6381–6388. https://doi.org/10.1128/JVI.78.12.6381-6388.2004

Gao, G.-P., Alvira, M. R., Wang, L., Calcedo, R., Johnston, J., & Wilson, J. M. (2002). Novel adeno-associated viruses from rhesus monkeys as vectors for human gene therapy. *Proceedings of the National Academy of Sciences*, *99*(18), 11854–11859. https://doi.org/10.1073/pnas.182412299

Gao, X., Tao, Y., Lamas, V., Huang, M., Yeh, W.-H., Pan, B., … Liu, D. R. (2018). Treatment of autosomal dominant hearing loss by in vivo delivery of genome editing agents. *Nature*, *553*(7687), 217–221. https://doi.org/10.1038/nature25164

Garner, J. P. (2014). The Significance of Meaning: Why Do Over 90% of Behavioral Neuroscience Results Fail to Translate to Humans, and What Can We Do to Fix It? *ILAR Journal*, *55*(3), 438–456. https://doi.org/10.1093/ilar/ilu047

Gates, H. W., Romba, J. J., & Martin, P. (1963). Response latencies in the rhesus monkey as a function of tone intensity. *U.S. Army Human Engineering Laboratories*, *Technical Memorandum 3-63*, 1–15. https://doi.org/10.21236/AD0647822

Géléoc, G. S. G., & Holt, J. R. (2014). Sound Strategies for Hearing Restoration. *Science*, *344*(6184), 1241062. https://doi.org/10.1126/science.1241062

Glueckert, R., Johnson Chacko, L., Rask-Andersen, H., Liu, W., Handschuh, S., & Schrott-Fischer, A. (2018). Anatomical basis of drug delivery to the inner ear. *Hearing Research*, *368*, 10–27. https://doi.org/10.1016/j.heares.2018.06.017

Gopen, Q., Rosowski, J. J., & Merchant, S. N. (1997). Anatomy of the normal human cochlear aqueduct with functional implications. *Hearing Research*, *107*(1–2), 9–22. https://doi.org/10.1016/S0378-5955(97)00017-8

Gourevitch, G. (1970). Detectability of tones in quiet and in noise by rats and monkeys. In W.C. Stebbins (Ed.), *Animal psychoacoustics: the design and conduct of sensory experiments.* (pp. 67–97). New York, NY: Appleton-Century-Crofts.

Grinn, S. K., Wiseman, K. B., Baker, J. A., & Le Prell, C. G. (2017). Hidden Hearing Loss? No Effect of Common Recreational Noise Exposure on Cochlear Nerve Response Amplitude in Humans. *Frontiers in Neuroscience*, *11*. https://doi.org/10.3389/fnins.2017.00465

Guo, Y., Zhang, P., Sheng, Q., Zhao, S., & Hackett, T. A. (2016). lncRNA expression in the auditory forebrain during postnatal development. *Gene*, *593*(1), 201–216. https://doi.org/10.1016/j.gene.2016.08.027

Hackett, T. A., Guo, Y., Clause, A., Hackett, N. J., Garbett, K., Zhang, P., … Mirnics, K. (2015). Transcriptional maturation of the mouse auditory forebrain. *BMC Genomics*, *16*(1). https://doi.org/10.1186/s12864-015-1709-8

Harada, T., & Tokuriki, M. (1997). Brain-stem auditory evoked potentials in the common marmoset (Callithrix jacchus). *Electroencephalography and Clinical Neurophysiology/Evoked Potentials Section*, *104*(1), 43–50. https://doi.org/10.1016/S0168-5597(96)96015-3

Harris, J. D. (1967). Relations Among Aftereffects of Acoustic Stimulation. *The Journal of the Acoustical Society of America*, *42*(6), 1306–1324. https://doi.org/10.1121/1.1910720

Hauser, S. N., Burton, J. A., Mercer, E. T., & Ramachandran, R. (2018). Effects of noise overexposure on tone detection in noise in nonhuman primates. *Hearing Research*, *357*, 33–45. https://doi.org/10.1016/j.heares.2017.11.004

Hawkins, J. E., Johnsson, L.-G., Stebbins, W. C., Moody, D. B., & Coombs, S. L. (1976). Hearing Loss and Cochlear Pathology in Monkeys After Noise Exposure. *Acta Oto-Laryngologica*, *81*(3–6), 337–343. https://doi.org/10.3109/00016487609119971

Hawkins, J. E., & Stevens, S. S. (1950). The Masking of Pure Tones and of Speech by White Noise. *The Journal of the Acoustical Society of America*, *22*(1), 6–13. https://doi.org/10.1121/1.1906581

Heffner, H. E., & Heffner, R. S. (1990). Effect of bilateral auditory cortex lesions on sound localization in Japanese macaques. *Journal of Neurophysiology*, *64*(3), 915–931. https://doi.org/10.1152/jn.1990.64.3.915

Heffner, H., & Heffner, R. (1984). Temporal lobe lesions and perception of species-specific vocalizations by macaques. *Science*, *226*(4670), 75–76. https://doi.org/10.1126/science.6474192

Heffner, H., & Masterton, B. (1975). Contribution of auditory cortex to sound localization in the monkey (Macaca mulatta). *Journal of Neurophysiology*, *38*(6), 1340–1358. https://doi.org/10.1152/jn.1975.38.6.1340

Heffner, Henry E, & Heffner, R. S. (2007). Hearing Ranges of Laboratory Animals. *Journal of the American Association for Laboratory Animal Science*, *46*(1), 20–22.

Heffner, R. S. (2004). Primate hearing from a mammalian perspective. *The Anatomical Record*, *281A*(1), 1111–1122. https://doi.org/10.1002/ar.a.20117

Henderson, D., Subramaniam, M., & Boettcher, F. (1993). Individual Susceptibility to Noise-Induced Hearing loss. *Ear and Hearing*, *14*(3), 152–168.

Heppner, D. G., Kemp, T. L., Martin, B. K., Ramsey, W. J., Nichols, R., Dasen, E. J., … Adams, M. (2017). Safety and immunogenicity of the rVSVΔG-ZEBOV-GP Ebola virus vaccine candidate in healthy adults: A phase 1b randomised, multicentre, double-blind, placebo-controlled, dose-response study. *The Lancet Infectious Diseases*, *17*(8), 854–866. https://doi.org/10.1016/S1473-3099(17)30313-4

Hickox, A. E., Larsen, E., Heinz, M. G., Shinobu, L., & Whitton, J. P. (2017). Translational issues in cochlear synaptopathy. *Hearing Research*, *349*, 164–171. https://doi.org/10.1016/j.heares.2016.12.010

Hienz, R. D., Turkkan, J. S., & Harris, A. H. (1982). Pure tone thresholds in the yellow baboon (Papio cynocephalus). *Hearing Research*, *8*(1), 71–75. https://doi.org/10.1016/0378-5955(82)90035-1

Hocherman, S., Benson, D. A., Goldstein, M. H., Heffner, H. E., & Hienz, R. D. (1976). Evoked unit activity in auditory cortex of monkeys performing a selective attention task. *Brain Research*, *117*(1), 51–68. https://doi.org/10.1016/0006-8993(76)90555-2

Hoffmann, T. J., Keats, B. J., Yoshikawa, N., Schaefer, C., Risch, N., & Lustig, L. R. (2016). A Large Genome-Wide Association Study of Age-Related Hearing Impairment Using

Electronic Health Records. *PLoS Genetics*, *12*(10). https://doi.org/10.1371/journal.pgen.1006371

Holt, J. R., & Vandenberghe, L. H. (2012). Gene Therapy for Deaf Mice Goes Viral. *Molecular Therapy*, *20*(10), 1836–1837. https://doi.org/10.1038/mt.2012.196

Hopp, S. L., Sinnott, J. M., Owren, M. J., & Petersen, M. R. (1992). Differential Sensitivity of Japanese Macaques (Macaca fuscata) and Humans (Homo sapiens) to Peak Position Along a Synthetic Coo Call Continuum. *Journal of Comparative Psychology*, *106*(2), 128–136.

Hosoya, M., Fujioka, M., Kobayashi, R., Okano, H., & Ogawa, K. (2016). Overlapping expression of anion exchangers in the cochlea of a non-human primate suggests functional compensation. *Neuroscience Research*, *110*, 1–10. https://doi.org/10.1016/j.neures.2016.04.002

Hosoya, M., Fujioka, M., Ogawa, K., & Okano, H. (2016). Distinct Expression Patterns Of Causative Genes Responsible For Hereditary Progressive Hearing Loss In Non-Human Primate Cochlea. *Scientific Reports*, *6*(1). https://doi.org/10.1038/srep22250

Hunter-Duvar, I. M., & Bredberg, G. (1974). Effects of intense auditory stimulation: Hearing losses and inner ear changes in the chinchilla. *The Journal of the Acoustical Society of America*, *55*(4), 795–801. https://doi.org/10.1121/1.1914602

Hunter-Duvar, I. M., & Elliott, D. N. (1972). Effects of Intense Auditory Stimulation: Hearing Losses and Inner Ear Changes in the Squirrel Monkey. *The Journal of the Acoustical Society of America*, *52*(4B), 1181–1192. https://doi.org/10.1121/1.1913230

Hunter-Duvar, I. M., & Elliott, D. N. (1973). Effects of intense auditory stimulation: Hearing losses and inner ear changes in the squirrel monkey. II. *The Journal of the Acoustical Society of America*, *54*(5), 1179–1183. https://doi.org/10.1121/1.1914364

Igarashi, M., Mauldin, L., & Jerger, J. (1979). Impedance Audiometry in the Squirrel Monkey: Effect of Transection of Crossed Olivocochlear Bundle. *Archives of Otolaryngology - Head and Neck Surgery*, *105*(5), 258–259. https://doi.org/10.1001/archotol.1979.00790170028007

Isgrig, K., & Chien, W. W. (2019). Surgical Methods for Inner Ear Gene Delivery in Neonatal Mouse. In F. P. Manfredsson & M. J. Benskey (Eds.), *Viral Vectors for Gene Therapy: Methods and Protocols* (pp. 221–226). https://doi.org/10.1007/978-1-4939-9065-8_13

Jerger, J., Mauldin, L., & Igarashi, M. (1978a). Impedance Audiometry in the Squirrel Monkey: Effect of Middle Ear Surgery. *Archives of Otolaryngology - Head and Neck Surgery*, *104*(4), 214–224. https://doi.org/10.1001/archotol.1978.00790040036008

Jerger, J., Mauldin, L., & Igarashi, M. (1978b). Impedance Audiometry in the Squirrel Monkey: Sensorineural Losses. *Archives of Otolaryngology - Head and Neck Surgery*, *104*(10), 559–563. https://doi.org/10.1001/archotol.1978.00790100013003

Jordan, V. M., Pinheiro, M. L., Chiba, K., & Jimenez, A. (1973). Cochlear pathology in monkeys exposed to impulse noise. *Acta Oto-Laryngologica*, *76*(sup312), 16–30. https://doi.org/10.3109/00016487309125497

Joris, P. X., Bergevin, C., Kalluri, R., Laughlin, M. M., Michelet, P., Heijden, M. van der, & Shera, C. A. (2011). Frequency selectivity in Old-World monkeys corroborates sharp cochlear tuning in humans. *Proceedings of the National Academy of Sciences*, *108*(42), 17516–17520. https://doi.org/10.1073/pnas.1105867108

Katsuki, Y., Suga, N., & Kanno, Y. (1962). Neural Mechanism of the Peripheral and Central Auditory System in Monkeys. *The Journal of the Acoustical Society of America*, *34*(9B), 1396–1410. https://doi.org/10.1121/1.1918357

Kim, M.-A., Ryu, N., Kim, H.-M., Kim, Y.-R., Lee, B., Kwon, T.-J., … Kim, U.-K. (2019). Targeted Gene Delivery into the Mammalian Inner Ear Using Synthetic Serotypes of Adeno-Associated Virus Vectors. *Molecular Therapy - Methods & Clinical Development*, *13*, 197–204. https://doi.org/10.1016/j.omtm.2019.01.002

Kimura, R. S. (1975). The ultrastructure of the organ of corti. *International Review of Cytology*, *42*, 173–222.

Kirk, E. C., & Gosselin-Ildari, A. D. (2009). Cochlear Labyrinth Volume and Hearing Abilities in Primates. *The Anatomical Record*, *292*(6), spc1–spc1. https://doi.org/10.1002/ar.20923

Klein, A. J., & Mills, J. H. (1981). Physiological and psychophysical measures from humans with temporary threshold shift. *The Journal of the Acoustical Society of America*, *70*(4), 1045–1053. https://doi.org/10.1121/1.386955

Knipper, M., Van Dijk, P., Nunes, I., Rüttiger, L., & Zimmermann, U. (2013). Advances in the neurobiology of hearing disorders: Recent developments regarding the basis of tinnitus and hyperacusis. *Progress in Neurobiology*, *111*, 17–33. https://doi.org/10.1016/j.pneurobio.2013.08.002

Kojima, S. (1990). Comparison of Auditory Functions in the Chimpanzee and Human. *Folia Primatologica*, *55*(2), 62–72. https://doi.org/10.1159/000156501

Konopka, G., & Geschwind, D. H. (2010). Human brain evolution: Harnessing the genomics (r)evolution to link genes, cognition, and behavior. *Neuron*, *68*(2), 231–244. https://doi.org/10.1016/j.neuron.2010.10.012

Köppl, C., Wilms, V., Russell, I. J., & Nothwang, H. G. (2018). Evolution of Endolymph Secretion and Endolymphatic Potential Generation in the Vertebrate Inner Ear. *Brain, Behavior and Evolution*, *92*(1–2), 1–31. https://doi.org/10.1159/000494050

Kraus, N., Smith, D. I., Reed, N. L., Willott, J., & Erwin, J. (1985). Auditory brainstem and middle latency responses in non-human primates. *Hearing Research*, *17*(3), 219–226. https://doi.org/10.1016/0378-5955(85)90066-8

Kujawa, S. G., & Liberman, M. C. (2009). Adding Insult to Injury: Cochlear Nerve Degeneration after "Temporary" Noise-Induced Hearing Loss. *Journal of Neuroscience*, *29*(45), 14077–14085. https://doi.org/10.1523/JNEUROSCI.2845-09.2009

Kumar, S., & Hedges, S. B. (1998). A molecular timescale for vertebrate evolution. *Nature*, *392*(6679), 917–920. https://doi.org/10.1038/31927

Lakatos, P., Musacchia, G., O'Connell, M. N., Falchier, A. Y., Javitt, D. C., & Schroeder, C. E. (2013). The spectrotemporal filter mechanism of auditory selective attention. *Neuron*, *77*(4), 750–761. https://doi.org/10.1016/j.neuron.2012.11.034

Lasky, R. E., Beach, K. E., & Laughlin, N. K. (2000). Immittance and Otoacoustic Emissions in Rhesus Monkeys and Humans. *International Journal of Audiology*, *39*(2), 61–69. https://doi.org/10.3109/00206090009073055

Lasky, R. E., Luck, M. L., Torre, P., & Laughlin, N. (2001). The effects of early lead exposure on auditory function in rhesus monkeys. *Neurotoxicology and Teratology*, *23*(6), 639–649. https://doi.org/10.1016/S0892-0362(01)00175-1

Lasky, R. E., Maier, M. M., Snodgrass, E. B., Laughlin, N. K., & Hecox, K. E. (1995). Auditory evoked brainstem and middle latency responses in Macaca mulatta and humans. *Hearing Research*, *89*(1–2), 212–225. https://doi.org/10.1016/0378-5955(95)00140-7

Lasky, R. E., Snodgrass, E. B., Laughlin, N. K., & Hecox, K. E. (1995). Distortion product otoacoustic emissions in Macaca mulatta and humans. *Hearing Research*, *89*(1–2), 35–51. https://doi.org/10.1016/0378-5955(95)00120-1

Lasky, R. E., Soto, A. A., Luck, M. L., & Laughlin, N. K. (1999). Otoacoustic emission, evoked potential, and behavioral auditory thresholds in the rhesus monkey (Macaca mulatta). *Hearing Research*, *136*(1–2), 35–43. https://doi.org/10.1016/S0378-5955(99)00100-8

Lavinsky, J., Ge, M., Crow, A. L., Pan, C., Wang, J., Salehi, P., … Friedman, R. A. (2016). The Genetic Architecture of Noise-Induced Hearing Loss: Evidence for a Gene-by-Environment Interaction. *G3: Genes|Genomes|Genetics*, *6*(10), 3219–3228. https://doi.org/10.1534/g3.116.032516

Le Prell, C. G., Dell, S., Hensley, B., Hall, J. W., Campbell, K. C. M., Antonelli, P. J., … Guire, K. (2012). Digital Music Exposure Reliably Induces Temporary Threshold Shift in Normal-Hearing Human Subjects. *Ear & Hearing*, *33*(6), 44–58.

Le Prell, C. G., & Moody, D. B. (1997). Perceptual salience of acoustic features of Japanese monkey coo calls. *Journal of Comparative Psychology*, *111*(3), 261–274.

Le Prell, C. G., Niemiec, A. J., & Moody, D. B. (2001). Macaque thresholds for detecting increases in intensity: Effects of formant structure. *Hearing Research*, *162*, 29–42.

Lemus, L., Hernández, A., & Romo, R. (2009). Neural codes for perceptual discrimination of acoustic flutter in the primate auditory cortex. *Proceedings of the National Academy of Sciences of the United States of America*, *106*(23), 9471–9476. https://doi.org/10.1073/pnas.0904066106

Liberman, M. (1982). Single-neuron labeling in the cat auditory nerve. *Science*, *216*(4551), 1239–1241. https://doi.org/10.1126/science.7079757

Liberman, M. C. (1978). Auditory-nerve response from cats raised in a low-noise chamber. *The Journal of the Acoustical Society of America*, *63*(2), 442–455. https://doi.org/10.1121/1.381736

Liberman, M. C., & Dodds, L. W. (1984). Single-neuron labeling and chronic cochlear pathology. III. Stereocilia damage and alterations of threshold tuning curves. *Hearing Research*, *16*(1), 55–74. https://doi.org/10.1016/0378-5955(84)90025-X

Liberman, M. C., Epstein, M. J., Cleveland, S. S., Wang, H., & Maison, S. F. (2016). Toward a Differential Diagnosis of Hidden Hearing Loss in Humans. *PLOS ONE*, *11*(9), e0162726. https://doi.org/10.1371/journal.pone.0162726

Lichtenhan, J. T., Hartsock, J., Dornhoffer, J. R., Donovan, K. M., & Salt, A. N. (2016). Drug delivery into the cochlear apex: Improved control to sequentially affect finely spaced

regions along the entire length of the cochlear spiral. *Journal of Neuroscience Methods*, *273*, 201–209. https://doi.org/10.1016/j.jneumeth.2016.08.005

Lonsbury-Martin, B. L., & Martin, G. K. (1981). Effects of moderately intense sound on auditory sensitivity in rhesus monkeys: Behavioral and neural observations. *Journal of Neurophysiology*, *46*(3), 563–586. https://doi.org/10.1152/jn.1981.46.3.563

Lonsbury-Martin, B. L., & Martin, G. K. (1988). Incidence of spontaneous otoacoustic emissions in macaque monkeys: A replication. *Hearing Research*, *34*(3), 313–317. https://doi.org/10.1016/0378-5955(88)90011-1

Lonsbury-Martin, B. L., Martin, G. K., & Bohne, B. A. (1987). Repeated TTS exposures in monkeys: Alterations in hearing, cochlear structure, and single-unit thresholds. *The Journal of the Acoustical Society of America*, *81*(5), 1507–1518. https://doi.org/10.1121/1.394503

Lonsbury-Martin, B. L., Martin, G. K., Probst, R., & Coats, A. C. (1988). Spontaneous otoacoustic emissions in a nonhuman primate. II. Cochlear anatomy. *Hearing Research*, *33*(1), 69–93. https://doi.org/10.1016/0378-5955(88)90021-4

Luz, G. A., & Hodge, D. C. (1971). Recovery from Impulse-Noise Induced TTS in Monkeys and Men: A Descriptive Model. *The Journal of the Acoustical Society of America*, *49*(6B), 1770–1777. https://doi.org/10.1121/1.1912580

Luz, G. A., & Lipscomb, D. M. (1973). Susceptibility to damage from impulse noise: Chinchilla versus man or monkey. *The Journal of the Acoustical Society of America*, *54*(6), 1750–1754. https://doi.org/10.1121/1.1914475

Luz, G. A., Mosko, J. D., Fletcher, J. L., & Fravel, W. J. (1973). The relation between temporary threshold shift and permanent threshold shift in rhesus monkeys exposed to impulse noise. *Acta Oto-Laryngologica*, *76*(sup312), 5–15. https://doi.org/10.3109/00016487309125496

Maison, S. F., & Liberman, M. C. (2000). Predicting Vulnerability to Acoustic Injury with a Noninvasive Assay of Olivocochlear Reflex Strength. *The Journal of Neuroscience*, *20*(12), 4701–4707. https://doi.org/10.1523/JNEUROSCI.20-12-04701.2000

Maison, S. F., & Rauch, S. D. (2017). Ethical considerations in noise-induced hearing loss research. *The Lancet*, *390*(10098), 920–922. https://doi.org/10.1016/S0140-6736(17)31875-5

Makishima, T., Rodriguez, C. I., Robertson, N. G., Morton, C. C., Stewart, C. L., & Griffith, A. J. (2005). Targeted disruption of mouse Coch provides functional evidence that DFNA9 hearing loss is not a COCH haploinsufficiency disorder. *Human Genetics*, *118*(1), 29–34. https://doi.org/10.1007/s00439-005-0001-4

Mangham, C. A., & Miller, J. M. (1976). Effects of an experimental acoustic neurinoma on stapedius reflex activity. *The Journal of the Acoustical Society of America*, *60*(S1), S104–S105. https://doi.org/10.1121/1.2003060

Manohar, S., Ramchander, P. V., Salvi, R., & Seigel, G. M. (2019). Synaptic Reorganization Response in the Cochlear Nucleus Following Intense Noise Exposure. *Neuroscience*, *399*, 184–198. https://doi.org/10.1016/j.neuroscience.2018.12.023

Manohar, Senthilvelan, Jamesdaniel, S., Ding, D., Salvi, R., Seigel, G. M., & Roth, J. A. (2016). Quantitative PCR analysis and protein distribution of drug transporter genes in the rat cochlea. *Hearing Research*, *332*, 46–54. https://doi.org/10.1016/j.heares.2015.10.020

Marques-Bonet, T., Ryder, O. A., & Eichler, E. E. (2009). Sequencing Primate Genomes: What Have We Learned? *Annual Review of Genomics and Human Genetics*, *10*(1), 355–386. https://doi.org/10.1146/annurev.genom.9.081307.164420

Martin, G. K., Lonsbury-Martin, B. L., Probst, R., & Coats, A. C. (1985). Spontaneous otoacoustic emissions in the nonhuman primate: A survey. *Hearing Research*, *20*(1), 91–95. https://doi.org/10.1016/0378-5955(85)90062-0

Martin, G. K., Lonsbury-Martin, B. L., Probst, R., & Coats, A. C. (1988). Spontaneous otoacoustic emissions in a nonhuman primate. I. Basic features and relations to other emissions. *Hearing Research*, *33*(1), 49–68. https://doi.org/10.1016/0378-5955(88)90020-2

Martin, P., Romba, J. J., & Gates, H. W. (1962). A method for the study of hearing loss and recovery in rhesus monkeys. *U.S. Army Human Engineering Laboratories*, *Technical Memorandum 11-62*, 1–31.

Mashiko, H., Yoshida, A. C., Kikuchi, S. S., Niimi, K., Takahashi, E., Aruga, J., … Shimogori, T. (2012). Comparative Anatomy of Marmoset and Mouse Cortex from Genomic Expression. *Journal of Neuroscience*, *32*(15), 5039–5053. https://doi.org/10.1523/JNEUROSCI.4788-11.2012

Matsuzaki, S., Hosoya, M., Okano, H., Fujioka, M., & Ogawa, K. (2018). Expression pattern of EYA4 in the common marmoset (Callithrix jacchus) cochlea. *Neuroscience Letters*, *662*, 185–188. https://doi.org/10.1016/j.neulet.2017.10.030

May, B., Moody, D. B., & Stebbins, W. C. (1989). Categorical perception of conspecific communication sounds by Japanese macaques. *The Journal of the Acoustical Society of America*, *85*(2), 837–847. https://doi.org/10.1121/1.397555

May, B., Moody, D. B., Stebbins, W. C., & Norat, M. A. (1986). Sound localization of frequency-modulated sinusoids by Old World monkeys. *The Journal of the Acoustical Society of America*, *80*(3), 776–782. https://doi.org/10.1121/1.393952

McFadden, D., Pasanen, E. G., Raper, J., Lange, H. S., & Wallen, K. (2006). Sex differences in otoacoustic emissions measured in rhesus monkeys (Macaca mulatta). *Hormones and Behavior*, *50*(2), 274–284. https://doi.org/10.1016/j.yhbeh.2006.03.012

McGill, T. J. I., & Schuknecht, H. F. (1976). Human cochlear changes in noise induced hearing loss. *The Laryngoscope*, *86*(9), 1293–1302. https://doi.org/10.1288/00005537-197609000-00001

Mills, J. H., Adkins, W. Y., & Gilbert, R. M. (1981). Temporary threshold shifts produced by wideband noise. *The Journal of the Acoustical Society of America*, *70*(2), 390–396. https://doi.org/10.1121/1.386774

Mitchell, C., & Silver, D. L. (2018). Enhancing our brains: Genomic mechanisms underlying cortical evolution. *Seminars in Cell & Developmental Biology*, *76*, 23–32. https://doi.org/10.1016/j.semcdb.2017.08.045

Moody, D. B. (1994). Detection and discrimination of amplitude-modulated signals by macaque monkeys. *The Journal of the Acoustical Society of America*, *95*(6), 3499–3510. https://doi.org/10.1121/1.409967

Moody, D. B., Le Prell, C. G., & Niemiec, A. J. (1998). Monaural phase discrimination by macaque monkeys: Use of multiple cues. *The Journal of the Acoustical Society of America*, *103*(5), 2618–2623. https://doi.org/10.1121/1.422782

Moody, D. B., Stebbins, W. C., Hawkins, J. E., & Johnsson, L.-G. (1978). Hearing loss and cochlear pathology in the monkey (Macaca) following exposure to high levels of noise. *Archives of Oto-Rhino-Laryngology*, *220–220*(1–2), 47–72. https://doi.org/10.1007/BF00456301

Moody, D. B., Stebbins, W. C., & Iglauer, C. (1971). Auditory generalization gradients for response latency in the monkey. *Journal of the Experimental Analysis of Behavior*, *16*(1), 105–111.

Moody, D. B., Winger, G., Woods, J. H., & Stebbins, W. C. (1980). Effect of ethanol and of noise on reaction time in the monkey: Variation with stimulus level. *Psychopharmacology*, *69*(1), 45–51. https://doi.org/10.1007/BF00426520

Moore, B. C. J. (1996). Perceptual consequences of cochlear hearing loss and their implications for the design of hearing aids. *Ear and Hearing*, *17*(2), 133–161.

Mutai, H., Miya, F., Shibata, H., Yasutomi, Y., Tsunoda, T., & Matsunaga, T. (2018). Gene expression dataset for whole cochlea of Macaca fascicularis. *Scientific Reports*, *8*(1). https://doi.org/10.1038/s41598-018-33985-9

Myint, A., White, C. H., Ohmen, J. D., Li, X., Wang, J., Lavinsky, J., … Friedman, R. A. (2016). Large-scale Phenotyping of Noise-Induced Hearing Loss in 100 Strains of Mice. *Hearing Research*, *332*, 113–120. https://doi.org/10.1016/j.heares.2015.12.006

Nadol, J. B. (1983). Serial Section Reconstruction of the Neural Poles of Hair Cells in the Human Organ Of Corti. I. Inner Hair Cells. *The Laryngoscope*, *93*(5), 599–614. https://doi.org/10.1002/lary.1983.93.5.599

Nadol, J. B. (1988). Comparative anatomy of the cochlea and auditory nerve in mammals. *Hearing Research*, *34*(3), 253–266. https://doi.org/10.1016/0378-5955(88)90006-8

Ng, C.-W., Navarro, X., Engle, J. R., & Recanzone, G. H. (2015). Age-related changes of auditory brainstem responses in nonhuman primates. *Journal of Neurophysiology*, *114*(1), 455–467. https://doi.org/10.1152/jn.00663.2014

Ng, C.-W., Plakke, B., & Poremba, A. (2014). Neural correlates of auditory recognition memory in the primate dorsal temporal pole. *Journal of Neurophysiology*, *111*(3), 455–469. https://doi.org/10.1152/jn.00401.2012

Nielsen, D. W., Burnham, J., & Talley, C. (1978). Squirrel monkey temporary threshold shift from 48-h exposures to low-frequency noise. *The Journal of the Acoustical Society of America*, *64*(2), 478–484. https://doi.org/10.1121/1.382020

Nielsen, D. W., Franseen, L., & Fowler, D. (1984). The Effects of Interruption on Squirrel Monkey Temporary Threshold Shift to a 96-Hour Noise Exposure. *International Journal of Audiology*, *23*(3), 297–308. https://doi.org/10.3109/00206098409072841

Nomoto, M. (1980). Representation of Cochlear Innervation Patterns in Single Auditory Nerve Fiber Responses. *The Japanese Journal of Physiology*, *30*(1), 31–40. https://doi.org/10.2170/jjphysiol.30.31

Nomoto, M., Suga, N., & Katsuki, Y. (1964). Discharge pattern and inhibition of primary auditory nerve fibers in the monkey. *Journal of Neurophysiology*, *27*(5), 768–787.

O'Connor, K. N., Barruel, P., Hajalilou, R., & Sutter, M. L. (1999). Auditory temporal integration in the rhesus macaque (Macaca mulatta). *The Journal of the Acoustical Society of America*, *106*(2), 954–965. https://doi.org/10.1121/1.427108

O'Connor, K. N., Johnson, J. S., Niwa, M., Noriega, N. C., Marshall, E. A., & Sutter, M. L. (2011). Amplitude modulation detection as a function of modulation frequency and stimulus duration: Comparisons between macaques and humans. *Hearing Research*, *277*(1–2), 37–43. https://doi.org/10.1016/j.heares.2011.03.014

Osmanski, M. S., Song, X., Guo, Y., & Wang, X. (2016). Frequency discrimination in the common marmoset (Callithrix jacchus). *Hearing Research*, *341*, 1–8. https://doi.org/10.1016/j.heares.2016.07.006

Osmanski, M. S., & Wang, X. (2011). Measurement of absolute auditory thresholds in the common marmoset (Callithrix jacchus). *Hearing Research*, *277*(1–2), 127–133. https://doi.org/10.1016/j.heares.2011.02.001

Ota, C. Y., & Kimura, R. S. (1980). Ultrastructural study of the human spiral ganglion. *Acta Oto-Laryngologica*, *89*, 53–62.

Park, J. Y., Clark, W. W., Coticchia, J. M., Esselman, G. H., & Fredrickson, J. M. (1995). Distortion product otoacoustic emissions in rhesus (Macaca mulatta) monkey ears: Normative findings. *Hearing Research*, *86*(1–2), 147–162. https://doi.org/10.1016/0378-5955(95)00065-C

Perkins, R. E., & Morest, D. K. (1975). A study of cochlear innervation patterns in cats and rats with the Golgi method and Nomarski optics. *The Journal of Comparative Neurology*, *163*(2), 129–158. https://doi.org/10.1002/cne.901630202

Perlman, R. L. (2016). Mouse models of human disease. *Evolution, Medicine, and Public Health*, *2016*(1), 170–176. https://doi.org/10.1093/emph/eow014

Petersen, M., Beecher, M., Zoloth, Moody, D., & Stebbins, W. (1978). Neural lateralization of species-specific vocalizations by Japanese macaques (Macaca fuscata). *Science*, *202*(4365), 324–327. https://doi.org/10.1126/science.99817

Petersen-Jones, S. M., & Komáromy, A. M. (2015). Dog Models for Blinding Inherited Retinal Dystrophies. *Human Gene Therapy Clinical Development*, *26*(1), 15–26. https://doi.org/10.1089/humc.2014.155

Petkov, C. I., O'Connor, K. N., & Sutter, M. L. (2003). Illusory Sound Perception in Macaque Monkeys. *The Journal of Neuroscience*, *23*(27), 9155–9161. https://doi.org/10.1523/JNEUROSCI.23-27-09155.2003

Pfingst, B. E. (1993). Comparison of spectral and nonspectral frequency difference limens for human and nonhuman primates. *The Journal of the Acoustical Society of America*, *93*(4), 2124–2129. https://doi.org/10.1121/1.406673

Pfingst, B. E., Laycock, J., Flammino, F., Lonsbury-Martin, B., & Martin, G. (1978). Pure tone thresholds for the rhesus monkey. *Hearing Research*, *1*, 43–47.

Phillips, K. A., Bales, K. L., Capitanio, J. P., Conley, A., Czoty, P. W., 't Hart, B. A., … Voytko, M. L. (2014). Why primate models matter: Why Primate Models Matter. *American Journal of Primatology*, *76*(9), 801–827. https://doi.org/10.1002/ajp.22281

Pineda, J. A., Holmes, T. C., Swick, D., & Foote, S. L. (1989). Brain-stem auditory evoked potentials in squirrel monkey (Saimiri sciureus). *Electroencephalography and Clinical Neurophysiology*, *73*, 12.

Pinheiro, M., Jordan, V., & Luz, G. A. (1973). The relationship between permanent threshold shift and the loss of hair cells in monkeys exposed to impulse noise. *Acta Oto-Laryngologica*, *76*(sup312), 31–40. https://doi.org/10.3109/00016487309125498

Plum, A., Winterhager, E., Pesch, J., Lautermann, J., Hallas, G., Rosentreter, B., … Willecke, K. (2001). Connexin31-Deficiency in Mice Causes Transient Placental Dysmorphogenesis but Does Not Impair Hearing and Skin Differentiation. *Developmental Biology*, *231*(2), 334–347. https://doi.org/10.1006/dbio.2000.0148

Prosen, C. A., Moody, D. B., Sommers, M. S., & Stebbins, W. C. (1990). Frequency discrimination in the monkey. *The Journal of the Acoustical Society of America*, *88*(5), 2152–2158. https://doi.org/10.1121/1.400112

Prosen, Cynthia A., & Moody, D. B. (1995). Rise-time difference thresholds in the monkey. *The Journal of the Acoustical Society of America*, *97*(1), 697–700. https://doi.org/10.1121/1.413060

Pugh, J. E., Horwitz, M. R., & Anderson, D. J. (1974). Cochlear electrical activity in noise-induced hearing loss: Behavioral and electrophysiological studies in primates. *Archives of Otolaryngology*, *100*, 36–40.

Pugh, J. E., Horwitz, M. R., Anderson, D. J., & Singleton, E. F. (1973). A chronic implant for recording of cochlear potentials in primates. *American Journal of Physical Anthropology*, *38*(2), 351–355. https://doi.org/10.1002/ajpa.1330380232

Pugh, J. E., Moody, D. B., & Anderson, D. J. (1979). Electrocochleography and experimentally induced loudness recruitment. *Archives of Oto-Rhino-Laryngology*, *224*(3–4), 241–255. https://doi.org/10.1007/BF01108782

Rask-Andersen, H., Li, H., Löwenheim, H., Müller, M., Pfaller, K., Schrott-Fischer, A., & Glueckert, R. (2017). Supernumerary human hair cells—signs of regeneration or impaired development? A field emission scanning electron microscopy study. *Upsala Journal of Medical Sciences*, *122*(1), 11–19. https://doi.org/10.1080/03009734.2016.1271843

Rattay, F., Potrusil, T., Wenger, C., Wise, A. K., Glueckert, R., & Schrott-Fischer, A. (2013). Impact of Morphometry, Myelinization and Synaptic Current Strength on Spike Conduction in Human and Cat Spiral Ganglion Neurons. *PLOS ONE*, *8*(11), 1–17.

Raymond, L. A., Wallace, D., Berman, N. E., Marcario, J., Foresman, L., Joag, S. V., … Cheney, P. D. (1998). Auditory brainstem responses in a Rhesus Macaque model of neuro-AIDS. *Journal of Neurovirology*, *4*(5), 512–520. https://doi.org/10.3109/13550289809113495

Recanzone, G. H., Jenkins, W. M., Hradek, G. T., & Merzenich, M. M. (1991). A behavioral frequency discrimination paradigm for use in adult primates. *Behavior Research Methods, Instruments, &amp Computers*, *23*(3), 357–369. https://doi.org/10.3758/BF03203397

Rhesus Macaque Genome Sequencing and Analysis Consortium, Gibbs, R. A., Rogers, J., Katze, M. G., Bumgarner, R., Weinstock, G. M., … Zwieg, A. S. (2007). Evolutionary and Biomedical Insights from the Rhesus Macaque Genome. *Science*, *316*(5822), 222–234. https://doi.org/10.1126/science.1139247

Riazi, M., Marcario, J. K., Samson, F. K., Kenjale, H., Adany, I., Staggs, V., … Cheney, P. D. (2009). Rhesus Macaque Model of Chronic Opiate Dependence and Neuro-AIDS: Longitudinal Assessment of Auditory Brainstem Responses and Visual Evoked Potentials. *Journal of Neuroimmune Pharmacology*, *4*(2), 260–275. https://doi.org/10.1007/s11481-009-9149-3

Rocchi, F., Dylla, M. E., Bohlen, P. A., & Ramachandran, R. (2017). Spatial and temporal disparity in signals and maskers affects signal detection in non-human primates. *Hearing Research*, *344*, 1–12. https://doi.org/10.1016/j.heares.2016.10.013

Romba, J. J. (1962). The rhesus monkey in hearing loss research. *Report from the Eighth Annual Army Human Factors Engineering Conference*, 163–171.

Romba, J. J., & Gates, H. W. (1964). Hearing loss in the rhesus monkey after repeated exposures to identical noises. *U.S. Army Human Engineering Laboratories*, *Technical Memorandum 3-64*, 1–11.

Russell, S., Bennett, J., Wellman, J. A., Chung, D. C., Yu, Z.-F., Tillman, A., … Maguire, A. M. (2017). Efficacy and safety of voretigene neparvovec (AAV2-hRPE65v2) in patients with RPE65-mediated inherited retinal dystrophy: A randomised, controlled, open-label, phase 3 trial. *The Lancet*, *390*(10097), 849–860. https://doi.org/10.1016/S0140-6736(17)31868-8

Ryan, A., & Dallos, P. (1975). Effect of absence of cochlear outer hair cells on behavioural auditory threshold. *Nature*, *253*, 44–46.

Salt, Alec N., & Hirose, K. (2018). Communication pathways to and from the inner ear and their contributions to drug delivery. *Hearing Research*, *362*, 25–37. https://doi.org/10.1016/j.heares.2017.12.010

Salt, Alec N., & Plontke, S. K. (2018). Pharmacokinetic principles in the inner ear: Influence of drug properties on intratympanic applications. *Hearing Research*, *368*, 28–40. https://doi.org/10.1016/j.heares.2018.03.002

Salt, A.N., Hartsock, J. J., Gill, R. M., King, E., Kraus, F. B., & Plontke, S. K. (2016). Perilymph pharmacokinetics of locally-applied gentamicin in the guinea pig. *Hearing Research*, *342*, 101–111. https://doi.org/10.1016/j.heares.2016.10.003

Saunders, J. C., Dear, S. P., & Schneider, M. E. (1985). The anatomical consequences of acoustic injury: A review and tutorial. *The Journal of the Acoustical Society of America*, *78*(3), 833–860. https://doi.org/10.1121/1.392915

Scheib, B. T., Stebbins, W. C., & Moody, D. B. (1975). Temporary threshold shift in nonhuman primates resulting from chronic exposure to a 2-kHz octave band of noise. *The Journal of the Acoustical Society of America*, *57*(S1), S41–S41. https://doi.org/10.1121/1.1995227

Scheib, B. T., Stebbins, W. C., Moody, D. B., Johnsson, L. -G., & Muraski, A. A. (1975). Auditory threshold shift in nonhuman primates chronically exposed to low-level noise. *The Journal of the Acoustical Society of America*, *58*(S1), S89–S90. https://doi.org/10.1121/1.2002379

Schrauwen, I., Hasin-Brumshtein, Y., Corneveaux, J. J., Ohmen, J., White, C., Allen, A. N., … Friedman, R. A. (2016). A comprehensive catalogue of the coding and non-coding transcripts of the human inner ear. *Hearing Research*, *333*, 266–274. https://doi.org/10.1016/j.heares.2015.08.013

Scott, B. H., Mishkin, M., & Yin, P. (2012). Monkeys have a limited form of short-term memory in audition. *Proceedings of the National Academy of Sciences*, *109*(30), 12237–12241. https://doi.org/10.1073/pnas.1209685109

Seiden, H. R. (1957). *Auditory Acuity of the Marmoset Monkey (Hapale jacchus).*

Serafin, J. V., Moody, D. B., & Stebbins, W. C. (1982). Frequency selectivity of the monkey's auditory system: Psychophysical tuning curves. *The Journal of the Acoustical Society of America*, *71*(6), 1513–1518. https://doi.org/10.1121/1.387851

Shepherd, R. K., Xu, S. A., & Clark, G. M. (1994). Partial hearing loss in the macaque following the co-administration of kanamycin and ethacrynic acid. *Hearing Research*, *72*(1–2), 89–98. https://doi.org/10.1016/0378-5955(94)90209-7

Sinnott, J. M., Beecher, M. D., Moody, D. B., & Stebbins, W. C. (1976). Speech sound discrimination by monkeys and humans. *The Journal of the Acoustical Society of America*, *60*(3), 687–695. https://doi.org/10.1121/1.381140

Sinnott, Joan M. (1989). Detection and discrimination of synthetic English vowels by Old World monkeys (*C e r c o p i t h e c u s* , *M a c a c a*) and humans. *The Journal of the Acoustical Society of America*, *86*(2), 557–565. https://doi.org/10.1121/1.398235

Sinnott, Joan M., & Brown, C. H. (1993a). Effects of varying signal and noise levels on pure-tone frequency discrimination in humans and monkeys. *The Journal of the Acoustical Society of America*, *93*(3), 1535–1540. https://doi.org/10.1121/1.406811

Sinnott, Joan M., & Brown, C. H. (1993b). Effects of varying signal duration on pure-tone frequency discrimination in humans and monkeys. *The Journal of the Acoustical Society of America*, *93*(3), 1541–1546. https://doi.org/10.1121/1.406812

Sinnott, Joan M., Petersen, M. R., & Hopp, S. L. (1985). Frequency and intensity discrimination in humans and monkeys. *The Journal of the Acoustical Society of America*, *78*(6), 1977–1985. https://doi.org/10.1121/1.392654

Sinnott, Joan M., Powell, L. A., & Camchong, J. (2006). Using monkeys to explore perceptual "loss" versus "learning" models in English and Spanish voice-onset-time perception. *The Journal of the Acoustical Society of America*, *119*(3), 1585–1596. https://doi.org/10.1121/1.2162440

Sivian, L. J., & White, S. D. (1933). On minimum audible sound fields. *The Journal of the Acoustical Society of America*, *4*, 288–321.

Sliwinska-Kowalska, M., & Pawelczyk, M. (2013). Contribution of genetic factors to noise-induced hearing loss: A human studies review. *Mutation Research/Reviews in Mutation Research*, *752*(1), 61–65. https://doi.org/10.1016/j.mrrev.2012.11.001

Sly, D. J., Campbell, L., Uschakov, A., Saief, S. T., Lam, M., & O'Leary, S. J. (2016). Applying Neurotrophins to the Round Window Rescues Auditory Function and Reduces Inner Hair Cell Synaptopathy After Noise-induced Hearing Loss: *Otology & Neurotology*, *37*(9), 1223–1230. https://doi.org/10.1097/MAO.0000000000001191

Sommers, M. S., Moody, D. B., Prosen, C. A., & Stebbins, W. C. (1992). Formant frequency discrimination by Japanese macaques (Macaca fuscata). *The Journal of the Acoustical Society of America*, *91*(6), 3499–3510. https://doi.org/10.1121/1.402839

Song, Q., Shen, P., Li, X., Shi, L., Liu, L., Wang, J., … Wang, J. (2016). Coding deficits in hidden hearing loss induced by noise: The nature and impacts. *Scientific Reports*, *6*(1). https://doi.org/10.1038/srep25200

Sousa, A. M. M., Meyer, K. A., Santpere, G., Gulden, F. O., & Sestan, N. (2017). Evolution of the Human Nervous System Function, Structure, and Development. *Cell*, *170*(2), 226–247. https://doi.org/10.1016/j.cell.2017.06.036

Spankovich, C., Griffiths, S. K., Lobariñas, E., Morgenstein, K. E., de la Calle, S., Ledon, V., … Le Prell, C. G. (2014). Temporary threshold shift after impulse-noise during video game play: Laboratory data. *International Journal of Audiology*, *53*(sup2), S53–S65. https://doi.org/10.3109/14992027.2013.865844

Starr, A., Picton, T. W., Sininger, Y., Hood, L. J., & Berlin, C. I. (1996). Auditory neuropathy. *Brain*, *119*, 741–753.

Stebbins, William C. (1966). Auditory reaction time and the derivation of equal loudness contours for the monkey. *Journal of the Experimental Analysis of Behavior*, *9*(2), 135–142.

Stebbins, William C. (1973). Hearing of old world monkeys (Cercopithecinae). *American Journal of Physical Anthropology*, *38*(2), 357–364. https://doi.org/10.1002/ajpa.1330380233

Stebbins, William C., Hawkins, J. E., Johnsson, L.-G., & Moody, D. B. (1979). Hearing thresholds with outer and inner hair cell loss. *American Journal of Otolaryngology*, *1*(1), 15–27. https://doi.org/10.1016/S0196-0709(79)80004-6

Stebbins, William C., & Miller, J. M. (1964). Reaction time as a function of stimulus intensity for the monkey. *Journal of the Experimental Analysis of Behavior*, *7*(4), 309–312.

Stebbins, William C., Miller, J. M., Johnsson, L.-G., & Hawkins, J. E. (1969). Ototoxic Hearing Loss and Cochlear Pathology in the Monkey. *Annals of Otology, Rhinology & Laryngology*, *78*(5), 1007–1025. https://doi.org/10.1177/000348946907800508

Sun, W., Zhang, L., Lu, J., Yang, G., Laundrie, E., & Salvi, R. (2008). Noise Exposure Induced Enhancement of Auditory Cortex Response and Changes in Gene Expression. *Neuroscience*, *156*(2), 374–380. https://doi.org/10.1016/j.neuroscience.2008.07.040

Suzuki, J., Corfas, G., & Liberman, M. C. (2016). Round-window delivery of neurotrophin 3 regenerates cochlear synapses after acoustic overexposure. *Scientific Reports*, *6*(1). https://doi.org/10.1038/srep24907

Suzuki, J., Hashimoto, K., Xiao, R., Vandenberghe, L. H., & Liberman, M. C. (2017). Cochlear gene therapy with ancestral AAV in adult mice: Complete transduction of inner hair cells without cochlear dysfunction. *Scientific Reports*, *7*(1). https://doi.org/10.1038/srep45524

Suzuki, S., Suzuki, N., Mori, J.-I., Oshima, A., Usami, S., & Hashizume, K. (2007). micro-Crystallin as an intracellular 3,5,3'-triiodothyronine holder in vivo. *Molecular Endocrinology (Baltimore, Md.)*, *21*(4), 885–894. https://doi.org/10.1210/me.2006-0403

Thompson, G. C., Stach, B. A., & Jerger, J. F. (1984). Effect of Ketamine on the Stapedius Reflex in the Squirrel Monkey. *Archives of Otolaryngology - Head and Neck Surgery*, *110*(1), 22–24. https://doi.org/10.1001/archotol.1984.00800270026007

Tomlinson, R. W. W., & Schwarz, D. W. F. (1988). Perception of the missing fundamental in nonhuman primates. *The Journal of the Acoustical Society of America*, *84*(2), 560–565. https://doi.org/10.1121/1.396833

Torre, P., & Fowler, C. G. (2000). Age-related changes in auditory function of rhesus monkeys (Macaca mulatta). *Hearing Research*, *142*(1–2), 131–140. https://doi.org/10.1016/S0378-5955(00)00025-3

Tsunada, J., Liu, A. S. K., Gold, J. I., & Cohen, Y. E. (2016). Causal contribution of primate auditory cortex to auditory perceptual decision-making. *Nature Neuroscience*, *19*(1), 135–142. https://doi.org/10.1038/nn.4195

Valero, M.D., Burton, J. A., Hauser, S. N., Hackett, T. A., Ramachandran, R., & Liberman, M. C. (2017). Noise-induced cochlear synaptopathy in rhesus monkeys (Macaca mulatta). *Hearing Research*, *353*, 213–223. https://doi.org/10.1016/j.heares.2017.07.003

Valero, Michelle D., Hancock, K. E., & Liberman, M. C. (2016). The middle ear muscle reflex in the diagnosis of cochlear neuropathy. *Hearing Research*, *332*, 29–38. https://doi.org/10.1016/j.heares.2015.11.005

Valero, Michelle D., Hancock, K. E., Maison, S. F., & Liberman, M. C. (2018). Effects of cochlear synaptopathy on middle-ear muscle reflexes in unanesthetized mice. *Hearing Research*, *363*, 109–118. https://doi.org/10.1016/j.heares.2018.03.012

Van Laer, L., Carlsson, P.-I., Ottschytsch, N., Bondeson, M.-L., Konings, A., Vandevelde, A., … Camp, G. V. (2006). The contribution of genes involved in potassium-recycling in the inner ear to noise-induced hearing loss. *Human Mutation*, *27*(8), 786–795. https://doi.org/10.1002/humu.20360

Van Laer, L., Pfister, M., Thys, S., Vrijens, K., Mueller, M., Umans, L., … Van Camp, G. (2005). Mice lacking Dfna5 show a diverging number of cochlear fourth row outer hair

cells. *Neurobiology of Disease*, *19*(3), 386–399. https://doi.org/10.1016/j.nbd.2005.01.019

Verschooten, E., Desloovere, C., & Joris, P. X. (2018). High-resolution frequency tuning but not temporal coding in the human cochlea. *PLOS Biology*, *16*(10), e2005164. https://doi.org/10.1371/journal.pbio.2005164

Wang, H., Zhao, H., Huang, X., Sun, K., & Feng, J. (2018). Comparative cochlear transcriptomics of echolocating bats provides new insights into different nervous activities of CF bat species. *Scientific Reports*, *8*(1). https://doi.org/10.1038/s41598-018-34333-7

Wang, L., Kempton, J. B., & Brigande, J. V. (2018). Gene Therapy in Mouse Models of Deafness and Balance Dysfunction. *Frontiers in Molecular Neuroscience*, *11*. https://doi.org/10.3389/fnmol.2018.00300

Wang, Y., Hirose, K., & Liberman, M. C. (2002). Dynamics of Noise-Induced Cellular Injury and Repair in the Mouse Cochlea. *Journal of the Association for Research in Otolaryngology*, *3*(3), 248–268. https://doi.org/10.1007/s101620020028

Ward, W. D. (1960). Recovery from High Values of Temporary Threshold Shift. *The Journal of the Acoustical Society of America*, *32*(4), 497–500. https://doi.org/10.1121/1.1908111

Ward, W. D., Glorig, A., & Sklar, D. L. (1959). Temporary Threshold Shift from Octave-Band Noise: Applications to Damage-Risk Criteria. *The Journal of the Acoustical Society of America*, *31*(4), 522–528. https://doi.org/10.1121/1.1907746

Wichmann, T., Bergman, H., & DeLong, M. R. (2018). Basal ganglia, movement disorders and deep brain stimulation: Advances made through non-human primate research. *Journal of Neural Transmission (Vienna, Austria: 1996)*, *125*(3), 419–430. https://doi.org/10.1007/s00702-017-1736-5

Wienicke, A., Hausler, U., & Jurgens, U. (2001). Auditory frequency discrimination in the squirrel monkey. *J Comp Physiol A*, *187*(3), 189–195. https://doi.org/10.1007/s003590100189

Wojtczak, M., Beim, J. A., & Oxenham, A. J. (2017). Weak Middle-Ear-Muscle Reflex in Humans with Noise-Induced Tinnitus and Normal Hearing May Reflect Cochlear Synaptopathy. *ENeuro*, *4*(6). https://doi.org/10.1523/ENEURO.0363-17.2017

Yankaskas, K., Hammill, T., Packer, M., & Zuo, J. (2017). Editorial: Auditory injury – A military perspective. *Hearing Research*, *349*, 1–3. https://doi.org/10.1016/j.heares.2017.04.010

Zeng, H., Shen, E. H., Hohmann, J. G., Oh, W. S., Bernard, A., Royall, J. J., … Jones, A. R. (2012). Large-scale cellular-resolution gene profiling in human neocortex reveals species-specific molecular signatures. *Cell*, *149*(2), 483–496. https://doi.org/10.1016/j.cell.2012.02.052

Zheng, F., & Zuo, J. (2017). Cochlear hair cell regeneration after noise-induced hearing loss: Does regeneration follow development? *Hearing Research*, *349*, 182–196. https://doi.org/10.1016/j.heares.2016.12.011

Zoloth, S., Petersen, M., Beecher, M., Green, S., Marler, P., Moody, D., & Stebbins, W. (1979). Species-specific perceptual processing of vocal sounds by monkeys. *Science*, *204*(4395), 870–873. https://doi.org/10.1126/science.108805

CHAPTER 2

Effects of noise-induced cochlear damage on auditory nerve encoding

This review was prepared in partial fulfillment of the Vanderbilt University Neuroscience Graduate Program qualifying examination. The review was written in 2018 and was published in *Vanderbilt Reviews Neuroscience* (2020, Vol. 12), the official open-access journal of the Vanderbilt Brain Institute. Minor revisions were made in this Chapter, per committee comments.

2.1 ABSTRACT

Exposure to loud sounds is one of the most common causes of hearing loss, affecting nearly one-fourth of adults in the United States. Depending on the intensity and duration of exposure, noise can damage various components of the inner ear, including inner or outer hair cells, hair cell stereocilia, or inner hair cell ribbon synapses. These anatomical disturbances lead to changes in the central auditory system that manifest as communication difficulties. Depending on the site of lesion, cochlear damage causes different changes in auditory nerve encoding and listening abilities. Identifying these unique deficit profiles will contribute to stronger clinical predictions of the severity and extent of cochlear damage and the particular site of lesion. These advances will play a vital role in identifying appropriate therapeutic recommendations for the prevention and treatment of noise-induced cochlear pathology. This review discusses cochlear anatomy and auditory nerve physiology in normal conditions and following noise-induced cochlear damage.

2.2 INTRODUCTION

Affecting over 60 million U.S. adults (Goman & Lin, 2016; Hoffman et al., 2017), hearing loss is a growing public health concern. Exposure to loud sounds is one of the most common causes of hearing loss. Depending on the intensity and duration of exposure, noise can temporarily or permanently damage delicate structures within the inner ear (Spoendlin & Brun, 1973). These anatomical disturbances lead to changes in the central auditory system that manifest as hearing difficulties (Furman et al., 2013; Ma & Young, 2006; Miller et al., 1997; Shaheen & Liberman, 2018; Wang et al., 2002). Hearing impairment can be extremely

detrimental to verbal communication, leading to increased listening effort, frustration among conversational partners, and social isolation. Some forms of hearing loss are manageable with standard audiologic rehabilitation devices, such as hearing aids or cochlear implants. However, many people with normal audiologic exams or mild losses not suitable for hearing aids (nearly two-thirds of Americans with hearing loss; Goman & Lin, 2016) still report significant hearing difficulties. Additionally, even patients who are considered successful hearing aid or cochlear implant users report significant difficulty listening in background noise.

While disruptions in any part of the auditory pathway can manifest in hearing difficulties, this review will focus on noise-induced cochlear injury. Damage to the cochlea propagates throughout the auditory system, leading to substantial changes in neuronal encoding of sound and auditory perception. These changes occur at every stage of the auditory system, from the auditory nerve through the auditory cortex and beyond. This review will focus on the first step beyond the cochlea – the auditory nerve. First, a brief overview of cochlear anatomy and function will be provided. Next, basic features of auditory nerve encoding will be described. This will be followed by a description of noise-induced cochlear damage and its consequences on auditory nerve encoding. Finally, the perceptual consequences of cochlear hearing loss will be briefly discussed.

The literature on auditory nerve encoding is vast, spanning over 75 years and 10,000 publications. An exhaustive review of this literature is beyond the scope of this paper and has already been completed by several authors in a variety of intellectual contexts (Heil & Peterson, 2015; Henry & Heinz, 2013; Kiang, 1965; Young, 2012). This review will provide a focused discussion of the relationship between cochlear anatomy and basic auditory nerve physiology, under normal conditions and following cochlear injury.

2.3 THE COCHLEA: A SOPHISTICATED BIOLOGICAL SOUND PROCESSOR

Sound transduction begins with sound pressure waves being funneled by the pinna into the external ear canal. The eardrum vibrates in response to the pressure waves, which in turn vibrates the three ossicles of the middle ear: the malleus, incus, and stapes. The stapes then transmits this mechanical vibration into a fluid shear in the inner ear organ of hearing: the cochlea.

The cochlea is a membranous, fluid-filled structure that transforms mechanical vibrations into electrical potentials for transmission to the brain. Located within the temporal bone, this delicate snail-shaped structure is comprised of three compartments – the scala tympani, scala media, and scala vestibuli – which are separated by two membranes – Reissner's membrane (RM) and the basilar membrane (BM). Housed within the scala media below RM and on top of the BM is the organ of Corti. Several cell types are situated on top of the BM with the tectorial membrane (TM) resting on top. These membranes run the length of the cochlear spiral with varying thickness and stiffness, generating a gradient of preferred vibration frequency. This gradient establishes the tonotopic organization of the cochlea, with high frequency sounds encoded toward the base and low frequency sounds encoded toward the apex.

Mammals have one row of inner hair cells (IHCs) and three rows of outer hair cells (OHCs) along the length of the organ of Corti, summing to approximately 3,000 IHCs and 10,000 OHCs per cochlea depending on the species. Much like the rods and cones of the retina, the IHCs and OHCs serve different roles in the cochlea (Ryan & Dallos, 1975). The OHCs are motile cells that serve as the cochlear amplifier, providing gain for low sounds by enhancing the vibration of the BM. The IHCs are sensory receptor cells that transduce vibrations of the BM to activate the auditory nerve to transmit information about sound to the brain. From this, it is clear that cochlear damage affecting the OHCs vs. the IHCs will manifest as distinct hearing pathologies.

IHCs and OHCs have apical stereocilia that contact the TM. When sound vibrates the BM, hair cells are pressed against the TM, causing the stereocilia to bend and open mechanically-gated ion channels. The fluid surrounding the organ of Corti, called the endolymph, has a high concentration of potassium (K+). When the ion channels open, K+ enters the hair cell and generates a graded electrical potential, stimulating the release of glutamate. This excitatory neurotransmission generates action potentials in the auditory nerve, thereby establishing the first neural code in the central auditory system.

2.4 THE AUDITORY NERVE: TRANSMITTING SOUND TO THE BRAIN

2.4.1 Auditory Nerve Anatomy

Arguably the most important step in the auditory pathway, the auditory nerve establishes the neural code of the auditory system. A branch of the vestibulocochlear cranial nerve VIII, the

auditory nerve is comprised of roughly 30,000 spiral ganglion cells, including afferents and efferents (Hinojosa et al., 1985; Nadol, 1988). These bipolar neurons have cell bodies housed in the modiolus of the cochlea and two axonal projections. The peripheral axons innervate the cochlear hair cells and the central axons project to the cochlear nucleus.

Afferent fibers can be classified as Type I or Type II auditory nerve fibers (ANFs). Type I ANFs are the primary fibers responsible for sound transmission to the brain and comprise approximately 90-95% of neurons in the auditory nerve (Young, 2012). In most mammals, Type I ANFs are myelinated, though human Type I ANFs are only myelinated on the axon and not the cell body (Nadol, 1988; Ota & Kimura, 1980; Rattay et al., 2013). The IHCs are innervated by approximately 10-30 ANFs, depending upon species and frequency place within the cochlea (Liberman, 2017). Each Type I ANF usually makes one synapse on one IHC, but ANF branching and innervation of 2-3 adjacent IHCs has been observed (Fernandez, 1951; Kimura, 1975; Liberman, 1982; Nadol, 1983; Perkins & Morest, 1975).

Type II ANFs are unmyelinated and smaller in diameter compared to Type I ANFs. Each Type II ANF synapses with several OHCs (mean 7, range 1-30, up to 100 in cats; Liberman & Simmons 1985; Weisz et al., 2012; M. Charles Liberman, personal communication). Type II fibers do not exhibit sound-evoked activity (Brown, 1994; Robertson, 1984), but can spike in response to broad OHC activation (Weisz et al., 2014). The role of Type II ANFs is poorly understood. Some evidence suggests these fibers may act as nociceptors during acoustic trauma and following cochlear damage (Flores et al., 2015; Liu et al., 2015; Weisz et al., 2021). One study suggested that Type II neurons activate the medial olivocochlear reflex for otoprotection (Froud et al., 2015), but this was disproven (Maison et al., 2016). The remainder of this review will focus on Type I ANFs.

IHCs and Type I ANFs are connected by a specialized synapse. Each IHC contains electron-dense presynaptic ribbons that serve as an anchor for synaptic vesicles (Nouvian et al., 2006). The ribbons are opposed by a postsynaptic density in the ANF that contains a localized patch of AMPA glutamate receptors (Liberman et al., 2011). The spatial concentration of synaptic vesicles and AMPA receptors allows for rapid neurotransmission while maintaining a large vesicular store. The ribbon synapse directly supports the high temporal precision necessary for many auditory system functions, such as temporal fine structure encoding and sound localization. Ribbon synapses vary in size along the IHC circumference, with larger and

narrower ribbons on the modiolar side and smaller and rounder ribbons on the pillar side (Liberman et al., 2011). The opposing ANFs also differ in diameter and *spontaneous firing rate* (SR), defining three main subclasses of Type I ANFs. ANFs with low spontaneous rates (LSR; <1 spike/sec) and medium spontaneous rates (MSR; 1-18 spikes/sec) have smaller diameters and innervate the larger modiolar synaptic ribbons (Liberman, 1982; Liberman, 2017; Merchan-Perez & Liberman, 1996). High spontaneous rate ANFs (HSR; >18 spikes/sec) have larger diameters and synapse with the smaller pillar ribbons.

2.4.2 Auditory Nerve Physiology

In addition to differences in size and innervation site, ANFs exhibit different sound-evoked response properties, which vary somewhat according to SR. Threshold tuning curves are used to identify several basic response properties of ANFs. Tones are played across a range of frequencies and intensities while spikes are recorded. The tuning curve is plotted as the lowest sound intensity that evokes a response for a given frequency. ANFs exhibit V-shaped tuning curves, with a tip of maximum sensitivity that is defined as the unit's *characteristic frequency* (CF) (Liberman, 1978). At each cochlear frequency place, and even within a given IHC, there is a somewhat uniform distribution of units from each SR class (Liberman, 1982; Liberman, 1978), though some species show a more unimodal distribution of SRs and fewer HSRs in the high frequencies (Huet et al., 2016; Taberner & Liberman, 2005). The lowest sound level at which an ANF responds to its CF is defined as the unit's *threshold*. Overall, SR is inversely correlated with CF threshold; LSR ANFs have higher thresholds and HSR ANFs have lower thresholds (Huet et al., 2016; Kiang et al., 1976; Liberman, 1978; Sumner & Palmer, 2012; Taberner & Liberman, 2005; Yates, 1991). However, it is important to note that thresholds vary by >50 dB SPL within a given SR class, especially for LSR ANFs (Huet et al., 2016; Liberman, 1978; Schmiedt, 1989).

The width of the tuning curve can be measured at a set intensity level above the threshold (e.g. 10 dB). The *tuning bandwidth* (e.g. Q10) is used to assess the frequency selectivity of the ANF. Tuning bandwidth increases linearly with increasing CF, while relative bandwidth decreases with increasing CF (Liberman, 1978). Tuning curve bandwidth is similar across SR classes for units of the same CF (Heil & Peterson, 2015; Kiang, 1965; Liberman, 1978).

Rate-level functions demonstrate the change in sound-evoked firing rate (e.g. to a CF tone or broadband noise) as a function of stimulus intensity. Firing rate increases monotonically with increasing sound level (Kiang, 1965). At high sound levels above the unit's threshold, HSR unit firing rates saturate and plateau, whereas LSR unit firing rates may continue to increase beyond the limits of the equipment (Heil & Peterson, 2015; Winter et al., 1990). Maximum ANF firing rate at saturation increases with increasing CF and typically does not exceed 300 spikes/second (Kiang, 1965; Liberman, 1978; Rose et al., 1971). The *dynamic range* of the rate-level function is related to SR; LSR ANFs have larger dynamic ranges and HSR ANFs have smaller dynamic ranges (Kiang, 1965; Liberman, 1978; Sumner & Palmer, 2012; Taberner & Liberman, 2005). In response to off-frequency (i.e. non-CF) stimuli, rate-level functions are shallower with higher thresholds.

ANFs can be further characterized according to their temporal firing properties. A peristimulus time histogram (PSTH) can be constructed by presenting several repetitions of the same stimulus and then binning and averaging the spiking responses. Termed a "primary-like response", the PSTH for most ANFs has a sharp onset response followed by an initial rapid (a few msec) and then slower (tens of msec) exponential decay to a constant, sustained firing rate (Galambos & Davis, 1943; Heil & Peterson, 2015; Kiang, 1965; Ruggero, 1992). The rate of decay is determined by stimulus characteristics and properties of IHC vesicle release at the synapse, a discussion of which is beyond the scope of this review and has been discussed elsewhere (Heil & Peterson, 2015). When recording PSTHs across multiple stimulus levels, first-spike latency decreases with increasing stimulus level and with increasing CF (due to signal propagation through the cochlear length) (Huet et al., 2016). LSR ANFs also exhibit longer first-spike latencies than HSR ANFs (Huet et al., 2016). For ANFs with a high probability of spiking at stimulus onset, the sharp onset peak is sometimes followed by a notch in the PSTH (called "primary-like with notch"), demonstrating the refractoriness of the fiber (Heil & Peterson, 2015; Ruggero, 1992). For ANFs with spontaneous activity, offset suppression is often noted following stimulus cessation (Heil & Peterson, 2015; Kiang, 1965; Ruggero, 1992).

ANF firing synchronizes to the phase of low-frequency tones and the envelope of complex stimuli, known as phase locking (Joris & Yin, 1992; Kiang, 1965; Rose et al., 1971). Depending on the species, ANFs can phase lock up to approximately 4000 Hz (Verschooten et al., 2018). Phase locking can be assessed by vector strength, or the firing rate as a function of the

stimulus phase (plotted as a period histogram). LSR fibers have greater vector strength than HSR fibers (Joris & Yin, 1992) and vector strength decreases with increasing modulation frequency up to the phase-locking limit (as demonstrated by modulation transfer functions) (Ruggero, 1992).

In the auditory nerve physiology literature, numerous studies have investigated responses to complex stimuli, such as tones in noise, harmonic complexes, vowels, and speech (Costalupes et al., 1984; Costalupes, 1985; Heinz, 2007; G. Le Prell et al., 1996; Rhode et al., 1978; Ruggero, 1973; Sinex & Geisler, 1984). One example is two-tone suppression, where an ANF's response to a tone can be suppressed by the presence of a second tone (Kiang, 1965). These complex, nonlinear response properties are certainly of interest in the context of cochlear pathology, as they are inevitably impacted by cochlear damage and have greater relevance to real-world listening environments. However, this review will focus on the effects of cochlear pathology on basic response properties, since these changes have been more thoroughly described (but see Miller et al., 1997).

There is rich literature describing both basic and complex auditory nerve response properties in detail in several common laboratory animals, including cats, guinea pigs, chinchillas, ferrets, gerbils, rats, and mice (Galambos & Davis, 1943; Heinz & Swaminathan, 2009; Huet et al., 2016; Kiang, 1965; Schmiedt, 1989; Sumner & Palmer, 2012; Taberner & Liberman, 2005; Tasaki, 1954; Zhang et al., 1990; Clock Eddins et al., 1998). Across these species, response properties are generally well-conserved and have served to define our understanding of the auditory nerve. Surprisingly few studies have investigated auditory nerve properties in phylogenetically similar model species, such as nonhuman primates (Joris et al., 2011; Katsuki et al., 1962; Nomoto, 1980; Nomoto et al., 1964; Verschooten et al., 2018). However, the limited data available suggest that monkeys starkly contradict the aforementioned assumptions demonstrated in other species. Nomoto et al. (1964) showed no relationship between SR and sound-evoked threshold or dynamic range for macaque monkeys. Data from squirrel monkeys also suggest a weak relationship between SR and threshold (Rose et al., 1971; Ruggero, 1973), but this was not explicitly evaluated. Macaque ANFs have sharper tuning curves (Joris et al., 2011) and a lower upper limit of phase locking (Verschooten et al., 2018) than other laboratory species. These contradictory findings beg further research in a phylogenetically-similar model species to better predict responses in the human auditory nerve.

2.5 NOISE EXPOSURE: DAMAGE TO THE AUDITORY PERIPHERY AND ITS CONSEQUENCES

Sensorineural hearing loss (SNHL) can be caused by exposure to loud sounds, aging, ototoxic drugs, congenital abnormalities, genetic mutations, immune or cardiovascular disorders, etc. The variety of mechanisms that can induce SNHL is indicative of the heterogeneity of the accompanying cochlear damage. Depending on the site of lesion and extent of damage, the degree and configuration of SNHL and its associated perceptual deficits can vary extensively. Histological corroboration of noise-induced cochlear pathologies is limited in humans. In this respect, animal models of noise-induced hearing loss are invaluable in developing our understanding of the peripheral and central consequences of this pathology. A variety of animals have been used to model noise-induced hearing loss, including mice (Kujawa & Liberman, 2009; Ohlemiller et al., 2000; Wang et al., 2002), guinea pigs (Drescher & Eldredge, 1974; Lurie et al., 1944; Spoendlin & Brun, 1973), chinchillas (Clark & Bohne, 1978; Dallos & Harris, 1978; Hunter-Duvar & Bredberg, 1974; Ward & Duvall, 1971), cats (Kiang et al., 1976; Miller et al., 1963), and nonhuman primates (Hunter-Duvar & Elliott, 1973; Moody et al., 1978; Romba & Gates, 1964; Valero et al., 2017). These studies developed sensitive and reliable methods to characterize hearing loss severity and anatomical damage secondary to noise exposure.

Noise exposure causes maximal cochlear damage at and above the frequency of noise exposure (Moody et al., 1978; although low frequency (<1kHz) exposures may behave differently). For narrowband noise or pure tones, peak damage typically occurs at a half octave above the frequency of the noise. For broadband noise exposures, peak damage typically occurs in the mid- to high-frequency region (due to a peak in the middle ear transfer function) (Moody et al., 1978). With longer durations or higher intensities of noise exposure, damage spreads toward the high frequencies and then the low frequencies. Cochlear damage secondary to noise exposure is thought to result from mechanical damage to the hair cells and glutamate excitotoxicity causing damage and eventual cell death in ANFs (reviewed in Pujol & Puel, 1999). OHC damage typically precedes IHC damage following noise exposure, indicating greater susceptibility of OHCs compared to IHCs (Clark & Bohne, 1978; Hawkins et al., 1976). OHC damage, including stereocilia damage or cell loss, results in decreased sensitivity and broader spectral tuning (Liberman & Dodds, 1984a, 1984b; Ryan & Dallos, 1975). In contrast,

IHC stereocilia damage leads to decreased sensitivity with preserved spectral tuning. Cochlear damage can also affect the stria vascularis, leading to a decrease in the endolymphatic K+ concentration and disrupting hair cell potentials (Young, 2012).

Recent work in animal models has expanded our understanding of noise-induced hearing pathology to include a previously unidentified class of cochlear damage, termed synaptopathy (Kujawa & Liberman, 2009). Following temporary noise-induced threshold shifts or in aging, animals exhibit isolated loss of IHC ribbon synapses and subsequent ANF degeneration without loss of IHCs or OHCs. Synapse loss is greater on the modiolar side of the IHC, leading to preferential degeneration of LSR ANFs (Furman et al., 2013; Song et al., 2016). Animals with synaptopathy have normal hearing sensitivity as assessed by ABR or behavioral hearing assessment, but a reduced response from the auditory nerve (Wave I of the ABR) (Kujawa & Liberman, 2009). Synaptopathy can also occur in combination with IHC or OHC loss associated with SNHL (Fernandez et al., 2015; Kujawa & Liberman, 2015; Valero et al., 2017).

Post-mortem studies of human temporal bones do show age-related loss of ribbon synapses and auditory nerve degeneration in the absence of hair cell loss (Viana et al., 2015; Wu et al., 2018). However, there is no evidence to date that humans suffer from noise-induced synaptopathy. Furthermore, while the predicted consequences of synaptopathy resemble those of common patient concerns, it is entirely unknown whether the speech-in-noise complaints of humans with normal hearing are related to a peripheral pathology (Guest et al., 2018; Hickox et al., 2017).

2.6 CONSEQUENCES OF COCHLEAR DAMAGE ON AUDITORY NERVE ENCODING

Noise exposures causing hair cell loss or synaptopathy disrupt neuronal encoding of sound in ANFs innervating the damaged cochlear regions. One goal for studies of auditory nerve encoding following cochlear pathology is to identify unique patterns of degraded response properties to predict the underlying cochlear damage and resulting perceptual deficits. Specifically, do hair cell loss and synapse loss produce different changes in the auditory nerve? Can we predict the integrity and site of lesion of the cochlea based on auditory nerve responses and associated perceptual deficits? The answers to these questions become relevant when

probing the relationship between sensory input and perceptual output – a mystery that has plagued scientists and philosophers for centuries.

Following noise-induced SNHL, ANFs exhibit decreased spontaneous and sound-evoked firing rates (Kale & Heinz, 2012; Liberman & Dodds, 1984a; Liberman & Kiang, 1984; Scheidt et al., 2010; Wang et al., 1997). IHC loss results in silencing of afferent neurons (i.e. no spontaneous or sound-evoked activity; Wang et al., 1997), whereas selective OHC loss or combined OHC and IHC loss result in elevated thresholds and broadened tuning curves (Evans, 1975; Heinz & Young, 2004; Liberman & Dodds, 1984b; Miller et al., 1997). Rate-level functions typically exhibit steeper slopes and compressed dynamic ranges secondary to elevated thresholds following OHC loss (Heinz & Young, 2004; Liberman & Kiang, 1984; Young, 2012).

SNHL also disrupts temporal coding in ANFs. Selective OHC loss does not affect first spike latency or PSTH shape (Dallos & Harris, 1978). However, combined OHC and IHC loss results in reduced first spike latency, increased onset response, faster onset adaptation, and slower recovery from adaptation (Scheidt et al., 2010). Impaired ANFs can phase-lock to the same range of modulation frequencies as normal ANFs (Kale & Heinz, 2012). Affected ANFs exhibit decreased synchronization to CF and broadband amplitude-modulated stimuli (Salvi, Henderson, et al., 1979), but enhanced synchronization to off-frequency components in complex stimuli due to broader spectral filters (Miller et al., 1997). Temporal fine structure coding is severely distorted in the presence of background noise (Henry & Heinz, 2013), but envelope coding is enhanced following SNHL (Henry et al., 2016; Kale & Heinz, 2012). In summary, SNHL alters both spectral and temporal aspects of suprathreshold auditory nerve encoding.

ANFs with CFs in the region of hair cell loss exhibit the greatest changes in neuronal encoding (Young, 2012). More specifically, greater threshold shifts and tuning curve bandwidths are observed at cochlear frequency places with the greatest amount of hair cell loss (Heinz & Young, 2004; Liberman, 1984; Liberman & Dodds, 1984b; Miller et al., 1997). However, the range of ANFs with elevated thresholds often exceeds the region of hair cell loss, suggesting that some encoding deficits may occur due to more subtle cochlear pathology (Liberman, 1984; Liberman & Kiang, 1978; Salvi et al., 1979). Similarly, behavioral thresholds are not well predicted by the cytocochleogram (Clark & Bohne, 1978; Hunter-Duvar & Bredberg, 1974; Hunter-Duvar & Elliott, 1972, 1973; Jordan et al., 1973; Lonsbury-Martin et al., 1987; Moody et al., 1978; Scheib et al., 1975). After chronic SNHL, fewer ANFs are encountered in the damaged

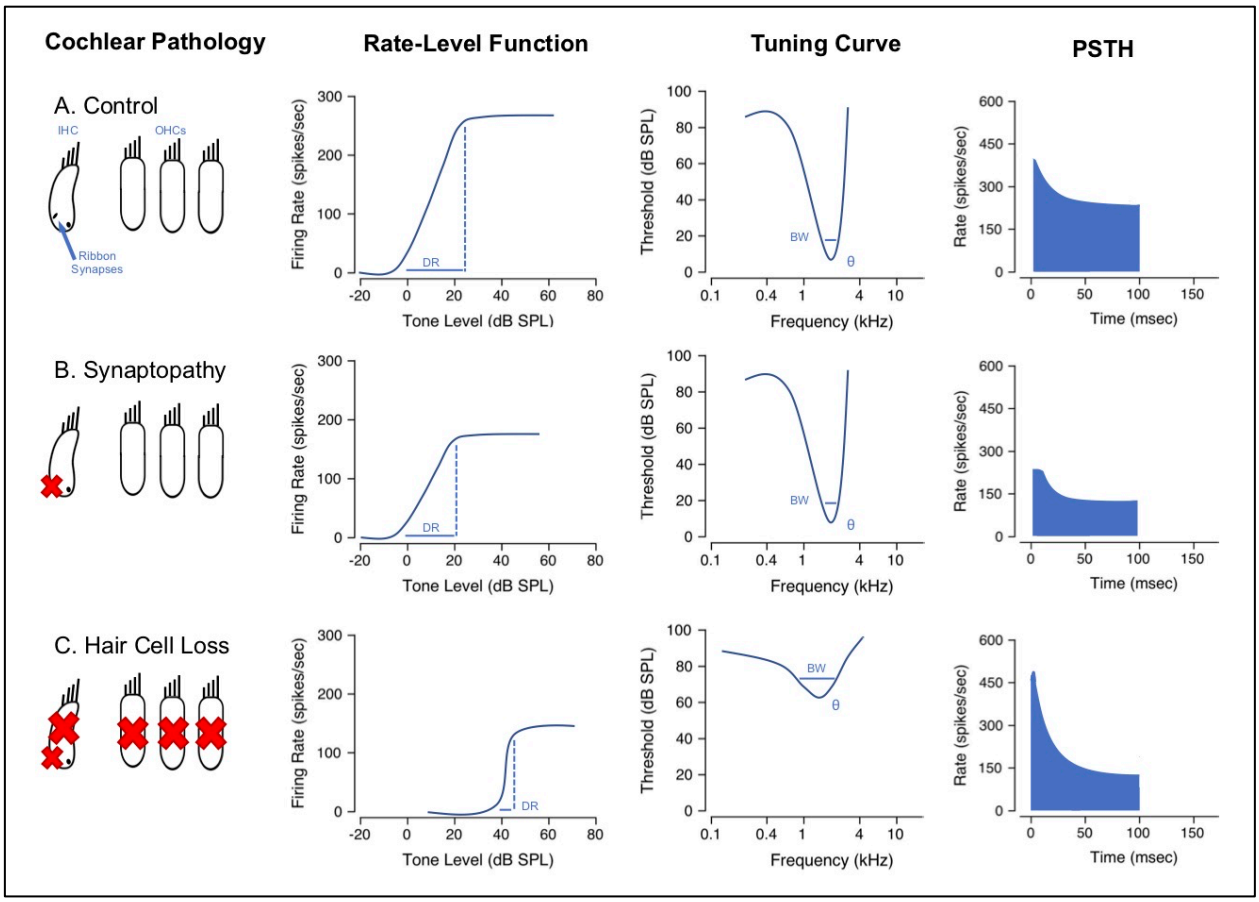

Figure 2.1 Cochlear pathology results in unique patterns of coding deficits for different sites of lesion. In comparison to control ears, synaptopathy results in loss of IHC ribbon synapses, especially on the modiolar side. Sensorineural hearing loss results in loss of IHCs, OHCs, and synapses. Following cochlear pathology, rate-level functions show changes in dynamic range and peak evoked firing rate. Tuning curves broaden and thresholds are elevated with OHC loss. PSTHs differ in mean and variability of first spike latency and sustained firing rate. PSTH = peristimulus time histogram; IHC = inner hair cell; OHC = outer hair cell; DR = dynamic range; BW = bandwidth; θ = threshold

frequency region, due to denervation and subsequent ANF degeneration (Liberman & Dodds, 1984a; Miller et al., 1997; Spoendlin, 1984). ANF degeneration occurs across all SR classes, leading to sparse coding across stimulus intensities (Dallos & Harris, 1978; Heil & Peterson, 2015; Liberman & Dodds, 1984a). ANFs originating from regions that are histologically normal may or may not exhibit changes to their response properties (Dallos & Harris, 1978; Liberman, 1984; Liberman & Kiang, 1978; Salvi et al., 1979).

Due to the relatively recent discovery of synaptopathy, there are very few studies investigating its effect on auditory nerve integrity. Despite the paucity of data, a few noteworthy trends are apparent. Noise-induced synaptopathy causes primary neural degeneration (i.e. progressive ANF loss) with a disproportionate loss of LSR fibers (Fernandez et al., 2015;

Furman et al., 2013; Kujawa & Liberman, 2006; Lin et al., 2011; Song et al., 2016; but see Suthakar & Liberman, 2021). Tuning curve bandwidths and thresholds remain normal for all ANFs (Furman et al., 2013). Rate-level function dynamic ranges and PSTH adaptation constants also remain normal following synapse loss (Furman et al., 2013). In one study, peak and total firing rates decreased and first spike latency was more variable (Song et al., 2016). Similar temporal encoding deficits have been observed in a mutant mouse model that lacks inner hair cell ribbon synapses (Buran et al., 2010). These changes in temporal coding integrity following synaptopathy may be a consequence of poorer neurotransmission efficiency and ANF denervation. However, another study found increased peak and sustained firing rates and decreased first spike latency jitter (Suthakar & Liberman 2021), which may be caused by enlargement of the remaining ribbons. Loss of ANFs may lead to stochastic undersampling of the stimulus and negatively impact perception (Lopez-Poveda, 2014).

Overall, synaptopathy and hair cell loss appear to have distinct patterns of degraded auditory nerve encoding (Figure 2.1). These effects predict different patterns of perceptual deficits. It is important to consider species differences in cochlear innervation and auditory nerve physiology when interpreting these data for translation to clinical populations.

2.7 CENTRAL AUDITORY PATHWAYS: BEYOND THE PERIPHERY

Downstream of the auditory nerve, central auditory brain structures process and transform the incoming information, ultimately resulting in auditory perception. However, if the incoming signal is degraded, the output of the system will also be degraded to some extent due to the propagation of the incoming encoding deficits. While auditory nerve encoding is significantly altered following cochlear damage, these deficits combine with changes to central processing to produce hearing difficulties. Compensatory mechanisms can help overcome some aspects of the degraded ANF signal. For example, in response to decreased peripheral input, central auditory neurons exhibit increased spontaneous and evoked firing rates secondary to reduced inhibitory neurotransmission (Cai et al., 2009; Chambers et al., 2016; Ma & Young, 2006; Mulders & Robertson, 2013; Noreña & Eggermont, 2003; Seki & Eggermont, 2003; Vogler et al., 2014; Wang et al., 2002). This phenomenon, termed *central gain*, helps maintain the sensitivity of the central auditory system following injury. However, central gain also results in impaired temporal processing and sound localization and is thought to cause tinnitus

(Eggermont, 2015; Knipper et al., 2013; Noreña & Eggermont, 2003). A comprehensive review of this and other changes in the central auditory system following cochlear damage is beyond the scope of this review and has been described in detail by others (Caspary et al., 2008).

2.8 HEARING LOSS: MANIFESTATIONS OF PERIPHERAL AND CENTRAL CHANGES FOLLOWING NOISE EXPOSURE

Given the high prevalence of SNHL in humans, the perceptual consequences have been thoroughly studied and described using numerous clinical and psychoacoustic measures. SNHL causes global perceptual deficits, including poorer audibility, decreased frequency and temporal resolution, poorer sound localization, distorted loudness and pitch perception, and degraded speech understanding (Moore, 1985, 1996). These findings align with the observations described above for the auditory nerve. The lowest ANF thresholds correspond with the behavioral audiogram in normal hearing and noise-exposed animals (Dallos & Harris, 1978; Salvi et al., 1979; Sumner & Palmer, 2012; Taberner & Liberman, 2005), suggesting that the auditory nerve serves as a rate-limiting step for auditory perceptual abilities. Greater severity of SNHL (i.e. hair cell loss and threshold shift) is associated with greater perceptual deficits, though with considerable inter-subject variability. These hearing impairments result in communication difficulties for people with SNHL, especially in complex listening environments. The most common complaint of patients with hearing loss is difficulty listening in noisy environments. While current audiological rehabilitation devices, such as hearing aids and cochlear implants, can improve audibility, they are limited in their capacity to restore more complex auditory cues.

To date, the perceptual consequences of synaptopathy have not been identified. Due to the inability to directly assess IHC synapse counts or integrity *in vivo*, human work is limited to studies of individuals at high risk for synaptopathy and post-mortem histological investigations, with little to no direct corroboration of these data sets. The selective loss of LSR ANFs in synaptopathy predicts difficulties with suprathreshold processing, such as listening for signals in background noise (Bharadwaj et al., 2014; Oxenham, 2016; Plack et al., 2014). Modest signal in noise detection deficits have been reported for animals with synaptopathy (Lobarinas et al., 2016, 2017). However, speech in noise perception ability does not relate to lifetime noise exposure (Guest et al., 2018). Furthermore, human studies show mixed results on the relationship between lifetime noise exposure metrics and standard synaptopathy diagnostics from the animal literature

(e.g. Wave I amplitude) (Bramhall et al., 2017; Guest et al., 2018; Le Prell, 2019). Other non-invasive measures of synaptopathy, such as the middle ear muscle reflex and envelope following response, may be more sensitive diagnostic tools (Bharadwaj et al., 2019; Shaheen et al., 2015; Valero et al., 2016, 2018). However, since it is not known whether humans indeed suffer from noise-induced synaptopathy, the sensitivity and specificity of these diagnostic measures are unclear.

While animal models permit combined studies of noise exposure conditions and cochlear histology not possible in humans, most animals have limited capacity to perform complex auditory tasks that mimic the challenging listening environments experienced by patients. Many species can learn to detect tones in quiet, yielding a basic behavioral audiogram. However, as numerous studies indicate, the audiogram is a poor predictor of the severity or extent of cochlear pathology (Clark & Bohne, 1978; Hunter-Duvar & Bredberg, 1974; Hunter-Duvar & Elliott, 1972, 1973; Jordan et al., 1973; Lonsbury-Martin et al., 1987; Moody et al., 1978; Scheib et al., 1975). Despite this limitation, the audiogram continues to be considered the clinical gold standard for hearing loss diagnosis. There is an urgent need for more sensitive and specific clinical diagnostic tools that can be used to differentiate among cochlear pathologies.

Ideally, the perceptual consequences of synaptopathy would be identified in a histologically validated model capable of performing complex listening tasks. This approach supports direct structure-function correlations by comparing frequency-specific perceptual deficits with the extent and location of damage within the cochlea. These studies could be complemented by investigations of neuronal encoding along the pathologic auditory pathway to understand how the peripheral and central auditory pathways contribute to auditory perception.

2.9 FUTURE DIRECTIONS: PREDICTING COCHLEAR DAMAGE

A thorough understanding of the anatomical, physiological, and perceptual effects of noise-induced hearing loss is vital with the emergence of therapeutics for the prevention and treatment of noise-induced hearing pathology. Differential diagnosis of cochlear pathology – from hair cell loss to synaptopathy to ANF degeneration and beyond – will be essential for determining appropriate recommendations. A combination of behavioral and physiological assays will likely provide the best insight into underlying pathophysiology. Diagnostic tools need

to be identified and validated in histologically characterized animal models to provide the translational strength necessary to meet medical standards.

2.10 REFERENCES

Bharadwaj, H. M., Mai, A. R., Simpson, J. M., Choi, I., Heinz, M. G., & Shinn-Cunningham, B. G. (2019). Non-Invasive Assays of Cochlear Synaptopathy – Candidates and Considerations. *Neuroscience*, *407*, 53–66. https://doi.org/10.1016/j.neuroscience.2019.02.031

Bharadwaj, H. M., Verhulst, S., Shaheen, L., Liberman, M. C., & Shinn-Cunningham, B. G. (2014). Cochlear neuropathy and the coding of supra-threshold sound. *Frontiers in Systems Neuroscience*, *8*. https://doi.org/10.3389/fnsys.2014.00026

Bramhall, N. F., Konrad-Martin, D., McMillan, G. P., & Griest, S. E. (2017). Auditory Brainstem Response Altered in Humans With Noise Exposure Despite Normal Outer Hair Cell Function: *Ear and Hearing*, *38*(1), e1–e12. https://doi.org/10.1097/AUD.0000000000000370

Brown, M. C. (1994). Antidromic responses of single units from the spiral ganglion. *J Neurophysiol, 71*(5), 1835-1847.

Buran, B. N., Strenzke, N., Neef, A., Gundelfinger, E. D., Moser, T., & Liberman, M. C. (2010). Onset Coding Is Degraded in Auditory Nerve Fibers from Mutant Mice Lacking Synaptic Ribbons. *Journal of Neuroscience*, *30*(22), 7587–7597. https://doi.org/10.1523/JNEUROSCI.0389-10.2010

Cai, S., Ma, W.-L. D., & Young, E. D. (2009). Encoding Intensity in Ventral Cochlear Nucleus Following Acoustic Trauma: Implications for Loudness Recruitment. *Journal of the Association for Research in Otolaryngology*, *10*(1), 5–22. https://doi.org/10.1007/s10162-008-0142-y

Caspary, D. M., Ling, L., Turner, J. G., & Hughes, L. F. (2008). Inhibitory neurotransmission, plasticity and aging in the mammalian central auditory system. *Journal of Experimental Biology*, *211*(11), 1781–1791. https://doi.org/10.1242/jeb.013581

Chambers, A. R., Resnik, J., Yuan, Y., Whitton, J. P., Edge, A. S., Liberman, M. C., & Polley, D. B. (2016). Central Gain Restores Auditory Processing following Near-Complete

Cochlear Denervation. *Neuron*, *89*(4), 867–879. https://doi.org/10.1016/j.neuron.2015.12.041

Clark, W. W., & Bohne, B. A. (1978). Animal Model for the 4-kHz Tonal Dip. *Annals of Otology, Rhinology & Laryngology*, *87*(4_suppl), 1–16. https://doi.org/10.1177/00034894780870S401

Clock Eddins, A., Salvi, R. J., Wang, J., & Powers, N. L. (1998). Threshold-duration functions of chinchilla auditory nerve fibers. *Hearing Research*, *119*, 135–141.

Costalupes, J. A. (1985). Representation of tones in noise in the responses of auditory nerve fibers in cats. I. Comparison with detection thresholds. *Journal of Neuroscience*, *5*(12), 3261–3269.

Costalupes, J. A., Young, E. D., & Gibson, D. J. (1984). Effects of continuous noise backgrounds on rate response of auditory nerve fibers in cat. *Journal of Neurophysiology*, *51*(6), 1326–1344. https://doi.org/10.1152/jn.1984.51.6.1326

Dallos, P., & Harris, D. (1978). Properties of auditory nerve responses in absence of outer hair cells. *Journal of Neurophysiology*, *41*(2), 365–383. https://doi.org/10.1152/jn.1978.41.2.365

Drescher, D. G., & Eldredge, D. H. (1974). Species differences in cochlear fatigue related to acoustics of outer and middle ears of guinea pig and chinchilla. *The Journal of the Acoustical Society of America*, *56*(3), 929–934. https://doi.org/10.1121/1.1903350

Eggermont, J. J. (2015). Animal models of spontaneous activity in the healthy and impaired auditory system. *Frontiers in Neural Circuits*, *9*. https://doi.org/10.3389/fncir.2015.00019

Evans, E. F. (1975). The Sharpening of cochlear frequency selectivity in the normal and abnormal cochlea. *International Journal of Audiology*, *14*(5–6), 419–442. https://doi.org/10.3109/00206097509071754

Fernandez, C. (1951). The innervation of the cochlea (guinea pig). *The Laryngoscope*, *61*(12), 1152–1172.

Fernandez, K. A., Jeffers, P. W. C., Lall, K., Liberman, M. C., & Kujawa, S. G. (2015). Aging after Noise Exposure: Acceleration of Cochlear Synaptopathy in “Recovered” Ears. *Journal of Neuroscience*, *35*(19), 7509–7520. https://doi.org/10.1523/JNEUROSCI.5138-14.2015

Flores, E. N., Duggan, A., Madathany, T., Hogan, A. K., Márquez, F. G., Kumar, G., Seal, R. P., Edwards, R. H., Liberman, M. C., & García-Añoveros, J. (2015). A Non-canonical Pathway from Cochlea to Brain Signals Tissue-Damaging Noise. *Current Biology*, *25*(5), 606–612. https://doi.org/10.1016/j.cub.2015.01.009

Froud, K. E., Wong, A. C. Y., Cederholm, J. M. E., Klugmann, M., Sandow, S. L., Julien, J.-P., Ryan, A. F., & Housley, G. D. (2015). Type II spiral ganglion afferent neurons drive medial olivocochlear reflex suppression of the cochlear amplifier. *Nature Communications*, *6*(1). https://doi.org/10.1038/ncomms8115

Furman, A. C., Kujawa, S. G., & Liberman, M. C. (2013). Noise-induced cochlear neuropathy is selective for fibers with low spontaneous rates. *Journal of Neurophysiology*, *110*(3), 577–586. https://doi.org/10.1152/jn.00164.2013

Galambos, R., & Davis, H. (1943). The response of single auditory-nerve fibers to acoustic stimulation. *Journal of Neurophysiology*, *6*(1), 39–57. https://doi.org/10.1152/jn.1943.6.1.39

Goman, A. M., & Lin, F. R. (2016). Prevalence of Hearing Loss by Severity in the United States. *American Journal of Public Health*, *106*(10), 1820–1822. https://doi.org/10.2105/AJPH.2016.303299

Guest, H., Munro, K. J., Prendergast, G., Millman, R. E., & Plack, C. J. (2018). Impaired speech perception in noise with a normal audiogram: No evidence for cochlear synaptopathy and no relation to lifetime noise exposure. *Hearing Research*, *364*, 142–151. https://doi.org/10.1016/j.heares.2018.03.008

Hawkins, J. E., Johnsson, L.-G., Stebbins, W. C., Moody, D. B., & Coombs, S. L. (1976). Hearing Loss and Cochlear Pathology in Monkeys After Noise Exposure. *Acta Oto-Laryngologica*, *81*(3–6), 337–343. https://doi.org/10.3109/00016487609119971

Heil, P., & Peterson, A. J. (2015). Basic response properties of auditory nerve fibers: A review. *Cell and Tissue Research*, *361*(1), 129–158. https://doi.org/10.1007/s00441-015-2177-9

Heinz, M. G. (2007). Spatiotemporal Encoding of Vowels in Noise Studied with the Responses of Individual Auditory-Nerve Fibers. In B. Kollmeier, G. Klump, V. Hohmann, U. Langemann, M. Mauermann, S. Uppenkamp, & J. Verhey (Eds.), *Hearing – From Sensory Processing to Perception* (pp. 107–115). Springer Berlin Heidelberg.

Heinz, M. G., & Swaminathan, J. (2009). Quantifying Envelope and Fine-Structure Coding in Auditory Nerve Responses to Chimaeric Speech. *Journal of the Association for Research in Otolaryngology*, *10*(3), 407–423. https://doi.org/10.1007/s10162-009-0169-8

Heinz, M. G., & Young, E. D. (2004). Response Growth With Sound Level in Auditory-Nerve Fibers After Noise-Induced Hearing Loss. *Journal of Neurophysiology*, *91*(2), 784–795. https://doi.org/10.1152/jn.00776.2003

Henry, K. S., & Heinz, M. G. (2013). Effects of sensorineural hearing loss on temporal coding of narrowband and broadband signals in the auditory periphery. *Hearing Research*, *303*, 39–47. https://doi.org/10.1016/j.heares.2013.01.014

Henry, K. S., Kale, S., & Heinz, M. G. (2016). Distorted Tonotopic Coding of Temporal Envelope and Fine Structure with Noise-Induced Hearing Loss. *Journal of Neuroscience*, *36*(7), 2227–2237. https://doi.org/10.1523/JNEUROSCI.3944-15.2016

Hickox, A. E., Larsen, E., Heinz, M. G., Shinobu, L., & Whitton, J. P. (2017). Translational issues in cochlear synaptopathy. *Hearing Research*, *349*, 164–171. https://doi.org/10.1016/j.heares.2016.12.010

Hinojosa, R., Seligsohn, R., & Lerner, S. A. (1985). Ganglion cell counts in the cochleae of patients with normal audiograms. *Acta Oto-Laryngologica*, *99*(1–2), 8–13.

Hoffman, H. J., Dobie, R. A., Losonczy, K. G., Themann, C. L., & Flamme, G. A. (2017). Declining Prevalence of Hearing Loss in US Adults Aged 20 to 69 Years. *JAMA Otolaryngology–Head & Neck Surgery*, *143*(3), 274. https://doi.org/10.1001/jamaoto.2016.3527

Huet, A., Batrel, C., Tang, Y., Desmadryl, G., Wang, J., Puel, J.-L., & Bourien, J. (2016). Sound coding in the auditory nerve of gerbils. *Hearing Research*, *338*, 32–39. https://doi.org/10.1016/j.heares.2016.05.006

Hunter-Duvar, I. M., & Bredberg, G. (1974). Effects of intense auditory stimulation: Hearing losses and inner ear changes in the chinchilla. *The Journal of the Acoustical Society of America*, *55*(4), 795–801. https://doi.org/10.1121/1.1914602

Hunter-Duvar, I. M., & Elliott, D. N. (1972). Effects of Intense Auditory Stimulation: Hearing Losses and Inner Ear Changes in the Squirrel Monkey. *The Journal of the Acoustical Society of America*, *52*(4B), 1181–1192. https://doi.org/10.1121/1.1913230

Hunter-Duvar, I. M., & Elliott, D. N. (1973). Effects of intense auditory stimulation: Hearing losses and inner ear changes in the squirrel monkey. II. *The Journal of the Acoustical Society of America*, *54*(5), 1179–1183. https://doi.org/10.1121/1.1914364

Jordan, V. M., Pinheiro, M. L., Chiba, K., & Jimenez, A. (1973). Cochlear pathology in monkeys exposed to impulse noise. *Acta Oto-Laryngologica*, *76*(sup312), 16–30. https://doi.org/10.3109/00016487309125497

Joris, P. X., Bergevin, C., Kalluri, R., Laughlin, M. M., Michelet, P., Heijden, M. van der, & Shera, C. A. (2011). Frequency selectivity in Old-World monkeys corroborates sharp cochlear tuning in humans. *Proceedings of the National Academy of Sciences*, *108*(42), 17516–17520. https://doi.org/10.1073/pnas.1105867108

Joris, P. X., & Yin, T. C. T. (1992). Responses to amplitude-modulated tones in the auditory nerve of the cat. *The Journal of the Acoustical Society of America*, *91*(1), 215–232. https://doi.org/10.1121/1.402757

Kale, S., & Heinz, M. G. (2012). Temporal modulation transfer functions measured from auditory-nerve responses following sensorineural hearing loss. *Hearing Research*, *286*(1–2), 64–75. https://doi.org/10.1016/j.heares.2012.02.004

Katsuki, Y., Suga, N., & Kanno, Y. (1962). Neural Mechanism of the Peripheral and Central Auditory System in Monkeys. *The Journal of the Acoustical Society of America*, *34*(9B), 1396–1410. https://doi.org/10.1121/1.1918357

Kiang, N. Y. S., Liberman, M. C., & Levine, R. A. (1976). Auditory-Nerve Activity in Cats Exposed to Ototoxic Drugs and High-Intensity Sounds. *Annals of Otology, Rhinology & Laryngology*, *85*(6), 752–768. https://doi.org/10.1177/000348947608500605

Kiang, N. Y.-S. (1965). *Discharge patterns of single fibers in the cat's auditory nerve: Vol. Research Mongraph No. 35*. The M.I.T. Press.

Kimura, R. S. (1975). The ultrastructure of the organ of corti. *International Review of Cytology*, *42*, 173–222.

Knipper, M., Van Dijk, P., Nunes, I., Rüttiger, L., & Zimmermann, U. (2013). Advances in the neurobiology of hearing disorders: Recent developments regarding the basis of tinnitus and hyperacusis. *Progress in Neurobiology*, *111*, 17–33. https://doi.org/10.1016/j.pneurobio.2013.08.002

Kujawa, S. G., & Liberman, M. C. (2006). Acceleration of Age-Related Hearing Loss by Early Noise Exposure: Evidence of a Misspent Youth. *Journal of Neuroscience*, *26*(7), 2115–2123. https://doi.org/10.1523/JNEUROSCI.4985-05.2006

Kujawa, S. G., & Liberman, M. C. (2009). Adding Insult to Injury: Cochlear Nerve Degeneration after "Temporary" Noise-Induced Hearing Loss. *Journal of Neuroscience*, *29*(45), 14077–14085. https://doi.org/10.1523/JNEUROSCI.2845-09.2009

Kujawa, S. G., & Liberman, M. C. (2015). Synaptopathy in the noise-exposed and aging cochlea: Primary neural degeneration in acquired sensorineural hearing loss. *Hearing Research*, *330*, 191–199. https://doi.org/10.1016/j.heares.2015.02.009

Le Prell, C. G. (2019). Effects of noise exposure on auditory brainstem response and speech-in-noise tasks: A review of the literature. *International Journal of Audiology*, *58*(sup1), S3–S32. https://doi.org/10.1080/14992027.2018.1534010

Le Prell, G., Sachs, M., & May, B. (1996). Representation of Vowel-like Spectra by Discharge Rate Responses of Individual Auditory-Nerve Fibers. *Aud Neurosci*, *2*(3), 275–288.

Liberman, L. D., Wang, H., & Liberman, M. C. (2011). Opposing Gradients of Ribbon Size and AMPA Receptor Expression Underlie Sensitivity Differences among Cochlear-Nerve/Hair-Cell Synapses. *Journal of Neuroscience*, *31*(3), 801–808. https://doi.org/10.1523/JNEUROSCI.3389-10.2011

Liberman, M. (1982). Single-neuron labeling in the cat auditory nerve. *Science*, *216*(4551), 1239–1241. https://doi.org/10.1126/science.7079757

Liberman, M. C. (1978). Auditory-nerve response from cats raised in a low-noise chamber. *The Journal of the Acoustical Society of America*, *63*(2), 442–455. https://doi.org/10.1121/1.381736

Liberman, M. C. (1984). Single-neuron labeling and chronic cochlear pathology. I. Threshold shift and characteristic-frequency shift. *Hearing Research*, *16*(1), 33–41. https://doi.org/10.1016/0378-5955(84)90023-6

Liberman, M. C. (2017). Noise-induced and age-related hearing loss: New perspectives and potential therapies. *F1000Research*, *6*, 927. https://doi.org/10.12688/f1000research.11310.1

Liberman, M. C., & Dodds, L. W. (1984a). Single-neuron labeling and chronic cochlear pathology. II. Stereocilia damage and alterations of spontaneous discharge rates. *Hearing Research*, *16*(1), 43–53. https://doi.org/10.1016/0378-5955(84)90024-8

Liberman, M. C., & Dodds, L. W. (1984b). Single-neuron labeling and chronic cochlear pathology. III. Stereocilia damage and alterations of threshold tuning curves. *Hearing Research*, *16*(1), 55–74. https://doi.org/10.1016/0378-5955(84)90025-X

Liberman, M. C., & Kiang, N. Y. S. (1978). Acoustic trauma in cats: Cochlear pathology and auditory nerve activity. *Acta Oto-Laryngologica*, *86*(sup358), 1–63. https://doi.org/10.3109/00016487809127889

Liberman, M. C., & Kiang, N. Y.-S. (1984). Single-neuron labeling and chronic cochlear pathology. IV. Stereocilia damage and alterations in rate- and phase-level functions. *Hearing Research*, *16*(1), 75–90. https://doi.org/10.1016/0378-5955(84)90026-1

Liberman, M. C. & Simmons, D. D. (1985). Applications of neuronal labeling techniques to the study of the peripheral auditory system. *J Acoust Soc Am, 78*(1), 312-319.

Lin, H. W., Furman, A. C., Kujawa, S. G., & Liberman, M. C. (2011). Primary Neural Degeneration in the Guinea Pig Cochlea After Reversible Noise-Induced Threshold Shift. *Journal of the Association for Research in Otolaryngology*, *12*(5), 605–616. https://doi.org/10.1007/s10162-011-0277-0

Liu, C., Glowatzki, E., & Fuchs, P. A. (2015). Unmyelinated type II afferent neurons report cochlear damage. *Proceedings of the National Academy of Sciences*, *112*(47), 14723–14727. https://doi.org/10.1073/pnas.1515228112

Lobarinas, E., Salvi, R., & Ding, D. (2016). Selective Inner Hair Cell Dysfunction in Chinchillas Impairs Hearing-in-Noise in the Absence of Outer Hair Cell Loss. *Journal of the Association for Research in Otolaryngology*, *17*(2), 89–101. https://doi.org/10.1007/s10162-015-0550-8

Lobarinas, E., Spankovich, C., & Le Prell, C. G. (2017). Evidence of "hidden hearing loss" following noise exposures that produce robust TTS and ABR wave-I amplitude reductions. *Hearing Research*, *349*, 155–163. https://doi.org/10.1016/j.heares.2016.12.009

Lonsbury-Martin, B. L., Martin, G. K., & Bohne, B. A. (1987). Repeated TTS exposures in monkeys: Alterations in hearing, cochlear structure, and single-unit thresholds. *The*

Journal of the Acoustical Society of America, *81*(5), 1507–1518. https://doi.org/10.1121/1.394503

Lopez-Poveda, E. A. (2014). Why do I hear but not understand? Stochastic undersampling as a model of degraded neural encoding of speech. *Frontiers in Neuroscience*, *8*. https://doi.org/10.3389/fnins.2014.00348

Lurie, M. H., Davis, H., & Hawkins, J. E. (1944). Acoustic trauma of the organ of corti in the guinea pig. *The Laryngoscope*, *54*(8), 375–386.

Ma, W.-L. D., & Young, E. D. (2006). Dorsal cochlear nucleus response properties following acoustic trauma: Response maps and spontaneous activity. *Hearing Research*, *216–217*, 176–188. https://doi.org/10.1016/j.heares.2006.03.011

Maison, S., Liberman, L. D., & Liberman, M. C. (2016). Type II Cochlear Ganglion Neurons Do Not Drive the Olivocochlear Reflex: Re-Examination of the Cochlear Phenotype in Peripherin Knock-Out Mice. *eNeuro, 3*(4), 1-11.

Merchan-Perez, A., & Liberman, M. C. (1996). Ultrastructural differences among afferent synapses on cochlear hair cells: Correlations with spontaneous discharge rate. *The Journal of Comparative Neurology*, *371*(2), 208–221. https://doi.org/10.1002/(SICI)1096-9861(19960722)371:2<208::AID-CNE2>3.0.CO;2-6

Miller, J. D., Watson, C. S., & Covell, W. P. (1963). Deafening effects of noise on the cat. *Acta Oto-Laryngologica*, *Suppl 176*, 6–91.

Miller, R. L., Schilling, J. R., Franck, K. R., & Young, E. D. (1997). Effects of acoustic trauma on the representation of the vowel /ɛ/ in cat auditory nerve fibers. *The Journal of the Acoustical Society of America*, *101*(6), 3602–3616. https://doi.org/10.1121/1.418321

Moody, D. B., Stebbins, W. C., Hawkins, J. E., & Johnsson, L.-G. (1978). Hearing loss and cochlear pathology in the monkey (Macaca) following exposure to high levels of noise. *Archives of Oto-Rhino-Laryngology*, *220–220*(1–2), 47–72. https://doi.org/10.1007/BF00456301

Moore, B. C. J. (1985). Frequency selectivity and temporal resolution in normal and hearing impaired listeners. *British Journal of Audiology*, *19*, 189–201.

Moore, B. C. J. (1996). Perceptual consequences of cochlear hearing loss and their implications for the design of hearing aids. *Ear and Hearing*, *17*(2), 133–161.

Mulders, W. H. A. M., & Robertson, D. (2013). Development of hyperactivity after acoustic trauma in the guinea pig inferior colliculus. *Hearing Research*, *298*, 104–108. https://doi.org/10.1016/j.heares.2012.12.008

Nadol, J. B. (1983). Serial Section Reconstruction of the Neural Poles of Hair Cells in the Human Organ Of Corti. I. Inner Hair Cells. *The Laryngoscope*, *93*(5), 599–614. https://doi.org/10.1002/lary.1983.93.5.599

Nadol, J. B. (1988). Comparative anatomy of the cochlea and auditory nerve in mammals. *Hearing Research*, *34*(3), 253–266. https://doi.org/10.1016/0378-5955(88)90006-8

Nomoto, M. (1980). Representation of Cochlear Innervation Patterns in Single Auditory Nerve Fiber Responses. *The Japanese Journal of Physiology*, *30*(1), 31–40. https://doi.org/10.2170/jjphysiol.30.31

Nomoto, M., Suga, N., & Katsuki, Y. (1964). Discharge pattern and inhibition of primary auditory nerve fibers in the monkey. *Journal of Neurophysiology*, *27*(5), 768–787.

Noreña, A. J., & Eggermont, J. J. (2003). Changes in spontaneous neural activity immediately after an acoustic trauma: Implications for neural correlates of tinnitus. *Hearing Research*, *183*(1–2), 137–153. https://doi.org/10.1016/S0378-5955(03)00225-9

Nouvian, R., Beutner, D., Parsons, T. D., & Moser, T. (2006). Structure and Function of the Hair Cell Ribbon Synapse. *Journal of Membrane Biology*, *209*(2–3), 153–165. https://doi.org/10.1007/s00232-005-0854-4

Ohlemiller, K. K., Wright, J. S., & Heidbreder, A. F. (2000). Vulnerability to noise-induced hearing loss in 'middle-aged' and young adult mice: A dose–response approach in CBA, C57BL, and BALB inbred strains. *Hearing Research*, *149*(1–2), 239–247. https://doi.org/10.1016/S0378-5955(00)00191-X

Ota, C. Y., & Kimura, R. S. (1980). Ultrastructural study of the human spiral ganglion. *Acta Oto-Laryngologica*, *89*, 53–62.

Oxenham, A. J. (2016). Predicting the Perceptual Consequences of Hidden Hearing Loss. *Trends in Hearing*, *20*. https://doi.org/10.1177/2331216516686768

Perkins, R. E., & Morest, D. K. (1975). A study of cochlear innervation patterns in cats and rats with the Golgi method and Nomarski optics. *The Journal of Comparative Neurology*, *163*(2), 129–158. https://doi.org/10.1002/cne.901630202

Plack, C. J., Barker, D., & Prendergast, G. (2014). Perceptual Consequences of "Hidden" Hearing Loss. *Trends in Hearing*, *18*, 233121651455062. https://doi.org/10.1177/2331216514550621

Pujol, R., & Puel, J.-L. (1999). Excitotoxicity, Synaptic Repair, and Functional Recovery in the Mammalian Cochlea: A Review of Recent Findings. *Annals of the New York Academy of Sciences*, *884*(1), 249–254. https://doi.org/10.1111/j.1749-6632.1999.tb08646.x

Rattay, F., Potrusil, T., Wenger, C., Wise, A. K., Glueckert, R., & Schrott-Fischer, A. (2013). Impact of Morphometry, Myelinization and Synaptic Current Strength on Spike Conduction in Human and Cat Spiral Ganglion Neurons. *PLOS ONE*, *8*(11), 1–17.

Rhode, W. S., Geisler, C. D., & Kennedy, D. T. (1978). Auditory nerve fiber response to wide-band noise and tone combinations. *Journal of Neurophysiology*, *41*(3), 692–704. https://doi.org/10.1152/jn.1978.41.3.692

Robertson, D. (1984). Horseradish peroxidase injection of physiologically characterized afferent and efferent neurones in the guinea pig spiral ganglion. *Hear Res, 15*(2), 113-121.

Romba, J. J., & Gates, H. W. (1964). Hearing loss in the rhesus monkey after repeated exposures to identical noises. *U.S. Army Human Engineering Laboratories*, *Technical Memorandum 3-64*, 1–11.

Rose, J. E., Hind, J. E., Anderson, D. J., & Brugge, J. F. (1971). Some effects of stimulus intensity on response of auditory nerve fibers in the squirrel monkey. *Journal of Neurophysiology*, *34*(4), 685–699. https://doi.org/10.1152/jn.1971.34.4.685

Ruggero, M. A. (1973). Response to noise of auditory nerve fibers in the squirrel monkey. *Journal of Neurophysiology*, *36*(4), 569–587. https://doi.org/10.1152/jn.1973.36.4.569

Ruggero, M. A. (1992). Physiology and Coding of Sound in the Auditory Nerve. In R. R. Fay (Ed.), *The Mammalian Auditory Pathway: Neurophysiology* (Vol. 2, pp. 34–93). Springer-Verlag.

Ryan, A., & Dallos, P. (1975). Effect of absence of cochlear outer hair cells on behavioural auditory threshold. *Nature*, *253*, 44–46.

Salvi, R. J., Hamernik, R. P., & Henderson, D. (1979). Auditory nerve activity and cochlear morphology after noise exposure. *Archives of Oto-Rhino-Laryngology*, *224*(1–2), 111–116. https://doi.org/10.1007/BF00455233

Salvi, R. J., Henderson, D., & Hamernik, R. P. (1979). Single auditory nerve fiber and action potential latencies in normal and noise-treated chinchillas. *Hearing Research*, *1*, 237–251.

Scheib, B. T., Stebbins, W. C., Moody, D. B., Johnsson, L. -G., & Muraski, A. A. (1975). Auditory threshold shift in nonhuman primates chronically exposed to low-level noise. *The Journal of the Acoustical Society of America*, *58*(S1), S89–S90. https://doi.org/10.1121/1.2002379

Scheidt, R. E., Kale, S., & Heinz, M. G. (2010). Noise-induced hearing loss alters the temporal dynamics of auditory-nerve responses. *Hearing Research*, *269*(1–2), 23–33. https://doi.org/10.1016/j.heares.2010.07.009

Schmiedt, R. A. (1989). Spontaneous rates, thresholds and tuning of auditory-nerve fibers in the gerbil: Comparisons to cat data. *Hearing Research*, *42*(1), 23–35. https://doi.org/10.1016/0378-5955(89)90115-9

Seki, S., & Eggermont, J. J. (2003). Changes in spontaneous firing rate and neural synchrony in cat primary auditory cortex after localized tone-induced hearing loss. *Hearing Research*, *180*(1–2), 28–38. https://doi.org/10.1016/S0378-5955(03)00074-1

Shaheen, L. A., & Liberman, M. C. (2018). Cochlear Synaptopathy Changes Sound-Evoked Activity Without Changing Spontaneous Discharge in the Mouse Inferior Colliculus. *Frontiers in Systems Neuroscience*, *12*. https://doi.org/10.3389/fnsys.2018.00059

Shaheen, L. A., Valero, M. D., & Liberman, M. C. (2015). Towards a Diagnosis of Cochlear Neuropathy with Envelope Following Responses. *Journal of the Association for Research in Otolaryngology*, *16*(6), 727–745. https://doi.org/10.1007/s10162-015-0539-3

Sinex, D. G., & Geisler, C. D. (1984). Comparison of the responses of auditory nerve fibers to consonant–vowel syllables with predictions from linear models. *The Journal of the Acoustical Society of America*, *76*(1), 116–121. https://doi.org/10.1121/1.391106

Song, Q., Shen, P., Li, X., Shi, L., Liu, L., Wang, J., Yu, Z., Stephen, K., Aiken, S., Yin, S., & Wang, J. (2016). Coding deficits in hidden hearing loss induced by noise: The nature and impacts. *Scientific Reports*, *6*(1). https://doi.org/10.1038/srep25200

Spoendlin, H. (1984). Factors Inducing Retrograde Degeneration of the Cochlear Nerve. *Annals of Otology, Rhinology & Laryngology*, *93*(4_suppl), 76–82. https://doi.org/10.1177/00034894840930S415

Spoendlin, H., & Brun, J. P. (1973). Relation Of Structural Damage To Exposure Time And Intensity In Acoustic Trauma. *Acta Oto-Laryngologica*, *75*(2–6), 220–226. https://doi.org/10.3109/00016487309139699

Sumner, C. J., & Palmer, A. R. (2012). Auditory nerve fibre responses in the ferret: Auditory nerve fibre responses in ferrets. *European Journal of Neuroscience*, *36*(4), 2428–2439. https://doi.org/10.1111/j.1460-9568.2012.08151.x

Suthakar, K. & Liberman, M. C. (2021). Auditory-nerve responses in mice with noise-induced cochlear synaptopathy. *J Neurophysiol, 126*(6), 2027-2038.

Taberner, A. M., & Liberman, M. C. (2005). Response Properties of Single Auditory Nerve Fibers in the Mouse. *Journal of Neurophysiology*, *93*(1), 557–569. https://doi.org/10.1152/jn.00574.2004

Tasaki, I. (1954). Nerve impulses in individual auditory nerve fibers of guinea pig. *Journal of Neurophysiology*, *17*(2), 97–122. https://doi.org/10.1152/jn.1954.17.2.97

Valero, M. D., Burton, J. A., Hauser, S. N., Hackett, T. A., Ramachandran, R., & Liberman, M. C. (2017). Noise-induced cochlear synaptopathy in rhesus monkeys (Macaca mulatta). *Hearing Research*, *353*, 213–223. https://doi.org/10.1016/j.heares.2017.07.003

Valero, M. D., Hancock, K. E., & Liberman, M. C. (2016). The middle ear muscle reflex in the diagnosis of cochlear neuropathy. *Hearing Research*, *332*, 29–38. https://doi.org/10.1016/j.heares.2015.11.005

Valero, M. D., Hancock, K. E., Maison, S. F., & Liberman, M. C. (2018). Effects of cochlear synaptopathy on middle-ear muscle reflexes in unanesthetized mice. *Hearing Research*, *363*, 109–118. https://doi.org/10.1016/j.heares.2018.03.012

Verschooten, E., Desloovere, C., & Joris, P. X. (2018). High-resolution frequency tuning but not temporal coding in the human cochlea. *PLOS Biology*, *16*(10), e2005164. https://doi.org/10.1371/journal.pbio.2005164

Viana, L. M., O'Malley, J. T., Burgess, B. J., Jones, D. D., Oliveira, C. A. C. P., Santos, F., Merchant, S. N., Liberman, L. D., & Liberman, M. C. (2015). Cochlear neuropathy in human presbycusis: Confocal analysis of hidden hearing loss in post-mortem tissue. *Hearing Research*, *327*, 78–88. https://doi.org/10.1016/j.heares.2015.04.014

Vogler, D. P., Robertson, D., & Mulders, W. H. A. M. (2014). Hyperactivity following unilateral hearing loss in characterized cells in the inferior colliculus. *Neuroscience*, *265*, 28–36. https://doi.org/10.1016/j.neuroscience.2014.01.017

Wang, J., Ding, D., & Salvi, R. J. (2002). Functional reorganization in chinchilla inferior colliculus associated with chronic and acute cochlear damage. *Hearing Research*, *168*(1–2), 238–249. https://doi.org/10.1016/S0378-5955(02)00360-X

Wang, J., Powers, N. L., Hofstetter, P., Trautwein, P., Ding, D., & Salvi, R. (1997). Effects of selective inner hair cell loss on auditory nerve fiber threshold, tuning and spontaneous and driven discharge rate. *Hearing Research*, *107*(1–2), 67–82. https://doi.org/10.1016/S0378-5955(97)00020-8

Wang, Y., Hirose, K., & Liberman, M. C. (2002). Dynamics of Noise-Induced Cellular Injury and Repair in the Mouse Cochlea. *Journal of the Association for Research in Otolaryngology*, *3*(3), 248–268. https://doi.org/10.1007/s101620020028

Ward, W. D., & Duvall, A. J. (1971). Behavioral and Ultrastructural Correlates of Acoustic Trauma. *Annals of Otology, Rhinology & Laryngology*, *80*(6), 881–896. https://doi.org/10.1177/000348947108000615

Weisz, C. J. C., Glowatzki, E., & Fuchs, P. A. (2014). Excitability of Type II Cochlear Afferents. *Journal of Neuroscience*, *34*(6), 2365–2373. https://doi.org/10.1523/JNEUROSCI.3428-13.2014

Weisz, C. J. C., Lehar, M., Hiel, H., Glowatzki, E., & Fuchs, P. A. (2012). Synaptic Transfer from Outer Hair Cells to Type II Afferent Fibers in the Rat Cochlea. *Journal of Neuroscience*, *32*(28), 9528–9536. https://doi.org/10.1523/JNEUROSCI.6194-11.2012

Weisz, C. J. C., Williams, S. G., Eckard, C. S., Divito, C. B., Ferreira, D. W., Fantetti, K. N., Dettwyler, S. A., Cai, H. M., Rubio, M. E., Kandler, K., & Seal, R. P. (2021). Outer Hair Cell Glutamate Signaling through Type II Spiral Ganglion Afferents Activates Neurons in the Cochlear Nucleus in Response to Nondamaging Sounds. *J Neurosci, 41*(13), 2930-2943.

Winter, I. M., Robertson, D., & Yates, G. K. (1990). Diversity of characteristic frequency rate-intensity functions in guinea pig auditory nerve fibres. *Hearing Research*, *45*(3), 191–202. https://doi.org/10.1016/0378-5955(90)90120-E

Wu, P. Z., Liberman, L. D., Bennett, K., de Gruttola, V., O'Malley, J. T., & Liberman, M. C. (2018). Primary Neural Degeneration in the Human Cochlea: Evidence for Hidden Hearing Loss in the Aging Ear. *Neuroscience*. https://doi.org/10.1016/j.neuroscience.2018.07.053

Yates, G. K. (1991). Auditory-nerve spontaneous rates vary predictably with threshold. *Hearing Research*, *57*(1), 57–62. https://doi.org/10.1016/0378-5955(91)90074-J

Young, E. D. (2012). Neural coding of sound with cochlear damage. In *Noise-induced hearing loss: Scientific advances* (pp. 87–135). Springer.

Zhang, W., Salvi, R. J., & Saunders, S. S. (1990). Neural correlates of gap detection in auditory nerve fibers of the chinchilla. *Hearing Research*, *46*(3), 181–200. https://doi.org/10.1016/0378-5955(90)90001-6

SECTION I: AUDITORY PERCEPTION IN NORMAL HEARING MACAQUE MONKEYS

CHAPTER 3

Frequency selectivity in macaque monkeys measured using a notched-noise method

When establishing an animal model of human hearing and hearing disorders, it is important to consider the similarities and differences in auditory perceptual abilities. Different aspects of auditory perception can be probed using precisely designed psychoacoustic paradigms. The most familiar measure of auditory perception is the audiogram, which assesses hearing sensitivity through the detection of tones in quiet. The addition of masking noise affords measurement of suprathreshold auditory functions, such as temporal resolution, spatial hearing, and frequency resolution. Studies of nonhuman primate auditory perceptual abilities are broadly summarized in Chapter 1. In the following study, frequency selectivity was assessed in normal hearing macaque monkeys by measuring tone detection in the presence of spectrally-notched noise. The results suggest that macaques have similar or slightly broader frequency selectivity than humans.

Burton, J. A., Dylla, M. E., & Ramachandran, R. (2018). Frequency selectivity in macaque monkeys measured using a notched-noise method. Hear Res, 357, 73-80. https://doi.org/10.1016/j.heares.2017.11.012

3.1 ABSTRACT

The auditory system is thought to process complex sounds through overlapping bandpass filters. Frequency selectivity as estimated by auditory filters has been well quantified in humans and other mammalian species using behavioral and physiological methodologies, but little work has been done to examine frequency selectivity in nonhuman primates. In particular, knowledge

of macaque frequency selectivity would help address the recent controversy over the sharpness of cochlear tuning in humans relative to other animal species. The purpose of our study was to investigate the frequency selectivity of macaque monkeys using a notched-noise paradigm. Four macaques were trained to detect tones in noises that were spectrally notched symmetrically and asymmetrically around the tone frequency. Masked tone thresholds decreased with increasing notch width. Auditory filter shapes were estimated using a rounded exponential function. Macaque auditory filters were symmetric at low noise levels and broader and more asymmetric at higher noise levels with broader low-frequency and steeper high-frequency tails. Macaque filter bandwidths (BW3dB) increased with increasing center frequency, similar to humans and other species. Estimates of equivalent rectangular bandwidth (ERB) and filter quality factor (Q_{ERB}) suggest macaque filters are broader than human filters. These data shed further light on frequency selectivity across species and serve as a baseline for studies of neuronal frequency selectivity and frequency selectivity in subjects with hearing loss.

3.2 INTRODUCTION

Frequency selectivity, or the ability to resolve the different frequency components of a complex sound, is a fundamental property of the auditory system. Characterization of individual perceptual abilities and the anatomical and physiological correlates of these abilities reveals important contributions to one's ability to hear in noisy environments. Decades of work have investigated frequency selectivity in humans, primarily through behavioral tasks, as well as a variety of animal models, using a combination of behavioral and physiological methodologies. These studies suggest that the auditory system utilizes overlapping bandpass filters for the detection and resolution of complex sounds (e.g. Fletcher 1940; Patterson and Nimmo-Smith 1980). These auditory filters are known to broaden in individuals with hearing impairment, serving as a likely contributor to difficulties with speech in noise perception (Tyler et al. 1984; Glasberg and Moore 1986, Desloge et al. 2012).

Little work has been done to examine frequency selectivity in nonhuman primates. Nonhuman primates are an ideal animal model for human hearing, due to their close phylogenetic relationship to humans and the similarities in their ability to detect auditory signals in noise (e.g. Dylla et al., 2013). Early auditory filter measurements in macaques were found to be similar to those for humans (Gourevitch 1970) and more recent filter measurements in

marmosets showed that frequency selectivity was generally comparable to that for humans, at least for some frequencies (Osmanski et al. 2013). In contrast, physiological measures using stimulus frequency otoacoustic emissions (SFOAEs) indicate poorer frequency selectivity for macaques than for humans (Joris et al., 2011). These discordant results are one example of the impact of methodology on measures of frequency selectivity. Comprehensive characterization of frequency selectivity in nonhuman primates using comparable methodologies to previous human experiments across both behavioral and physiological measures would contribute important information toward the controversy regarding the sharpness of human cochlear tuning (e.g. Shera et al. 2002; Ruggero & Temchin 2005; Lopez-Poveda & Eustaquio-Martin 2013). Here we report on behavioral frequency selectivity in macaque monkeys across their audible frequency range. These data provide the basis for ongoing and future investigations of the neurophysiological representations of frequency selectivity and changes in frequency selectivity following noise-induced hearing loss.

3.2.1 Methodological considerations in the measurement of frequency selectivity

While there are a variety of methods used to study frequency selectivity, the notched-noise paradigm (described in detail by Patterson and Nimmo-Smith 1980) has been used routinely to study auditory filters in humans with normal hearing (e.g. Glasberg et al., 1984; Oxenham and Simonson 2006; Eustaquio-Martin and Lopez-Poveda 2011; Lopez-Poveda and Eustaquio-Martin 2013) and with hearing loss (Tyler et al. 1984; Glasberg and Moore 1986, Desloge et al. 2012). This body of research determined that auditory filter bandwidth increases with increasing signal frequency (e.g. Moore et al. 1990; Rosen and Stock 1992; Shailer et al. 1990) and filter shape becomes more asymmetric at higher masker levels (e.g. Moore and Glasberg 1987).

Due to the compressive nonlinearity of the auditory periphery, filter shape and width vary significantly depending on probe and masker level, frequency composition of the masker, use of fixed signal or masker level, and timing between signal and masker (e.g. Houtgast 1977; Glasberg and Moore 1982; Glasberg et al. 1984; Niemiec et al. 1992; Rosen and Baker 1998; Eustaquio-Martin and Lopez-Poveda 2011; Lopez-Poveda and Eustaquio-Martin 2013). The significant impact of methodology on filter sharpness complicates definitions and comparisons of frequency selectivity within and across species. Therefore, these comparisons require critical review and have been under debate in recent years. In particular, estimates of frequency

selectivity using fixed signal level and fixed masker level paradigms should be compared with caution (Eustaquio-Martin and Lopez-Poveda 2011; Lopez-Poveda and Eustaquio-Martin 2013). Despite this, many studies make comparisons across species and between behavioral and physiological studies in an attempt to describe the evolutionary basis and neuronal origins of frequency selectivity (e.g. Fay 1988; Evans et al. 1989; Shera et al. 2002; Joris et al. 2011). Unsurprisingly, the conclusions from these studies are variable and inconsistent.

These discrepancies in the literature motivate our investigation of auditory filters in a single model species using a single methodology in both physiological and behavioral experiments. We elected to use a fixed masker level notched-noise paradigm. This design limits the opportunity for off-frequency listening, provides ease of comparison to the wealth of human and non-primate mammalian behavioral data using fixed masker levels, and supplements physiological measurements of frequency selectivity in humans, macaques, and other mammals.

3.3 METHODS

Experiments were conducted on four macaques: three male rhesus monkeys (*Macaca mulatta*) that were seven (monkey C) and ten (monkeys B and L) years of age at the time of testing, and one bonnet monkey (*Macaca radiata*) that was nine years of age at the time of testing (monkey G). All procedures were approved by the Animal Care and Use Committee at Vanderbilt University Medical Center and were in strict compliance with the National Institutes of Health guidelines for animal research.

All experiments were conducted in sound treated booths (Industrial Acoustics Corp, NY) that measured 1.8 m x 1.8 m x 2 m. During experiments, the monkeys were seated in an acrylic primate chair that was designed for comfort and with no obstruction to sounds on either side of the head (Audio chair, Crist Instrument Co., Hagerstown, MD). The subject's head was fixed to the chair such that the head was directly facing the middle of the loudspeaker at a distance of 35 inches from the ears. The loudspeaker (SA1 loudspeaker, Madisound, WI) and amplifier (SLA2, Applied Research Technologies, Rochester, NY) were able to deliver sounds between 50 Hz and 40 kHz. Calibration using a ½" probe microphone placed at the approximate entrance of the subjects' ear canals revealed that the output of the loudspeaker varied less than ±3 dB across the frequency range. Tones and noise were delivered from the same loudspeaker.

The monkeys were prepared for behavioral experiments by a surgical procedure, described in detail by Dylla et al. (2013). Briefly, during this surgical procedure, each monkey was implanted with a PEEK or titanium head holder (Crist Instruments, Hagerstown, MD) on the skull. This was used to position the monkey's head in a fixed location during experiments, so that the sound location and level were constant relative to the monkey's ears across trials and days. The monkeys were then trained to perform a behavioral Go/No-Go lever release task using fluid reward as positive reinforcement (for details, see Dylla et al. 2013).

3.3.1 Behavioral task

The monkeys were trained to detect 200-ms tones with 10-ms rise and fall times that were embedded in continuous noise. Signals were generated with onset phase of 0˚ and a sampling rate of 97.6 kHz. Monkeys initiated trials by pressing down on a lever (Model 829 Single Axis Hall Effect Joystick, P3America, San Diego, CA). The lever state was sampled at a rate of 24.4 kHz. After a variable hold time, a signal (tone) was presented on about 80% of trials. On hearing the tone, the monkey was required to release the lever within a 600-ms response window after the offset of the tone. The response window began with the onset of the stimulus, and the monkeys were free to respond even before stimulus offset. If the lever was released correctly on signal trials (hit), the monkey was rewarded with fluid. There were no penalties for not releasing the lever (miss), as this was taken to indicate non-detection. Catch trials were those in which no signal was played. Incorrect lever releases on catch trials (false alarms) were penalized with a timeout (6-10 seconds) in which no tone was presented (noise continued playing).

The experiments were controlled by a computer running OpenEx software (System 3, TDT Inc., Alachua, FL). The sound pressure level (SPL) of each tone could take values over a 60 dB range within each block. The different tone levels were randomly interleaved with catch trials and repeated 15-30 times each using the method of constant stimuli. Broadband noise was generated using one of the TDT System 3 functions, which generated flat spectrum noise that was then band-limited to 40 kHz. The level of the broadband noise is specified as the spectrum level, in dB SPL/Hz. The overall sound pressure level may be computed by adding the spectrum level to $10*\log_{10}$(bandwidth in Hz).

3.3.2 Procedure

The notched-noise paradigm was modeled after the methods of Patterson and Nimmo-Smith (1980) and Glasberg et al. (1984). Both symmetric and asymmetric notches were used to derive auditory filter shapes.

Symmetric notches were used for signal frequencies of 0.5, 1, 2, 4, 8, 16, 24, and 32 kHz, spanning nearly the entire audible frequency range of macaques (e.g., Pfingst et al. 1978). Tone detection performance was measured in broadband noise (5-40000 Hz, 30 or 50 dB spectrum level) and notched-noise. The normalized half-notchwidth from the stimulus (tone) frequency, f_0, to each edge of the notch, expressed as $\Delta f/f_0$, was 0.0, 0.05, 0.1, 0.2, 0.3, 0.5, 0.6, 0.65, and 0.8. (Note: Due to bandwidth limitations of the system, 24 kHz was not tested at 0.8 half notch width and 32 kHz was not tested at half notch widths greater than 0.2.)

Asymmetric notches were also used for the signal frequencies of 2 and 16 kHz. Upward shifted notches were obtained with the high frequency edge of the lower band of noise $0.2f_0$ closer to f_0 than the low frequency edge of the higher band of noise, while maintaining a particular notch width. Downward shifted notches were obtained with the lower band of noise $0.2f_0$ farther from f_0 than the higher band of noise. For an illustration of the stimulus setup, see the inset graphs in Figures 3 and 4 of Patterson and Nimmo-Smith (1980). Values of $\Delta f/f_0$ for the asymmetric notch conditions were 0.3, 0.4, 0.5, 0.6, 0.65, and 0.8. All asymmetric testing was completed using both the 30 and 50 dB SPL/Hz masker.

3.3.3 Calculation of behavioral thresholds

Data were analyzed according to signal detection theoretic methods, as described in Dylla et al. (2013) and Bohlen et al. (2014). Briefly, the hit rate at each tone level (*H(level)*) and false alarm rate (*FA*) were calculated based on the number of releases at each tone level and on catch trials respectively within a block. Based on signal detection theory, *H(level)* and *FA* were then converted into units of standard deviation of a standard normal distribution (z-score, norminv in MATLAB) to estimate *d'* according to $d'(level) = z\big(H(level)\big) - z(FA)$ (Macmillan and Creelman, 2005). Because we wanted these results to serve as a baseline for neurophysiological studies where we would measure distributions of responses to (noise) and (signal+noise), we converted the Go/No-Go analysis to a 2AFC analysis and calculated the probability correct (pc) at each tone level as follows: $pc(level) = z^{-1}(d'(level)/2)$. Here, the inverse z transform (z^{-1}) converts a unique number of standard deviations of a standard normal distribution into a probability correct (normcdf in MATLAB). The conversion of *d'* to the *pc* measure was to

facilitate the comparison of psychometric functions with neurometric functions obtained from neuronal responses using distribution free methods. The traditional threshold estimated at *d'*=1 corresponds to *pc*=0.76.

To obtain a smooth relationship between *pc* and *level*, psychometric functions were fitted with a modified Weibull cumulative distribution function (cdf) according to $pc(level)_{fit} = c - d * e^{-\left(\frac{level}{\lambda}\right)^k}$, where *level* is the tone level (in dB SPL), λ represents the threshold parameter and *k* corresponds to the slope parameter. *c* represents the saturation probability correct, and *d* is the estimate of chance performance. Threshold was calculated from the fit as the tone level that would cause a pc_{fit} value of 0.76.

3.3.4 Filter shape and bandwidth analyses

Tone detection thresholds obtained from the Weibull cdf fits at various notch widths were fitted assuming that each side of the auditory filter was a rounded exponential. This was done using publicly available software developed by B. C. J. Moore and B. R. Glasberg. The ROEXPR program was used for symmetric filter estimates and the ROEX3 program was used for asymmetric filter estimates. In both of these programs, the default settings were used. The rounded exponential (roex) filter shape is described by: $W(g) = (1 - r) * (1 + p * g) * e^{-p*g} + r$, where *g* is the normalized deviation from the center frequency, and *p* and *r* are adjustable parameters. A larger value of *p* indicates a larger slope and therefore a narrower filter. *r* corresponds to the shallow tail of the filter. Additionally, processing efficiency (*k*) was calculated directly from the fitting process (see Patterson et al. 1982), with a smaller value of *k* (in dB) indicating more efficient processing. The *W(g)* filter parameter values were iteratively adjusted in the software so as to achieve the smallest RMS difference between the predicted and actual threshold values. The width of the filter was measured 3 dB down from the peak (BW3dB) and was used to define frequency selectivity. ERB values, another metric used to describe frequency selectivity, were calculated from the *p* values, according to: $ERB = 4 * f_0/p$. Quality factors of the perceptual filter (Q_{ERB}), which provide a dimensionless measure of the sharpness of filter tuning, were calculated from the ERB, according to Shera et al. (2002): $Q_{ERB} = f_0/ERB$. BW3dB, ERB, and Q_{ERB} values were compared across species using published data sets.

3.4 RESULTS

3.4.1 Macaque filter shapes and bandwidths

Figure 3.1 shows the behavioral data used to derive a perceptual auditory filter. Figure 3.1A shows the psychometric functions for Monkey B for an 8 kHz signal in a 30-dB spectrum level masker. Psychometric functions are shown for notched-noise maskers with g values of 0 (black), 0.1 (red), 0.5 (green), and 0.65 (blue). As shown in other studies, the tone detection threshold decreased (threshold level indicated by the dashed lines, leftward shift of the dynamic range) with increasing notch width. Figure 3.1B shows the threshold (in dB SPL) of the 8 kHz tone as a function of notch width. Filter parameter values were used to generate the auditory filter shown in Figure 3.1C. The horizontal dashed line in Figure 3.1C indicates the half power bandwidth of the auditory filter function, which was defined as BW3dB.

3.4.1.1 Auditory filters across frequencies

Figure 3.2 shows tone detection threshold as a function of notch width for various tone frequencies in the symmetric notch condition. For all four subjects, the lowest frequencies (0.5 kHz, 1 kHz, red) yielded the shallowest functions and the highest frequencies (16 kHz, 32 kHz, blue) yielded the steepest functions. A steeper slope indicates a more sharply tuned filter. These data suggest that auditory filters become progressively relatively narrower (on a logarithmic frequency scale) with increasing frequency. The symmetric auditory filters generated from the functions in Figure 3.2 are shown for each subject in Figure 3.3. Absolute filter bandwidth increased with increasing frequency, consistent with the extensive literature on human auditory filters (e.g. Moore and Glasberg, 1987).

3.4.1.2. Auditory filters across masker levels and asymmetric masker configurations

Masker intensity affects the bandwidth and asymmetry of auditory filters (e.g. Moore et al. 1990; Rosen and Stock 1989; 1992; Eustaquio-Martin and Lopez-Poveda; 2011; explained in Lopez-Poveda and Eustaquio-Martin, 2013). Our macaque subjects showed similar masker level effects to those observed previously in human and animal studies. Representative auditory filter shapes are shown for one subject at 2 kHz (Figure 3.4A) and 16 kHz (Figure 3.4B) with 30 (blue) and 50 (red) dB/Hz maskers in both symmetric (dashed line) and asymmetric (solid line) masking conditions. Filter bandwidth and symmetry changed minimally with increasing noise level at 2 kHz. A more pronounced effect of noise level was observed at 16 kHz, with a broader, more asymmetric filter (broad lower side, steep upper side) at the higher noise level.

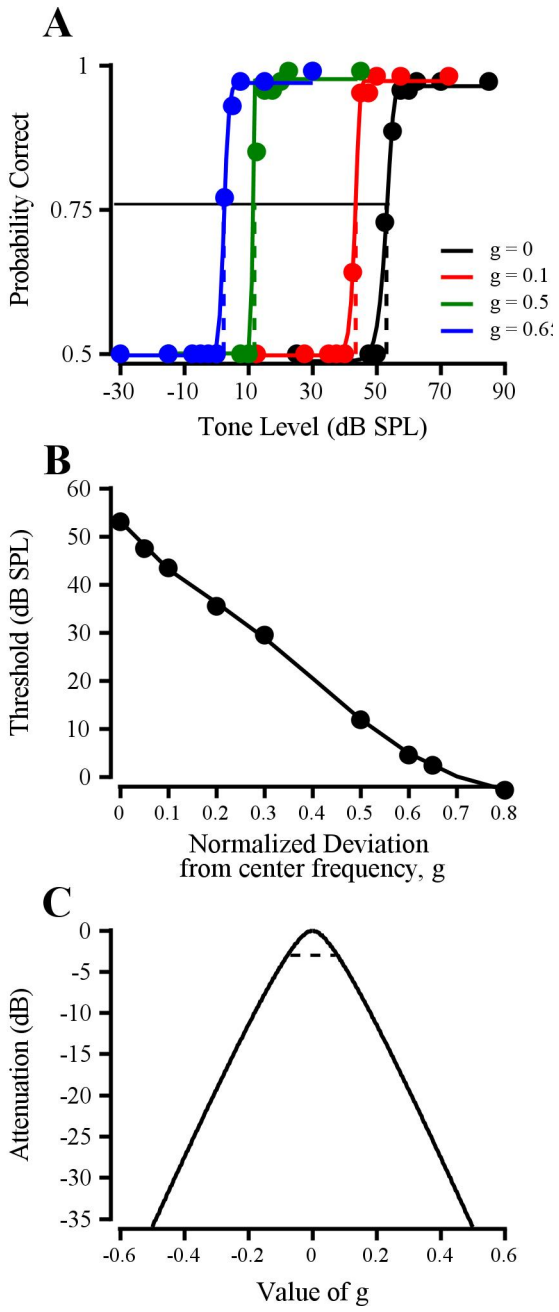

Figure 3.1 Estimation of an auditory filter shape from the notched-noise paradigm. A: Psychometric functions for detecting an 8-kHz tone in a 30 dB/Hz masker, with g values of 0 (black), 0.1 (red), 0.5 (green), and 0.65 (blue). Threshold is the signal level that would evoke 0.76 probability correct (indicated by dashed lines). B: Thresholds from (A) plotted as a function of g (normalized deviation from center frequency). C: Auditory filter shape for an 8-kHz tone in 30 dB/Hz noise (from data in B). Dashed line indicates the half power point of the filter; the bandwidth of the filter at the half-power point was taken as BW3dB. Data are from Monkey B.

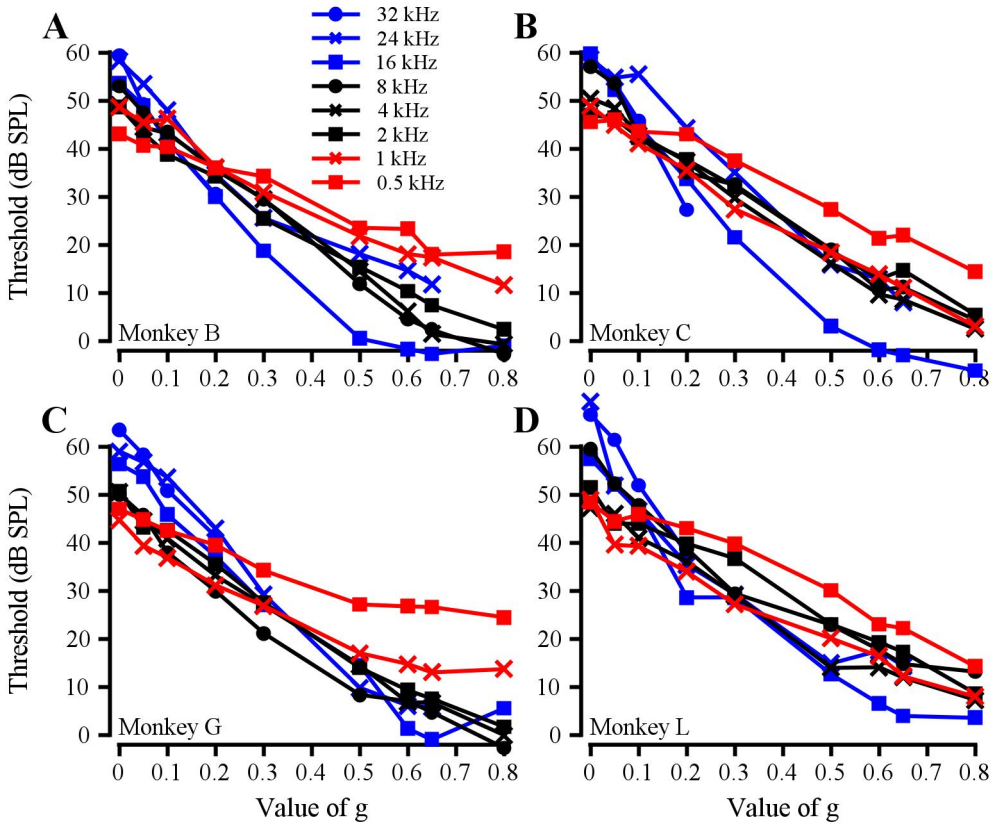

Figure 3.2 Threshold as a function of g at each frequency tested for each subject. A – D. Data from monkeys B, C, G, L, respectively.

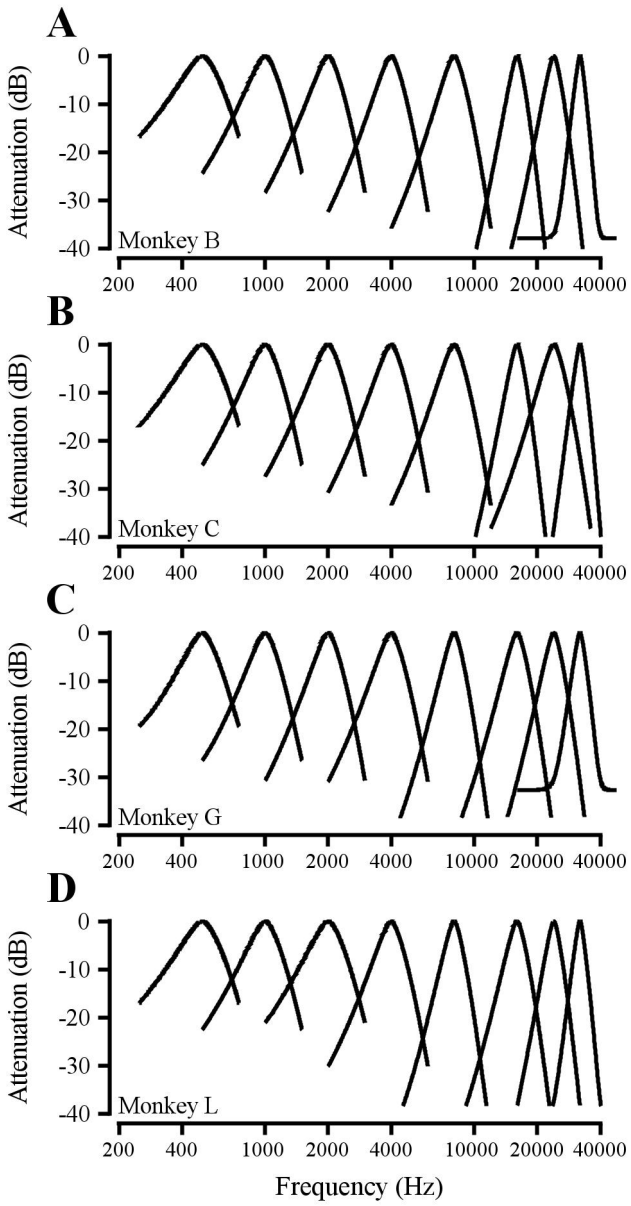

Figure 3.3 Auditory filters across the macaque audible frequency range. A – D. Data from monkeys B, C, G, L, respectively.

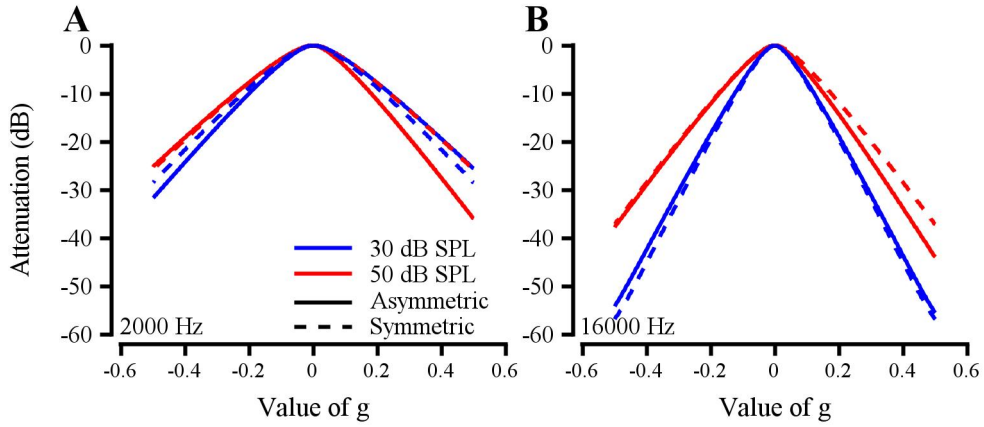

Figure 3.4 Auditory filter shape and asymmetry as a function of masker level. Data are from Monkey B. A: Symmetric (dashed lines) and asymmetric (solid lines) auditory filter shapes for a 2 kHz tone with 30 (blue) and 50 (red) dB/Hz maskers. B: Similar to A, but for a 16 kHz tone.

Additionally, filter asymmetry was small for 30 dB/Hz masker conditions at both 2 and 16 kHz, while more pronounced asymmetry occurred at 50 dB/Hz masker conditions for both signal frequencies. These findings are consistent with previous work (Weber 1977; Pick 1980; Patterson 1971).

3.4.2 Characterizing macaque frequency selectivity

Half power bandwidth (BW3dB), equivalent rectangular bandwidth (ERB), and quality factor (Q_{ERB}) were calculated for the auditory filters for each subject at each probe frequency. Values were derived from symmetric 30 dB masker level filters unless otherwise specified. Due to low variability in filter shape and frequency selectivity metrics across subjects, mean data will be highlighted in the following section. Individual and mean BW3dB values are listed by frequency in Table 3.1.

Table 3.1 – BW3dB values for individual monkeys and their mean.

Frequency (kHz)	Monkey B	Monkey C	Monkey G	Monkey L	Mean (Std. Dev.)
0.5	143	143	123	143	138 (10)
1	215	210	195	230	213 (14)
2	380	390	354	480	401 (55)
4	680	706	700	720	702 (17)
8	1240	1320	1040	1000	1150 (155)
16	1648	1680	2160	2000	1872 (249)
24	2520	3624	2808	2328	2820 (571)
32	2105	2368	2592	2336	2350 (199)

Note: BW3dB values were obtained using filters estimated from 30 dB SPL/Hz maskers.

BW3dB values increased approximately linearly as a function of frequency (Figure 3.5, mean = red circles, range = gray shaded area; slope = 0.084, R^2 = 0.8376, $p = 6.8\text{x}10^{-14}$). Values were consistent with previous macaque critical bandwidth data (Gourevitch 1970; blue circles) from 0.5 to 4 kHz and were lower over the 8 to 32 kHz range. Macaque BW3dB values were plotted against previous data collected from humans (Desloge et al. 2012, notched-noise; black diamonds). BW3dB values from the present study of macaques seem to align well with BW3dB values from humans, but differences may not be clear using this metric due to scaling.

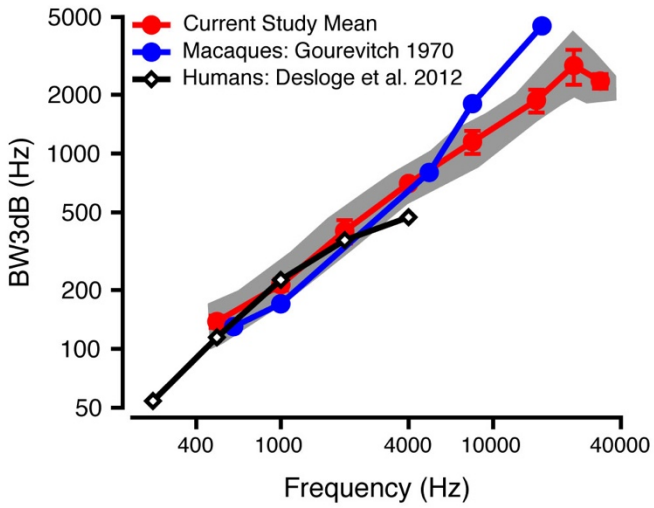

Figure 3.5 BW3dB values as a function of frequency. Mean macaque BW3dB data from current study (mean: red circles; standard deviation: error bars) are plotted against previous macaque data using band-widening techniques (Gourevitch 1970; blue circles) and BW3dB data from humans (Desloge et al., 2012; unfilled black diamonds). The gray shaded area shows the range of the macaque BW3dB values in the current study.

BW3dB values were also calculated for symmetric and asymmetric filters at 2 and 16 kHz for the 30 and 50 dB masker levels (mean data listed in Table 3.2). BW3dB values were generally smaller using asymmetric filter shapes compared to symmetric filter shapes. BW3dB values were greater at the higher masker level for both symmetric and asymmetric filters.

Table 3.2 – BW3dB values obtained from symmetric and asymmetric notched-noise at 30 and 50 dB SPL/Hz.

Frequency (kHz)	Mean BW3dB @ 30 dB (Std. Dev)	Mean BW3dB @ 50 dB (Std. Dev.)
2, symmetric	401 (55)	478 (64)
2, asymmetric	362 (45)	384 (45)
16, symmetric	1872 (249)	2422 (386)
16, asymmetric	1874 (294)	2124 (436)

Note: Summary data based on 4 monkeys

ERB values were calculated based on the values of p derived from the rounded exponential fit. Individual and mean macaque ERB values are listed by frequency in Table 3.3 and mean ERB values are plotted as a function of tone frequency in Figure 3.6 (mean: red circles; standard deviation: error bars; range indicated by gray shaded area). The ERB increased with increasing signal frequency and this was well described by a power function of the signal

frequency (exponent = 0.098, R^2 = 0.8565, $p = 3.5\text{x}10^{-14}$). Macaque ERB values were compared to ERB values from humans (black, all notched-noise; circles: Moore et al. 1990; unfilled squares: Glasberg and Moore 1986; triangles: Shailer et al. 1990; unfilled diamonds: Desloge et al. 2012), marmosets (blue circles: Osmanski et al. 2013, notched-noise), and chinchillas (green squares: Niemiec et al. 1992, notched-noise). Macaque ERB values were comparable to some human ERB data sets (compare red circles with unfilled diamonds, Figure 3.6), but were globally broader than most human ERB values and ERBs for marmosets and chinchillas.

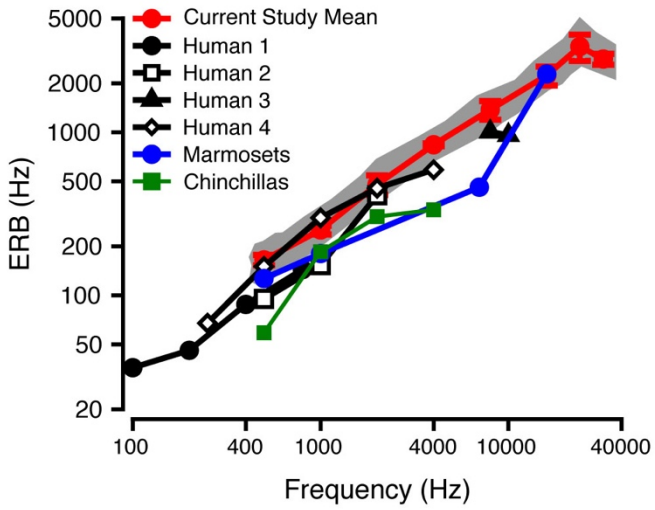

Figure 3.6 ERB as a function of frequency. Mean macaque ERB data from current study (mean: red circles; standard deviation: error bars) are compared to ERB data obtained using notched-noise methods for humans (black; filled circles (Human1): Moore et al. 1990; unfilled squares (Human2): Glasberg and Moore 1986; filled triangles (Human3): Shailer et al. 1990; unfilled diamonds (Human4): Desloge et al. 2012), marmosets (blue; Osmanski et al. 2013), and chinchillas (green; Niemiec et al. 1992). The gray shaded area shows the range of the macaque ERB values in the current study.

Table 3.3 – ERB values in Hz for individual macaques and their mean.

Frequency (kHz)	Monkey B	Monkey C	Monkey G	Monkey L	Mean (Std. Dev.)
0.5	171	171	146	171	165 (13)
1	255	250	233	272	252 (16)
2	452	465	423	576	479 (67)
4	812	847	842	856	839 (19)
8	1488	1576	1250	1194	1377 (184)
16	1963	2000	2570	2415	2237 (302)
24	3028	4229	3380	2807	3361 (625)
32	2560	2826	3107	2777	2817 (225)

Note: ERBs obtained using filters estimated from 30 dB SPL/Hz maskers.

Q_{ERB} values also reflect this trend, with generally lower Q_{ERB} values for the macaque as compared to most human data sets (except for data from Desloge et al. 2012), suggesting poorer frequency selectivity in macaques. Individual and mean Q_{ERB} data are listed in Table 3.4. Figure 3.7 shows mean macaque data (red circles) plotted against behavioral data for humans (black circles: Moore et al. 1990; unfilled black squares: Glasberg and Moore 1986; black triangles: Shailer et al. 1990; unfilled diamonds: Desloge et al. 2012; black line: Shera et al. 2002;),

marmosets (blue circles: Osmanski et al. 2013), and chinchillas (green squares: Niemiec et al. 1992). Interestingly, both the marmoset and chinchilla ERB and Q_{ERB} are comparable to the human values and actually seem to suggest narrower spectral tuning than humans and macaques depending upon which data set and frequencies are being compared.

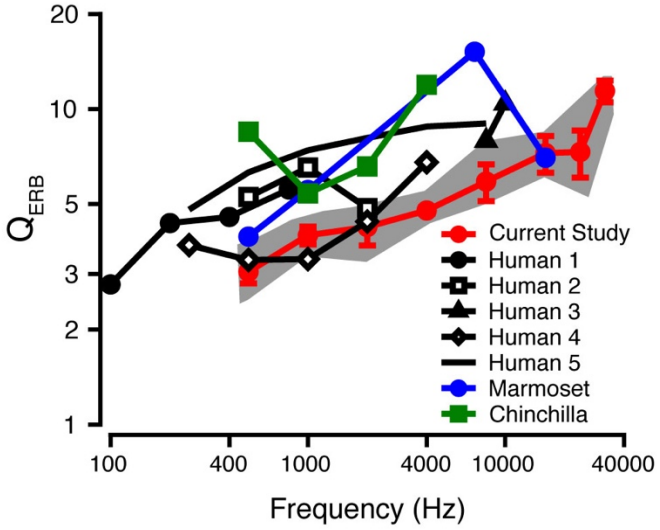

Figure 3.7 Q_{ERB} as a function of frequency. Mean macaque behavioral Q_{ERB} data (red circles; standard deviation error bars) are compared to behavioral Q_{ERB} data for humans (black; filled circles (Human1): Moore et al. 1990; unfilled squares (Human2): Glasberg and Moore 1986; filled triangles (Human3): Shailer et al. 1990; unfilled diamonds (Human4): Desloge et al. 2012; solid line (Human5): Shera et al. 2002;), marmosets (blue; Osmanski et al. 2013), and chinchillas (green; Niemiec et al. 1992). The gray shaded area shows the range of the macaque Q_{ERB} values in the current study.

Table 3.4 –Q_{ERB} values for individual monkeys and their mean.

Frequency (kHz)	Monkey B	Monkey C	Monkey G	Monkey L	Mean (Std. Dev.)
0.5	2.93	2.93	3.43	2.93	3.05 (0.25)
1	3.93	4.00	4.30	3.68	3.98 (0.26)
2	4.43	4.30	4.73	3.48	4.23 (0.54)
4	4.93	4.73	4.75	4.68	4.77 (0.11)
8	5.38	5.08	6.40	6.70	5.89 (0.78)
16	8.15	8.00	6.23	6.63	7.25 (0.97)
24	7.93	5.68	7.10	8.55	7.31 (1.2)
32	12.50	11.33	10.30	11.53	11.41 (0.90)

Note: Q_{ERB} values obtained using filters estimated from 30 dB SPL/Hz maskers.

3.5 DISCUSSION

This study provides a comprehensive description of behavioral auditory filters in nonhuman primates. Changes in filter shape and bandwidth according to frequency, noise masker level, and asymmetry were similar to those observed in humans and other non-primate species. Macaque filters were generally broader than those for humans, suggesting poorer frequency selectivity.

3.5.1 Effect of noise level and signal frequency on auditory filter shapes

The present study is one of the first to examine auditory filters across the audible frequency range of a species and to use sample frequencies across the audible range to check for frequency dependent effects of noise level or asymmetry. Macaque auditory filters were broader and more asymmetric at the higher masker level and at higher signal frequencies. The majority of previous studies site similar effects of noise level (e.g. Rosen and Stock 1992; Patterson 1971; Pick 1980; Moore and Glasberg 1987) and signal frequency (e.g. Weber 1977; Pick 1980; Rosen and Stock 1989; Moore et al. 1990; Glasberg and Moore 1986; Shailer et al. 1990), though some report no effect of masker level on filter width (see Pick (1980) for further discussion). It is likely that methodological differences, such as masker type or stimulus frequency, or even the details of the task itself, contribute to these discrepancies, due to cochlear nonlinearity (Rosen and Stock 1992; Lopez-Poveda and Eustaquio-Martin 2013).

Humans and macaques have different audible frequency ranges: the macaque audible range is approximately 55 Hz-45 kHz (Pfingst et al. 1978; Stebbins et al. 1966), while humans can hear from 20 Hz-20 kHz (Sivian and White 1933; Hawkins and Stevens 1950). The lowest tone thresholds of macaques are between 1 and 16 kHz (Pfingst et al. 1978; Dylla et al. 2013) whereas the lowest tone thresholds of humans are between 0.5 and 8 kHz (Sivian and White 1933; Hawkins and Stevens 1950). It is likely that frequency-specific characteristics of auditory filters will vary among species based on this difference. For example, Shailer et al. (1990) noted smaller ERB values at 8 and 10 kHz in humans than expected based on extrapolation of classical filter bandwidth values. However, this reduction from a linear relationship was not observed in the macaques in the current study until 16 kHz. The large variability across subjects in auditory filter shape observed at 8 and 10 kHz with increasing noise level in humans (Shailer et al. 1990) may also be related to the variable filter asymmetry and bandwidth with increasing noise levels we observed for our macaques at 16 kHz. Therefore, we suggest that similarities in frequency-specific filter effects may emerge if the species' audible range is taken into account.

3.5.2 Describing macaque frequency selectivity

In evaluating an animal's utility as a model for human hearing, one needs a basic understanding of the animal's psychophysical auditory abilities, such as frequency selectivity (Fay 1988). One previous review suggests that small laboratory animals, such as mice (Ehret 1976), rats (Gourevitch 1965), chinchillas (Niemiec et al. 1992), and cats (Nienhuys and Clark

1979; Pickles 1979), have broader auditory filters than humans (see Figure 8 in Fay 1988), which may implicate an evolutionary aspect of frequency selectivity. In contrast, a more recent review comparing only among data obtained using a fixed masker level suggests comparable tuning across mammals and birds (Ruggero and Temchin 2005). A perfunctory comparison of our macaque data suggests broader tuning than for the human, marmoset, and chinchilla (see Figure 3.7, all notched-noise data).

However, as described in the introduction, methodology is known to have a significant impact on estimates of frequency selectivity (Glasberg et al. 1984; Niemiec et al. 1992; Eustaquio-Martin and Lopez-Poveda 2011; Lopez-Poveda and Eustaquio-Martin 2013), so data comparisons must be made sensibly. When comparing to one study that employed a similar fixed signal level methodology, our BW3dB, ERB and Q_{ERB} values suggest that frequency selectivity is similar for monkeys and humans (e.g. Desloge et al. 2012). However, comparisons to most other human studies indicate sharper tuning for humans compared to macaques (e.g. Moore et al. 1990; Glasberg and Moore 1986).

Previous studies have compared frequency selectivity across species using comparisons across methodologies. For example, Shera et al. (2002) found lower Q_{ERB} values for cats and guinea pigs than for humans using fixed signal level SFOAE measurements, indicating broader frequency selectivity in these animals (see their Figure 1). While these data could be interpreted together due to the use of similar methodologies (though this is questioned in Lopez-Poveda and Eustaquio-Martin 2013), they should be compared to the current behavioral data, obtained with a fixed masker level, with caution. Q_{ERB} values calculated from our behavioral measurements in macaques were considerably lower than those obtained previously using SFOAEs and in ANF recordings (Joris et al. 2011; data not shown). When comparing human SFOAE data to human behavioral data, a similar disparity in Q_{ERB} values obtained by behavioral and physiological methodologies was noted. However, the utility of this comparison is questionable, since the physiological estimates of frequency selectivity were obtained using a fixed signal level and the behavioral estimates were obtained using a fixed masker level (for a discussion of the problems with these comparisons, see Eustaquio-Martin and Lopez-Poveda 2011; Lopez-Poveda and Eustaquio-Martin 2013).

Some of the variation in estimates of frequency selectivity at high frequencies may also be a result of not taking into account the frequency response of the transducer (Moore et al.

1990; Shailer et al. 1990). In our study, calibrations were routinely performed to ensure that all signals and masking noises were presented at equivalent levels across subjects and testing sessions. Thus, the observed narrowing of filter bandwidths at high frequencies may reflect a true characteristic of the macaque auditory system. Previous work has suggested that a modified *a priori* notched-noise method yields more symmetrical, steep filters at high frequencies (10 kHz) by taking into account the middle ear transfer function (Glasberg and Moore 1990, 2000; Kowalewski 2014).

In summary, these data will serve as comparisons for ongoing physiological measures of frequency selectivity in single units along the auditory pathway. These investigations of neuronal frequency selectivity will contribute toward an understanding of the underlying computations, circuitry, and transformations that generate perceptual frequency selectivity in normal hearing and hearing impaired subjects.

3.6 ACKNOWLEDGMENTS

The authors would like to acknowledge Mary Feurtado for her assistance with the surgical procedures to prepare subjects for experiments, Bruce Williams and Roger Williams for building experimental hardware, and Corey Mondul for his assistance with data collection. The authors would like to acknowledge the helpful comments of Dr. B. C. J. Moore and two anonymous reviewers during the review of this manuscript. The authors would also like to acknowledge the National Institutes of Health and the National Institute on Deafness and Other Communication Disorders for funding this research through the following grant support: R01 DC 011092 (PI: Ramnarayan Ramachandran) and T35 DC008763-08 (PI: Linda J. Hood).

3.7 REFERENCES

Cohen, A. (1961). Further investigation of the effects of intensity upon the pitch of pure tones. *J. Acoust. Soc. Am., 33*(10), 1363-1376.

Desloge, J. G., Reed, C. M., Braida, L. D., Perez, Z. D., and Delhorne, L. A. (2012). Auditory-filter characteristics for listeners with real and simulated hearing impairment. *Trends in Amplification, 16*(1), 19-39.

Dylla, M., Hrnicek, A., Rice, C., and Ramachandran, R. (2013). Detection of tones and their modification by noise in nonhuman primates. *J. Assoc. Res. Otolaryngol, 14*, 547-560.

Ehret, G. (1976). Critical bands and filter characteristics in the ear of the housemouse (*Mus musculus*). *Biol. Cybernetics, 24*, 35-42.

Eustaquio-Martín, A. and Lopez-Poveda, E. A. (2011). Isoresponse versus isoinput estimates of cochlear filter tuning. *J. Assoc. Res. Otolaryngol., 12*(3), 281-299.

Evans, E. F. (1977). Frequency selectivity at high signal levels of single units in cochlear nerve and nucleus. In E. F. Evans and J. P. Wilson (Eds.), *Psychophysics and Physiology of Hearing* (185-192). London, Academic Press.

Evans, E. F., Pratt, S. R., and Cooper, N. P. (1989). Correspondence between behavioural and physiological frequency selectivity in the guinea pig. *Br. J. Audiol., 23*(2), 151-152.

Fay, R. R. (1988). Comparative psychoacoustics. *Hearing Research, 34*, 295-306.

Fletcher, H. (1940). Auditory patterns. *Rev. Mod. Phys., 12*, 47-65.

Glasberg, B. R. and Moore, B. C. J. (1982). Auditory filter shapes in forward masking as a function of level. *J. Acoust. Soc. Am., 71*, 946-949.

Glasberg, B. R., Moore, B. C. J., and Nimmo-Smith, I. (1984). Comparison of auditory filter shapes derived with three different maskers. *J. Acoust. Soc. Am., 75*(2), 536-544.

Glasberg, B. R., Moore, B. C. J., Patterson, R. D., and Nimmo-Smith, I. (1984). Dynamic range and asymmetry of the auditory filter. *J. Acoust. Soc. Am., 76*(2), 419-427.

Glasberg, B. R. and Moore, B. C. J. (1990). Derivation of auditory filter shapes from notched-noise data. *Hear. Res. 47*, 103-138.

Glasberg, B. R. and Moore, B. C. J. (2000). Frequency selectivity as a function of level and frequency measured with uniformly exciting notched noise. *J. Acoust. Soc. Am. 108*, 2318-2328.

Gourevitch, G. (1965). Auditory masking in the rat. *J. Acoust. Soc. Am., 37*(3), 439-443.

Gourevitch, G. (1970). Detectability of tones in quiet and in noise by rats and monkeys. In W. C. Stebbins (Ed.), *Animal Psychoacoustics: The Design and Conduct of Sensory Experiments* (pp. 67-97). New York, NY: Appleton-Century-Crofts.

Hawkins, J. E. and Stevens, S. S. (1950). The masking of pure tones and of speech by white noise. *J. Acoust. Soc. Am., 22*(1), 6-13.

Houtgast, T. (1977). Auditory-filter characteristics derived from direct-masking data and pulsation-threshold data with a rippled-noise masker. *J. Acoust. Soc. Am., 62*(2), 409-415.

Joris, P. X., Bergevin, C., Kalluri, R., McLaughlin, M., Michelet, P., van der Heijden, M., and Shera, C. A. (2011). Frequency selectivity in Old-World monkeys corroborates sharp cochlear tuning in humans. *PNAS, 108*(42), 17516-17520.

Kowalewski, B. (2014). Modified notched-noise method for investigation of auditory filter shapes at high frequencies. In *Forum Acusticum*. Retrieved from http://www.fa2014.agh.edu.pl/fa2014_cd/article/RS/R17_11.pdf.

Lopez-Poveda, E.A. and Eustaquio-Martín, A. (2013). On the controversy about the sharpness of human cochlear tuning. *J. Assoc. Res. Otolaryngol., 14*(5), 673-686.

Macmillan, N. A. and Creelman, C. D. (2005). *Detection Theory: A User's Guide, 2nd Ed.* Mahwah, NJ: Lawrence Erlbaum Associates.

Moore, B. C. J., & Glasberg, B. R. (1981). Auditory filter shapes derived in simultaneous and forward masking. *J. Acoust. Soc. Am.*, *70*(4), 1003-1014.

Moore, B. C. J. and Glasberg, B. R. (1987). Formulae describing frequency selectivity as a function of frequency and level, and their use in calculating excitation patterns. *Hear. Res., 28*, 209-225.

Moore, B. C. J., Peters, R. W., and Glasberg, B. R. (1990). Auditory filter shapes at low center frequencies. *J. Acoust. Soc. Am., 88*(1), 132-140.

Niemiec, A. J., Yost, W. A., and Shofner, W. P. (1992). Behavioral measures of frequency selectivity in the chinchilla. *J. Acoust. Soc. Am., 92*(5), 2636-2649.

Nienhuys, T. G. W. and Clark, G. M. (1979). Critical bands following the selective destruction of cochlear inner and outer hair cells. *Acta Otolaryngol, 88*, 350-358.

Osmanski, M. S., Song, X., and Wang, X. (2013). The role of harmonic resolvability in pitch perception in a vocal nonhuman primate, the common marmoset (*Callithrix jacchus*). *J. Neurosci, 33*(21), 9161-9168.

Oxenham, A. J. and Simonson, A. M. (2006). Level dependence of auditory filters in nonsimultaneous masking as a function of frequency. *J. Acoust. Soc. Am., 119*(1), 444-453.

Patterson, R. D. (1971). Effect of amplitude on auditory filter shape. *J. Acoust. Soc. Am., 49*(1A), 81.

Patterson, R. D., Nimmo-Smith, I., Weber, D. L., and Milroy, R. (1982). The deterioration of hearing with age: Frequency selectivity, the critical ratio, the audiogram, and speech threshold. *J. Acoust. Soc. Am., 72*(6), 1788-1803.

Patterson, R. D. and Nimmo-Smith, I. (1980). Off-frequency listening and auditory filter asymmetry. *J. Acoust. Soc. Am., 67*(1), 229-245.

Pfingst, B. E., Laycock, J., Flammino, F., Lonsbury-Martin, B, and Martin, G. (1978). Pure tone thresholds for the rhesus monkey. *Hearing Research, 1*, 43-47.

Pick, G. F. (1980). Level dependence of psychophysical frequency resolution and auditory filter shape. *J. Acoust. Soc. AM., 68*(4), 1085-1095.

Pickles, J. O. (1979). Psychophysical frequency resolution in the cat as determined by simultaneous masking and its relation to auditory-nerve resolution. *J. Acoust. Soc. Am., 66*(6), 1725-1732.

Rosen, S. and Stock, D. (1992). Auditory filter bandwidths as a function of level at low frequencies (125 Hz – 1 kHz). *J. Acoust. Soc. Am., 92*(2), 773-781.

Ruggero, M. A. and Temchin, A. N. (2005). Unexceptional sharpness of frequency tuning in the human cochlea. *PNAS, 102*(51), 18614-18619.

Scharf, B. (1970). Critical bands. In J. Tobias (Ed.), *Foundations of Modern Auditory Theory, Vol. 1* (pp. 159-202). New York, NY: Academic Press, Inc.

Shailer, M. J., Moore, B. C. J., Glasberg, B. R., Watson, N., and Harris, S. (1990). Auditory filter shapes at 8 and 10 kHz. *J. Acoust. Soc. Am., 88*(1), 141-148.

Shera, C. A., Guinan, J. J., and Oxenham, A. J. (2002). Revised estimates of human cochlear tuning from otoacoustic and behavioral measurements. *PNAS, 99*(5), 3318-3323.

Sivian, L. J. and White, S. D. (1933). On minimum audible sound fields. *J. Acoust. Soc. Am., 4*(4), 288-321.

Stebbins, W. C., Green, S., and Miller, F. L. (1966). Auditory sensitivity of the monkey. *Science, 153*(3744), 1646-1647.

Weber, D. L. (1977). Growth of masking and the auditory filter. *J. Acoust. Soc. Am., 62*(2), 424-429.

SECTION II: CHANGES IN COCHLEAR ANATOMY, AUDITORY PHYSIOLOGY, AND AUDITORY PERCEPTION IN MACAQUE MONKEYS FOLLOWING NOISE-INDUCED PERMANENT THRESHOLD SHIFTS

CHAPTER 4

Changes in audiometric threshold and frequency selectivity correlate with cochlear histopathology in macaque monkeys with permanent noise-induced hearing loss

As reviewed in Chapter 1, acoustic overexposure can cause permanent hearing impairment associated with damage to the cochlea, such as hair cell loss. Although the audiogram is the standard clinical metric for assessing cochlear hearing loss, it can be a poor predictor of the severity and location of damage within the cochlea. We previously established a nonhuman primate model of noise-induced sensorineural hearing loss. As described in publications prepared with my colleagues (Valero et al. 2017, Hauser et al. 2018), acoustic overexposure abolished distortion product otoacoustic emissions, elevated auditory brainstem response thresholds, and caused significant loss of outer hair cells, inner hair cells, and ribbon synapses. Behavioral measures of hearing sensitivity, threshold shift rate, and temporal resolution revealed significant hearing impairments in quiet, steady-state noise, and amplitude-modulated noise. Audiometric thresholds and threshold shift rates were significantly correlated with the severity of cochlear histopathology.

In this study, we evaluated frequency selectivity, another aspect of hearing abilities, in macaques before and after acoustic overexposure. We then correlated this perceptual measure with hearing sensitivity loss and with metrics of cochlear histopathology: inner hair cell, outer hair cell, and ribbon synapse counts. The results suggested that audiometric thresholds and auditory filter widths were highly correlated with each other, as well as the severity and location of cochlear damage. Using more sophisticated statistical modeling than in our previous study (Hauser et al. 2018) allowed us to show that the best predictions of hearing abilities came from models that included both hair cell and synapse counts.

Burton, J. A., Mackey, C. A., MacDonald, K. S., Hackett, T. A., & Ramachandran, R. (2020). Changes in audiometric threshold and frequency selectivity correlate with cochlear histopathology in macaque monkeys with permanent noise-induced hearing loss. *Hear Res*, *398*, 108082. https://doi.org/10.1016/j.heares.2020.108082

4.1 ABSTRACT

Exposure to loud noise causes damage to the inner ear, including but not limited to outer and inner hair cells (OHCs and IHCs) and IHC ribbon synapses. This cochlear damage impairs auditory processing and increases audiometric thresholds (noise-induced hearing loss, NIHL). However, the exact relationship between the perceptual consequences of NIHL and its underlying cochlear pathology are poorly understood. This study used a nonhuman primate model of NIHL to relate changes in frequency selectivity and audiometric thresholds to indices of cochlear histopathology. Three macaques (one *Macaca mulatta* and two *Macaca radiata*) were trained to detect tones in quiet and in noises that were spectrally notched around the tone frequency. Audiograms were derived from tone thresholds in quiet; perceptual auditory filters were derived from tone thresholds in notched-noise maskers using the rounded-exponential fit. Data were obtained before and after a four-hour exposure to a 50-Hz noise centered at 2 kHz at 141 or 146 dB SPL. Noise exposure caused permanent audiometric threshold shifts and broadening of auditory filters at and above 2 kHz, with greater changes observed for the 146-dB-exposed monkeys. The normalized bandwidth of the perceptual auditory filters was strongly correlated with audiometric threshold at each tone frequency. While changes in audiometric threshold and perceptual auditory filter widths were primarily determined by the extent of OHC survival, additional variability was explained by including interactions among OHC, IHC, and ribbon synapse survival. This is the first study to provide within-subject comparisons of auditory filter bandwidths in an animal model of NIHL and correlate these NIHL-related perceptual changes with cochlear histopathology. These results expand the foundations for ongoing investigations of the neural correlates of NIHL-related perceptual changes.

4.2 INTRODUCTION

Hearing impairment causes significant perceptual deficits across the frequency and time domains (e.g. Moore, 1995). These deficits have been studied for decades using psychophysical measures in humans and animal models in order to quantify the perceptual changes underlying the global hearing difficulties reported by hearing impaired patients. Temporal and frequency resolution are impaired for many patients with hearing loss (e.g. Florentine et al. 1980; Hall and Grose 1989; Moore 1985; Moore 1995; Reed et al. 2009), with the degree of impairment often being related to severity of hearing loss. While quantifying these behavioral impairments helps guide appropriate treatment and rehabilitation strategies, the identification of specific underlying cochlear damage and associated neural changes provides an additional therapeutic target and helps elucidate the variability in rehabilitative success.

The link between auditory perception and indices of cochlear histopathology has been examined in animal models of ototoxicity, age-related hearing loss, and noise-induced hearing loss. Many of these studies were conducted in small-animal models (e.g. chinchilla: Ward & Duvall 1971, Clark & Bohne 1978, Ryan et al. 1979, Hamernik et al. 1989; cat: Miller et al. 1963; see early review by Saunders et al. 1991), and there is a comparatively smaller literature in nonhuman primates (reviewed in Burton et al. 2019). Most of this work was limited to examinations of audiometric thresholds, with little characterization of higher level auditory perceptual characteristics (however, see Radziwon et al. 2019). Systematic studies using the macaque model are relatively new and may serve as a bridge between the rodent and human literatures on noise-induced hearing loss (NIHL).

Our laboratory previously established a model of NIHL in macaque monkeys (Valero et al. 2017; Hauser et al. 2018). The macaque NIHL model provides the advantages of a close phylogenetic relationship to humans, thorough knowledge of the history of noise exposure, the ability to successfully complete complex listening tasks, and the opportunity to utilize more invasive neuroscientific methodologies such as single-unit neurophysiology and post-mortem cochlear histology and neuroanatomy (Burton et al. 2019). Noise overexposure to a narrowband stimulus resulted in frequency-specific but variable loss across subjects of outer hair cells (OHCs), inner hair cells (IHCs), and inner hair cell ribbon synapses (Valero et al. 2017). This anatomical damage was accompanied by perceptual deficits as measured by elevated tone detection thresholds in quiet, decreased threshold shift rates during masked tone detection, and

decreased release from masking during tone detection in sinusoidally amplitude modulated noise masker (Hauser et al. 2018). The characterization of this NIHL model is extended here to examine perceptual frequency selectivity measured using the notched-noise method in noise-exposed macaques. The aims of this study were 1) to examine the relationship between severity of noise-induced hearing loss and loss of frequency selectivity and 2) to examine the relationship between indices of cochlear histopathology as measured by OHC, IHC, and ribbon synapse survival and loss of hearing sensitivity and frequency selectivity. To the best of the authors' knowledge, this is the first report of perceptual auditory filters in an animal model of NIHL.

4.3 METHODS

Experiments were conducted on one male rhesus macaque (*Macaca mulatta,* Monkey L, ten years old at the time of noise exposure) and two male bonnet macaques (*Macaca radiata*, Monkey E and G, eleven and nine years old at the time of exposure, respectively), as well as a cohort of non-exposed male control subjects with normal hearing sensitivity (*Macaca mulatta, n* = 5, 6-10 years old). Macaques were maintained on a 12:12-h light:dark cycle and all procedures occurred between 8 AM and 6 PM during their light cycle. Monkeys E and G were socially housed; however, all other subjects were individually housed, per incompatibility for social housing as identified by repeated behavioral assessments. The macaques had visual, auditory, and olfactory contact with conspecifics maintained within the housing room, as well as daily visual, auditory, or olfactory supplemental enrichment. All procedures were approved by the Animal Care and Use Committee at the Vanderbilt University Medical Center and were in strict compliance with the National Institutes of Health guidelines for animal research.

Experiments were conducted in sound treated booths (Industrial Acoustics Corp, NY; Acoustic Systems, Austin, TX). During the task, monkeys sat in an acrylic primate chair that was custom designed for comfort and with no obstruction to sounds on either side of their heads (Audio chair, Crist Instrument Co., Hagerstown, MD). Monkeys were head-fixed via a surgically-implanted titanium head holder and trained to perform a Go/No-Go lever release task using fluid reward as positive reinforcement (for details about surgical preparation and behavioral task, see Dylla et al. 2013; Burton et al. 2018a). The monkey's head was fixed to the chair such that the head and ears directly faced the center of a loudspeaker at a distance of 36 inches. The loudspeaker (SA1 loudspeaker, Madisound, WI) and amplifier (SLA2, Applied

Research Technologies, Rochester, NY) were able to deliver sounds between 50 Hz and 40 kHz. Calibration using a 1/4" probe microphone (model 378C01, PCB Piezotronics Inc., Depew, NY) placed at the approximate entrance of the subjects' ear canals revealed that the output of the speakers varied by approximately ±3 dB across the frequency range. Tones and noise were delivered from the same loudspeaker.

4.3.1 Noise exposure

The details of the noise exposure matched those in in Valero et al. (2017) and Hauser et al. (2018). Briefly, the monkeys were treated with atropine (0.04 mg/kg) and sedated with a mixture of ketamine (10-15 mg/kg) and midazolam (0.05 mg/kg IM) prior to intubation. Sedation was maintained with 1-2% isoflurane and vital signs were monitored throughout the procedure. The noise exposure was conducted in a sound treated booth (Acoustic Systems, Austin, TX) while the monkey was lying prone on a table with the head slightly elevated. Closed-field loudspeakers (MF1, Tucker-Davis Technologies) were coupled to the subject's ears using 10 cm long PE tubing and pediatric ER-3A insert earphones that were trimmed and deeply inserted into each ear canal. A 50-Hz band of noise centered at 2 kHz was presented simultaneously to both ears via the insert earphones for four hours.

Monkey L was exposed at 141 dB SPL and Monkeys E and G were exposed at 146 dB SPL. This design allowed us to examine changes in frequency selectivity with varying degrees of hearing impairment and cochlear damage. The level of the exposure stimulus varied by less than 0.3 dB SPL over the course of the four-hour procedure. The monkeys were monitored intensively for a minimum of 72 hours post-procedure. Auditory brainstem responses and distortion product otoacoustic emissions were measured in separate sedated procedures pre- and post-exposure to supplement behavioral measures of hearing impairment (for further details, see Hauser et al. 2018).

4.3.2 Behavioral task

The behavioral task was identical to the methods described in Burton et al. (2018a). Briefly, the monkeys were trained to detect tones in quiet or embedded in noise maskers. To initiate a trial, the monkey pressed down on a lever (Model 829 Single Axis Hall Effect Joystick, P3America, San Diego, CA). After a variable hold time, a signal (tone, 80% of trials) or catch trial (no tone, 20% of trials) was presented. Upon correct lever release on signal trials, the monkey received a fluid reward. If the monkey did not release the lever during a signal trial, this

was taken to indicate non-detection, and no reward or penalty was administered. Lever release on catch trials resulted in a timeout penalty.

The experiments were controlled by a computer running OpenEx software (System 3, TDT Inc., Alachua, FL). Within each block, tone sound pressure levels spanned a 60 dB range and were randomly interleaved with catch trials. Flat spectrum broadband noise was generated from a uniform distribution and band-limited to 40 kHz. In experiments using masking noise, the level was constant at 50 dB SPL.

4.3.2.1 Tone detection in quiet

Pre- and post-exposure audiograms for each monkey were determined from tone detection performance in quiet, as reported previously (Hauser et al. 2018). Signal frequencies of 0.125, 0.25, 0.5, 1, 1.414, 2, 2.828, 4, 8, 16, and 32 kHz were chosen to span the audible range of macaques (Pfingst et al. 1978; Dylla et al. 2013) in octave steps with additional resolution near the noise exposure band. Audiograms were obtained prior to noise exposure and serial audiograms were obtained over the course of several weeks following noise exposure. Audiometric threshold shifts at each frequency were quantified by taking the difference between the post-exposure and pre-exposure tone detection thresholds in quiet at that frequency.

Here, we report audiometric threshold shifts from two post-exposure timepoints. The first set of audiometric threshold shifts were obtained a minimum of 5 weeks after the subject's noise exposure and just prior to collection of the data used to estimate frequency selectivity (Figure 4.1A; "Early Post-Exposure"). Post-exposure frequency selectivity data were not collected until a minimum of 60 days after the exposure, well after initial temporary threshold shifts had stabilized.

The second set of post-exposure audiometric thresholds were obtained following frequency selectivity data collection (Figure 4.1B; "Late Post-Exposure"). Due to the large behavioral task sets for each subject and variable completion rates for each task, post-exposure survival times were variable across subjects. Unexpectedly, we observed extensive changes in audiometric thresholds throughout post-exposure survival for two of the three subjects (Monkeys E and G). Late post-exposure audiometric thresholds were collected within one month of euthanasia for Monkeys L and E. Audiometric thresholds could not be obtained at a later time point for Monkey G, due to limited behavioral performance and likely profound deafness in the mid to high frequencies.

4.3.2.2 Tone detection in notched-noise masker

Modeled after Patterson and Nimmo-Smith (1980) and Glasberg et al. (1984b), the notched-noise methods used here were similar to those described in Burton et al. (2018a). In brief, tone detection performance was measured in the presence of two 50 dB SPL narrowband noise maskers (bandwidth = 0.4*f_0) placed symmetrically and asymmetrically around the tone frequency. Signal frequencies (f_0) were 0.5, 1, 1.414, 2, 2.828, 4, 8, and 16 kHz. (Note: 32 kHz was not tested due to bandwidth limitations of the speaker, which prevented the upper notched-noise bands from being presented at the specified level.) The normalized half notch widths ($\Delta f/f_0$) of the symmetric noise notches were 0.0, 0.05, 0.1, 0.2, 0.3, 0.5, 0.6, 0.65, and 0.8. Upward and downward shifted asymmetric notches were generated by shifting the high frequency edge of the lower band of noise $0.2f_0$ closer or farther from f_0, respectively, while maintaining a particular notch width ($\Delta f/f_0$ = 0.3, 0.4, 0.5, 0.6, 0.65, and 0.8). Detection performance was measured and filters estimated pre-exposure and beginning a minimum of 60 days after noise exposure.

4.3.3 Calculation of behavioral thresholds

Behavioral performance was analyzed according to signal detection theoretic methods, as described in Dylla et al. (2013), Bohlen et al. (2014), and Burton et al. (2018a). Briefly, at each tone level (*level*), hit rate was calculated (*H(level)*) based on the proportion of releases on trials with the tone at that sound level. False alarm rate (*FA*) was calculated based on the proportion of releases on catch trials. Based on signal detection theory, *H(level)* and *FA* were then converted into units of standard deviation of a standard normal distribution (*z*-score, norminv in MATLAB) to estimate *d'* according to $d'(level) = z\big(H(level)\big) - z(FA)$ (Macmillan and Creelman 2005). Because we wanted these results to serve as a baseline for neurophysiological studies where we would measure (noise) and (signal+noise) representation distributions, we converted the Yes/No analysis to a 2-alternative forced choice analysis and calculated the behavioral accuracy at each tone level using the probability correct (*pc*) metric as follows: $pc(level) = z^{-1}(d'(level)/2)$. Here, the inverse z transform (z^{-1}) converts a unique number of standard deviations of a standard normal distribution into a probability correct (normcdf in MATLAB). The conversion of *d'* to the *pc* measure was to facilitate the comparison of psychometric functions with neurometric functions obtained from neuronal responses using distribution free methods. The traditional threshold estimated at *d'*=1 corresponds to *pc(level)*=0.76.

The psychometric functions were fitted with a modified Weibull cumulative distribution function (cdf) according to $pc(level)_{fit} = c - d * e^{-\left(\frac{level}{\lambda}\right)^k}$, where *level* was the tone level (in dB SPL), λ represents the threshold parameter and *k* corresponds to the slope parameter. *c* represents the saturation probability correct, and *d* was the estimate of chance performance. Threshold was calculated from the fit as the tone level that resulted in a pc_{fit} value of 0.76.

4.3.4 Filter shape and bandwidth analyses

Assuming that each side of the auditory filter was a rounded exponential, estimates of filter shape were obtained from the tone detection thresholds as a function of notch width, as reported in Burton et al. (2018a). Briefly, asymmetric filter estimates were obtained using the default settings in the publicly available ROEX3 program, developed by B. C. J. Moore and B. R. Glasberg. The rounded exponential (roex) filter shape is described by: $W(g) = (1 - r) * (1 + p * g) * e^{-p*g} + r$, where g is the normalized deviation from the tone frequency ($g = \Delta f/f_0$), and *p* and *r* are adjustable parameters. A larger value of *p* indicates a larger slope and therefore a narrower filter. For asymmetric filters, p_l and p_u are used to describe the lower and upper sides of the filter, respectively. *r* corresponds to the shallow tail of the filter. The *W(g)* filter parameter values were iteratively adjusted in the software so as to achieve the smallest RMS difference between the predicted and actual threshold values.

Equivalent rectangular bandwidths were calculated from the p_l and p_u values, according to Glasberg et al. (1984b): $ERB(f_0) = f_0 * (2/p_l + 2/p_u)$. Change in frequency selectivity with hearing impairment was quantified according to the ratio: $ERB_{post-exposure}(f_0)/ERB_{baseline}\ (f_0)$.

4.3.5 Cochlear histological preparation and quantification

Histology and imaging were performed using procedures detailed previously (Valero et al. 2017). Briefly, following completion of the behavioral assays, animals were euthanized by an overdose of sodium pentobarbital (130 mg/kg), followed immediately by transcardial perfusion (2 liters 0.9% phosphate-buffered saline, PBS; 2 liters 4% phosphate-buffered paraformaldehyde, PFA). The round and oval windows were opened, cochleas perfused through the scala tympani with PFA, submerged in PFA for 2 hours, then transferred to 0.12 M EDTA for decalcification.

Decalcified cochleas were dissected into quarter turns to obtain epithelial whole mounts of the organ of Corti containing the hair cells and most of the osseous spiral lamina at each

location from base to apex. Immunohistochemistry was used to label pre-synaptic ribbons (mouse IgG1 anti-CtBP2 (C-terminal binding protein 2); BD Transduction Labs; 1:200); ii) glutamate receptor patches (mouse IgG2 anti-GluA2; Millipore; 1:200), iii) hair cell cytoplasm (rabbit anti-myo7a (myosin VIIa); Proteus Biosciences; 1:200), and iv) cochlear afferent and efferent fibers (chicken anti-NFH (neurofilament-H); Chemicon; 1:1000). Tissue was incubated in species-appropriate fluorescent secondary antibody conjugates (AlexaFluor) for secondary detection.

The tissue was imaged on a Leica SP8 confocal microscope, using a 63X glycerol objective (1.3 N.A.), to acquire 3-dimensional image stacks at each of 8 octave-spaced positions along the cochlear spiral from 0.125 to 32 kHz, with half-octave spacing in regions of significant hair cell loss. The frequency correlate of each image stack was computed from a cochlear frequency map based on a Greenwood function (Greenwood 1990), assuming an upper frequency limit of 45 kHz. OHC, IHC, and ribbon synapse counts were averaged across two adjacent stacks for each cochlear place. Amira software (Visage Imaging) was used to quantify IHC afferent synapses from confocal z-stacks by identification of thresholded CtBP2-labeled puncta within hair cells. Normative ribbon synapse counts (per IHC) were defined as the mean count within non-exposed ears for each frequency region. Synapse counts from the exposed cochleas were compared to the normative values to determine percentage synapse survival along the cochlear length. Hair cell survival was assessed in low-power confocal z-stacks by counting cuticular plates normalized to the expected number of hair cells within each row.

4.3.6 Statistical analyses

All statistical analyses were completed in MATLAB (2018a; Mathworks Inc.). One-sample *t*-tests were used to compare post-exposure *ERB* values for each subject to mean *ERB* values compiled from pre-exposure and control macaques across different tone frequencies. Bonferroni corrections were applied to adjust for multiple comparisons. Specifically, *p*-values of 0.05, 0.01, and 0.001 were adjusted to 0.0023, 4.55×10^{-4}, and 4.55×10^{-5}, respectively, since twenty-two comparisons were completed.

Using the "fitlm" and "fitnlm" functions in MATLAB, simple linear regressions and exponential nonlinear regressions were applied to the normalized ERB (ERB/f_0) by absolute audiometric threshold data (Figure 4.6A) to compare with previous literature. All data points were included in each regression analysis. The best model was determined according to the

lowest Bayesian information criterion (BIC) value, which adds a penalty for the number of model parameters in order to avoid overfitting. These same analyses were completed for data comparing the ERB ratio and audiometric threshold shift (Figure 4.6B), and for data comparing OHC, IHC, and ribbon synapse survival with audiometric threshold shift (Figure 4.8) and *ERB* ratio (Figure 4.9). Finally, stepwise multivariate linear regression models ("stepwiselm", with and without interactions included) were used to describe the relationship between audiometric threshold shift or *ERB* ratio with frequency and indices of cochlear histopathology (OHC, IHC, and ribbon synapse survival). This model fitting procedure systematically removes factors and interaction terms that do not add significant explanatory power to the model. The "plotResiduals" function was used to assess whether linear regressions were appropriate for use in the models.

In an attempt to provide the most legitimate comparisons, we used audiometric threshold shift data from two post-exposure timepoints (see Section 4.3.2.1) in the following ways: 1) audiometric threshold shifts from the early post-exposure timepoint were compared to frequency selectivity metrics due to the close relationship in time and 2) audiometric threshold shifts from the late post-exposure timepoint were compared to the indices of cochlear histopathology (OHC, IHC, and ribbon synapse survival) due to their closer relationship in time. While regressions between the frequency selectivity data and cochlear histology are inconvenienced by a long and variable time delay between behavioral data collection and cochlear harvesting, we believe that this represents a conservative comparison that still provides meaningful insight into the relationship between cochlear integrity and a facet of auditory perception.

4.4 RESULTS

4.4.1 Tone detection in quiet

Tone detection in quiet was assessed before and after noise exposure in order to assess the degree of permanent hearing impairment. Figure 4.1A shows audiometric threshold shifts for the three noise-exposed subjects, roughly 5 weeks post-exposure and just prior to measurement of frequency selectivity ("Early Post-Exposure"). Significant threshold shifts were observed at and above the center frequency of the exposure band (grey box; 2 kHz), as reported in Hauser et al. (2018). Threshold shifts were similar for Monkeys L and E and greatest for Monkey G, even though both Monkeys G and E were exposed at 146 dB SPL, and Monkey L was exposed at 141

dB SPL. All monkeys showed a peak in threshold shift roughly one half octave above the exposure band, which is similar to the high frequency, notched configuration observed in humans with noise-induced hearing loss (Gelfand 2009). Both monkeys exposed at the higher level showed a second peak in their threshold shift patterns at the highest frequency tested. This extreme basal peak, while tonotopically inappropriate given the exposure band, is typical of permanent threshold shifts after acute exposures (e.g. Moody et al. 1978).

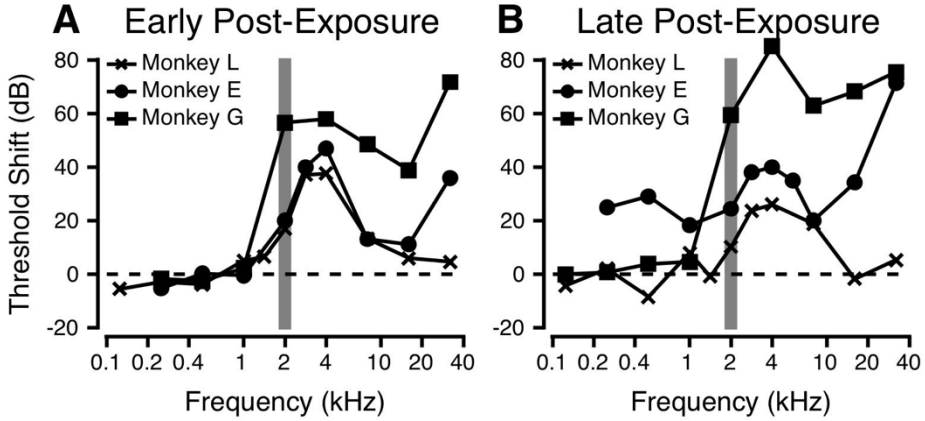

Figure 4.1. Audiometric threshold shift (dB) plotted as a function of frequency (kHz) for Monkey L (×), Monkey E (○), and Monkey G (□). Threshold shift was calculated as (post-exposure threshold – pre-exposure threshold). A. Early post-exposure threshold shifts collected a minimum of 5 weeks after the noise exposure and just prior to frequency selectivity data collection. B. Late post-exposure threshold shifts collected just prior to euthanasia (Monkey L and E) or at a later time point several months after frequency selectivity data collection (Monkey G).

Audiometric thresholds were monitored for 7 to 27 months post-exposure (Figure 4.1B; "Late Post-Exposure"). While the general patterns remained similar, the severity of threshold shift increased for the two cases exposed at 146 dB SPL (Monkeys E and G). Such ongoing threshold shifts are consistent with reports of accelerated age-related audiometric shifts in mice and humans with NIHL (Fernandez et al. 2015; Gates et al. 2000). Due to this change in audiometric thresholds over time, each timepoint was utilized for different comparisons, as outlined in Section 4.3.6.

4.4.2 Auditory filters

Tone detection thresholds in notched-noise maskers were obtained from psychometric functions (Figure 4.2). Prior to noise exposure (Figure 4.2A), tone detection threshold (dashed line) decreased with increasing notch width ($g = \Delta f/f_0$; normalized deviation from the tone frequency) as expected (e.g. Patterson and Nimmo-Smith 1980; Burton et al. 2018a). Post-

exposure, at frequencies with significant threshold elevation (such as 2.828 kHz, Figure 4.2B), thresholds decreased less for the same increase in notch width. At the same frequency and notch widths, Monkey G (with the poorest tone in quiet thresholds) also had higher masked thresholds than Monkey L and E.

Figure 4.3 compares pre- and post-exposure thresholds in notched-noise maskers centered around different tone frequencies, plotted as a function of *g* value. As reported

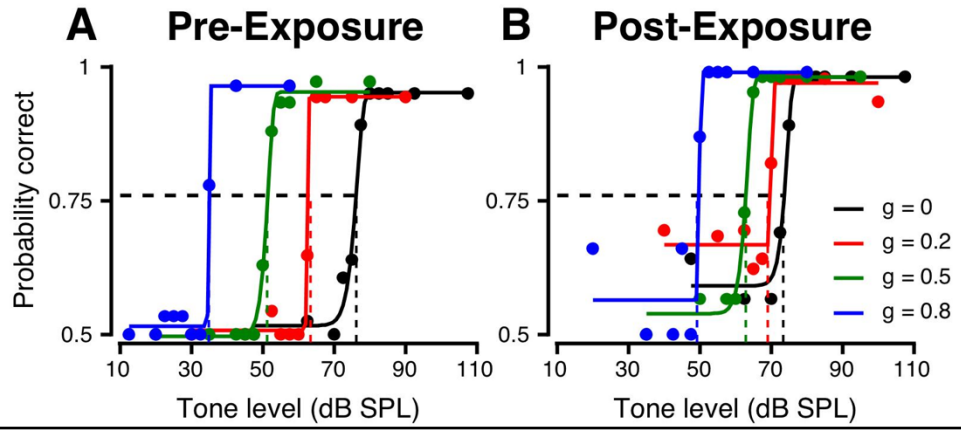

Figure 4.2. Psychometric functions for the detection of tones in notched noise. A: Psychometric functions for detection of a 2.828 kHz tone in a 50 dB SPL/Hz masker in a normal hearing macaque (Monkey L, pre-exposure). Lines of different colors represent various *g* values. *g*-values shown are 0 (black), 0.2 (red), 0.5 (green), and 0.8 (blue). B: Similar to A, but following noise exposure at 141 dB SPL for 4 hours (Monkey L, post-exposure). In both panels, horizontal dashed line represents *pc* = 0.76, and the vertical lines represent the tone levels required to evoke such performance.

previously, pre-exposure threshold vs. *g* functions had negative slopes (Figure 4.3A-C) (Burton et al. 2018a). Post-exposure (Figure 4.3D-F), these functions were usually shallower for frequencies ≥ 2 kHz (red lines). In particular, the 2-8 kHz functions were nearly flat post-exposure, suggesting broader filters after damage.

Perceptual auditory filters obtained using asymmetric notches are shown in Figure 4.4 for each subject before and after noise exposure. Pre-exposure, relative filter bandwidths (Figure 4.4A-C) decreased with increasing tone frequency, consistent with previous reports (e.g. Moore and Glasberg 1987; Burton et al. 2018a). Post-exposure, filters appear unchanged at frequencies < 2 kHz (Figure 4.4D-F; black) and were generally broader at frequencies ≥ 2 kHz (Figure 4.4D-F; red), except at 16 kHz for Monkey L and at 8 and 16 kHz for Monkey E.

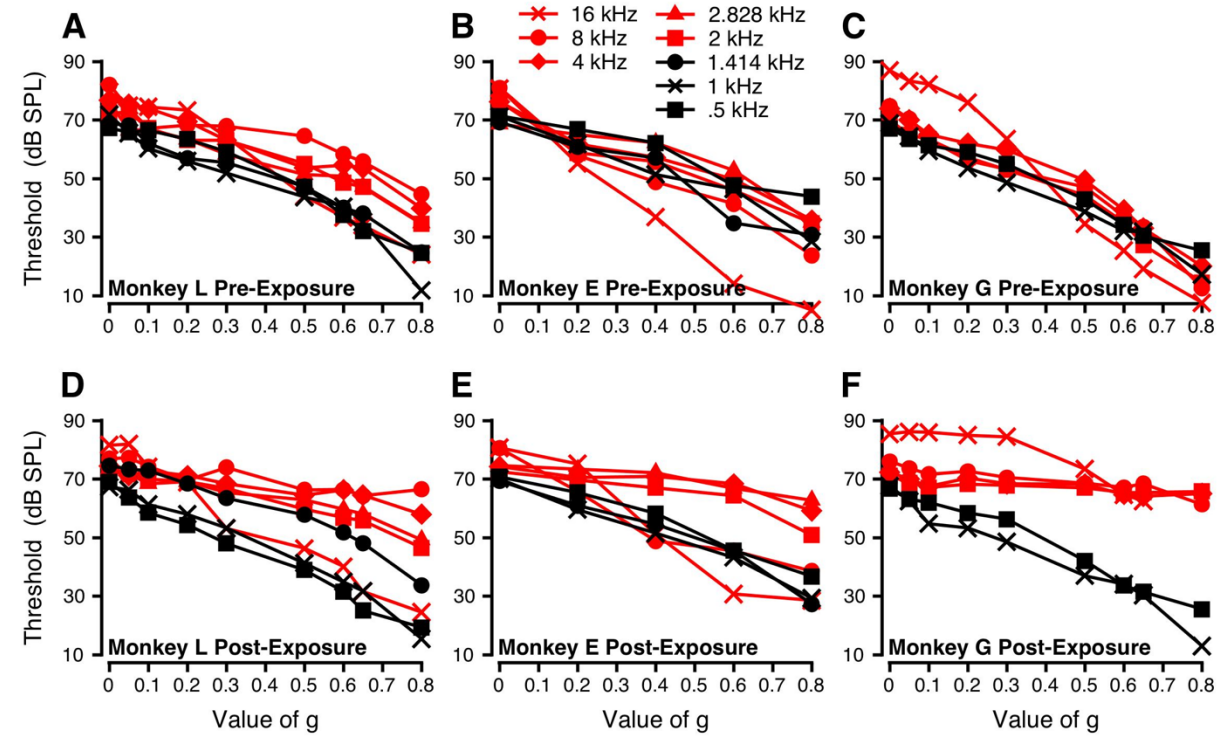

Figure 4.3. Threshold (in dB SPL) as a function of *g*, the normalized notch width. A-C: Pre-exposure data for Monkey L, E, and G, respectively. D-F: Post-exposure data for Monkey L, E, & G, respectively. Frequencies below the noise exposure band are shown in black (0.5 kHz: □, 1 kHz: ×, 1.414 kHz: ○). Frequencies at and above the noise exposure band are shown in red (2 kHz: □, 2.828 kHz: △, 4 kHz: ◇, 8 kHz: ○, 16 kHz: ×).

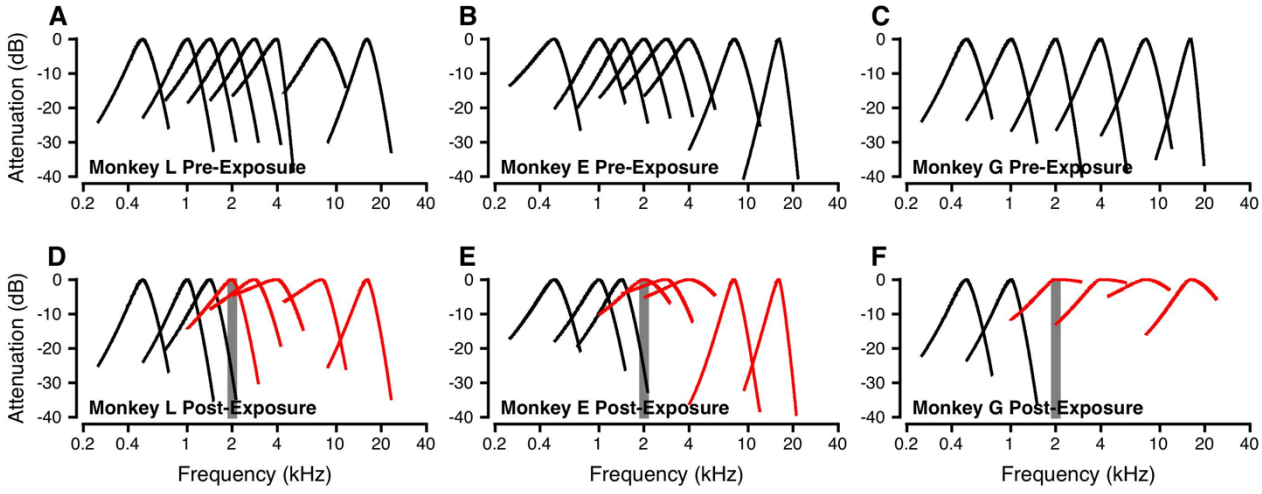

Figure 4.4. Asymmetric auditory filters across the macaque audible frequency range. A-C: Pre-exposure filters estimated for Monkey L, E, and G, respectively. D-F: Post-exposure filters estimated for Monkey L, E, and G, respectively. Filters for frequencies below the noise exposure band are shown in black (0.5-1.414 kHz). Filters for frequencies at and above the noise exposure band are shown in red (2-16 kHz). Gray bars illustrate the spectral range of the noise exposure stimulus.

To quantify filter shapes, the equivalent rectangular bandwidth (*ERB*) was measured (Figure 4.5A and Table 4.1). Pre-exposure, *ERB* values increased with increasing frequency, consistent with previous reports in other species and in macaques (e.g. Humans: Glasberg and Moore, 1986; Macaques: Burton et al. 2018a; Marmosets: Osmanski et al. 2013; Chinchilla: Niemiec et al. 1992). Post-exposure *ERB* values (Figure 4.5A, red lines) were significantly greater (i.e. broader tuning) at most frequencies above the exposure band, when compared to five normal-hearing macaques (Figure 4.5A, black, mean and standard deviation; see Table 4.2 for one-sample *t*-test statistics).

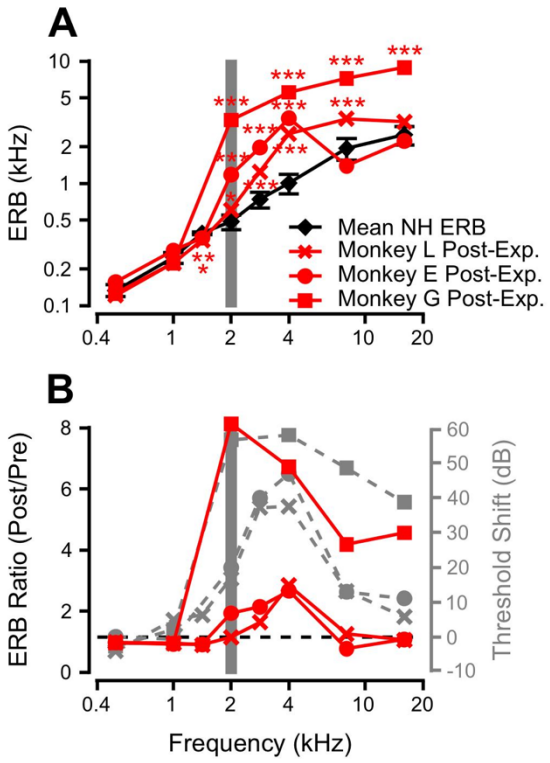

Figure 4.5. Filter bandwidth estimates. A: Equivalent rectangular bandwidth (*ERB*) as a function of frequency. Mean data (± one standard deviation) for pre-exposure and control macaques (◇) and post-exposure data for Monkey L (×), Monkey E (○), and Monkey G (□). Post-exposure *ERB* values that significantly differed from mean control values are marked with asterisks (see Table 4.2 for statistics). B: *ERB* ratio (post-exposure/pre-exposure, red) as a function of frequency for Monkey L (×), Monkey E (○), and Monkey G (□). The horizontal dashed line represents an *ERB* ratio of 1, and indicates equal pre- and post-exposure *ERB* values. Early post-exposure audiometric threshold shifts for each subject (from Figure 1A) are plotted in gray for comparison with the same symbol designations. Gray bars illustrate the spectral range of the noise exposure stimulus.

Table 4.1 – ERB values (in Hz) of asymmetric auditory filters for a cohort of normal hearing macaques and for Monkey L, Monkey E, and Monkey G before and after noise exposure.

Frequency (kHz)	Mean (stdev) Normative ERB Values	Monkey L ERB Values		Monkey E ERB Values		Monkey G ERB Values	
		Pre-Exposure	Post-Exposure	Pre-Exposure	Post-Exposure	Pre-Exposure	Post-Exposure
0.5	133.1 (15.22)	124.7	120.9	160.5	156.0	130.7	125.6
1	246.2 (25.54)	234.7	222.9	305.6	282.4	237.7	222.5
1.414	390.3 (8.34)	384.7	342.6	391.2	357.3	--	--
2	483.8 (64.83)	532.5	606.1	607.4	1173.0	405.5	3296.7
2.828	735.8 (105.3)	762.9	1243.1	918.6	1961.5	--	--
4	1002.2 (182.8)	895.7	2539.7	1283.9	3410.4	825.5	5548.0
8	1932.8 (393.0)	2693.8	3364.9	1799.8	1389.8	1729.6	7229.4
16	2491.3 (425.2)	3023.2	3189.1	2067.9	2218.5	1947.1	8869.6

Table 4.2 – One-sample *t*-tests comparing post-exposure *ERB* values for Monkey L, Monkey E, and Monkey G to mean *ERB* values from a normal hearing cohort (including pre-exposure values for Monkeys L, E, and G).

Frequency (kHz)	***df*** **(*n*-1)**	**Monkey L**		**Monkey E**		**Monkey G**	
		t	***p*-value**	***t***	***p*-value**	***t***	***p*-value**
0.5	5	-1.96	0.1078	3.68	0.0142	-1.20	0.2839
1	7	-2.58	0.0365	4.00	0.00518	-2.63	0.0338
1.414	4	-12.80	0.00022**	-8.86	0.00090*	--	--
2	7	5.34	0.00108*	30.07	0.00001***	122.73	0.00001***
2.828	6	12.75	0.00001***	30.80	0.00001***	--	--
4	7	23.79	0.00001***	37.26	0.00001***	70.33	0.00001***
8	7	10.31	0.00002***	-3.91	0.005831	38.12	0.00001***
16	7	4.64	0.00237	-1.82	0.1124	42.43	0.00001***

* significant at $p < 0.05$ level after Bonferroni correction to $p = 0.0023$

** significant at $p < 0.01$ level after Bonferroni correction to $p = 4.55*10^{-4}$

*** significant at $p < 0.001$ level after Bonferroni correction to $p = 4.55*10^{-5}$

The *ERB* ratio (post-exposure ERB/pre-exposure ERB) allows for within-subject normalization, with values > 1 indicating broader filters post-exposure. Plotting ERB ratios (red in Figure 4.5B) with the audiometric threshold shifts from Figure 4.1A (grey in Figure 4.5B) shows that filter bandwidths were wider at frequencies with larger threshold shifts, consistent with previous reports in humans (e.g. Tyler et al. 1984; Glasberg and Moore 1986; Desloge et al. 2012).

4.4.3 Frequency selectivity as a function of hearing impairment

To further compare frequency selectivity and audiometric threshold shift, normalized *ERB* (*ERB*/f_0) was plotted as a function of absolute audiometric threshold (dB SPL) for each subject using pre- and early post-exposure values (Figure 4.6A), after Glasberg and Moore (1986). Linear and nonlinear regressions were compared to determine the best fit. The relation between normalized *ERB* and audiometric threshold was best described by a one-term exponential function ($y = 0.2368 + 0.0086 * e^{(0.0836*x)}$; $R^2 = 0.885$, $p = 1.54\text{x}10^{-19}$) according to the BIC, as shown by the solid black line.

The relation between *ERB* ratios (post-exposure/pre-exposure) and audiometric threshold shift was also best fit with a one-term exponential function (Figure 4.6B; $y = 0.854 + 0.1166 * e^{(0.0698*x)}$; $R^2 = 0.889$, $p = 2.50\text{e-}9$) according to the BIC. The exponential relations in Figures 4.6A and 4.6B show that frequency selectivity is relatively unaffected with up to approximately 30 dB of audiometric threshold shift, but degrades rapidly as thresholds rise above that value.

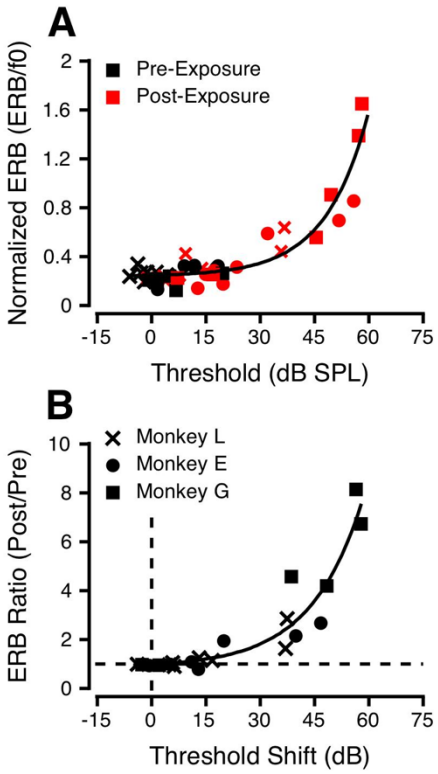

Figure 4.6. Relationship between audiometric changes and changes in the bandwidth of perceptual filters. A: Normalized *ERB* (*ERB*/f_0) as a function of absolute audiometric threshold (dB SPL) for Monkey L (×), Monkey E (○), and Monkey G (□), pre-exposure (black) and post-exposure (red; early post-exposure timepoint). The solid black line is a single exponential fit to all data points ($y = 0.2368 + 0.0086 * e^{(0.0483*x)}$). B: *ERB* ratio (post-exposure ERB/pre-exposure ERB) as a function of audiometric threshold shift (early post-exposure – pre-exposure) for Monkey L (×), Monkey E (○), and Monkey G (□). The horizontal dashed line indicates an *ERB* ratio of 1 (equal pre- and post-exposure *ERB* values). The vertical dashed line indicates a threshold shift of 0 (equivalent pre- and post-exposure audiometric thresholds). The solid black line is a single exponential fit to all data points ($y = 0.854 + 0.117 * e^{(0.0698*x)}$).

4.4.4 Audiometric threshold shift and frequency selectivity as a function of cochlear histopathology

Cochleas were extracted for histopathological analysis at various delays after the late post-exposure audiometric threshold shifts in Figure 4.1B (for details, see Section 4.3.2.1). As expected, hair cell loss was more extensive among OHCs than IHCs, and was worse at high-frequency regions (above the exposure band) than below (Figure 4.7). The loss of IHC ribbon synapses extended a bit further apically than the loss of IHCs (Figure 4.7B'', 4.7C''). However, all three survival metrics in each ear followed similar apical-basal patterns. The degree of lesion asymmetry between the two ears was unexpectedly large for two of the subjects. Nevertheless, since the behavioral measures were obtained free-field, we elected to average the histopathological metrics across both ears of each animal. This approach is supported by several studies reporting that binaural thresholds are lower than monaural thresholds, implying binaural summation during signal detection (e.g. Gage 1932; Shaw, Newman, & Hirsh, 1947; Hirsh 1948;

Pollack 1948; Hempstock, Bryan, & Webster 1966; Heil 2014) as opposed to listening with the "better ear". Consistent with this, the regression and mixed effects analyses that were conducted using the "better ear" or the "poorer ear" histological data generally resulted in poorer, often non-significant models (data not shown).

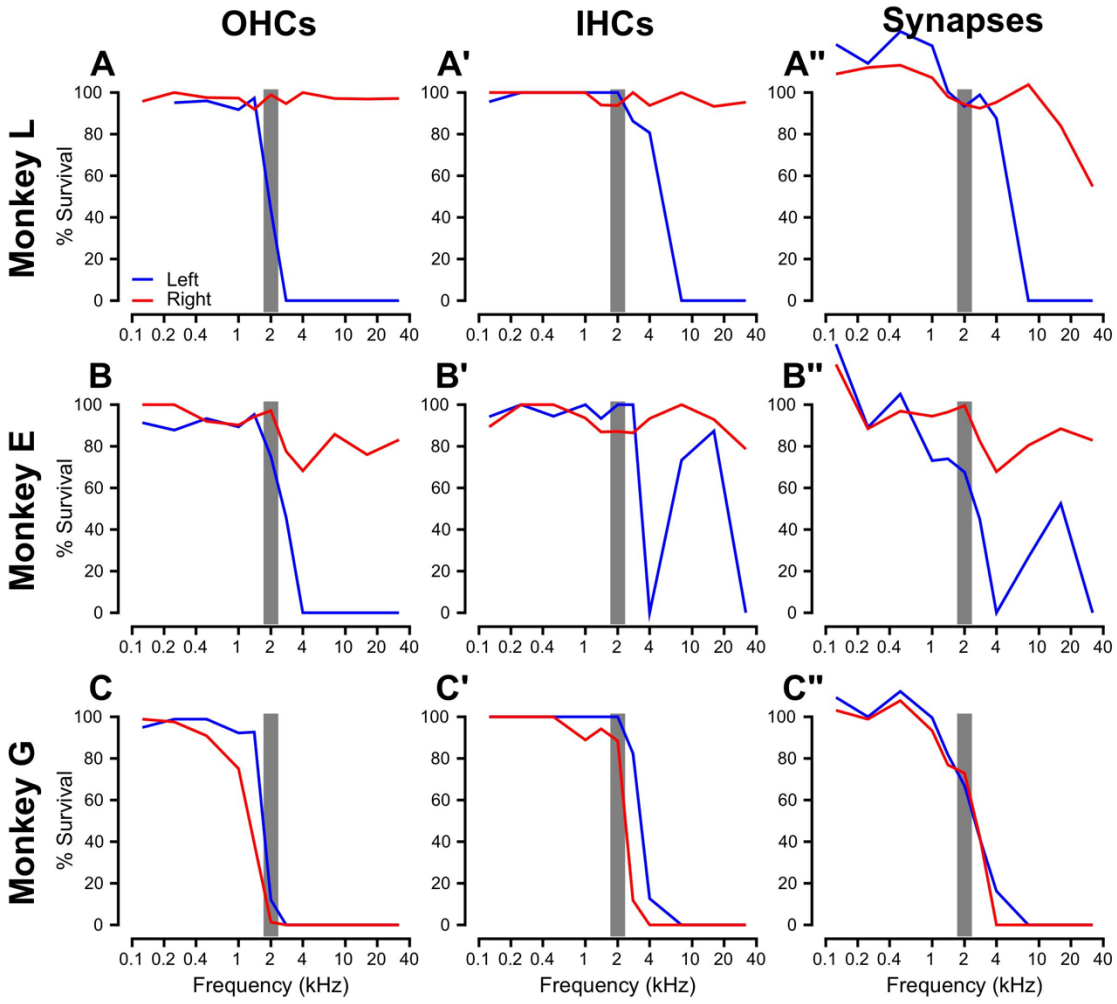

Figure 4.7. Percentage survival of outer hair cells (A, B, C), inner hair cells (A', B', C'), and ribbon synapses (A", B", C") as a function of cochlear frequency place for each of the noise-exposed monkeys. Data are shown for each subject (Monkey L: A-A"; Monkey E: B-B"; Monkey G: C-C") with separate traces for the left ear (blue) and right ear (red). Gray bars illustrate the spectral range of the noise exposure stimulus.

Figure 4.8 shows the relations between late post-exposure audiometric threshold shifts and each histopathological metric at the appropriate cochlear place. As expected, threshold shifts were negatively correlated with all three metrics. According to the BIC, one-term exponential functions provided the best fit for mean survival of OHCs ($y = 0.0095 + 72.71 * e^{(-0.0236*x)}$; $R^2 = 0.701$, $p = 1.56e\text{-}07$), IHCs ($y = 4.128 * + 69.54 * e^{(-0.0199*x)}$; $R^2 = 0.554$, $p = 2.76e\text{-}05$),

and ribbon synapses ($y = -63.19 * + 130.11 * e^{(-0.0057*x)}$; $R^2 = 0.586$, $p = 1.04e\text{-}05$). These models suggest that audiometric threshold shift increases exponentially with increasing severity of cochlear damage.

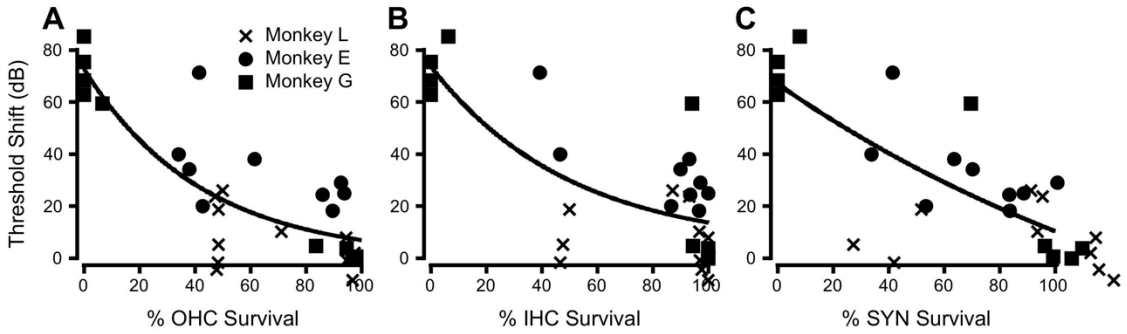

Figure 4.8. Relationship between audiometric threshold shift and cochlear histopathology. A: Late post-exposure audiometric threshold shift as a function of outer hair cell survival at each corresponding signal/cochlear frequency place for Monkey L (×), Monkey E (○), and Monkey G (□). The solid black line is a one term exponential fit to all data points ($y = 0.0095 + 72.71*\exp(x*(-0.0236))$). B: Same as in A, but for inner hair cell survival. Data are fit with a one term exponential function ($y = 4.128 + 69.54*\exp(x*(-0.0199))$). C: Same as in A and B, but for ribbon synapse survival. Data are fit with a one term exponential function ($y = -63.19 + 130.11*\exp(x*(-0.0057))$).

ERB ratio was also negatively correlated with survival of OHCs, IHCs, and ribbon synapses (Figure 4.9). However, for this outcome measure, linear models provided the best fit for mean survival of OHCs ($y = 4.7965 + x*(-0.045429)$; $R^2 = 0.603$, $p = 2.13e\text{-}05$), IHCs ($y = 4.5207 + x*(-0.03125)$; $R^2 = 0.28$, $p = 0.011$), and ribbon synapses ($y = 4.4397 + x*(-0.031949)$; $R^2 = 0.326$, $p = 0.0055$). These models suggest that *ERB* ratio increases linearly with increasing

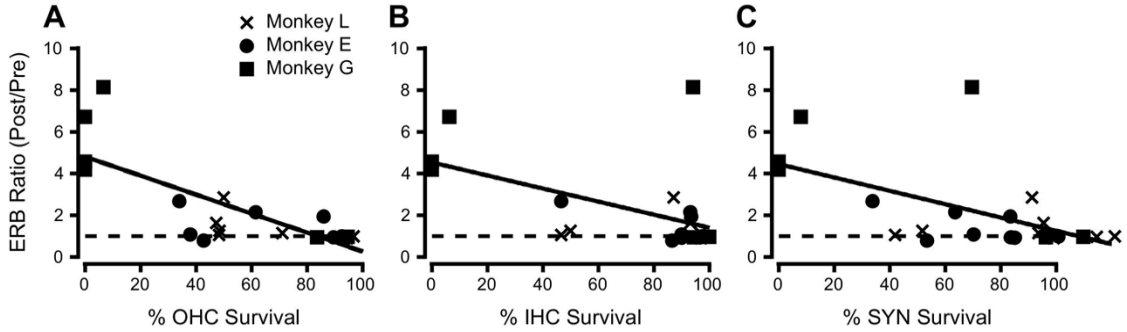

Figure 4.9. Relationship between frequency selectivity and cochlear histopathology. A: *ERB* ratio as a function of outer hair cell survival at each corresponding signal/cochlear frequency place for Monkey L (×), Monkey E (○), and Monkey G (□). The solid black line is a linear fit to all data points ($y = 4.7965 + x*(-0.045429)$). An *ERB* ratio of 1 (horizontal dashed line) indicates equivalent pre- and post-exposure *ERB* values. B: Same as in A, but for inner hair cell survival. Data are fit with a linear function ($y = 4.5207 + x*(-0.03125)$). C: Same as in A and B, but for ribbon synapse survival. Data are fit with a linear function ($y =$

severity of cochlear damage. Similar models were obtained for normalized *ERB* (data not shown). Considering the long and variable delay between behavioral testing and histological analysis, the observed correlations may underestimate the strength of this relationship.

Since many of these measures co-varied, stepwise multivariate linear regression was used to model their relative contributions to audiometric threshold shift (Table 4.3.1 and 4.3.2) and frequency selectivity (Table 4.4.1 and 4.4.2). Models contained frequency and mean OHC, IHC, and ribbon synapse survival as predictor variables, and either audiometric threshold shift (late post-exposure timepoint) or *ERB* ratio as the dependent variable. When excluding variable interactions, the models included OHC survival as a significant coefficient (see Table 4.3.1 and 4.4.1 for coefficient statistics):

$Threshold\ Shift \sim 1 + OHC$ (R^2 = 0.626, p = 3.24e-07)

$ERB\ Ratio \sim 1 + OHC + Frequency$ (R^2 = 0.797, p = 2.67e-07)

However, when including interaction components, the models included several main effects and interaction terms (see Tables 4.3.2 and 4.4.2 for coefficient statistics):

$Threshold\ Shift \sim 1 + Frequency + OHC + IHC + Synapses + OHC * Frequency + IHC * Frequency + Synapses * Frequency + OHC * IHC + IHC * Synapses$ (R^2 = 0.893, p = 2.00e-07)

$ERB\ Ratio \sim 1 + Frequency + OHC + IHC + Synapses + Synapses * IHC + Synapses * OHC + Synapses * Frequency + IHC * Frequency$ (R^2 = 0.953, p = 2.2e-07)

Models including interaction terms provided higher R^2 values and were more favorable than the models excluding interaction terms according to the BIC values (see Table 4.5). It is important to note that the BIC aggressively penalizes models with a greater number of parameters in order to avoid overfitting. Overall, these models suggest that audiometric threshold shift and frequency selectivity may be primarily attributed to OHC loss, but additional variability may be determined by complex patterns of cochlear damage and interactions across cochlear components.

Table 4.3.1 – Stepwise multivariate linear regression model (without interactions) for describing audiometric threshold shift as a function of frequency and mean OHC, IHC, and ribbon synapse survival.

Term	**Coefficient**	***p*-value**
Intercept	61.641	1.76e-10
OHC	-0.61654	3.24e-07

Table 4.3.2 – Stepwise multivariate linear regression model (with interactions) for describing audiometric threshold shift as a function of frequency and mean OHC, IHC, and ribbon synapse survival.

Term	**Coefficient**	***p*-value**
Intercept	60.444	6.58e-05
Frequency	0.51428	0.38596
OHC	-5.1493	0.0045536
IHC	0.53219	0.031685
Synapses	2.5694	0.1508
OHC:Frequency	0.057208	0.045242
IHC:Frequency	-0.092825	0.0049246
Synapses:Frequency	0.067793	0.086125
OHC:IHC	0.050427	0.0071199
IHC:Synapses	-0.03513	0.055364

Table 4.4.1 – Stepwise multivariate linear regression model (without interactions) for describing frequency selectivity as a function of frequency and mean OHC, IHC, and ribbon synapse survival.

Term	**Coefficient**	***p*-value**
Intercept	6.8806	1.46e-09
Frequency	-0.21248	0.00043
OHC	-0.064223	5.91e-08

Table 4.4.2 – Stepwise multivariate linear regression model (with interactions) for describing frequency selectivity as a function of frequency and mean OHC, IHC, and ribbon synapse survival.

Term	**Coefficient**	***p*-value**
Intercept	5.2072	1.30e-05
Frequency	-0.049711	0.46
OHC	-0.3574	1.29e-05
IHC	0.32491	5.31e-05
Synapses	-0.15587	0.0043
IHC:Frequency	-0.033111	7.60e-05
Synapses:Frequency	0.039443	0.00015
Synapses:OHC	0.0038163	9.07e-05
Synapses:IHC	-0.0023705	0.0015

Table 4.5 – Comparing stepwise multivariate linear regression models with and without interactions for describing audiometric threshold shift and frequency selectivity as a function of frequency and mean OHC, IHC, and ribbon synapse survival.

	Audiometric Threshold Shift			**ERB Ratio**		
Stepwise Linear Regression Model	R^2	***p*-value**	**BIC Value**	R^2	***p*-value**	**BIC Value**
Without Interactions	0.626	3.24e-07	250.48	0.797	2.67e-07	66.50
With Interactions	0.893	2.00e-07	241.14	0.953	2.2e-07	53.02

4.5 DISCUSSION

These findings provide the first pre- and post-noise exposure, within-subject comparisons of auditory filter bandwidths in an animal model, along with post-exposure cochlear histological characterization. Due to the sophisticated behavioral capabilities of these subjects, hearing impaired macaques provide a valuable model system for investigating the mechanisms underlying the degradation of auditory performance following cochlear damage (Stebbins 1982; Burton et al. 2019). The relationship between cochlear damage and auditory performance is expected to be complex, since perception is the product of many neurophysiological and computational processing steps. These investigations will help draw connections between the

extensive literature on human psychoacoustics in the presence of hearing loss and physiological and anatomical investigations of animal auditory neuroscience.

4.5.1 Relationship between frequency selectivity and audiometric threshold following noise exposure

Macaque perceptual filter widths increased with increasing severity of NIHL, indicating poorer frequency selectivity with greater hearing impairment. Since the current study used an identical masker level for pre- and post-exposure measurements, differences in filter width cannot be attributed to differences in masking condition – a factor that often complicates comparisons between normal hearing and hearing-impaired listeners. These findings recapitulate numerous studies of auditory filters in humans with hearing impairment (e.g. Tyler et al. 1984; Glasberg and Moore 1986; Peters and Moore 1992; Leek and Summers 1993; Bernstein and Oxenham 2006; Hopkins and Moore 2011; Desloge et al. 2012; Shen et al. 2019). Furthermore, this study provides additional evidence for a relationship between degree of hearing loss and perceptual filter bandwidth for losses beyond a mild hearing impairment. Although some previous studies (e.g. Glasberg and Moore 1986; Laroche et al. 1992) have suggested using a linear fit for thresholds beyond a mild hearing loss (i.e. using a ~30 dB inflection point to delineate normal vs. impaired frequency selectivity), the current data and others (Dubno & Dirks 1989; Shen et al. 2019) support an exponential relationship. This exponential relationship may not have been apparent in the former studies because the data were collected at one tone frequency (1 kHz) across many subjects without regard to the frequency of greatest impairment (Glasberg and Moore 1986; Laroche et al. 1992). The current data and that of Shen et al. (2019) was compiled across multiple signal frequencies and subjects. Further factors that may contribute to the different trends observed include the inclusion of ERB values greater than 1.0, as well as differences in species.

As demonstrated here and in many previous investigations, perceptual frequency selectivity is typically normal or near normal for audiometric thresholds up to 30-40 dB HL and variably impaired in subjects with more than a mild hearing loss (Ryan et al. 1979; Hall et al. 1984; Glasberg and Moore 1986; Peters and Moore 1992; Florentine 1992; Laroche et al. 1992; Leek and Summers 1993; Sommers and Humes 1993; Moore 1995; Hopkins and Moore 2011; Desloge et al. 2012; Shen et al. 2019). Subsequently, auditory filter shapes are also highly variable across individuals with hearing impairment. For example, the low- and high- frequency

sides of filters can be affected independently (Tyler et al. 1984), as was seen in the 8 kHz filter from Monkey L (see Figure 4.4A and 4.4D). Additionally, measures of frequency selectivity can remain variable even when hearing thresholds (Lutman et al. 1991) or stimulus presentation level (Leek and Summers 1993; Sommers and Humes, 1993; Florentine et al. 1980; Desloge et al. 2012) were accounted for, with filter widths ranging from normal to 4-5 times the normal bandwidth for thresholds of 50 dB HL (Pick et al. 1977).

4.5.2 Relationship between noise-induced audiometric threshold shift and cochlear histopathology

An inverse relationship between indices of cochlear histopathology and hearing sensitivity has consistently been observed (e.g. Schuknecht 1955; Miller et al. 1963; Stebbins et al. 1979; Hauser et al. 2018). Several animal studies point to OHC loss as the primary determinant of the first 30-50 dB of hearing impairment (e.g. Ryan & Dallos 1975; Hawkins et al. 1976; Stebbins et al. 1979; Hamernik et al. 1989), whereas fractional IHC loss and selective ribbon synapse loss (i.e. synaptopathy) typically do not result in permanent threshold shifts (e.g. Lobarinas et al. 2013; Kujawa & Liberman 2009; Liberman & Kujawa 2017; Burton et al. 2018b). Liberman & Dodds (1984) report that both OHC and IHC damage can result in decreased sensitivity, but with distinct effects on other regions of the tuning curve. However, audiometric thresholds remain variable and difficult to predict purely based on OHC or IHC survival counts (e.g. Clark & Bohne 1978; Ward & Duvall 1971; Hunter-Duvar & Bredberg 1974; Hunter-Duvar & Elliott 1972, 1973; Moody et al. 1978; Luz et al. 1973; Suga & Lindsay 1976; Lonsbury-Martin et al. 1987; Ward & Duvall 1971; Schuknecht & Gacek 1993; Landegger et al. 2016). Stereocilia condition may be an important determinant of threshold shifts (Liberman & Dodds 1984; Engström 1984; Wang et al. 2002), since surviving hair cells are often severely compromised. Unfortunately, we have not yet developed methods to assess stereocilia condition in cochleas also prepared for counting ribbon synapses and hair cells.

The current data and stepwise multivariate linear regression modeling suggest that, while OHC damage plays a predominant role in determining audiometric threshold, interactions among cochlear structures may also contribute to the variability observed in previous work. While ribbon synapse loss alone is not known to cause audiometric threshold shifts (i.e. hidden hearing loss), the accumulation of additional cases and types of cochlear pathologies alongside immunohistochemical quantification of multiple cochlear components could improve

understanding of the relationship between audiometric threshold shift and bilateral OHC, IHC, and ribbon synapse loss.

Finally, a high degree of inter-subject and across-ear variability was observed in degree of noise-induced audiometric threshold shift and cochlear damage. Inter-subject differences in noise susceptibility have been reported previously (Bohne et al. 1999), and appear to be significantly greater for more genetically heterogeneous species (i.e. guinea pigs, nonhuman primates) compared to inbred mouse strains (Wang et al. 2002). However, a unique and unexpected finding in this study was the marked asymmetry in cochlear histopathology for two of the subjects. This contrasts with studies that suggest a high degree of within-subject across-ear symmetry (Bohne et al. 1999), but is consistent with reports of differential susceptibility between ears in humans (Chung et al. 1983; Landegger et al. 2016).

4.5.3 Relationship between noise-induced changes in perceptual frequency selectivity and cochlear histopathology

In the current study, little or no change in frequency selectivity was observed at frequencies with very little or no OHC, IHC, or ribbon synapse loss. Frequency selectivity degraded with increasing damage; in particular, OHC survival seemed to be a large contributor to auditory filter width. Previous work by Smith and colleagues (1987) showed impaired psychophysical tuning curves in patas monkeys with selective damage to outer hair cells. Taken together, these data are consistent with the idea that the active mechanism of the OHCs is a predictor of both the absolute sensitivity and frequency selectivity of the normal cochlea, as has been previously suggested (Glasberg & Moore 1986). These data are also consistent with reports that OHC loss is a major contributor to the first 30-40 dB of permanent hearing loss (Saunders et al. 1991).

Individual differences in frequency selectivity of hearing-impaired subjects may be explained in part by differences in underlying pathology. Even when the etiology of hearing loss is matched (e.g. noise-induced), filter widths may still be significantly variable for a given degree of threshold elevation (Laroche et al. 1992). This variability may be accounted for by the interaction components identified in the stepwise multivariate linear regression model. For example, frequency selectivity may be even broader when there is both OHC and ribbon synapse loss (i.e. OHC*Synapses interaction), as compared to OHC loss alone. Evaluation of stereocilia

condition may provide additional predictive power (Liberman & Dodds 1984) and should be assessed in future studies.

The relationship between cochlear damage and perceptual frequency selectivity remains highly variable, even in controlled animal studies (Ryan et al. 1979; Nienhuys and Clark 1979; Marean et al. 1998). These three studies examined changes in frequency selectivity as measured by psychophysical tuning curves (Ryan et al. 1979) or auditory filter widths (Nienhuys & Clark 1979; Marean et al. 1998) before and after ototoxic kanamycin treatment in animal models. Ryan et al. (1979) observed variable elevation of tuning curve thresholds, loss of tuning curve tips, and slight broadening of tuning curve widths in chinchillas with greater than 50 dB of hearing loss, which was typically associated with combined OHC and IHC loss. Similarly, Neinhuys and Clark (1979) found that filter bandwidths were unaffected in kanamycin-treated cats, even in the presence of complete OHC loss in the implicated frequency regions, unless IHC loss also exceeded 40%, providing further support for a model including interaction components. Finally, changes in notched-noise derived auditory filter width correlated with audiometric threshold shift in kanamycin-treated starlings (Marean et al., 1998), which exhibit mixed OHC and IHC loss. These correlations persisted throughout the course of kanamycin treatment and audiometric threshold recovery following hair cell regeneration. Given that estimates of perceptual frequency selectivity vary with methodology (e.g. Glasberg et al. 1984a, Eustaquio-Martin and Lopez-Poveda 2011), methodological differences should be noted and comparisons with the present study should be made with caution. While differences in species and methods of hearing loss induction also make comparisons difficult, these studies are still instructive for interpreting the present results, as they support a model in which perceptual frequency selectivity is determined by survival of multiple cochlear structures. This multivariate relationship was strongly supported in the current study ($R^2 = 0.953$), despite the long time delay (~4-18 months) between behavioral data collection and cochlear histopathological characterization that varied across subjects. The authors predict that the model could even be strengthened if the time delay was minimized.

4.5.4 Future directions: Frequency selectivity in other noise-induced cochlear pathologies

The approach of the present study could be extended to assess the relationship between cochlear histopathology and auditory perception in other pathologies. Recent investigations of noise-induced temporary threshold shifts (TTS) reveal that IHC ribbon synapse loss occurs prior to the OHC loss that is typically associated with permanent NIHL (Kujawa and Liberman, 2009;

Valero et al. 2017). Though TTS-induced synapse loss, or synaptopathy, does not result in decreased hearing sensitivity, it is suspected to affect suprathreshold auditory processing (e.g. Bharadwaj et al. 2014; Plack et al. 2014; Oxenham 2016). Frequency selectivity following TTS and the associated sub-clinical damage to the auditory periphery is not well-described. In a study of noise-exposed industrial workers, Bergman and colleagues (1992) found variable changes in frequency selectivity estimates accompanied by equally variable TTS after a work day. Acute TTS in humans also worsens frequency selectivity in noise-exposed normal hearing subjects (Feth et al. 1979; Klein and Mills 1981). However, the impaired frequency selectivity reported in these studies is likely dominated by reversible damage to OHCs during the TTS. Broader auditory filters and impaired frequency selectivity have been reported for normal hearing participants with impaired speech-in-noise perception, some of whom likely experienced synaptopathy subsequent to TTS (Pick and Evans 1983; Badri et al. 2011). Contributions from OHC loss cannot be ruled out in this study either, since many participants had subclinical audiometric notches and poorer extended high frequency thresholds compared to controls. Future studies examining frequency selectivity in animal models of synaptopathy could provide key evidence for distinguishing the contributions of specific cochlear components to impaired frequency selectivity and establishing appropriate therapeutic targets. These studies would also help establish the clinical utility of new methods for acquiring auditory filters, which may be both clinically feasible and sensitive to different hearing impairments (Shen et al. 2014; Shen et al. 2019).

4.6 ACKNOWLEDGMENTS

The authors would like to acknowledge Dr. Michelle Valero and the Liberman Lab for assistance with the histopathological analysis, Mary Feurtado for assistance with procedures involving anesthesia, Bruce Williams and Roger Williams for building experimental hardware, and Samantha Hauser, Evan Mercer, Jessica Feller, Namrata Temghare, and Alex Tarabillo for assistance with data collection. The authors thank Dr. Allison Leich Hilbun for her enthusiastic and expert assistance with the statistical analyses and modeling. The authors would also like to extend special acknowledgment to Dr. Brian C. J. Moore for his assistance with the rounded exponential fits, and to Dr. M. C. Liberman for helpful comments on earlier versions of the manuscript. Finally, the authors would like to acknowledge the National Institutes of Health and

the National Institute on Deafness and Other Communication Disorders for funding this research through the following grant support: R01 DC 011092 (PI: Ramnarayan Ramachandran), R01 DC 015988 (MPI: R. Ramachandran and B. Shinn-Cunningham), and T32 MH 064913 (PI: D. Winder). This study was also partly supported by the Vanderbilt Hobbs Discovery Grant to Ramnarayan Ramachandran.

4.7 REFERENCES

Badri, R., Siegel, J. H., and Wright, B. A. (2011). Auditory filter shapes and high-frequency hearing in adults who have impaired speech in noise performance despite clinically normal audiograms. *J Acoust Soc Am, 129*(2), 852-863.

Bergman, M., Najenson, T., Korn, C., Harel, N., Erenthal, P., and Sachartov, E. (1992). Frequency selectivity as a potential measure of noise damage susceptibility. *British Journal of Audiology, 26*(1), 15-22.

Bernstein, J. G. W. and Oxenham, A. J. (2006). The relationship between frequency selectivity and pitch discrimination: Sensorineural hearing loss. *J Acoust Soc Am, 120*(6), 3929-3945.

Bharadwaj, H. M., Verhulst, S., Shaheen, L, Liberman, M. C., and Shinn-Cunningham, B. G. (2014). Cochlear neuropathy and the coding of supra-threshold sound. *Frontiers in Systems Neuroscience, 8*(26), 1-17.

Bohlen, P., Dylla, M., Timms, C., and Ramachandran, R. (2014). Detection of modulated tones in modulated noise by non-human primates. *JARO, 15*, 801-821.

Bohne, B. A., Harding, G. W., Nordmann, A. S., Tseng, C. J., Liang, G. E., & Bahadori, R. S. (1999). Survival-fixation of the cochlea: a technique for following time-dependent degeneration and repair in noise-exposed chinchillas. *Hearing Research, 134,* 163-178.

Burton, J. A., Dylla, M. E., and Ramachandran, R. (2018a). Frequency selectivity in macaque monkeys measured using a notched-noise method. *Hearing Research, 357*, 73-80.

Burton, J. A., McCrate, J., Hauser, S., Mackey, C., Feller, J., & Ramachandran, R. (2018b). Temporal and spectral resolution in a nonhuman primate model of noise-induced hearing loss. Poster presented at the Auditory System Gordon Research Conference, Smithfield, RI.

Burton, J. A., Valero, M. D., Hackett, T. A., & Ramachandran, R. (2019). The use of nonhuman primates in studies of noise injury and treatment. *J Acoust Soc Am, 146*(5), 3770-3789.

Chung, D. Y., Willson, G. N., & Gannon, R. P. (1983). Lateral differences in susceptibility to noise damage. *Audiology*, 22(2), 199-205.

Clark, W. W. & Bohne, B. A. (1978). Animal model for the 4-kHz tonal dip. *Ann Otol Rhinol Laryngol, 87*(4 Pt 2 Suppl 51), 1-16.

Desloge, J. G., Reed, C. M., Braida, L. D., Perez, Z. D., and Delhorne, L. A. (2012). Auditory-filter characteristics for listeners with real and simulated hearing impairment. *Trends in Amplification, 16*(1), 19-39.

Dubno, J. R. and Dirks, D. D. (1989). Auditory filter characteristics and consonant recognition for hearing-impaired listeners. *J Acoust Soc Am, 85*(4), 1666-1675.

Dylla, M., Hrnicek, A., Rice, C., and Ramachandran, R. (2013). Detection of tones and their modification by noise in nonhuman primates. *JARO, 14*, 547-560.

Engström, B. (1984). Fusion of stereocilia on inner hair cells in man and in the rabbit, rat and guinea pig. *Scand Audiol, 13,* 87-92.

Eustaquio-Martin, A. and Lopez-Poveda, E. A. (2011). Isoresponse versus isoinput estimates of cochlear filter tuning. *J Assoc Res Otolaryngol, 12*(3), 281-299.

Feth, L. L., Oesterle, E. C., and Kidd, G. (1979). Frequency selectivity after noise exposure. *J Acoust Soc Am, 65*, S118.

Fernandez, K. A., Jeffers, P. W., Lall, K., Liberman, M. C., & Kujawa, S. G. (2015). Aging after noise exposure: acceleration of cochlear synaptopathy in "recovered" ears. *J Neurosci*, 35(19), 7509-7520.

Florentine, M. (1992). Effects of cochlear impairment and equivalent-threshold masking on psychoacoustic tuning curves. *Audiology, 31*, 241-253.

Florentine, M., Buus, S., Scharf, B., and Zwicker, E. (1980). Frequency selectivity in normally-hearing and hearing-impaired observers. *J Speech Hear Res, 23*, 646-669.

Gage, F. H. (1932). A note on the binaural threshold. *British Journal of Psychology*, 23(2), 148.

Gates, G. A., Schmid, P., Kujawa, S. G., Nam, B. H., & D'Agostino, R. (2000). Longitudinal threshold changes in older men with audiometric notches. *Hear Res*, 141(1-2), 220-228.

Gelfand, S. A. (2009). *Essentials of audiology* (3rd. ed.). New York, NY: Thieme Medical Publishers.

Glasberg, B. R. and Moore, B. C. J. (1986). Auditory filter shapes in subjects with unilateral and bilateral cochlear impairments. *J Acoust Soc Am, 79*(4), 1020-1033.

Glasberg, B. R., Moore, B. C. J., and Nimmo-Smith, I. (1984a). Comparison of auditory filter shapes derived with three different maskers. *J Acoust Soc Am, 75*(2), 536-544.

Glasberg, B. R., Moore, B. C. J., Patterson, R. D., and Nimmo-Smith, I. (1984b). Dynamic range and asymmetry of the auditory filter. *J Acoust Soc Am, 76*(2), 419-427.

Greenwood, D. D. (1990). A cochlear frequency-position function for several species – 29 years later. *J Acoust Soc Am 87*(6), 2591-2605.

Hall, J. W. and Grose, J. H. (1989). Spectrotemporal analysis and cochlear hearing impairment: Effects of frequency selectivity, temporal resolution, signal frequency, and rate of modulation. *J Acoust Soc Am, 85*(6), 2550-2562.

Hall, J. W., Tyler, R. S., and Fernandes, M. A. (1984). Factors influencing the masking level difference in cochlear hearing-impaired and normal-hearing listeners. *J Speech Hear Res, 27*, 145-154.

Hamernik, R. P., Patterson, J. H., Turrentine, G. A., and Ahroon, W. A. (1989). The quantitative relation between sensory cell loss and hearing thresholds. *Hearing Research, 38*, 199-212.

Hauser, S. N., Burton, J. A., Mercer, E. T., and Ramachandran, R. (2018). Effects of noise overexposure on tone detection in noise in nonhuman primates. *Hearing Research, 357,* 33-45.

Hawkins, J. E., Johnsson, L.-G., Stebbins, W. C., Moody, D. B., & Coombs, S. L. (1976). Hearing loss and cochlear pathology in monkeys after noise exposure. *Acta Otolaryngol, 81*, 337-343.

Heil, P. (2014). Towards a unifying basis of auditory thresholds: binaural summation. *JARO, 15*(2), 219-234.

Hempstock, T. I., Bryan, M. E., and Webster, J. B. C. (1966). Free field threshold variance. *Journal of Sound and Vibration, 4*, 33–44.

Hirsh, I. J. (1948). Binaural summation-a century of investigation. *Psychological Bulletin, 45*(3), 193.

Hopkins, K. and Moore, B. C. J. (2011). The effects of age and cochlear hearing loss on temporal fine structure sensitivity, frequency selectivity, and speech reception in noise. *J Acoust Soc Am, 130*(1), 334-349.

Hunter-Duvar, I. M. & Bredberg, G. (1974). Effects of intense auditory stimulation: Hearing losses and inner ear changes in the chinchilla. *J Acoust Soc Am, 55*(4), 795-801.

Hunter-Duvar, I. M. & Elliott, D. N. (1972). Effects of intense auditory stimulation: Hearing losses and inner ear changes in the squirrel monkey. *J Acoust Soc Am, 52*(4), 1181-1192.

Hunter-Duvar, I. M. & Elliott, D. N. (1973). Effects of intense auditory stimulation: Hearing losses and inner ear changes in the squirrel monkey. II. *J Acoust Soc Am, 54*(5), 1179-1183.

Klein, A. J. and Mills, J. H. (1981). Physiological and psychophysical measures from humans with temporary threshold shift. *J Acoust Soc Am, 70*(4), 1045-1053.

Kujawa, S. G. and Liberman, M. C. (2009). Adding insult to injury: Cochlear nerve degeneration after "temporary" noise-induced hearing loss. *J Neurosci, 29*(45), 14077-14085.

Landegger, L. D., Psaltis, D., & Stankovic, K. M. (2016). Human audiometric thresholds do not predict specific cellular damage in the inner ear. *Hearing Research, 335*, 83-93.

Laroche, C., Hétu, R., Quoc, H. T., Josserand, B., and Glasberg, B. (1992). Frequency selectivity in workers with noise-induced hearing loss. *Hearing Research, 64*, 61-72.

Leek, M. R. and Summers, V. (1993). Auditory filter shapes of normal-hearing and hearing-impaired listeners in continuous broadband noise. *J Acoust Soc Am, 94*(6), 3127-3137.

Liberman, M. C. & Dodds, L. W. (1984). Single-neuron labeling and chronic cochlear pathology. III. Stereocilia damage and alterations of threshold tuning curves. *Hearing Research, 16*, 55-74.

Liberman, M. C. & Kujawa, S. G. (2017). Cochlear synaptopathy in acquired sensorineural hearing loss: Manifestations and mechanisms. *Hearing Research, 349*, 138-147.

Lobarinas, E., Salvi, R., & Ding, D. (2013). Insensitivity of the audiogram to carboplatin induced inner hair cell loss in chinchillas. *Hearing Research, 302,* 113-120.

Lonsbury-Martin, B. L., Martin, G. K., & Bohne, B. A. (1987). Repeated TTS exposures in monkeys: Alterations in hearing, cochlear structure, and single-unit thresholds. *J Acoust Soc Am, 81*(5), 1507-1518.

Lutman, M. E., Gatehouse, S., & Worthington, A. G. (1991). Frequency resolution as a function of hearing threshold level and age. *J Acoust Soc Am, 89*(1), 320-328.

Luz, G. A., Mosko, J. D., Fletcher, J. L., & Fravel, W. J. (1973). The relation between temporary threshold shift and permanent threshold shift in rhesus monkeys exposed to impulse noise. *Acta Otolaryngol, 76*(Sup312), 5-15.

Macmillan, N. A. & Creelman, C. D. (2005). *Detection theory: A user's guide* (2nd ed.). Lawrence Erlbaum Associates, Mahwah, NJ.

Marean, G. C., Burt, J. M., Beecher, M. D., & Rubel, E. W. (1998). Auditory perception following hair cell regeneration in European starling (Sturnus vulgaris): Frequency and temporal resolution. *J Acoust Soc Am,103*(6), 3567-3580.

Miller, J. D., Watson, C. S., and Covell, W. P. (1963). Deafening effects of noise on the cat. *Acta Otolaryngol. Suppl. 176*, 1-84.

Moody, D. B., Stebbins, W. C., Hawkins, J. E., & Johnsson, L.-G. (1978). Hearing loss and cochlear pathology in the monkey (Macaca) following exposure to high levels of noise. *Arch Oto-Rhino-Laryng, 220,* 47-72.

Moore, B. C. J. (1995). Perceptual consequences of cochlear hearing loss and their implications for the design of hearing aids. *Ear & Hearing, 17*(2), 133-161.

Moore, B. C. J. (1985). Frequency selectivity and temporal resolution in normal and hearing-impaired listeners. *British Journal of Audiology, 19*, 189-201.

Moore, B. C. J. & Glasberg, B. R. (1987). Formulae describing frequency selectivity as a function of frequency and level, and their use in calculating excitation patterns. *Hear Res, 28*, 209-225.

Nienhuys, T. G. W. and Clark, G. M. (1979). Critical bands following the selective destruction of cochlear inner and outer hair cells. *Acta Oto-Laryngologica, 88,* 350–358.

Niemiec, A.J., Yost, W.A., Shofner, W.P. (1992). Behavioral measures of frequency selectivity in the chinchilla. *J Acoust Soc Am, 92*(5), 2636-2649.

Osmanski, M.S., Song, X., Wang, X., 2013. The role of harmonic resolvability in pitch perception in a vocal nonhuman primate, the common marmoset (Callithrix jacchus). *J Neurosci, 33*(21), 9161-9168.

Oxenham, A. J. (2016). Predicting the perceptual consequences of hidden hearing loss. *Trends in Hearing, 20,* 1-6.

Patterson, R. D. and Nimmo-Smith, I. (1980). Off-frequency listening and auditory filter asymmetry. *J. Acoust. Soc. Am., 67*(1), 229-245.

Peters, R. W. and Moore, B. C. J. (1992). Auditory filter shapes at low center frequencies in young and elderly hearing-impaired subjects. *J Acoust Soc Am, 91*(1), 256-266.

Pfingst, B. E., Laycock, J., Flammino, F., Lonsbury-Martin, B., and Martin, G. (1978). Pure tone thresholds for the rhesus monkey. *Hear Res, 1*, 43–47.

Pick, G. F. and Evans, E. F. (1983). Dissociation between frequency resolution and hearing threshold. In R. Klinke and R. Hartmann (Eds.), *Hearing: Physiological Bases and Psychophysics* (393-397). Berlin, Germany: Springer-Verlag.

Pick, G., Evans, E. F., and Wilson, J. P. (1977). Frequency resolution in patients with hearing loss of cochlear origin. In E.F. Evans and J.P. Wilson (Eds.), *Psychophysics and Physiology of Hearin*g (pp. 273-282). London: Academic Press.

Plack, C. J., Barker, D., & Prendergast, G. (2014). Perceptual consequences of "hidden" hearing loss. *Trends in Hearing, 18*, 1-11.

Pollack I. (1948). Monaural and binaural threshold sensitivity for tones and for white noise. *J Acoust Soc Am, 20,* 52–57.

Radziwon, K. E., Sheppard, A., & Salvi, R. J. (2019). Psychophysical changes in temporal processing in chinchillas with noise-induced hearing loss: A literature review. *J Acoust Soc Am, 146*(5), 3733-3742.

Reed, C. M., Braida, L. D., and Zurek, P. M. (2009). Review of the literature on temporal resolution in listeners with cochlear hearing impairment: A critical assessment of the role of suprathreshold deficits. *Trends in Amplification, 13*(1), 4-43.

Ryan, A. & Dallos, P. (1975). Effect of absence of cochlear outer hair cells on behavioural auditory threshold. *Nature, 253,* 44-46.

Ryan, A., Dallos, P., & McGee, T. (1979). Psychophysical tuning curves and auditory thresholds after hair cell damage in the chinchilla. *J Acoust Soc Am, 66*(2), 370-378.

Saunders, J. C., Cohen, Y. E., and Szymko, Y. M. (1991). The structural and functional consequences of acoustic injury in the cochlea and peripheral auditory system: A five year update. *J Acoust Soc Am, 90*(1), 136-146.

Schuknecht, H. F. (1955). Presbycusis. *The Laryngoscope, 65*(6), 402-419.

Schuknecht, H. F. and Gacek, M. R. (1993). Cochlear pathology in presbycusis. *Ann Otol Rhinol Laryngol 102*, 1-16.

Shaw, W. A., Newman, E. B., and Hirsh, I. J. (1947). The difference between monaural and binaural thresholds. *Journal of Experimental Psychology, 37,* 229–242.

Shen, Y., Kern, A. B., and Richards, V. M. (2019). Toward routine assessment of auditory filter shape. *JSLHR, 62*, 442-455.

Shen, Y., Sivakumar, R., and Richards, V. M. (2014). Rapid estimation of high-parameter auditory filter shapes. *J Acoust Soc Am, 136*(4), 1857–1868.

Smith, D. W., Moody, D. B., Stebbins, W. C., and Norat, M. A. (1987). Effects of outer hair cell loss on the frequency selectivity of the patas monkey auditory system. *Hearing Research, 29*, 125-138.

Sommers, M. S. and Humes, L. E. (1993). Auditory filter shapes in normal-hearing, noise-masked normal, and elderly listeners. *J Acoust Soc Am, 93*(5), 2903-2914.

Stebbins, W. C. (1982). Concerning the need for more sophisticated animal models in sensory behavioral toxicology. *Environmental Health Perspectives, 44*, 77-85.

Stebbins, W. C., Hawkins, J. E., Johnsson, L-G., & Moody, D. B. (1979). Hearing thresholds with outer and inner hair cell loss. *Am J Otolaryngology, 1*(1), 15-27.

Suga, F. & Lindsay, J. R. (1976). Histopathological observations of presbycusis. *Ann Otol, 85*, 169-184.

Tyler, R. S., Hall, J. W., Glasberg, B. R., Moore, B. C. J., and Patterson, R. D. (1984). Auditory filter asymmetry in the hearing impaired. *J Acoust Soc Am, 76*(5), 1363-1368.

Valero, M. D., Burton, J. A., Hauser, S. N., Hackett, T. A., Ramachandran, R., and Liberman, M. C. (2017). Noise-induced cochlear synaptopathy in rhesus monkeys (Macaca mulatta). *Hearing Research, 353*, 213-223.

Wang, Y., Hirose, K., & Liberman, M. C. (2002). Dynamics of noise-induced cellular injury and repair in the mouse cochlea. *JARO, 3*, 248-268.

Ward, W. D. & Duvall, A. J. (1971). Behavioral and ultrastructural correlates of acoustic trauma. *Ann Otol, 80*, 881-896.

SECTION III: COCHLEAR ANATOMY, AUDITORY PHYSIOLOGY, AND AUDITORY PERCEPTION IN MACAQUE MONKEYS FOLLOWING TEMPORARY NOISE-INDUCED HEARING LOSS

CHAPTER 5

General Introduction to Cochlear Synaptopathy

Of the 60 million Americans that experience hearing difficulties (Goman & Lin, 2016; Hoffman et al., 2017), approximately 5-20% present with normal audiological test results (Billings et al., 2018; Cooper & Gates, 1991; Grant et al., 2021; Hannula et al., 2011; Hind et al., 2011; Koerner et al., 2020; Kumar et al., 2007; Parthasarathy et al., 2020; Spankovich et al., 2018; Tremblay et al., 2015). This "hidden hearing loss" is commonly associated with difficulty listening in background noise, despite good hearing sensitivity (Kohrman et al., 2020; Schaette & McAlpine, 2011). Efforts to identify the specific site(s) of lesion underlying these hearing impairments have been a primary focus of hearing research in recent years.

Loss of inner hair cell ribbon synapses, or cochlear synaptopathy (SYN), is a newly discovered inner ear pathology thought to contribute to these hidden hearing difficulties (Kujawa & Liberman, 2006, 2009). SYN results in degradation of afferent auditory nerve fibers, including a disproportionate loss of those with low spontaneous firing rates (LSR) and high sound-evoked thresholds (Furman et al., 2013; Liberman et al., 2015; Schmiedt et al., 1996; but see Suthakar & Liberman, 2021). Because these more susceptible LSR neurons encode signals in noise (Costalupes, 1985), SYN is hypothesized to underlie hearing-in-noise impairments in the absence of overt hearing loss and outer hair cell dysfunction (Bharadwaj et al., 2014; Oxenham, 2016; Plack et al., 2014).

SYN can occur naturally with aging (Gleich et al., 2016; Sergeyenko et al., 2013; Steenken et al., 2021) or following acoustic overexposure that causes temporary threshold shifts (Kujawa & Liberman, 2009; Lin et al., 2011; Valero et al., 2017). Further, SYN both precedes and accompanies sensorineural hearing loss (Fernandez et al., 2020). SYN has been documented in several mammalian species including: mice (Fernandez et al., 2015; Kujawa & Liberman, 2009; Sergeyenko et al., 2013; Shi et al., 2015; Valero et al., 2018), gerbils (Gleich et al., 2016;

Steenken et al., 2021; Tziridis et al., 2021), rats (Lee et al., 2020; Mohrle et al., 2016; Singer et al., 2013), guinea pigs (Furman et al., 2013; Hickman et al., 2020; Lin et al., 2011; Liu et al., 2012; Shi et al., 2013; Song et al., 2016), chinchillas (Bharadwaj et al., 2021; Hickman et al., 2018), macaques (Valero et al., 2017), and humans (per temporal bone specimens) (Makary et al., 2011; Sagers et al., 2017; Viana et al., 2015; Wu et al., 2019; Wu et al., 2020, 2021). SYN may be reversible through innate regeneration (Hickman et al., 2020, 2021; Shi et al., 2015; Song et al., 2016) or therapeutic interventions (Chen et al., 2018; Sly et al., 2016; Suzuki et al., 2016; Wan et al., 2014), but can lead to accelerated auditory nerve degeneration over time (Fernandez et al., 2015; Kujawa & Liberman, 2009).

SYN was first identified in animal studies and emerged as a potential explanation for hidden hearing loss. Since its discovery, numerous studies in animal models and in humans have attempted to identify physiological and perceptual indices of this pathology and hearing-in-noise impairments. This approach diverges from traditional biomedical research, in which a symptom or patient complaint is identified and then experiments are conducted to determine the underlying mechanism. In this case, both the mechanism and patient complaint were known, but required further research to establish causality.

After more than ten years of research, the literature on correlations between SYN biomarkers and hearing-in-noise difficulties in humans yields inconsistent conclusions (Bharadwaj et al., 2019; Bramhall et al., 2019; DiNino et al., 2021; Hickox et al., 2017). Although scientists are no stranger to conflicting data, these mixed results have created doubt and confusion within the audiology and otolaryngology communities about the clinical significance of SYN (Dobie & Humes, 2017; Hall, 2017; Musiek et al., 2018; Salanger & Parker, 2018; Tumolo, 2020; Zeng, 2015). The manifestations of SYN may be subtle, dynamic over time, and difficult to capture with a standard clinical test battery (i.e. “hidden”). Because SYN cannot be histologically verified in living subjects, parallel research in animal models of SYN and humans at risk for SYN is essential for an enhanced understanding of SYN pathology and translation of diagnostic and treatment strategies to clinical practice.

In Section III, we describe a series of experiments investigating cochlear anatomy, auditory physiology, and hearing-in-noise abilities of macaques that underwent a single, high-level noise exposure intended to cause SYN. The exposure parameters were chosen based on prior studies of noise-induced hearing loss in nonhuman primates (reviewed in Chapter 1, Burton

et al., 2019), including previous work in our laboratory that established macaque models of noise-induced sensorineural hearing loss and SYN (Chapter 4, Burton et al., 2020; Hauser et al., 2018; Mackey et al., 2021; Valero et al., 2017). As discussed in Chapter 1, macaques are an ideal animal model for studying hearing disorders, given their similarity to human inner ear anatomy, auditory physiology, and susceptibility to noise-induced hearing loss (Burton et al., 2019). Macaque auditory function can be probed with complementary noninvasive physiological tests and behavioral psychoacoustic tone detection tests, resulting in a comprehensive account of the effects of experimental manipulations like SYN. Our study design includes characterization of hearing-in-noise abilities, physiological function, and cochlear histopathology in the same subjects, enabling direct correlations between structure and function.

Section III is organized as follows. General methods relevant to multiple chapters are described in Chapter 6. Each of the next five chapters discusses a different anatomical, physiological, or perceptual characteristic of our macaque model of SYN. Pertinent background literature is discussed in each chapter to motivate the experimental rationale. First, the inner ear histopathology generated by the acoustic overexposure is described in Chapter 7. This anatomical characterization is a critical component of this Section and serves as a foundation for the following chapters. Chapters 8 and 9 describe changes in afferent and efferent physiology following noise exposure using otoacoustic emissions, acoustic reflexes, and auditory brainstem response measures. In Chapters 10 and 11, the perceptual consequences of noise-induced temporary threshold shifts are described for six psychoacoustic paradigms. These data are among the first reports of how SYN pathologies can affect hearing-in-noise. Section III ends with a general discussion in Chapter 12, which attempts to synthesize the anatomical, physiological, and perceptual data together to form a revised understanding of SYN and identify areas for further research.

CHAPTER 6

General Materials and Methods

6.1 SUBJECTS

Young adult rhesus macaques (*Macaca mulatta*, *n* = 25; 5 females; 6-10 years old) were utilized in these studies. Subjects were randomly allocated to different groups for study as described in Table 6.1. Specific chapters and experiments will have the number and sex of subjects specified.

Table 6.1 Experimental groups and testing conditions

Group	Exposure Parameters	Experiments	Post-Exp. Survival Time	Total
I	N/A	Pre-exposure Physiology only	N/A	n = 9 male (M10, M22, Cel, Ch, De, Du, El, Ju, No), 1 female (M13)
II	120 dB SPL OBN (2-4 kHz), 4 h	Physiology only	2 months	n = 5 male (Alb*, Ced*, Do, Ki**, Ca)
III	120 dB SPL OBN (2-4 kHz), 4 h	Physiology & Behavior (Detection)	10 months	n = 4 male (Ar, Bi, Ga, Ha), 4 female (Lu, Ne, Op, Pi)
		Physiology & Behavior (Discrimination; not part of this dissertation)	10 months	n = 2 male (Da, Is)

*Pre-exposure audiogram, tone in steady-state noise, and overshoot were collected for these subjects

**Post-exposure audiogram and tone in steady-state noise data were collected for this subject

In addition to the cohort of subjects listed in Table 6.1, data from two subjects with sensorineural hearing loss (one with noise-induced permanent threshold shifts, one with likely congenital high frequency hearing loss) were included for comparison in some studies. Details about these subjects are included in Chapter 11.

Animals were maintained on a 12:12-h light:dark cycle. Veterinary assessments and experimental procedures occurred between 8:00 am – 5:00 pm during their light cycle. Four animals were socially housed. All other animals were individually housed due to incompatibility for social housing, but had visual, auditory, and olfactory contact with conspecifics maintained within the housing room. A commercial primate diet (Lab Diet 5037 or 5050, PMI Nutrition

International, Brentwood, MO) was provided twice daily and was supplemented with fresh produce and/or foraging items (seeds, dried fruit, nuts, etc.). Animals were provided manipulanda as well as auditory, visual, and olfactory enrichment on a rotational basis. Filtered municipal water was provided at least once a day as the animals were maintained on fluid restriction for study purposes. All animals were under the continuous care of veterinary staff and received semiannual comprehensive physical exams, including standard blood work (annual) and tuberculosis testing. Cranial implants (used for head fixation during psychophysical testing of parallel studies) were regularly cleaned with topical agents.

All research procedures were approved by the Institutional Animal Care and Use Committee at Vanderbilt University Medical Center.

6.2 PSYCHOPHYSICAL TONE DETECTION TASKS

Subjects (n=11, 4 females) were trained to perform a reaction-time Go/No-Go lever release task using fluid reward as positive reinforcement, as described previously (e.g. Bohlen et al., 2014; Burton et al., 2018; Dylla et al., 2013; Rocchi et al., 2017). Experiments were conducted in sound treated booths (Industrial Acoustics Corp, NY; Acoustic Systems, Austin, TX). During the task, subjects were seated in an acrylic primate chair that was custom designed for comfort and with no obstruction to sounds on either side of the head (Audio chair, Crist Instrument Co., Hagerstown, MD). During task performance, subjects were head-fixed via a surgically-implanted titanium head holder (for details about surgical preparation, see Dylla et al., 2013). The monkey's head was fixed to the chair such that the head and ears directly faced the center of a loudspeaker at a distance of 36 inches. The loudspeaker (SA1 loudspeaker, Madisound, WI) and amplifier (SLA2, Applied Research Technologies, Rochester, NY) were able to deliver sounds between 50 Hz and 40 kHz. Calibration using a 1/4" probe microphone (model 378C01, PCB Piezotronics Inc., Depew, NY) placed at the approximate entrance of the subjects' ear canals revealed that the output of the speakers varied by approximately ±3 dB across the frequency range. Tones and noise were delivered from the same speaker. All psychophysical tasks were performed in these diotic, open field testing conditions.

The behavioral task was identical to the methods described in Burton et al. (2018). Briefly, the monkeys were trained to detect tones in quiet or embedded in noise maskers. To initiate a trial, the monkey pressed down on a lever (Model 829 Single Axis Hall Effect Joystick,

P3America, San Diego, CA). After a variable hold time, a signal (tone, 85% of trials) or catch trial (no tone, 15% of trials) was presented. Upon correct lever release on signal trials, the monkey received a fluid reward. If the monkey did not release the lever during a signal trial, this was taken to indicate non-detection, and no reward or penalty was administered. Lever release on catch trials resulted in a timeout penalty.

The experiments were controlled by a computer running OpenEx software (System 3, TDT Inc., Alachua, FL). Within each block, tone sound pressure levels spanned a 60 dB range and were randomly interleaved with catch trials. Flat spectrum broadband noise was generated from a uniform distribution and band-limited to 40 kHz.

Behavioral performance was analyzed according to signal detection theoretic methods, as previously described (e.g. Bohlen et al., 2014; Burton et al., 2018; Dylla et al., 2013; Rocchi et al., 2017). Briefly, at each tone level (*level*), hit rate was calculated ($H(level)$) based on the proportion of releases on trials with the tone at that sound level. False alarm rate (FA) was calculated based on the proportion of releases on catch trials. Based on signal detection theory, $H(level)$ and FA were then converted into units of standard deviation of a standard normal distribution (z-score, norminv in MATLAB) to estimate *d'* according to $d'(level) = z(H(level)) - z(FA)$ (Macmillan and Creelman, 2005). Because we wanted these results to be able to serve as a baseline for neurophysiological studies where we would measure (noise) and (signal+noise) representation distributions, we converted the Yes/No analysis to a 2-alternative forced choice analysis and calculated the behavioral accuracy at each tone level using the probability correct (pc) metric as follows: $pc(level) = z^{-1}(d'(level)/2)$. Here, the inverse z transform (z^{-1}) converts a unique number of standard deviations of a standard normal distribution into a probability correct (normcdf in MATLAB). The conversion of *d'* to the *pc* measure was to facilitate the comparison of psychometric functions with neurometric functions obtained from neuronal responses using distribution free methods. The traditional threshold estimated at $d' = 1$ corresponds to $pc(level) = 0.76$.

Psychometric functions were fitted with a modified Weibull cumulative distribution function (cdf) according to:

$$pc(level)_{fit} = c - d * e \text{ ^ } -(level/\lambda)^k$$

where *level* was the tone level (in dB SPL), λ represents the threshold parameter, and k corresponds to the slope parameter. c represents the saturation probability correct, and d was the

estimate of chance performance. Threshold was calculated from the fit as the tone level that resulted in a pc_{fit} value of 0.76.

Tone detection paradigms were designed to assess hearing sensitivity, growth of masking, frequency selectivity, overshoot, and forward masking. Other tasks probing temporal resolution and spatial hearing were also performed by other researchers in the laboratory, generating a test battery that required approximately 10 months to complete. Specific stimulus parameters for the different tone detection tasks will be described in each chapter (Chapter 10: audiogram, tone in steady-state noise, tone in notched-noise; Chapter 11: overshoot, forward masking). Psychophysical performance was assessed before and after noise exposure; specific data collection timelines will be discussed in each chapter.

6.3 ANESTHETIC PROCEDURES

Animals were anesthetized for auditory brainstem response and otoacoustic emissions testing, as well as the noise exposure procedure. Initial sedation was induced with an intramuscular injection of ketamine (10 mg/kg) and midazolam (0.05 mg/kg). Animals were intubated and anesthesia was maintained with isoflurane (1-2%). All anesthetized procedures were conducted in a sound-treated booth (Industrial Acoustics Corp, NY; Acoustic Systems, Austin, TX). Subjects were monitored intensively for a minimum of 72 hours post-procedure.

6.4 NON-INVASIVE AUDIOLOGICAL ASSESSMENTS

6.4.1 Otoscopy and tympanometry

Prior to electrophysiologic testing or noise exposure, otoscopic examination (Welch Allyn) and tympanometry were conducted to assess the status of the external and middle ear. Using an Otowave 102-4 tympanometer (Amplivox, Eden Prairie, MN), a 226 Hz probe tone was presented while a pressure sweep (+200 to -400 dPa) was generated under a hermetic seal of the ear canal. We previously reported normal and abnormal tympanometric findings for macaques (Burton et al., 2022; Stahl et al., submitted). Middle ear fluid and tympanic membrane perforations were criteria for exclusion from the study.

6.4.2 Auditory brainstem response (ABR) testing

Auditory brainstem response (ABR) recording methods overlapped with previous publications from our laboratory (Hauser et al., 2018; Stahl et al., submitted; Valero et al., 2017).

ABRs were measured using subdermal needle electrodes (Rhythmlink) placed on the mastoid (active), vertex (reference), and shoulder (ground) connected to a Medusa 4Z preamplifier (Tucker-Davis Technologies). Impedances for subdermal needle electrodes were consistently less than 1 kΩ. A closed-field speaker (MF1, Tucker-Davis Technologies) was coupled to the ear with a pediatric ER-3A foam tip for stimulus delivery.

Stimuli were created in SigGenRZ and generated by an RZ6 Multi-I/O Processor (Tucker-Davis Technologies). Stimuli were presented at 27.7/s with an alternating stimulus polarity for two separate runs of 1024 repetitions. Stimuli were calibrated (+/- 1 dB) using a 0.5cc coupler and verified in the ear canal using a probe microphone system (Fonix 8000, Frye). Stimulus presentation, signal acquisition, and data analysis was completed using BioSigRZ software.

During online recording, the incoming signal was digitally filtered from 300-3000 Hz. Signals with amplitudes greater than 1 mV were rejected using the Artifact Rejection feature in BioSigRZ, and not included in the average. During offline analysis, the two artifact-free waveforms were averaged, inverted, and low-pass filtered at 1500 Hz to product a single ABR trace per condition (2048 repetitions).

ABR threshold was defined as the lowest sound level that elicited a visually identifiable response greater than the noise floor (40 nV). ABR Wave I, II, and IV peak-to-peak amplitudes and peak latencies were visually identified for each stimulus and level in order to derive input-output functions. Specific stimulus parameters for ABR testing are described in Chapter 9.

6.4.3 Otoacoustic emissions (OAE) testing

OAE testing was completed using a Scout Bio-logic OAE System (Natus, Pleasanton, CA). Recording methods overlapped with previous publications from our laboratory (Hauser et al., 2018; Stahl et al., submitted; Valero et al., 2017). A probe containing two speakers and one microphone was coupled to the ear with a pediatric foam tip.

Distortion product otoacoustic emissions (DPOAEs) were measured in response to tone pairs (f_2 = 0.5-10kHz, 8 points per octave; f_2/f_1 = 1.22; L_1-L_2 = 10 dB; L_1 = 70-25 dB in 5 dB steps). As previously described (Stahl et al., submitted), DPOAE amplitudes and input-output functions were derived. DPOAE threshold was defined as the lowest sound level that elicited a significant DP amplitude (>0 dB SPL, >6 dB signal to noise ratio). Transient-evoked otoacoustic emissions (TEOAEs) were measured in response to click trains (80μs, 80 dB pSPL).

6.5 NOISE EXPOSURE

Following baseline physiological and psychophysical characterization, subjects underwent a single noise exposure intended to generate cochlear synaptopathy. The details of the noise exposure were similar to those previously reported by our laboratory (Burton et al., 2020; Hauser et al., 2018; Valero et al., 2017). Following anesthetic induction and intubation, the subject was laid prone on a table with the head slightly elevated in a sound treated booth. Closed-field speakers (MF1, Tucker-Davis Technologies) were coupled to the ears using 1.5" PE tubing and pediatric ER-3A insert earphones that were deeply inserted into each ear canal. Octave-band noise (2-4 kHz) was presented simultaneously to both ears at 120 dB SPL for four hours. The level of the exposure stimulus varied by less than 0.3 dB SPL over the course of the four-hour procedure. As discussed in detail in Chapter 10, the noise exposure induced temporary threshold shifts that resolved within 3 weeks post-exposure as measured by DPOAEs and behavioral audiometry. Physiological and psychophysical assessments were completed before and after noise exposure; specific timelines for each experiment are detailed in their chapter.

6.6 COCHLEAR HISTOLOGICAL PREPARATION AND QUANTIFICATION

Following completion of the study, macaques were euthanized via overdose of sodium pentobarbital and sodium phenytoin (Euthasol; >120 mg/kg IV) and transcardially perfused with 0.9% phosphate-buffered saline and 4% phosphate-buffered paraformaldehyde (PFA). Temporal bones were extracted in order to harvest the cochlear tissue. The round and oval windows were opened, cochleas were perfused through the scala tympani with PFA, submerged in PFA for 2 hours, and then transferred to 0.12 M EDTA for decalcification. Decalcified cochleas underwent dissection, imaging, and immunohistochemical analysis as previously described (Valero et al. 2017). Briefly, decalcified cochleas were dissected into quarter turns to obtain epithelial whole mounts of the organ of Corti containing the hair cells and most of the osseous spiral lamina at each location from base to apex. Immunohistochemistry was used to label i) presynaptic ribbons (mouse IgG1 anti-CtBP2 (C-terminal binding protein 2); BD Transduction Labs; 1:200); ii) glutamate receptor patches (mouse IgG2 anti-GluA2; Millipore; 1:200), and iii) hair cell cytoplasm (rabbit anti-myo7a (myosin VIIa); Proteus Biosciences; 1:200). A fourth channel was used to label either cochlear afferent and efferent fibers (chicken anti-NFH (neurofilament-H);

Chemicon; 1:1000) or cochlear efferent fibers (goat anti-choline acetyltransferase (ChAT); Millipore #AB144P; 1:100). A fifth channel was included on some tissue to label the hair cell stereocilia (anti-ESPN (espin); Sigma #HPA028674; 1:200). Tissue was incubated in species-appropriate fluorescent secondary antibody conjugates (AlexaFluor) for secondary detection.

The tissue was imaged on a Leica SP8 confocal microscope, using a 63X glycerol objective (1.3 N.A.), to acquire 3-dimensional image stacks at each of 8 octave-spaced positions along the cochlear spiral from 0.125 to 32 kHz, with half-octave spacing in regions near the noise exposure band. The frequency correlate of each image stack was computed from a cochlear frequency map based on a Greenwood function (Greenwood, 1990), assuming an upper frequency limit of 45 kHz.

Hair cell survival was assessed in low-power confocal z-stacks by counting cuticular plates normalized to the expected number of hair cells within each row. Amira software (version 2019.4, Visage Imaging) was used to quantify IHC and OHC afferent synapses from confocal z-stacks by identification of thresholded CtBP2-labeled puncta within hair cells. Ribbon counts in each section were normalized to the number of hair cells (ribbons per hair cell). Amira software was also used to quantify efferent terminal density in the region near the outer hair cells (medial olivocochlear area) and near the inner hair cells (lateral olivocochlear area). Pixel counts of stained area were quantified using ImageJ software.

6.7 NOTES ABOUT SOUND LEVELS AND FIGURE CONVENTIONS

Throughout Section III, sound levels will be reported in "dB spectrum level" unless otherwise specified (such as MEMR elicitor levels, which are in dB SPL). Spectrum level refers to the sound pressure level in a 1 Hz band. This convention provides the most transparent reporting of sound level. Overall level (dB SPL) can be derived from spectrum level according to the following formula:

Overall Level = Spectrum Level + 10 * $\log_{10}$(bandwidth of the signal in Hz)

A few figure conventions are also worth mentioning. In figures showing mean data, error bars always illustrate ± 1 standard deviation from the mean. Many figures with frequency on the x-axis will include a gray box to illustrate the spectrum of the noise exposure band (2-4 kHz). Colors are used throughout figures to differentiate groups. Black typically indicates control data.

Green indicates data from human subjects. Pink and blue are used for female and male groups, respectively. Red indicates post-exposure data, with lighter shades for earlier time points and darker shades for later time points. Symbols are used to indicate different subjects or provide redundancy to color indices.

CHAPTER 7

Cochlear histopathological characterization of a macaque model of noise-induced synaptopathy: Effects of post-exposure survival time

7.1 INTRODUCTION

Acoustic overexposure causes damage to the inner ear and alters auditory physiology and perception. High sound levels generate large movements of the basilar membrane, causing mechanical stress on the inner and outer hair cells (IHCs, OHCs). The relationship between acoustic injury and hair cell loss have been a primary focus in the decades of research on noise-induced hearing loss (e.g. Hawkins et al., 1976; Liberman & Kiang, 1978; Lurie et al., 1944; Spoendlin & Brun, 1973). OHC loss is a hallmark of noise-induced and age-related sensorineural hearing loss (SNHL), but is only weakly correlated with the magnitude of hearing sensitivity loss and perceived hearing difficulties (e.g. Hunter-Duvar & Elliott, 1973; Landegger et al., 2016; Liberman & Kiang, 1978; Schuknecht & Gacek, 1993).

The functional inter-dependence of inner ear cell types and subcellular processes complicates the study of acoustic injury. In addition to hair cell loss, noise exposure causes excitotoxic swelling of afferent auditory nerve fibers (Le Prell et al., 2004; Puel et al., 1998) and damage to or loss of presynaptic IHC ribbons (Kujawa & Liberman, 2009). IHC ribbon loss, or cochlear synaptopathy (SYN), accompanies OHC loss (Fernandez et al., 2020; Valero et al., 2017) and also occurs in isolation (Kujawa & Liberman, 2009; Lin et al., 2011). SYN represents a naturally occurring deafferentation of the auditory system that reduces neurophysiological redundancy (e.g. fewer fibers discharging synchronously). Ribbon loss and hair cell loss are correlated (Valero et al., 2017; Wu et al., 2021), but SYN tends to outpace the manifestation of SNHL (Fernandez et al., 2015). SYN may underlie variability in hearing abilities among individuals with the same audiometric loss, as well as individuals who report hearing difficulties in background noise despite normal hearing sensitivity (i.e. hidden hearing loss; Schaette & McAlpine, 2011).

The advent of advanced imaging and staining techniques enabled detailed anatomical characterization of noise-induced hearing pathophysiology. Identifying the specific sites of lesion associated with noise damage will inform diagnostic and treatment options for individuals

with hearing difficulties. Important aspects to consider are: i) the time course of noise-induced inner ear pathology, including damage, repair, and progression; ii) species differences in the response to acoustic injury; iii) the relationship between inner ear integrity, auditory physiology, and hearing abilities.

Time-based changes in histopathology are a prominent feature noise-induced pathologies, including SYN. Some aspects of acoustic injury recover over time, while others accumulate or progress over time. For example, noise-induced temporary threshold shifts and associated outer hair cell dysfunction require time to fully recover; typically 1-3 weeks, depending on the species and exposure conditions (e.g. Furman et al., 2013; Kujawa & Liberman, 2009). Simultaneous with this recovery is the trigger of accelerated age-related hearing impairment and associated cochlear neural degeneration (Fernandez et al., 2015; Kujawa & Liberman, 2006). Although IHC ribbon loss was initially thought to be permanent or progressive with age, ribbon regeneration has been reported in guinea pigs (Hickman et al., 2020, 2021; Shi et al., 2013; Song et al., 2016) and some mouse strains (Kim et al., 2019; Shi et al., 2015). The functional consequences of IHC ribbon regeneration are unknown, but could have major implications for the dynamics of central compensation following peripheral injury.

Nonhuman primates are a useful model for human inner ear pathologies due to their phylogenetic similarity and comparable auditory anatomy and physiology. Like humans, nonhuman primates are less susceptible to acoustic injury than other animal models (Burton et al., 2019; Valero et al., 2017). We previously demonstrated that macaque monkeys exhibit isolated SYN (Valero et al., 2017) and ribbon synapse loss accompanying SNHL (Burton et al., 2020; Hauser et al., 2018; Mackey et al., 2021; Valero et al., 2017) following acoustic overexposure. Here, we provide a more comprehensive anatomical characterization of our macaque model of noise-induced SYN. We quantified OHC and IHC counts, OHC and IHC ribbon counts and sizes, and olivocochlear efferent terminal density following an acute noise exposure that caused a temporary threshold shift. Due to the overarching design of our study, macaques were divided into two experimental timelines, allowing us to assess the effect of post-exposure survival time on the dynamics of noise-induced inner ear damage by examining cochlear tissue at 2 months and 10 months post-exposure.

Please note that this Chapter only includes data from half of the subjects in this study, so the findings are preliminary. Final experiments and tissue processing are ongoing for the remaining animals and will be included in future analyses and publications.

7.2 MATERIALS AND METHODS

7.2.1 Subjects

Cochlear tissue was obtained from sixteen adult rhesus macaques (*Macaca mulatta*, 7-10 years old, 1 female). As described in the General Methods, subjects comprised three groups: unexposed controls ($n = 10$), short-term post-exposure survival (2 months; $n = 2$), and long-term post-exposure survival (10 months; $n = 4$).

7.2.2 Cochlear histology

Following completion of the study, subjects were euthanized and cochlear tissue was harvested for dissection and immunohistochemistry. Complete details of the histological preparations can be found in Chapter 6: General Methods. Immunolabeling and confocal imaging of cochlear whole mounts was conducted to quantify IHC and OHC counts, IHC and OHC ribbon counts and sizes, and efferent terminal densities. Data from noise-exposed subjects were compared to unexposed subjects to assess anatomical integrity along the cochlear length.

7.2.3 Statistical analyses

Statistical analyses were conducted using linear mixed effects models ("fitlme" in MATLAB 2018a). The dependent variable in the models was hair cell count, ribbon count, ribbon size, or efferent terminal density. Ear laterality, frequency, noise exposure status, and post-exposure survival time were entered as fixed effects into the model, while intercepts for individual subjects were entered as random effects. In all cases *p*-values were obtained by likelihood ratio testing of the model with the effect in question against the model without the effect in question. A significant *p*-value was defined as $p < 0.05$. *T*-statistics are reported for each model, similar to the *F*-statistic that is often reported for such models.

Ribbon volume distributions were compared using Kolmogorov-Smirnov two sample tests ("kstest2" in MATLAB 2018a). A Bonferroni correction was applied to adjust the significance level for multiple comparisons (18 comparisons, adjusted *p*-value = 0.0028).

7.3 RESULTS

7.3.1 Outer and inner hair cell counts

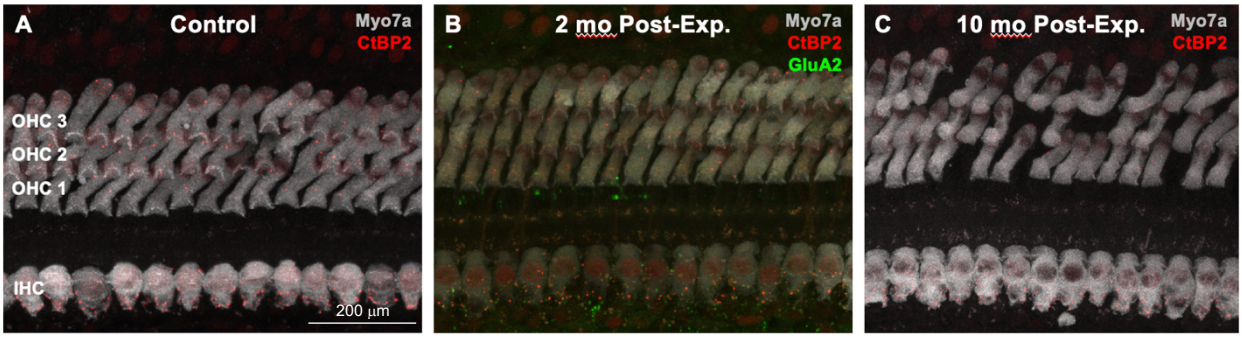

Figure 7.1 Confocal microscopic images (XY projection) of cochlear outer hair cells and inner hair cells at the 5.6kHz frequency place in a control (A) and in noise exposed subjects (B: 2 months, C: 10 months post-exposure). OHC = outer hair cell. IHC = inner hair cell.

Like humans, macaques have three to four rows of OHCs and one row of IHCs (Figure 7.1; Bredberg, 1968; Johnsson & Hawkins, 1967; Lonsbury-Martin et al., 1988). Hair cell survival along the cochlear length was calculated as the number of hair cells present divided by the total number of hair cells expected. Unexposed controls had nearly full complements of OHCs and IHCs across frequencies (Figure 7.1A; Figure 7.2, black symbols). Similar to controls, little to no IHC loss was observed at 2 and 10 months post-exposure (Figure 7.1B-C, Figure 7.2B; $R^2 = 0.15$, $t(df) = 0.25(296)$, $p = 0.558$), although there was a significant effect of frequency driven by the 5% IHC loss at 32kHz across groups ($t(df) = -3.81(296)$, $p = <0.000$). OHC loss was also minimal and not different from controls at 2 months post-exposure (Figure 7.1B; Figure 7.2A, red open symbols; $R^2 = 0.00$, $t(df) = 0.53(205)$, $p = 0.593$). In contrast, there was statistically significant OHC loss at 10 months post-exposure compared to controls (Figure 7.1C; Figure 7.2A, dark red symbols; $R^2 = 0.0$, $t(df) = -3.1417(244)$, $p = 0.002$). Inter-subject and across-ear variability was substantial, with 2 out of 8 ears showing <5% OHC loss

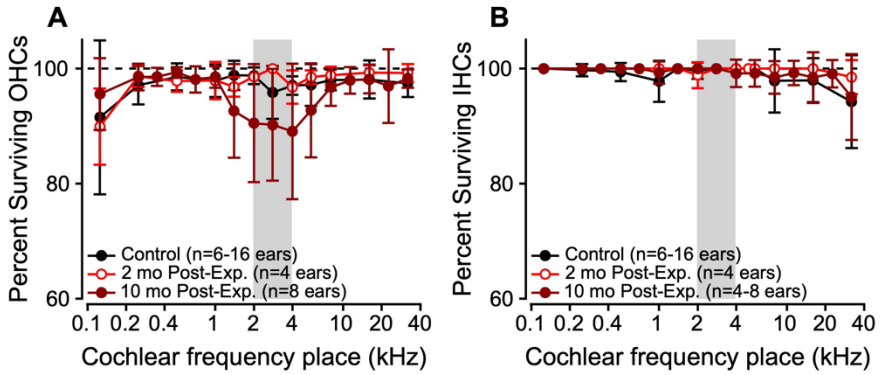

Figure 7.2 Outer hair cell survival (A) and inner hair cell survival (B) as a function of cochlear frequency place in controls (black, $n = 6$-16 ears per frequency) and at 2 (red, $n = 4$ ears) and 10 (dark red, $n = 8$ ears) months post-exposure. Error bars indicate ± 1 standard deviation from the mean. Gray boxes illustrate the noise exposure band.

and 6 out of 8 ears showing 12-32% OHC loss. This modest reduction (up to 11% on average) in OHC survival for frequencies near the noise exposure band did not significantly affect otoacoustic emission amplitudes or thresholds (see Chapter 8, Figure 8.7 and Tables 8.10, 8.11, 8.12, and 8.13).

7.3.2 Inner hair cell ribbons

IHCs contain presynaptic ribbon proteins that oppose postsynaptic glutamate receptors on afferent auditory nerve fibers. In Figure 7.3, IHC presynaptic puncta are labeled with the CtBP2 immunolabel (red) and postsynaptic glutamate receptor puncta in opposing auditory nerve fibers are labeled with the GluA2 immunolabel (green). The co-localization of pre- and postsynaptic puncta indicate a properly aligned synapse with the potential for afferent functional connectivity.

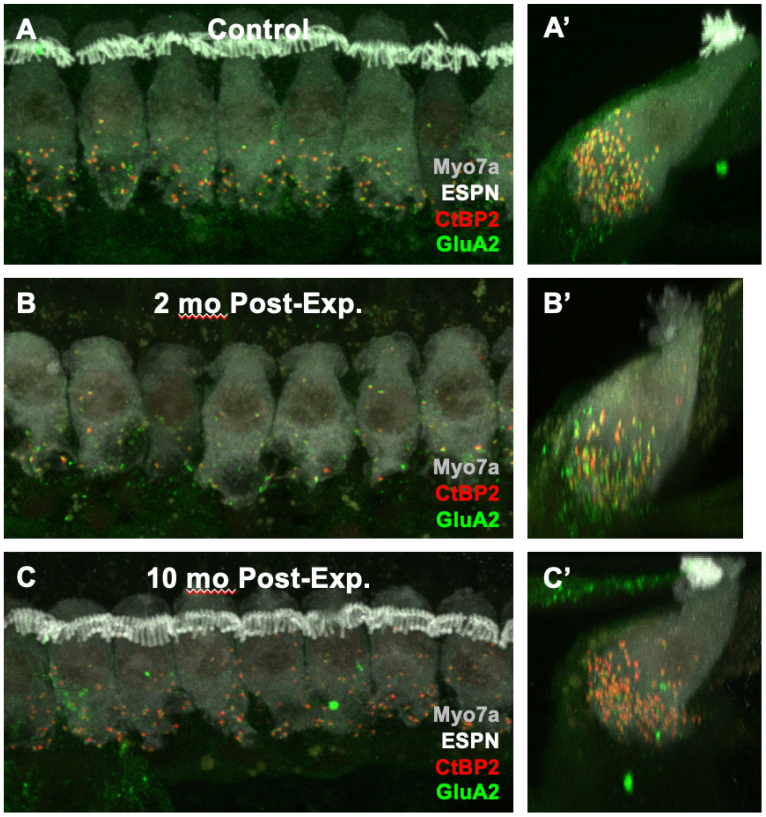

Figure 7.3 Confocal microscopic images of cochlear inner hair cells at the 5.6kHz frequency place in a control and in subjects 2 months post-exposure and 10 months post-exposure. A,B,C: XY projection. A',B',C': YZ projection.

IHC ribbon counts are plotted as a function of cochlear frequency

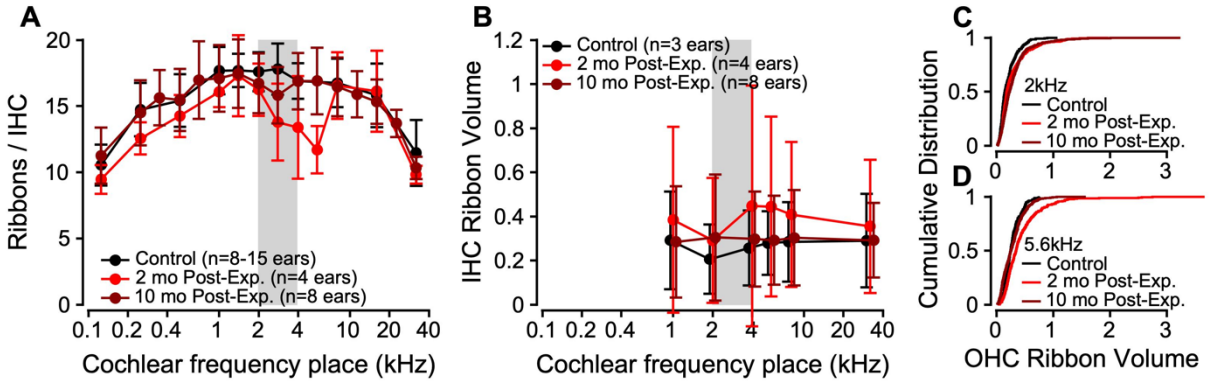

Figure 7.4 A,B. Mean ribbons per inner hair cell (A) and mean inner hair cell ribbon volume (B) as a function of cochlear frequency place in controls (black, *n* = 8-15 ears per frequency) and at 2 (red, *n* = 4 ears) and 10 (dark red, *n* = 8 ears) months post-exposure. Error bars indicate ± 1 standard deviation from the mean. C,D. Cumulative distribution functions of IHC ribbon volume at 2 kHz and 5.6 kHz cochlear frequency places.

place in Figure 7.4A. As reported previously (Valero et al. 2017), IHC ribbon counts were greatest in the mid-frequencies. At 2 months post-exposure, there was a significant reduction of IHC ribbons at frequencies near the noise exposure band (Figure 7.3B and B', Figure 7.4A, Table 7.1). In contrast, there was no significant difference in IHC ribbon counts for the 10 month post-exposure group compared to controls (Figure 7.3C and C', Figure 7.4A, Table 7.2).

IHC Ribbon Count_2 Month ~ Exposure + Frequency; $R^2 = 0.35$

Table 7.1 Linear mixed effects model for IHC ribbon count in controls vs. 2 months post-exposure

Variable	***T-statistic (df)***	***p-value***
Exposure	-2.15 (183)	0.033
Frequency	-3.00 (183)	0.003

IHC Ribbon Count_10 Month ~ Frequency; $R^2 = 0.41$

Table 7.2 Linear mixed effects model for IHC ribbon count in controls vs. 10 months post-exposure

Variable	***T-statistic (df)***	***p-value***
Exposure	-0.23 (226)	0.815
Frequency	-3.68 (226)	<0.001

IHC ribbon volumes were measured for all ribbons at a given cochlear frequency. Figure 7.4B illustrates mean IHC ribbon volumes as a function of cochlear frequency place in controls and at 2 and 10 months post-exposure. IHC ribbon volumes were similar on average across frequencies and groups, but highly variable within and across groups. Cumulative distribution functions revealed significant differences in IHC ribbon volume distributions across groups (Figure 7.4C-D). At 2 months post-exposure, there was a larger proportion of enlarged ribbons at frequencies near the noise exposure band compared to controls, as shown by the rightward shift and long upper tail in the cumulative distribution functions (red lines in Figure 7.4C-D; Table 7.3). At 10 months post-exposure, there was also a larger proportion of enlarged ribbons at 2 and 5.6 kHz compared to controls (dark red lines in Figure 7.4C-D; Table 7.3).

Table 7.3 Kolmogorov-Smirnov tests comparing IHC ribbon volume distributions from controls, 2 months post-exposure, and 10 months post-exposure

Frequency (kHz)	**2 Mo Post-Exp.**		**10 Mo Post-Exp.**	
	K-statistic	***p-value***	***K-statistic***	***p-value***
1	0.105	0.007	0.086	0.018
2	0.148	<0.000*	0.212	<0.000*
4	0.209	<0.000*	0.098	0.010
5.6	0.257	<0.000*	0.159	<0.000*
8	0.168	<0.000*	0.049	0.552
32	0.131	0.026	0.104	0.087

*significant after Bonferroni correction

7.3.3 Outer hair cell ribbons

OHCs also contain presynaptic ribbons that oppose Type II afferent auditory nerve fibers. In Figure 7.5, OHC presynaptic puncta are labeled with the CtBP2 immunolabel (red). There are fewer ribbons per OHC compared to IHCs and these ribbons are distributed in both the basal ("synaptic") and apical ("supranuclear") portions of the OHCs (Liberman & Liberman, 2016; Sobkowicz et al., 1986; Wood et al., 2021). Unfortunately, OHC ribbon staining in the 2 month post-exposure tissue was qualitatively poorer than the control and 10 month post-exposure samples, so those data were excluded from analyses.

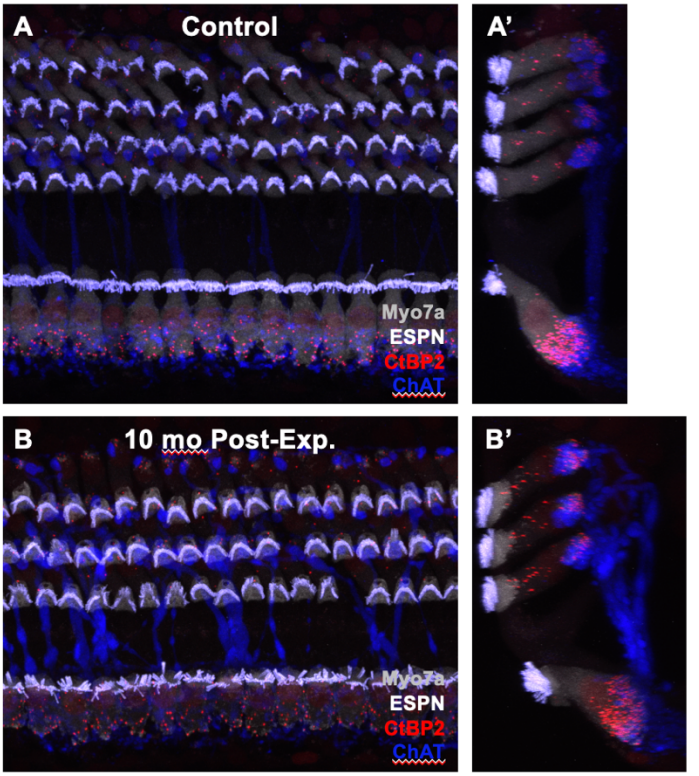

Figure 7.5 Confocal microscopic image of cochlear outer and inner hair cells at the 5.6kHz frequency place in a control (A) and in a noise-exposed subject (B, 10 months post-exposure). A,B: XY projection. A',B': YZ projection.

OHC ribbon counts are plotted as a function of cochlear frequency place in Figure 7.6A. The number of ribbons per OHC decreased with increasing frequency. Although

there was a significant effect of frequency on OHC ribbon count, there was no significant difference in OHC ribbon counts between controls and 10 months post-exposure (Table 7.4).

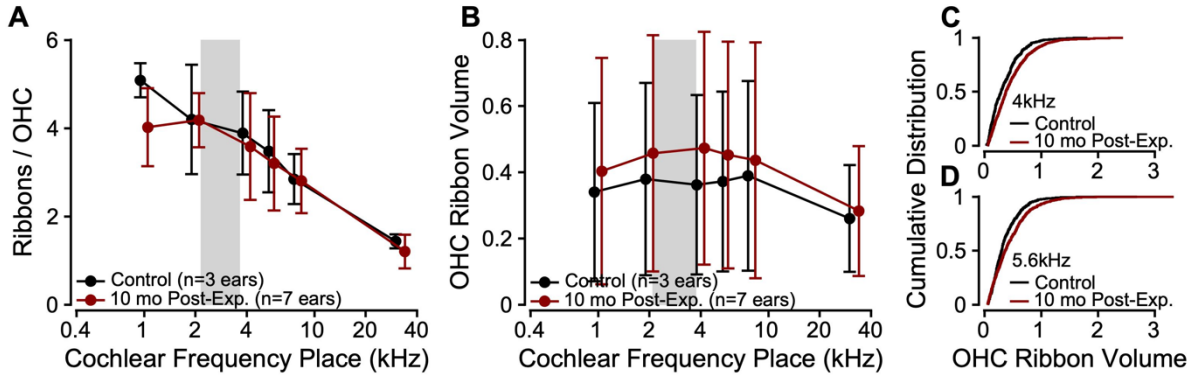

Figure 7.6 A,B. Ribbons per outer hair cell (A) and mean outer hair cell ribbon volume (B) as a function of cochlear frequency place in controls (black, $n = 3$ ears per frequency) and at 10 (dark red, $n = 7$ ears) months post-exposure. Error bars indicate ± 1 standard deviation from the mean. C,D. Cumulative distribution functions of OHC ribbon volume at 4kHz and 5.6 kHz cochlear frequency places.

OHC Ribbon Count_10 Month ~ Frequency; $R^2 = 0.73$

Table 7.4 Linear mixed effects model for OHC ribbon count in controls vs. 10 months post-exposure

Variable	***T-statistic (df)***	***p-value***
Exposure	-0.91 (56)	0.366
Frequency	-3.30 (56)	0.002

OHC ribbon volumes were measured for all ribbons across OHC rows at a given cochlear frequency place. Figure 7.6B illustrates mean OHC ribbon volumes as a function of cochlear frequency place in controls and at 10 months post-exposure. Like IHC ribbons, OHC ribbon volumes were similar on average across frequencies and groups, but highly variable within and across groups. Cumulative distribution functions revealed significant differences in OHC ribbon volume distributions across groups (Figure 7.6C-D). At 10 months post-exposure, there was a larger proportion of enlarged ribbons compared to controls at frequencies near the noise exposure band as shown by the rightward shift in the cumulative distribution functions (Figure 7.6C-D, Table 7.5).

Table 7.5 Kolmogorov-Smirnov tests comparing OHC ribbon volume distributions from controls and 10 months post-exposure

Frequency (kHz)	***K-statistic***	***p-value***
1	0.098	<0.001*
2	0.097	<0.001*
4	0.151	<0.001*
5.6	0.129	<0.001*
8	0.085	0.013
32	0.062	0.635

*significant after Bonferroni correction

7.3.4 Efferent terminal density

Olivocochlear efferent neurons are cholinergic and can be detected by a choline acetyltransferase antibody (ChAT; blue in Figure 7.5, white in Figure 7.7). Medial olivocochlear (MOC) neurons innervate the OHCs, whereas lateral olivocochlear (LOC) neurons innervate Type I afferent auditory nerve fibers near their synapse with the IHCs (Guinan, 2006). MOC and LOC innervation density were estimated from the area of ChAT staining within the OHC or IHC region, respectively (Figure 7.7; after Liberman & Liberman, 2019). Tunneling fibers and large axons were removed prior to analysis.

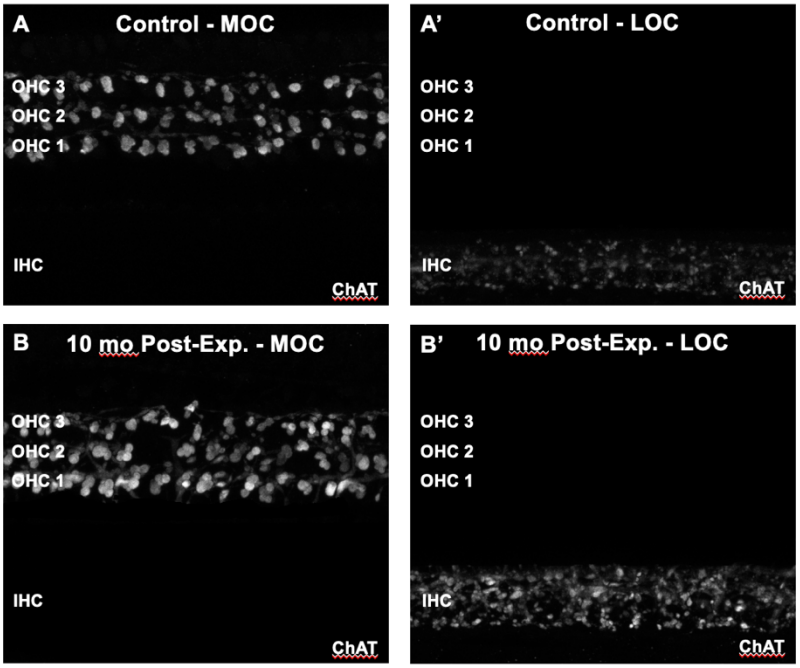

Figure 7.7 Immunolabeled (ChAT) olivocochlear efferent terminals at the 8kHz cochlear frequency place (XY projection). A. Medial olivocochlear neuron terminals in the outer hair cell region. A'. Lateral olivocochlear neuron terminals in the inner hair cell region. B,B'. Same as A and B, except from a noise-exposed subject (10 months post-exposure).

MOC innervation was densest in the mid- to high-frequency regions (Figure 7.8A), as previously reported in humans, cats, and rodents (Liberman & Liberman, 2019; Liberman et al.,

1990). MOC innervation density was also greater for OHC Row 1 than 2 than 3 (Brown, 2016; Liberman et al., 1990). There was no significant effect of noise exposure on MOC innervation density at 10 months post-exposure (Figure 7.8A, $t(df)$ = 0.98(119), p = 0.33).

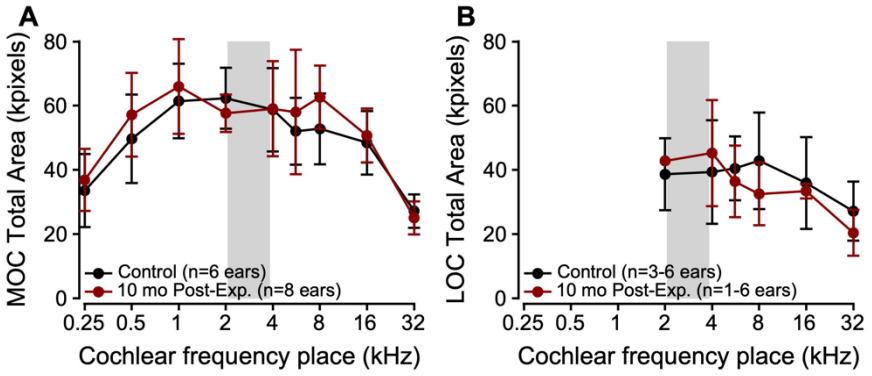

Figure 7.8 A. Medial olivocochlear efferent terminal area (kilopixels) as a function of cochlear frequency place for controls (black, n = 6) and at 10 months post-exposure (dark red, n = 8 ears) months post-exposure. Error bars indicate ± 1 standard deviation from the mean. B. Same as A, but for lateral olivocochlear terminal area.

LOC innervation density decreased with increasing frequency (Figure 7.8B), as previously reported in humans and cats (Liberman & Liberman, 2019; Liberman et al., 1990). LOC area was comparable to estimates in humans at corresponding cochlear frequency places (Liberman & Liberman, 2019). There was no significant effect of noise exposure on LOC innervation density at 10 months post-exposure (Figure 7.8B, $t(df)$ = -1.14(55), p = 0.26).

7.4 DISCUSSION

Here, we characterized cochlear anatomy in rhesus macaques with and without acoustic overexposure. Similar to our previous study (Valero et al., 2017), this macaque model of noise-induced SYN exhibited i) little to no IHC loss, ii) mild OHC loss at 10 months post-exposure, iii) 20-30% IHC ribbon loss at 2 months post-exposure that recovers by 10 months, iii) sustained enlargement of both IHC and OHC ribbons, and iv) no change in MOC or LOC innervation density. Overall, the cochlear histological consequences of noise exposure seem to be dynamic over long post-exposure survival times in macaques. Pending data from the remaining short- and long-term post-exposure survival subjects will help strengthen our conclusions, in light of the high inter-subject variability observed in some of the histological metrics.

7.4.1 Normal cochlear anatomy in the rhesus macaque

Macaques have three to four rows of OHCs and one row of IHCs (Figure 7.1 & 7.5; Johnsson & Hawkins, 1967; Lonsbury-Martin et al., 1988) like humans (Bredberg, 1968; Johnsson & Hawkins, 1967). As most mammals exhibit only three rows of OHCs, the functional

significance of these supernumerary OHCs in nonhuman primates and humans is unclear. Some research suggests that supernumerary hair cells may result from regenerative processes (Lefebvre et al., 2001; Rask-Andersen et al., 2017) and fourth row OHCs may alter the strength of otoacoustic emissions (Lonsbury-Martin et al., 1988). Regardless of their origin or function, this irregular feature appears common to nonhuman primates and humans.

Macaque IHC and OHC ribbon counts were similar to rodents (Furman et al., 2013; Hickox et al., 2017; Liberman & Liberman, 2016; Liberman et al., 2015; Wood et al., 2021) and estimates in humans (Wu et al., 2019). IHC ribbon counts also showed the characteristic inverted-U shape as a function of frequency. Macaque OHC ribbon counts decreased with increasing frequency as in cats (Liberman et al., 1990), whereas OHC ribbon counts in mice are similar across frequencies (Liberman & Liberman, 2016; Wood et al., 2021). The functional significance of this species difference is unknown, due to limited knowledge of the role of OHC ribbons and their opposing Type II afferent fibers.

Macaque IHC and OHC ribbons had variable volumes and shapes, as previously reported in other species (Weisz et al., 2012). The relative size of IHC and OHC ribbons seems to vary across species. Cats have larger IHC ribbons than OHC ribbons (Liberman et al., 1990); rats have similar IHC and OHC ribbon volumes (Weisz et al., 2012); and macaques have significantly smaller IHC ribbons than OHC ribbons ($k = 0.16$, $p < 0.001$). Whether these differences in synaptic body size and shape translate to functional differences is unknown.

In macaques, MOC innervation density was greatest in the mid-frequencies, whereas LOC innervation density was greatest in the low frequencies. These findings are consistent with the apical-basal gradients reported in humans (Liberman & Liberman, 2019). Macaque MOC innervation is intermediate to that of rodents (dense) and humans (sparse), whereas LOC innervation densities appear similar across species (Liberman & Liberman, 2019).

7.4.2 Cochlear histopathology in rhesus macaques following noise exposure: Species comparisons and effects of post-exposure survival time

7.4.2.1 Outer and inner hair cell survival

Rodent models of noise-induced SYN exhibit IHC ribbon loss in the absence of hair cell loss (e.g. Kujawa & Liberman, 2009). At 2 months post-exposure, macaques had minimal OHC and IHC loss. However, an average of 10% OHC loss was observed near the exposure band at 10 months post-exposure with substantial inter-subject and across-ear variability. Genetically

heterogeneous species, such as guinea pigs and macaques, show greater inter-animal variability in their response to acoustic injury than inbred mice (Wang et al., 2002).

Delayed emergence of OHC damage may indicate progression of inner ear injury over time (Fernandez et al., 2015; Kujawa & Liberman, 2006). In mice, a post-exposure survival of 10 months encompasses at least one quarter of the lifespan, introducing the confound of age-related decline. Macaques live up to 30-40 years, and age-related hearing loss begins around 15 years of age (Engle et al., 2013; Ng et al., 2015; Torre et al., 2004). Our macaques were 6-10 years old at the time of noise exposure and thus did not reach the onset of age-related hearing loss. Progressive OHC damage may be a characteristic of SYN previously attributed to aging. OHC loss may occur over time due to reduced strength of MOC feedback, which then renders the OHCs more vulnerable to damage.

Hook lesions, or complete hair cell loss in the basal tip of the cochlea, are reported in some models of noise-induced SYN (Liberman et al., 2015). There was no evidence of a hook lesion in our macaques, as there was normal OHC and IHC survival in the basal-most cochlear frequency region.

7.4.2.2 Inner hair cell ribbon counts

IHC ribbon loss occurs secondary to glutamate excitotoxicity (Hu et al., 2020; Kim et al., 2019). Our noise exposure reduced macaque IHC ribbon counts by 20-30%, and up to a maximum of 40%, at 2 months post-exposure. This model may represent a milder form of SYN compared to rodent models, which typically exhibit 50% IHC ribbon loss (Bharadwaj et al., 2021; Kujawa & Liberman, 2009; Lin et al., 2011; Singer et al., 2013). Given the high cost of nonhuman primates (Burton et al., 2019), it is not feasible to titrate noise level in the same way possible with rodents (Fernandez et al., 2020).

The IHC ribbon loss that was apparent at 2 months post-exposure was not present in macaques with 10 month post-exposure survivals. This finding is consistent with synaptic repair or regeneration, although there is no direct evidence for this conclusion. IHC ribbons are regenerated following acoustic overexposure in guinea pigs (Hickman et al., 2020, 2021; Shi et al., 2013; Song et al., 2016), but only in some mouse strains (Kim et al., 2019; Kujawa & Liberman, 2009; Liberman et al., 2015; Shi et al., 2015). In rodents that do show regeneration, ribbon recovery occurs within 1 month post-exposure. Therefore, it is possible that some IHC

ribbon loss had already recovered by 2 months post-exposure in our macaques. It is unknown whether the recovered ribbons and synapses function like native synapses.

Despite the absence of sustained IHC ribbon loss, we do observe significant, permanent changes in physiological function and perceptual abilities in our noise-exposed macaques (see Chapters 8 and 9). These data suggest that even a mild and temporary loss of synapses and their recovery can have lasting effects on auditory physiology and perception. Repaired or regenerated synaptic physiology may differ from innate synapses (Vincent et al., 2022). Additionally, SYN-related changes to the central auditory physiology, such as the inferior colliculus (Bakay et al., 2018; Shaheen & Liberman, 2018) and auditory cortex (Asokan et al., 2018), may not be reversed by peripheral repair.

7.4.2.3 Inner hair cell ribbon volumes

Enlarged IHC ribbon volumes have been observed in noise-induced SYN and age-related hearing loss (Furman et al., 2013; Hickman et al., 2020; Kim et al., 2019; Song et al., 2016; Stamataki et al., 2006; Valero et al., 2017). Ribbon enlargement occurs immediately following noise exposure (Liberman et al., 2015), but is independent of glutamate excitotoxic processes (Kim et al., 2019). Sustained ribbon enlargement is consistently observed up to 1-2 weeks post-exposure (Furman et al., 2013; Hickman et al., 2020; Kim et al., 2019; Liberman et al., 2015; Song et al., 2016), may be evident in guinea pigs through 1-6 months post-exposure (Hickman et al., 2020; Song et al., 2016), at 2 months post-exposure in macaques (Valero et al., 2017), and now appears as a persistent phenotype through even later post-exposure times in macaques.

The functional significance of enlarged ribbon volume is unknown, but likely affects synaptic physiology and Type I afferent auditory nerve fiber function. The capacity for tethering and fusing readily releasable vesicles varies with ribbon size (Becker et al., 2018; Matthews & Fuchs, 2010; Moser et al., 2020). Larger ribbons may tether more vesicles (Song et al., 2016), yielding greater multivesicular release and larger postsynaptic potentials. In a recent study of single-unit auditory nerve responses in synaptopathic mice, Suthakar and Liberman (2021) reported enhanced onset and sustained firing rates in response to tones in quiet and in noise. The SYN model used in this study also shows enlarged IHC ribbon volumes (Liberman et al., 2015), supporting the hypothesis that enlarged ribbons facilitate increased sound-evoked auditory nerve activity. However, auditory nerve recordings in guinea pigs do not show this same gain-of-

function (Song et al., 2016), so further work is needed to reconcile the discrepancies in these studies.

7.4.2.4 Outer hair cell ribbon synapses

Little work has investigated OHC ribbons, let alone in the context of noise exposure. The OHC afferent synapse does not appear to experience glutamate excitotoxicity like the IHC afferent synapse. OHC afferents, or Type II auditory nerve fibers, do not express the same type of AMPA receptors as IHC Type I afferent fibers (Liberman et al., 2011) and have not been reported to exhibit terminal swelling under conditions that are excitotoxic to Type I afferents.

Wood et al. (2021) provided the first characterization of OHC ribbons in a mouse model of noise-induced SYN. At 7 days post-exposure, mice exhibited increased counts and sizes of OHC ribbons compared to controls. Temporary threshold shifts had not yet resolved, but OHC loss was not significantly different from controls.

Our macaques showed larger OHC ribbon volumes, but no change in OHC ribbon counts. As suggested by Wood et al. (2021), changes in OHC ribbons may reflect a response to maximal acoustic stimulation or as compensation to mechanical trauma. Perhaps the increase in OHC ribbon count in the Wood et al. study is an acute response to acoustic injury, whereas enlarged OHC ribbons may reflect a chronic change in peripheral function following acoustic injury. As with IHC ribbons, the functional significance of enlarged OHC ribbons is not known. In this case, Type II afferent signaling could be impacted, and the functional contribution of these neurons is also debated (Liu et al., 2015; Maison et al., 2016; Weisz et al., 2012; Zhang & Coate, 2017). Impending data from macaques with shorter post-exposure survival durations will provide valuable insight to the nature of noise-induced OHC synaptic changes and how they compare to histopathologic changes of IHC ribbons.

7.4.2.5 Efferent terminal density

Olivocochlear efferent neurons project from the brainstem to the cochlea and mediate cochlear responses to incoming sound (Guinan, 2018). The MOC system mediates OHC motility, resulting in anti-masking and otoprotective functions (Guinan, 2006; Lopez-Poveda, 2018). MOC neurons are thought to receive input from low spontaneous rate ANFs (Liberman, 1988), which may be preferentially lost in SYN (Furman et al., 2013; Liberman et al., 2015; Schmiedt et al., 1996; but see Suthakar & Liberman, 2021), so MOC innervation and function could be impacted by IHC ribbon loss. Some studies in mice show reduced MOC innervation

density following noise-induced SYN (Boero et al., 2018; Qian et al., 2021) or age-related hearing loss (Boero et al., 2020; Grierson et al., 2022), and reduced MOC innervation in aging humans with minimal OHC loss (Liberman & Liberman, 2019). However, this study and others find no change in MOC innervation density in noise-exposed (Grierson et al., 2022) or aging mice (Kobrina et al., 2020). Etiology of inner ear damage may differentially affect the MOC system. MOC innervation and function may also change dynamically over time and vary across species.

Less is known about the unmyelinated LOC neurons, which synapse onto Type I afferent auditory nerve fiber dendrites (Guinan, 2018). As seen in the present data, LOC innervation density appears less affected by noise (Grierson et al., 2022) and age (Kobrina et al., 2020; Liberman & Liberman, 2019), although the location of LOC terminals may shift from afferent dendrites to IHCs in aging (Lauer et al., 2012).

7.4.2.6 Other inner ear structural elements

The inner ear sensory epithelium contains many other elements critical to its healthy function. Though not investigated here, the condition of hair cell stereocilia, supporting cells, and the stria vascularis can become pathological in response to a cochlear insult. Stereocilia fusion or damage can occur in the absence of hair cell loss, rendering hair cells functionally compromised (Engstrom, 1984; Liberman & Dodds, 1984a, 1984b; Liberman & Kiang, 1984; Wang et al., 2002). Supporting cells play an important role in inner ear response and homeostasis following injury, and may be less susceptible to inner ear damage than hair cells (Liu et al., 2015; Sugawara et al., 2005; Wan et al., 2013; Wang et al., 2002). Strial atrophy is a component of age-related hearing loss that minimally contributes to speech recognition abilities (Landegger et al., 2016; Wu et al., 2020, 2021), but some studies indicate changes in strial structure following noise exposure (Wang et al., 2002). Characterization of these and other inner ear structures will enhance our understanding of the relationship among inner ear cell types and their response to acoustic injury.

Another open question is whether ears with ribbon loss and recovery show degeneration of spiral ganglion cells. Delayed spiral ganglion cell degeneration is a hallmark of SYN in mice with permanent ribbon loss (Kujawa & Liberman, 2009), but this has not been investigated in animal models with ribbon recovery.

7.4.3 Implications for diagnostic testing

Anatomical characterization of SYN identifies sites of lesion to guide the development of diagnostic testing and therapeutic treatment strategies. Unlike SNHL, which can be readily diagnosed using otoacoustic emissions assays of OHC function, the more subtle cochlear changes accompanying SYN remain hidden from current clinical diagnostic approaches. If ribbon volume is indeed a prominent and permanent consequence of SYN, then physiological or psychophysical measures that probe according changes in synaptic physiology would be successful. If spiral ganglion cell degeneration does accompany ribbon loss and recovery, then assays probing gross auditory nerve function may be successful. In subsequent chapters, we discuss these and other possibilities in greater depth.

CHAPTER 8

Otoacoustic emissions, medial olivocochlear reflexes, and middle ear muscle reflexes in macaque monkeys following noise exposure intended to cause cochlear synaptopathy

8.1 INTRODUCTION

The loss of inner hair cell ribbon synapses, or cochlear synaptopathy (SYN), is a recently discovered inner ear pathology thought to contribute to hearing difficulties in background noise (Kujawa & Liberman, 2006, 2009). SYN results in degradation of afferent auditory nerve fibers, especially those with low spontaneous firing rates (LSR) and high thresholds to sound stimulation (Furman et al., 2013; Liberman et al., 2015; Schmiedt et al., 1996; but see Suthakar & Liberman, 2021). Hearing sensitivity is maintained by preserved outer hair cell (OHC) function and intact high spontaneous firing rate fibers with low sound thresholds. In contrast, the more susceptible LSR fibers encode signals in noise (Costalupes, 1985), leading to the hypothesis that SYN causes impaired auditory perception in background noise (Bharadwaj et al., 2014; Oxenham, 2016; Plack et al., 2014). Although SYN can be induced, measured, and verified in animal models, evidence for SYN in humans is mixed (Bharadwaj et al., 2019; Bramhall et al., 2019; DiNino et al., 2021; Hickox et al., 2017).

Among the top candidate biomarkers of SYN are assays that probe LSR fiber function, such as encoding of suprathreshold sounds. In addition to their role in afferent processing of signals in noise, LSR neurons may provide input to two auditory efferent pathways: the medial olivocochlear reflex (MOCR; Liberman, 1988) and middle ear muscle reflex (MEMR; Kobler et al., 1992; Liberman & Kiang, 1984; Liberman & Simmons, 1985). These feedback pathways contribute to unmasking of signals in noise and protect the ear from acoustic injury (Guinan, 2006; Kawase et al., 1993; Liberman & Guinan, 1998; Lopez-Poveda, 2018). If MOCR and MEMR inputs are diminished due to SYN-related loss of LSR fibers, these pathways may also degrade, further accentuating hearing in noise difficulties and increasing susceptibility to injury. Furthermore, MOCR and MEMR strength varies extensively in normal hearing adults (Backus & Guinan, 2007). This variability may cause intrinsic differences in hearing abilities (Abdala et al., 2014; Bidelman & Bhagat, 2015; de Andrade et al., 2011; de Boer & Thornton, 2008; de Boer et al., 2012; Giraud et al., 1997; Lauer et al., 2021; Mahoney et al., 1979; Mertes et al., 2019;

Shehorn et al., 2020; Smart et al., 2019) or susceptibility to acoustic injury (Fuente, 2015; Maison & Liberman, 2000; Smith & Keil, 2015), and may underlie differences in hearing abilities in background noise among normal hearing listeners (i.e. hidden hearing loss).

Aside from gross electrophysiological tests, such as the auditory brainstem response and envelope following response, the MEMR is the leading assay in studies of SYN. MEM motoneurons attenuate sound conduction through the middle ear by stiffening the ossicular chain via stapedius muscle contraction (Moller, 1962). Noninvasive MEMR measurements record changes in sound pressure levels of a probe stimulus in the ear canal. These changes in sound level increase with elicitor level and activate quickly after elicitor onset. The MEMR is reduced in rodents with noise-induced SYN (Bharadwaj et al., 2021; Valero et al., 2016; Valero et al., 2018) and in some humans at risk for SYN (Bharadwaj et al., 2021; Bramhall et al., 2022; Mepani et al., 2020; Shehorn et al., 2020; Wojtczak et al., 2017) (but see Causon et al., 2020; Guest et al., 2019; Higson, Morgan, et al., 1996).

Investigations of MOC efferent innervation and functional integrity following SYN are also emerging. MOC efferent neurons indirectly decrease sound-evoked excitation of inner hair cells by suppressing OHC amplification of incoming sounds (i.e. the cochlear amplifier) (Guinan, 2006; Lopez-Poveda, 2018). Otoacoustic emissions (OAEs) are a measure of OHC function routinely used in clinical audiology (Kemp, 1978). OAEs are suppressed in the presence of noise via the MOCR (Berlin, Hood, Wen, et al., 1993; Collet et al., 1992; Kujawa et al., 1993). One study reported decreased OAE suppression in a mouse model of noise-induced SYN, but this finding was attributed to the MEMR rather than the MOCR and efferent innervation was not histologically assessed (Valero et al., 2016). Other studies demonstrated reduced MOC innervation in synaptopathic mice, but did not functionally characterize MOCR strength (Boero et al., 2018; Boero et al., 2020; Maison et al., 2013; Qian et al., 2021). MOC projections and function also decline with age independent of OHC loss and elevated hearing thresholds (Abdala et al., 2014; Fu et al., 2010; Jacobson et al., 2003; Kim et al., 2002; Liberman & Liberman, 2019; Radtke-Schuller et al., 2015; Zhu et al., 2007), suggesting that MOC degradation may accompany age-related SYN. These converging anatomical and physiological consequences of SYN to the MOC pathway identify the MOCR as a candidate diagnostic test that requires further investigation.

Both the MOCR and MEMR can be elicited by noise, but their activation and responses differ in spectrum, intensity, and time course. The MOCR is elicited by moderate and high level broadband noise and reaches peak strength after 100 ms (Guinan, 2006). In contrast, the MEMR is maximally elicited by high level, low frequency noise and activates almost instantaneously after sound onset (Feeney et al., 2017; Margolis et al., 1980). Given the ease of measurement and similarity to current clinical tests, the MOCR and MEMR could be readily implemented for the diagnosis of SYN if they are sufficiently sensitive and specific (Bharadwaj et al., 2019; Bramhall et al., 2019; Hickox et al., 2017). Evaluation of the MOCR and further validation of the MEMR as SYN biomarkers is warranted, especially in an animal model with human-like auditory anatomy and physiology and susceptibility to noise-induced hearing loss (Burton et al., 2019).

Here, we measured OAEs, MOCRs, and MEMRs in macaques before and after noise exposure known to cause synaptopathy (Chapter 7). First, we characterized normative OAE, MOCR, and MEMR responses in normal hearing macaques and compared these responses to young normal hearing adults. Then, we repeated these measures in macaques following noise exposure known to cause SYN to monitor changes in OHC, MOCR, and MEMR function. The cross-species and within-subject design aspects allowed us to simultaneously assess the sensitivity and translatability of candidate SYN biomarkers.

8.2 MATERIALS AND METHODS

8.2.1 Subjects

Auditory function, as assessed by OAEs and MOCRs, was characterized in 15 adult rhesus macaques (*Macaca mulatta*, 7-9 years old, 4 female). Of these, 13 macaques (4 female) underwent testing before and after noise exposure. Only 4 macaques underwent MEMR testing, all after noise exposure.

Eleven young adults (20-30 years old, 6 female) were recruited to assess species differences in OAE, MOCR, and MEMR responses. Subjects had no self-reported history of middle-ear dysfunction, significant noise exposure, or neurological disorders. Prior to testing, audiometry was performed using insert earphones and a standard clinical audiometer to ensure normal hearing status (<25 dB HL) from 250-8000 Hz.

All research procedures were approved by the Institutional Animal Care and Use Committee and the Institutional Review Board at Vanderbilt University Medical Center.

Identical equipment and stimulus conditions were used for macaque and human testing. All testing was conducted in a sound-treated booth (ETS-Lindgren Acoustic Systems, Cedar Park, TX). For all human testing (awake), participants were seated in a chair and asked to remain quiet and still during testing. For awake measurements in macaques, subjects were seated in an acrylic primate chair and head-fixed for the duration of testing (approximately 10-20 minutes per session) in order to maintain stable probe placement in the ear and to minimize movement-related noise in the measures. For details about anesthetized measurements in macaques, see General Methods > Anesthetized Procedures.

8.2.2 Otoacoustic emission (OAE) and medial olivocochlear reflex (MOCR) testing

Distortion product otoacoustic emissions (DPOAEs) and transient evoked otoacoustic emissions (TEOAEs) were measured according to the methods described in General Methods > OAE Testing. Additional DPOAE testing was completed in some macaques using an ER10X probe system (Etymotic, Elk Grove Village, IL). Stimulus parameters were identical to those for the Scout DPOAE measurements, except f_2 = 1-32 kHz, 4 points per octave.

The MOCR was probed by suppression of OAEs by contralateral noise. A closed field speaker (MF1, Tucker-Davis Technologies) was coupled to the contralateral ear using an ER-3 or ER-3A foam ear tip. A broadband white noise (400-40000 Hz) was generated using Tucker-Davis Technologies hardware (RZ6 Multi I/O Processor) and OpenEx software. Noise was continuously presented at 40, 50, or 60 dB spectrum level while either DPOAEs (f_2 = 1-10kHz, 4 points per octave; f_2/f_1 = 1.22; L_1/L_2 = 65/55 dB SPL) or TEOAEs were being measured in the ipsilateral ear. OAE suppression was defined as the difference in OAE amplitudes when there was no contralateral noise and when the noise was present ($suppression = OAE_{noise} - OAE_{no\ noise}$).

8.2.3 Middle ear muscle reflex (MEMR) testing

Wideband middle ear muscle reflexes (WB-MEMRs) were measured using a FireFace audio interface (RME, Haimhausen, Germany) and the ER10X probe system following the methods of Keefe et al. (2017) and Bharadwaj et al. (2021). A train of 7 clicks (90 dB pSPL) were presented in alternation with 120 ms-long ipsilateral noise elicitors (500-8500 Hz, 60-108 dB SPL). For each elicitor level, this click + elicitor train was presented either 15 (humans) or 32 times (macaques) with an inter-trial interval of 1.5 seconds. The immittance measured in response to clicks two through seven were averaged and compared to the immittance measured in response to the first click. The resulting change in ear canal pressure, or absorbance, was

quantified as a function of frequency. The absolute value of this function between 500-2000 Hz was summed to derive the MEMR metric: *Δ absorbed power*, in dB.

8.2.4 Additional animal procedures

Following baseline characterization, macaques underwent a single noise exposure intended to generate cochlear synaptopathy (see General Methods). DPOAE amplitudes and thresholds, TEOAE amplitudes and suppression, and MEMRs were tested periodically following noise exposure (see Figure 8.1) to monitor changes in outer hair cell, MOCR, and MEMR function over time. After completion of the study, macaques were euthanized and cochlear tissues were harvested to assess cochlear integrity (Chapter 7).

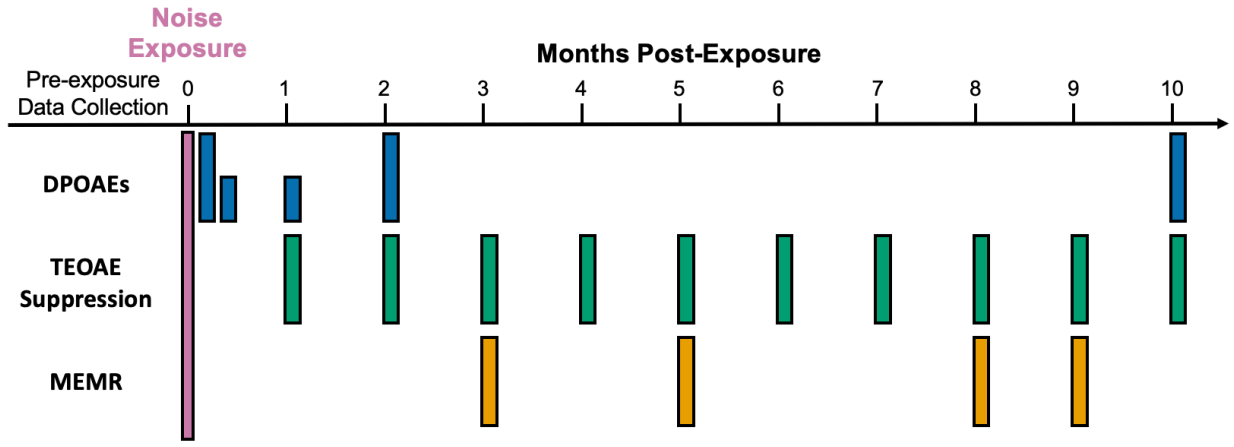

Figure 8.1 Timeline of post-exposure data collection in macaques. DPOAE amplitudes and thresholds were measured immediately post-exposure and at 2 and 9-10 months post-exposure. Some subjects also had abbreviated DPOAE testing at 1 day, 1 week, and 1 month post-exposure. TEOAE suppression was measured monthly post-exposure. MEMRs were measured in some subjects bi-monthly post-exposure.

8.2.5 Statistical analyses

Statistical analyses were conducted using linear mixed effects models ("fitlme") in MATLAB 2018a. The dependent variable in the models assessing the effects of species and noise exposure status was either OAE amplitude, OAE suppression, or MEMR threshold. Species, sex, ear laterality, DPOAE or TEOAE frequency, and noise exposure status (for macaques) were entered as fixed effects into the model, while intercepts for individual subjects were entered as random effects. In all cases *p*-values were obtained by likelihood ratio testing of the model with the effect in question against the model without the effect in question. A

significant *p*-value was defined as $p < 0.05$. *T*-statistics are reported for each model, similar to the *F*-statistic that is often reported for such models.

8.3 RESULTS

8.3.1 Otoacoustic emissions in macaques and humans

Distortion product otoacoustic emissions (DPOAEs) and transient-evoked otoacoustic emissions (TEOAEs) were measured in awake macaques and humans. Figure 8.2 illustrates mean DPOAE (A) and TEOAE amplitudes (B) for both species. Macaques had larger DPOAE amplitudes than humans from 2-10 kHz (Table 8.1), which may reflect differences in nonlinear distortion mechanisms across species, as well as differences in their audible ranges. In contrast, macaques and humans had similar TEOAE amplitudes across frequency components, suggesting that the mechanisms driving these reflection emissions are similar across species. This similarity is advantageous when measuring OAE suppression, as differences in OAE amplitudes could contribute to differences in the magnitude of OAE suppression measured.

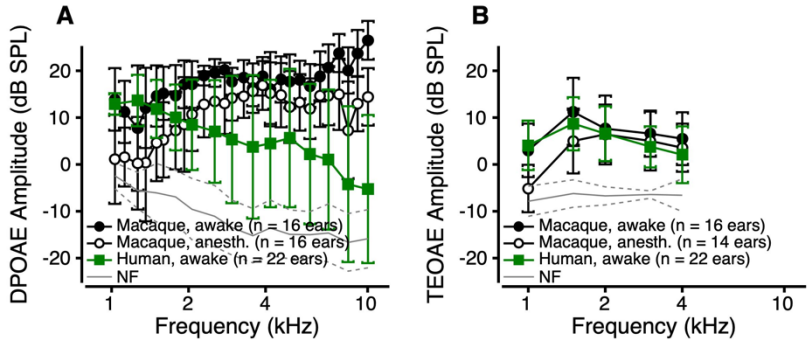

Figure 8.2 Mean otoacoustic emission amplitudes in macaques (black circles; awake: filled, anesthetized: open) and in humans (green squares; awake). A. DPOAE amplitude as a function of f_2 frequency. B. TEOAE amplitude as a function of frequency. Error bars indicate ± 1 standard deviation from the mean.

Linear mixed effects models were used to evaluate differences in DPOAE and TEOAE amplitudes according to species, sex, ear laterality, and frequency. DPOAE amplitudes differed across species, sex, and frequency according to:

*DPOAE Amplitude ~ Species + Frequency + Species*Sex + Species*Frequency;* $R^2 = 0.6399$

Table 8.1 Linear mixed effects model for DPOAE amplitude and species

Variable	***T-statistic (df)***	***p-value***
Species	-2.91 (754)	0.004
Frequency	-11.12 (754)	<0.001
Species*Sex	2.94 (754)	0.003
Species*Frequency	20.30 (754)	<0.001

TEOAE amplitudes did not differ significantly by species, sex, ear laterality, or frequency (all *p-values* > 0.05). These findings are consistent with previous reports that OAE amplitudes differ between humans and macaques, males and females, but not left and right ears (Lasky et al., 2000; Lasky et al., 1995; McFadden et al., 2009; McFadden et al., 2006).

Anesthesia is known to affect OAEs in animals and humans. Anesthesia typically results in smaller OAE amplitudes, but with differences across species and anesthetic agents (Cederholm et al., 2012; Ferber-Viart et al., 1998; Guven et al., 2006; Harel et al., 1997; Kim et al., 2012; Sheppard et al., 2018). DPOAE and TEOAE amplitudes from macaques under isoflurane anesthesia are shown in Figure 8.2 (open circles; compare to filled circles). DPOAE amplitudes were generally smaller under anesthesia than in awake subjects. Low frequency TEOAEs were also smaller under anesthesia, but high frequency TEOAE components were not different. Linear mixed effects models supported these observations, according to the following models (Table 8.2 and 8.3):

*DPOAE Amplitude ~ State + State*Frequency;* $R^2 = 0.51$

Table 8.2 Linear mixed effects model for macaque DPOAE amplitude and state

Variable	***T-statistic (df)***	***p-value***
State	-4.80 (964)	<0.001
State*Frequency	3.20 (964)	0.001

*TEOAE Amplitude ~ Sex + State*Frequency;* $R^2 = 0.4226$

Table 8.3 Linear mixed effects model for macaque TEOAE amplitude and state

Variable	***T-statistic (df)***	***p-value***
Sex	2.12 (140)	0.036
State*Frequency	2.62 (140)	0.010

These observations contribute knowledge about the effects of isoflurane anesthesia on DPOAEs and TEOAEs in macaques. OAE amplitude reductions may be caused by changes in cochlear or cerebral blood flow, middle-ear pressure or mechanics, or direct suppression of OHC function via unknown pharmacological effects of isoflurane that vary along the cochlear length (Cederholm et al., 2012; Ferber-Viart et al., 1998; Harel et al., 1997; Sheppard et al., 2018).

DPOAE and TEOAE amplitudes were compared within-species from 1-4kHz. Both species showed significant differences in DPOAE vs. TEOAE amplitudes with significant effects of frequency. Human TEOAEs were larger than DPOAEs (Table 8.4), whereas macaque DPOAEs were larger than TEOAEs (Table 8.5), consistent with previous reports after accounting for differences in stimulus level (Gorga et al., 1993; Lasky et al., 2000).

*Human OAE Amplitude ~ DPvsTE + DPvsTE*Frequency;* $R^2 = 0.5572$

Table 8.4 Linear mixed effects model for human DPOAE vs. TEOAE amplitudes

Variable	***T-statistic (df)***	***p-value***
DPvsTE	2.71 (209)	0.007
DPvsTE*Frequency	2.75 (209)	0.007

Macaque OAE Amplitude ~ DPvsTE + Frequency; $R^2 = 0.5993$

Table 8.5 Linear mixed effects model for macaque DPOAE vs. TEOAE amplitudes

Variable	***T-statistic (df)***	***p-value***
DPvsTE	-3.10 (149)	0.002
Frequency	2.02 (149)	0.045

8.3.2 Medial olivocochlear reflex as measured by otoacoustic emission suppression in macaques and humans

DPOAEs and TEOAEs were measured in awake macaques and humans in quiet and in the presence of contralateral broadband noise (40, 50, or 60 dB spectrum level) to elicit OAE suppression, a measure of the MOCR. An example of TEOAE suppression is shown for Monkey Al in Figure 8.3. OAE amplitudes were largest when there was no contralateral elicitor (Figure 8.3A, black, labeled 'No Noise') and

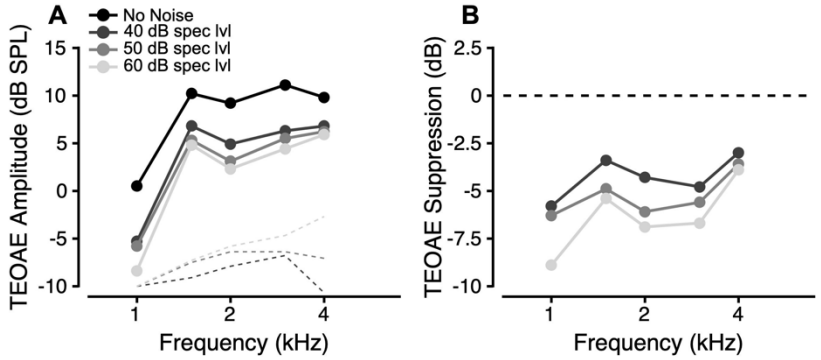

Figure 8.3 Exemplar TEOAE suppression data from Monkey Al, left ear. A. TEOAE amplitudes as a function of frequency in the presence of no noise (black) and 40, 50, or 60 dB spectrum level broadband noise (dark gray to light gray) presented in the contralateral ear. B. TEOAE suppression as a function of frequency with 40, 50, or 60 dB noise elicitors (dark gray to light gray, as in A).

reduced in the presence of contralateral noise (gray). OAE suppression was calculated as the difference in OAE amplitude with and without contralateral noise (*suppression* = OAE_{noise} – $OAE_{no\ noise}$; Figure 8.3B).

Figure 8.4 shows mean DPOAE suppression (A-C) and TEOAE suppression (A'-C') as a function of frequency with 40 (A, A'), 50 (B, B'), and 60 (C, C') dB spectrum level contralateral noise elicitors. Compared to humans (green squares), macaques had greater OAE suppression across most conditions. DPOAE and TEOAE suppression were greater in the low frequencies, as previously reported (Keppler et al., 2010; Kim et al., 2002; Kumar et al., 2013).

Species and its interactions were among the major contributing variables in linear mixed effects models assessing differences in OAE suppression according to species, ear, frequency, noise level (Tables 8.6 and 8.7). Of note, no female monkeys underwent DPOAE suppression testing, so the effects of sex on OAE suppression were not assessed.

*DPOAE Suppression ~ Species + Species*Ear + Species*Frequency + Ear*Frequency;* R^2 = 0.0994

Table 8.6 Linear mixed effects model for DPOAE suppression and species

Variable	***T-statistic (df)***	***p-value***
Species	-2.39 (1078)	0.017
Species*Ear	2.03 (1078)	0.043
Species*Frequency	3.51 (1078)	<0.001
Ear*Frequency	-2.71 (1078)	0.007

*TEOAE Suppression ~ Species + Frequency + Species*Ear + Frequency*Noise_Level;* R^2 = 0.4705

Table 8.7 Linear mixed effects model for TEOAE suppression and species

Variable	***T-statistic (df)***	***p-value***
Species	-2.68 (559)	0.007
Frequency	-2.00 (559)	0.046
Species*Ear	2.76 (559)	0.006
Frequency*Noise Level	2.62 (559)	0.009

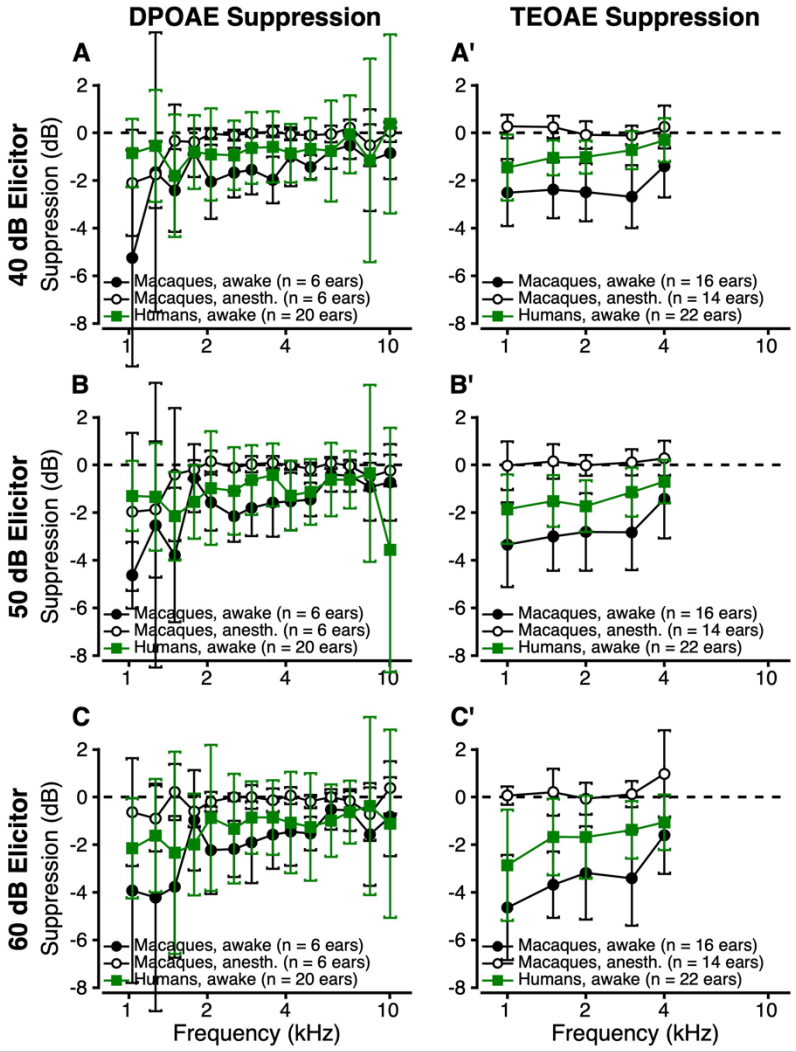

Figure 8.4 Mean OAE suppression in macaques (black circles; awake: filled, anesthetized: open) and in humans (green squares; awake). A, B, C. DPOAE suppression as a function of f_2 frequency with the 40, 50, or 60 dB spectrum level contralateral elicitor. A', B', C'. TEOAE suppression as a function of frequency with the 40, 50, or 60 dB spectrum level contralateral elicitor. Error bars indicate ± 1 standard deviation from the mean.

DPOAE and TEOAE suppression magnitudes were compared within-species from 1-4kHz using linear mixed effects models. Humans and monkeys showed no significant difference in DPOAE vs. TEOAE suppression across frequencies (all *p-values* > 0.05).

OAE suppression was also measured in anesthetized macaques. Consistent with previous reports (Boyev et al., 2002; Chambers et al., 2012; Guitton et al., 2004; Valero et al., 2016), OAE suppression was essentially absent under anesthesia across all stimulus conditions (Figure 8.4, open circles). State (awake vs. anesthetized) was one of the major contributing variables in linear mixed effects models assessing differences in OAE suppression according to state, ear, frequency, and noise level (Tables 8.8 and 8.9).

*DPOAE Suppression ~ Ear + Noise_Level + Ear*Noise_Level + State*Frequency;* $R^2 = 0.2215$

Table 8.8 Linear mixed effects model for macaque DPOAE suppression and state

Variable	***T-statistic (df)***	***p-value***
Ear	-2.44 (494)	0.015
Noise Level	-2.33 (494)	0.020
Ear*Noise Level	2.29 (494)	0.022
State*Frequency	-3.35 (494)	0.001

*TEOAE Suppression ~ Noise_Level + Noise_Level*Frequency + State*Frequency + State*Noise_Level;* $R^2 = 0.6633$

Table 8.9 Linear mixed effects model for macaque TEOAE suppression and state

Variable	***T-statistic (df)***	***p-value***
Noise Level	-4.55 (440)	<0.001
Noise Level*Frequency	3.38 (440)	<0.001
State*Frequency	-4.38 (440)	<0.001
State*Noise Level	4.24 (440)	<0.001

OAE suppression test-retest reliability was assessed as the absolute value of the difference in OAE suppression across two separate test sessions. Average DPOAE and TEOAE suppression test-retest values are plotted as a function of frequency in Figure 8.5. Across elicitor levels and frequencies, TEOAE suppression test-retest was lower, with average values of 1.36 and 1.17 dB for macaques and humans, respectively. In comparison, average DPOAE suppression test-retest was 1.89 and 1.77 dB for macaques and humans, respectively. The higher test-retest values for DPOAE suppression were likely driven by poorer reliability in the lowest and highest frequencies. The greater test-retest reliability of TEOAE suppression over DPOAE suppression is consistent with previous reports in humans (Kumar et al., 2013), and may be related to observations that DPOAE suppression is highly sensitive to minor changes in primary tone frequencies and levels (Wagner et al., 2007). The fact that both DPOAE and TEOAE suppression varies as a function of frequency suggests that TEOAE (but not DPOAE) suppression at lower frequencies may be the most reliable MOCR metric (i.e. larger suppression values and proportionally less test-retest variability).

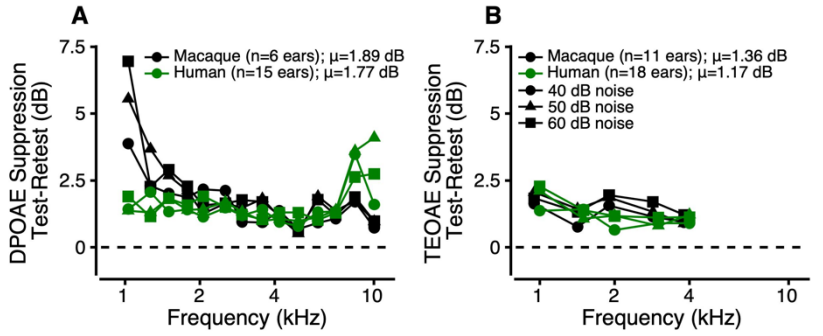

Figure 8.5 Mean OAE suppression test-retest reliability (absolute value ($suppression_{test} - suppression_{retest}$)) in macaques (black) and humans (green). A. DPOAE suppression test-retest reliability as a function of f_2 frequency with a 40 (circles), 50 (triangles), or 60 (squares) dB spectrum level contralateral elicitor. B. Same as A, but for TEOAE suppression test-retest reliability.

8.3.3 Middle ear muscle reflexes in humans

Wide-band middle ear muscle reflexes (WB-MEMRs) were measured in humans by assessing the change in click intensity evoked by an interleaved ipsilateral noise elicitor. Exemplar MEMRs from two human subjects are shown in Figure 8.6A & A'. Change in click level measured in the ear canal (Δ absorbed power) is plotted as a function of frequency for each of the elicitor levels. As elicitor level increased, the change in absorbed power also increased.

The absolute value of the change in absorbed power between 500-2000 Hz was summed and plotted as a function of elicitor level in Figure 8.6B. The level at which this function exceeded 0.1 dB was defined as the MEMR threshold. Figure 8.6C shows the mean MEMR threshold for humans (85.1 dB SPL; n = 18 ears). The distribution of MEMR thresholds revealed a wide range of values (73-99 dB SPL) that appeared to cluster in two groups. MEMR thresholds did not differ significantly according to sex or ear laterality (p-values > 0.05).

Unfortunately, the WB-MEMR assay was not developed in time to measure responses from macaques before noise exposure. Normative WB-MEMR measurements from a separate cohort of control macaques is pending. Post-exposure data are discussed in Section 8.3.6.

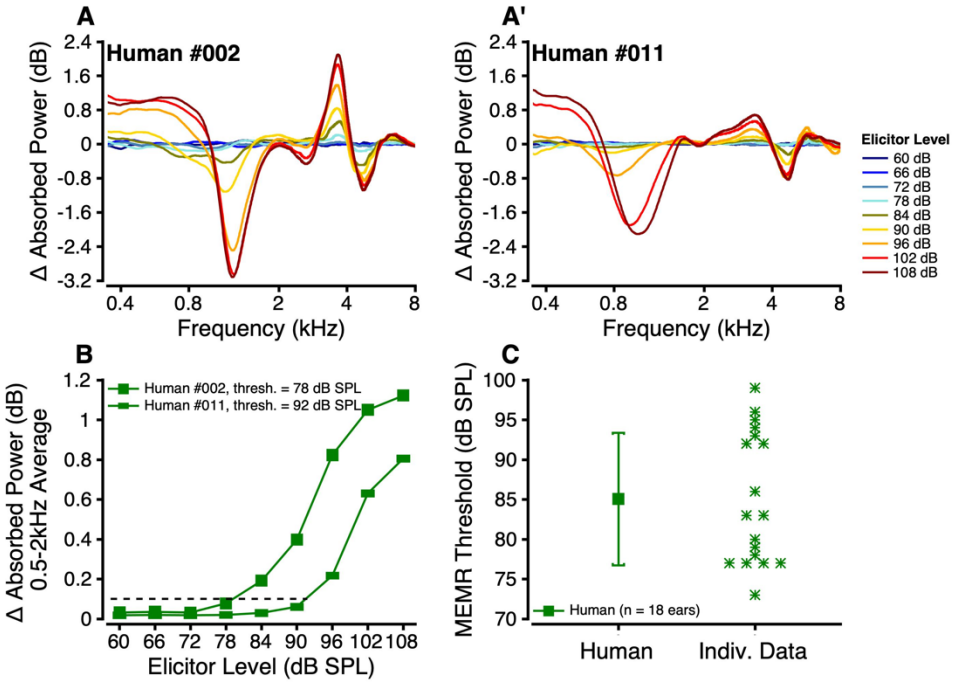

Figure 8.6 A,A'. Exemplar MEMR spectra from two female human subjects across elicitor levels. B. Change in absorbed power between 0.5-2kHz as a function of elicitor level. Functions are derived from the data in A and A'. Dashed line indicates the threshold cutoff value of 0.1 dB. C. Mean MEMR thresholds for humans (square; n = 18 ears). Error bars indicate ± 1 standard deviation from the mean. Individual data (stars) are also plotted to show the distribution of MEMR thresholds.

8.3.4 Otoacoustic emissions in macaques following noise exposure

We measured DPOAE amplitudes and thresholds in macaques following noise exposure intended to cause SYN to monitor OHC function. We elected to use DPOAEs since they are a routine component of clinical audiology assessments. Additionally, the larger amplitudes of

DPOAEs increase the sensitivity of DPOAE testing to subtle changes in OHC function compared to smaller amplitude TEOAEs.

Figure 8.7A shows DPOAE amplitudes as a function of f_2 frequency before exposure and immediately, 2 months, and 9-10 months post-exposure. DPOAE amplitudes were significantly reduced immediately following noise exposure, but recovered to pre-exposure amplitudes by 2 months post-exposure and were stable or increased (positive *T*-statistic) at 9-10 months post-exposure (Table 8.10). DPOAE thresholds followed a similar trend (Figure 8.7B): thresholds were elevated immediately after exposure, returned to pre-exposure values or improved slightly (negative *T*-statistic) by 2 months post-exposure, and were stable or improved at 9-10 months post-exposure (Table 8.11). These apparent improvements in DPOAE amplitudes and thresholds at 9-10 months post-exposure may be due to sampling, as not all subjects have reached this time point yet. Noise floors were consistent across testing time points.

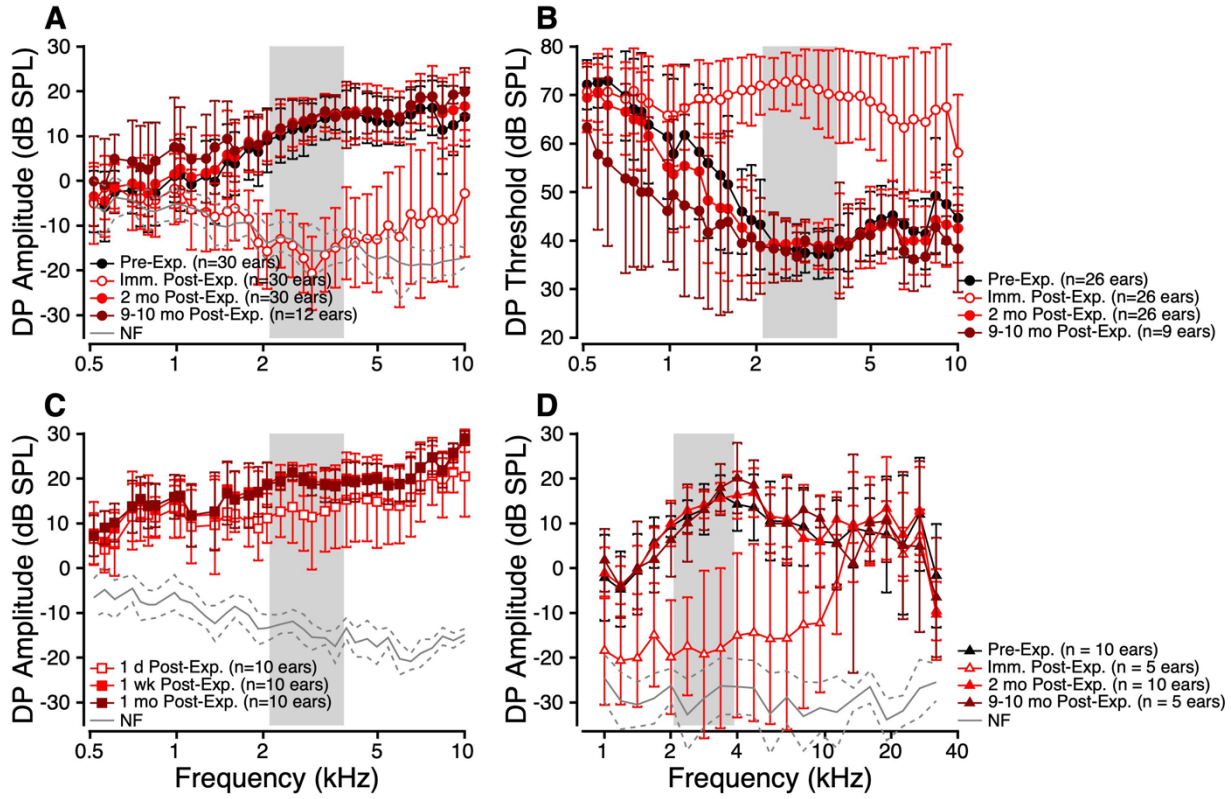

Figure 8.7 Mean macaque DPOAE amplitudes and thresholds before and after noise exposure. A. DPOAE amplitude as a function of f_2 frequency before noise exposure (black) and immediately (open red), 2 months (filled red), and 9-10 months (dark red) post-exposure. B. Same as A, except DPOAE threshold as a function of f_2 frequency. C. DPOAE amplitude as a function of f_2 frequency measured in awake macaques 1 day (open red), 1 week (filled red), or 1 month (dark red) post-exposure. D. Same as A, except DPOAEs were measured using a high frequency system (1-32 kHz; note the x-axis).

Table 8.10 Linear mixed effects models for macaque DPOAE amplitudes before and after noise exposure

Post-Exposure Time Point	***R-squared***	**Variable**	***T-statistic (df)***	***p-value***
Immediate	0.54	Exposure	-12.98 (1992)	<0.000
		Frequency	18.87 (1992)	<0.000
		Exposure*Frequency	-16.14 (1992)	<0.000
2 Months	0.44	Frequency	14.56 (1959)	<0.000
9-10 Months	0.47	Exposure	7.30 (1408)	<0.000
		Frequency	18.28 (1408)	<0.000
		Exposure*Frequency	-1.53 (1408)	<0.000

Table 8.11 Linear mixed effects models for macaque DPOAE thresholds before and after noise exposure

Post-Exposure Time Point	***R-squared***	**Variable**	***T-statistic (df)***	***p-value***
Immediate	0.52	Exposure	15.67 (1796)	<0.000
		Frequency	-13.90 (1796)	<0.000
		Exposure*Frequency	9.10 (1796)	<0.000
2 Months	0.29	Exposure	-3.26 (1809)	0.001
		Frequency	-10.64 (1809)	<0.000
9-10 Months	0.33	Exposure	-7.92 (1215)	<0.000
		Frequency	-12.886 (1215)	<0.000
		Exposure*Frequency	-3.50 (1215)	<0.000

In some macaques, DPOAEs were also measured while subjects were awake and head-fixed at 1 day, 1 week, and 1 month post-exposure to assess the time course of recovery from noise-induced temporary threshold shifts (Figure 8.7C). DPOAE amplitudes were significantly smaller at 1 day post-exposure, but similar at 1 week and 1 month post-exposure (see statistics in Table 8.12), suggesting recovery of outer hair cell function within 1 week.

Table 8.12 Linear mixed effects models for awake macaque DPOAE amplitudes before exposure and at early post-exposure times

Post-Exposure Time Point	***R-squared***	**Variable**	***T-statistic (df)***	***p-value***
Immediate	0.56	Exposure Frequency Exposure*Frequency	-13.26 (311) -5.39 (311) 7.13 (311)	<0.000 <0.000 <0.000
2 Months	0.10	none		
9-10 Months	0.23	none		

Additionally, high frequency DPOAEs were obtained in some subjects before and after noise exposure. High frequency DPOAEs provide information about OHC function through the extreme base (hook region) of the cochlea, which can be affected in noise exposures (Hawkins et al., 1976; Liberman et al., 2015; Liberman & Kiang, 1978). Similar changes in DPOAE amplitude were observed using this apparatus (Figure 8.7D), with significant reductions at frequencies near the noise exposure band immediately following exposure, but normal amplitudes at 2 and 9-10 months post-exposure (Table 8.13).

Table 8.13 Linear mixed effects models for macaque high frequency DPOAE amplitudes before and after noise exposure

Post-Exposure Time Point	***R-squared***	**Variable**	***T-statistic (df)***	***p-value***
1 Day vs. 1 Week	0.43	Exposure Frequency	4.73 (696) 3.59 (696)	<0.000 <0.000
1 Week vs. 1 Month	0.46	Frequency	4.13 (692)	<0.000

As a component of post-exposure TEOAE suppression testing (see next section), TEOAEs were measured monthly in noise-exposed macaques (data not shown). Similar to DPOAEs, TEOAE amplitudes were not different from pre-exposure values at 1 week, 1 month, or 2 months post-exposure (all *p-values* > 0.05), although sex differences persisted (1 week: $t(df)$ 2.37 (92) = , $p = 0.020$; 1 month: $t(df) = 3.11$ (92), $p = 0.003$; 2 months: $t(df) = 2.28$ (92), $p = 0.025$).

8.3.5 Medial olivocochlear reflex in macaques following noise exposure

TEOAE suppression was measured monthly in macaques following noise exposure intended to cause SYN in order to probe changes in MOCR strength. We elected to use TEOAEs due to the similar TEOAE amplitudes among macaques and humans, and the better TEOAE suppression test-retest reliability over DPOAE suppression. These factors increase the likelihood of successful translation of this candidate biomarker to human populations at risk for SYN.

TEOAE suppression was monitored monthly in macaques following noise exposure. Figure 8.8 illustrates mean TEOAE suppression as a function of post-exposure time at various frequency components (each panel). Data were combined across contralateral noise elicitors, due to similar trends across levels. Repeated measures ANOVAs were used to make comparisons between pre-exposure suppression values and each post-exposure time point. TEOAE suppression was weaker in the low frequencies at 1 and 2 months post-exposure (Table 8.14). Suppression was also reduced in the mid-frequencies at 4 months post-exposure. There were no changes in TEOAE suppression beyond 4 months post-exposure at any frequency component.

Table 8.14 Repeated measures ANOVA comparing macaque TEOAE suppression before and after noise exposure

Frequency (kHz)	**Post-Exposure Time Point**	***p-value***
1	1 Month	0.003*
	2 Months	0.002*
1.5	2 Months	0.000*
2	1 Month	0.001*
	2 Months	0.001*
	4 Months	0.002*
3	4 Months	<0.000*
4	none	

*significant after Bonferroni correction to $p = 0.005$

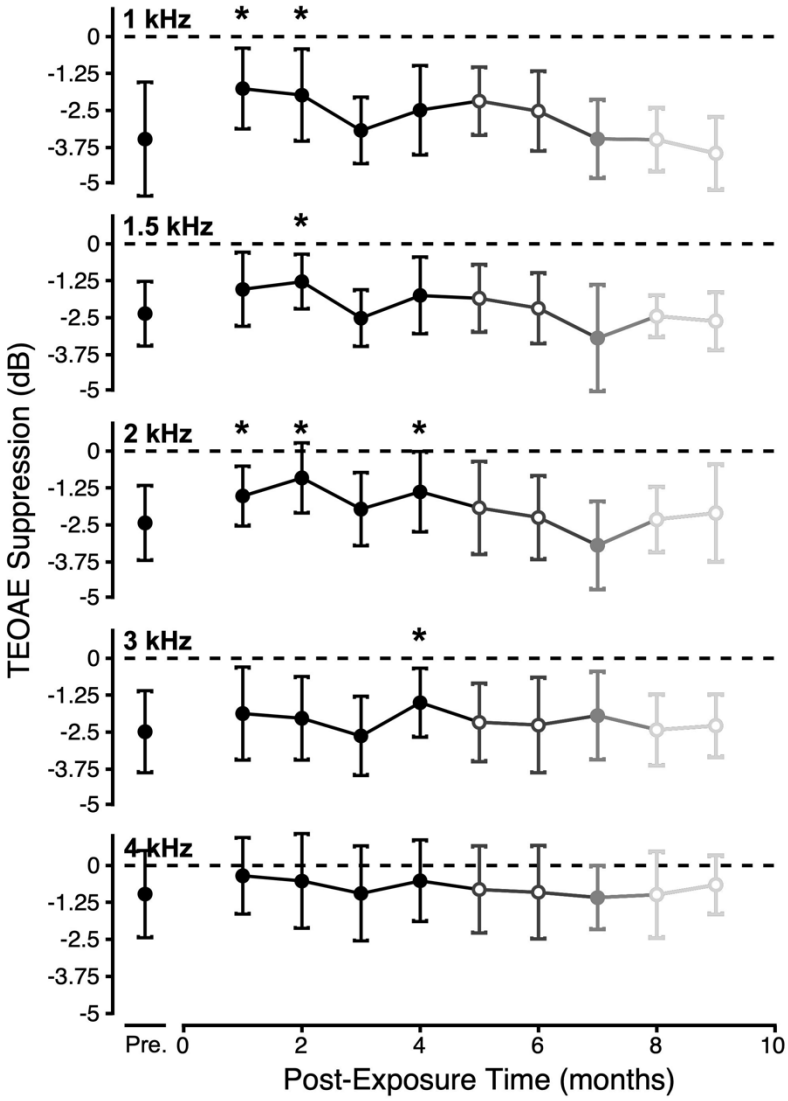

Figure 8.8 Mean macaque TEOAE suppression as a function of post-exposure time. Data are combined across 40, 50, and 60 dB contralateral noise elicitors. Each panel represents a different TEOAE frequency component. Color indicates number of ears: black = 10; dark gray open = 8; gray filled = 6; light gray open = 4. Dashed lines illustrate 0 dB suppression. Pre. = pre-exposure. Asterisks (*) indicate statistically significant differences compared to pre-exposure (see Table 8.14).

8.3.6 Middle ear muscle reflexes in macaques following noise exposure

WB-MEMRs were measured in awake macaques following noise exposure intended to cause SYN. Exemplar MEMRs from Monkey Pi (9 months post-exposure) and Monkey Da (3.5 months post-exposure) are shown in Figure 8.9A & A'. Compared to the human MEMR traces in Figure 8.6A & A', both monkeys showed attenuated responses. This difference is further illustrated in Figure 8.9B, which shows Δ absorbed power as a function of elicitor level for the same noise-exposed macaques (red) compared to humans (green).

WB-MEMRs were also measured in two noise-exposed macaques under isoflurane anesthesia. Awake and anesthetized MEMR functions from Monkey Pi left ear are shown for direct comparison in Figure 8.9B. No measurable MEMR responses were obtained under anesthesia (n = 4 ears; data not shown).

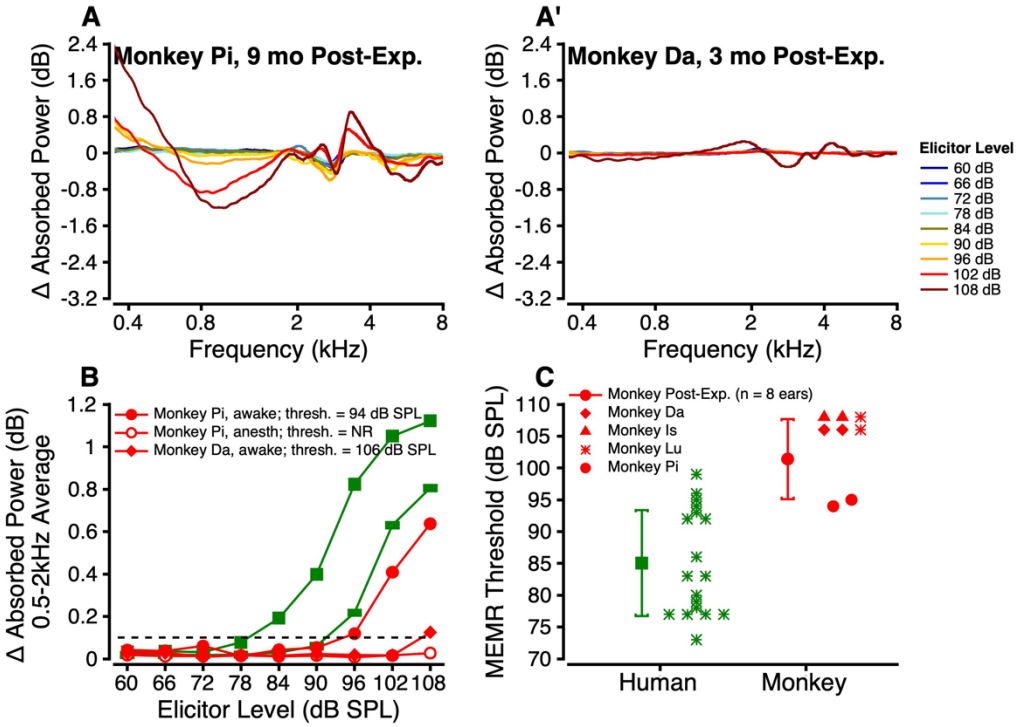

Figure 8.9 A,A'. Exemplar MEMR spectra from two awake, noise-exposed macaques across elicitor levels. B. Change in absorbed power between 0.5-2kHz as a function of elicitor level. Red functions are derived from the data in A and A'. Green functions are replotted from human data in Figure 6B. One function from an anesthetized subject (open red circles) is shown for comparison. Dashed line indicates the threshold cutoff value of 0.1 dB. C. Mean MEMR thresholds for humans (green square; n = 18 ears) and noise-exposed monkeys (red circle; n = 8 ears). Error bars indicate ± 1 standard deviation from the mean. Individual data (symbols) are also plotted to show the distribution of MEMR thresholds for each group.

Figure 8.9C shows mean MEMR thresholds for awake, noise-exposed macaques (101.4 dB SPL; n = 8 ears; red) to the re-plotted human data from Figure 8.6C (green). Monkeys were 3 (Da, diamonds), 5 (Is, triangles), 8 (Lu, stars), and 9 months (Pi, circles) post-exposure at the time of testing. Noise-exposed macaque MEMR thresholds were significantly higher than the human MEMR thresholds ($t(df)$ = 4.86 (24), $p < 0.001$); there were no significant effects of sex or ear laterality (p-values > 0.05). Due to the small size of this preliminary dataset, analyses of MEMR threshold as a function of post-exposure time were not pursued.

8.4 DISCUSSION

Here, we expanded on previous work describing normal auditory function in rhesus macaques with large datasets of DPOAEs and TEOAEs, DPOAE and TEOAE suppression, and WB-MEMRs. We also compared these normative macaque data to measurements in young normal hearing humans using the same stimuli and apparatuses for direct species comparisons. Finally, we measured TEOAE suppression and WB-MEMRs in macaques following noise exposure intended to cause SYN to evaluate noise-induced changes in auditory efferent function. Although it is difficult to tease apart the relative contributions of the MEMR and MOCR in some physiological assays and species (Marks & Siegel, 2017; Valero et al., 2018; Xu et al., 2017), these measures still represent candidate biomarkers of SYN agnostic to the specific driving mechanism.

8.4.1 Otoacoustic emissions in macaques and humans

Evoked otoacoustic emissions arise from two different mechanisms: linear reflection components (TEOAEs) and nonlinear distortion components (DPOAEs) (Shera & Guinan, 1999). Macaques are known to have robust DPOAEs and TEOAEs (Lasky et al., 1995; McFadden et al., 2006; Park et al., 1995) that decline with age (Fowler et al., 2010; Torre et al., 2004) and following experimental manipulations such as noise exposure (Hauser et al., 2018; Valero et al., 2017). The macaque DPOAE and TEOAE amplitudes reported here are consistent with previous reports (Lasky et al., 1995; McFadden et al., 2006; Park et al., 1995). We confirm previous work that shows larger DPOAE amplitudes in macaques than humans except at low frequencies (Lasky et al., 2000; Lasky et al., 1995- compare our Figure 8.2A with their Figure 1) and little or no sex differences in DPOAE amplitudes for macaques (McFadden et al., 2006) and humans (Dhar et al., 1998; McFadden et al., 2009; Moulin et al., 1993). In contrast, TEOAE

amplitudes are similar in macaques and humans, as previously reported (McFadden et al. 2006; but see Lasky et al. 2000). TEOAE amplitudes are larger in females of both species and show small species-specific ear differences (left > right in macaques, right > left in humans; McFadden et al., 2009; McFadden & Pasanen, 1998; McFadden et al., 2006). Of note, our macaque OAE data were collected throughout the year, and thus do not account for seasonal changes in hormone levels (McFadden et al., 2006).

Consistent with prior reports, macaque DPOAE amplitudes were larger than TEOAE amplitudes at corresponding frequencies (Lasky et al., 2000). In contrast, human DPOAE amplitudes were similar or slightly smaller than TEOAE amplitudes in this study (Figure 8.2) and in Gorga et al. (1993), but the opposite in McFadden et al. (2009). Differences across studies and species could be impacted by click and primary tone levels or the proportion of males and females. (Note: Our macaque TEOAE data have a larger proportion of females than the DPOAE data). Alternatively, differences in DPOAE vs. TEOAE measures in macaques and humans may reflect species differences in cochlear reflection and distortion mechanisms.

Following resolution of noise-induced temporary threshold shifts, macaques showed stable or improved DPOAE and TEOAE amplitudes and DPOAE thresholds, consistent with other animal models of noise-induced SYN (Bharadwaj et al., 2021; Kujawa & Liberman, 2009; Lin et al., 2011). Intact OAEs and only minimal loss of OHCs (Chapter 7, Figure 7.2A) indicate isolated synaptopathic damage with our noise exposure, minimizing confounds of hair cell damage in the interpretation of our physiological and behavioral findings.

8.4.2 Medial olivocochlear reflex: Species differences and effect of noise exposure

OAE suppression is a simple, non-invasive measure of MOCR efferent strength. Normative characterization is essential because OAE suppression varies extensively across species and measurement methods. This study provides the first report of OAE suppression in macaques. Awake macaques showed robust contralateral suppression of DPOAEs and TEOAEs across frequencies, which increased with increasing noise elicitor level (Hood et al., 1996). Macaques exhibited similar magnitudes of TEOAE and DPOAE suppression (TEOAE: mean = 2.76 dB, range = 1.4-4.64 dB; DPOAE: mean = 1.77 dB, range = 0.40-5.25 dB).

Previous reports of human contralateral OAE suppression range from 0.5-2 dB for TEOAEs (Berlin et al., 1995; Collet et al., 1992; Keppler et al., 2010; Mertes & Leek, 2016; Stuart & Daughtrey, 2016; Veuillet et al., 2001) and 0.5-2.25 dB for DPOAEs (Abdala et al.,

2014; Kim et al., 2002; Kumar et al., 2013; Wagner et al., 2007; Wicher & Moore, 2014). Here, we observed similar magnitudes of OAE suppression in humans (TEOAE: mean = 1.34 dB, range = 0.30 – 2.86 dB; DPOAE: mean = 1.06 dB, range = -0.38 – 2.34 dB). Macaque contralateral OAE suppression is significantly stronger than human suppression, as demonstrated by our direct within-study comparison and comparison to previous reports.

It is difficult to compare our data with OAE suppression measured in other animals, as most studies utilize low dose anesthesia to immobilize subjects during testing. This is problematic because anesthesia is known to attenuate the MOCR (see Figure 8.5; also Boyev et al., 2002; Chambers et al., 2012; Guitton et al., 2004; Valero et al., 2016). Awake DPOAE suppression by contralateral noise has been reported in single studies of mice (Chambers et al., 2012) and guinea pigs (Guitton et al., 2004), with suppression values of 6-14 dB and 5-6 dB, respectively. Taken together with the present macaque and human data, OAE suppression magnitude seems to mimic MOC innervation density: mice have dense MOC innervation and large DPOAE suppression, whereas humans have sparse MOC innervation and little DPOAE suppression, and guinea pigs and macaques lie in between (Liberman & Liberman, 2019).

Although OAE suppression is often attributed to the MOCR, contributions from the MEMR are known to occur for some species including mice (Valero et al., 2016), rabbits (Whitehead et al., 1991), and humans (Mertes, 2020), and vary with stimulus level and anesthetic state. We were not able to include experimental manipulations (e.g. nerve sectioning, chemical blocks, genetic modifications) or time-course analyses (Marks & Siegel, 2017; Xu et al., 2017) to isolate MEMR vs. MOCR responses. However, the noise-exposed macaque ipsilateral MEMR thresholds were approximately 94 dB SPL or greater, which exceeds or matches the three levels of contralateral noise used in the OAE suppression testing. Although ipsilateral and contralateral MEMR thresholds may not be symmetric, contralateral MEMR thresholds tend to be higher than ipsilateral (Borg & Moller, 1968; Fria et al., 1975; Guinan & McCue, 1987; Higson, Stephenson, et al., 1996; Kobler et al., 1992; Moller, 1962), suggesting minimal MEMR contributions to the measured OAE suppression. Pending MEMR data from unexposed macaques will be more informative for assessing MEMR contributions to OAE suppression in normal hearing monkeys.

Prior to changes in hearing sensitivity or outer hair cell function, the MOCR decreases with age in humans (Abdala et al., 2000; Kim et al., 2002) and rodents (Jacobson et al., 2003; Zhu et al., 2007), which mimics age-related decreases in MOC innervation prior to loss of OHCs

in humans (Liberman & Liberman, 2019) and rodents (Fu et al., 2010; Radtke-Schuller et al., 2015). The MOCR is also absent in individuals with auditory neuropathy (Abdala et al., 2000; Berlin, Hood, Cecola, et al., 1993; Hood et al., 2003), who have intact OHC function but grossly abnormal auditory nerve function (Moser & Starr, 2016; Starr et al., 1996). In mouse models of age-related and noise-induced SYN, MOC innervation density is reduced (Boero et al., 2018; Boero et al., 2020; Qian et al., 2021). Contrary to our predictions and these lines of evidence from the literature, we did not observe permanent changes in macaque MOCR strength as measured by contralateral suppression of TEOAEs. TEOAE suppression was reduced at 1-4 months post-exposure, but not at later post-exposure times. Differential explanations of this finding include: 1) the time course of synapse loss and recovery parallels the temporal dynamics of the MOCR, 2) central auditory system compensatory changes enhance top-down MOCR inputs, therefore cancelling out changes in afferent drive (Knudson et al., 2014), or 3) alternative MOCR assays may be more sensitive to SYN that contralateral TEOAE suppression. However, the lack of permanent changes in OAE suppression mimics the lack of change in MOC innervation density at late post-exposure times (Chapter 7, Figure 7.8A).

In future investigations of the MOCR and SYN, MOCR measurements could be optimized by 1) using elicitor levels known to fall below MEMR thresholds, 2) using binaural noise elicitors, which are known to elicit stronger MOCR magnitudes (Berlin et al., 1995), or 3) using compound action potential MOCR measures, which also result in larger MOCR magnitudes (Puria et al., 1996). Careful attention to contributions from MEMR vs. MOCR will help specify the site of lesion in SYN pathology. Refined MOCR methodology may reveal subtle permanent changes in MOC function that were not captured in this study. Of note, OAE-MOCR measures provide a faster and less invasive option than ABR-MOCR measures, especially for testing in animals or humans that would not tolerate extended ABR testing. If ABR-MOCR assays are pursued, results must be interpreted intelligently, as changes in afferent drive will also affect ABR responses.

8.4.3 Middle ear muscle reflex: Measurement and species differences, effect of noise exposure

MEMRs can be measured in a variety of ways, including ipsilateral vs. contralateral stimulation, tone vs. noise elicitors, and single frequency vs. wideband probes, resulting in a

range of threshold estimates and complicating comparisons across studies (Schairer et al., 2013). For example, MEMR thresholds are typically lower for ipsilateral elicitors (Wiley et al., 1987), noise elicitors (Margolis et al., 1980; Silman et al., 1978), and wideband probes (Feeney et al., 2017).

Few studies have reported MEMRs in nonhuman primates. In a single prior study of macaque MEMRs, an ipsilateral probe tone (220 Hz) was presented with ipsilateral pure tone elicitors (Mangham et al., 1982). MEMR thresholds were approximately 85 dB SPL for 0.5, 1, and 2 kHz, and just over 100 dB SPL for 4 kHz. Contralateral pure-tone MEMR thresholds in squirrel monkeys (probe = 1200 Hz) were similar (80-100 dB SPL, although with higher thresholds for low than high frequency tones), and contralateral broadband noise MEMR thresholds were approximately 80 dB SPL (Jerger et al., 1978a). Importantly, Mangham et al. (1982) found comparable MEMR thresholds in macaques and humans measured under identical conditions.

MEMRs are routinely measured in the audiology clinic using a probe tone and ipsilateral or contralateral tone or noise elicitors. Under these clinical testing parameters, human MEMR thresholds to broadband noise are typically 65-75 dB SPL (Dallos, 1964; Margolis et al., 1980; Silverman et al., 1983; Wiley et al., 1987; Wilson & McBride, 1978), with lower thresholds for ipsilateral than contralateral noise, although with considerable inter-subject variability (thresholds range from 55-95 dB SPL; Feeney et al., 2017; Wiley et al., 1987).

In this study, we used a wideband MEMR (WB-MEMR) that assesses changes in ear canal pressure across frequencies (Bharadwaj et al., 2021; Keefe et al., 2017). These wideband measures may result in lower MEMR threshold estimates than clinical MEMR paradigms using pure-tone probes (Feeney et al., 2017). Previous reports of ipsilateral WB-MEMR thresholds to broadband noise range from 65-70 dB SPL in humans (Bharadwaj et al., 2021; Feeney et al., 2017; Keefe et al., 2017) and 73 dB SPL in chinchillas (Bharadwaj et al., 2021); contralateral thresholds range from 77 dB SPL in humans (Bramhall et al., 2022) to 80 dB SPL in mice (Valero et al., 2018).

Macaques and humans exhibited band-pass absorbance functions, with peak changes in admittance between 500-2000 Hz and considerable variability in the peak of this function across subjects (Bharadwaj et al., 2021; Feeney et al., 2017). These functions mimic the tuning characteristics of stapedius motoneurons (Kobler et al., 1992). Mean human WB-MEMR

thresholds were 85 dB SPL and ranged from 73 to 99 dB SPL. This higher mean and large variability is intriguing, given the small sample size and small age range of the participants (20-30 years). Though individual studies of human WB-MEMRs do not show this extensive range of thresholds, this variability becomes apparent when comparing across studies (Feeney et al., 2017; Wiley et al., 1987). Pending data from normal hearing macaques will provide an interesting species comparison and could help elucidate the source of this variability (e.g. MEMR apparatus vs. subject sample).

MEMRs show variable sensitivity to sensorineural hearing loss, but generally decrease in amplitude and increase in threshold with more than a mild hearing loss (Jerger et al., 1978b; Letien & Bess, 1975; Lindgren et al., 1983; Margolis, 1993; Silman et al., 1978). Patients with auditory neuropathy consistently show elevated or absent MEMRs (Berlin et al., 2005). It follows that MEMRs may be sensitive to SYN (Bharadwaj et al., 2019; Bramhall et al., 2019), as the MEMR is seemingly uncoupled from audiometric hearing and more representative of neural function (Hickox et al., 2017). Indeed, animal studies show higher WB-MEMR thresholds and smaller WB-MEMR amplitudes in mice and chinchillas with histologically-verified SYN (Bharadwaj et al., 2021; Valero et al., 2016; Valero et al., 2018). Our noise-exposed macaques followed this trend, showing significantly elevated (n = 5 ears) or absent (n = 3) WB-MEMR thresholds compared to normal hearing humans. Although this is not an ideal comparison, such a stark difference in responses suggests impaired MEMR function in our macaques following noise exposure. Interestingly, our macaque WB-MEMR thresholds did not seem to vary with post-exposure time. This contrasts with our histological data that suggest recovery of SYN (Chapter 7). Though both the MEMR and histology datasets are preliminary, these findings could suggest persistent physiological changes despite recovery of inner hair cell ribbon counts. In the future, within-subject comparisons of MEMRs should be made before and after noise exposure, monitored over time, and coupled with cochlear histology to better assess the relationship between SYN dynamics and MEMR function.

In contrast to the consistent findings in animal research, studies of the MEMR in humans at risk for SYN (e.g. normal hearing sensitivity + older age, tinnitus, history of noise exposure, or reported hearing difficulties) show mixed findings. Clinical noise-elicited MEMR thresholds are higher in older adults with normal hearing compared to young adults, but this is not the case for tone-elicited MEMRs (Gelfand & Piper, 1981; Silman, 1979; Silverman et al., 1983). More

recently, studies using noise-elicited ipsilateral and contralateral WB-MEMRs show an association between greater SYN risk and higher MEMR thresholds or lower amplitudes (Bharadwaj et al., 2021; Bramhall et al., 2022; Mepani et al., 2020; Shehorn et al., 2020; Wojtczak et al., 2017). However, some studies using noise and tone elicitors of clinical MEMRs did not observe this same association (Causon et al., 2020; Guest et al., 2019; Higson, Morgan, et al., 1996). It is possible that the subjects did indeed have SYN, given the wide range of MEMR thresholds reported, but that the risk metrics were not predictive of inner ear status. Our participants also showed considerable variability in WB-MEMR thresholds, which could indicate underlying differences in cochlear integrity. Inter-subject variability in MEMR function may be intrinsic or related to risk factors that are unknown or difficult to quantify. Alternatively, noise-elicited WB-MEMRs may be a more sensitive biomarker of SYN than MEMRs measured with probe tones (Bharadwaj et al., 2019; Bramhall et al., 2019). Overall, our human and noise-exposed macaque MEMR data preliminarily support the utility of the WB-MEMR in the diagnosis of SYN.

CHAPTER 9

Auditory brainstem responses to masked clicks in macaque monkeys following noise exposure intended to cause cochlear synaptopathy

9.1 INTRODUCTION

Cochlear synaptopathy (SYN) is an inner ear pathology characterized by the selective loss of inner hair cell ribbon synapses, resulting in deafferentation of the auditory system and eventual degeneration of afferent auditory nerve fibers (Kujawa & Liberman, 2006, 2009). Some research has suggested that SYN leads to a preferential loss of auditory nerve fibers with low spontaneous firing rates and high sound-evoked thresholds (Furman et al., 2013; Liberman et al., 2015; Schmiedt et al., 1996; but see Suthakar & Liberman, 2021), which are more resistant to masking by background noise (Costalupes, 1985) and may be important for encoding signals in noisy environments (Bharadwaj et al., 2015; Bharadwaj et al., 2014). Because hair cells remain intact and only a small number of nerve fibers are needed to maintain hearing sensitivity, SYN has been described as "hidden hearing loss" as it is not readily identified using standard clinical audiometric approaches but may lead to poor signal encoding in noise (Schaette & McAlpine, 2011).

Due to the "hidden" nature of SYN, significant efforts have been made over the past decade to identify diagnostic biomarkers that are sensitive and specific to this subclinical pathology. Physiological assays that are designed to reveal responses from high threshold neurons may be of particular utility (Bharadwaj et al., 2019; Bharadwaj et al., 2014; Bramhall et al., 2019). In rodents, Wave I of the auditory brainstem response (ABR) can reliably predict the location and extent of synapse loss. Although ABR thresholds are unchanged, Wave I amplitudes are reduced at suprathreshold levels for stimuli within the region of synapse loss (Kujawa & Liberman, 2009). This change may reflect the loss of high threshold neurons that contribute to evoked potential responses at high stimulus levels (but see Bourien et al., 2014). This metric has shown mixed results in humans at risk for SYN. In some human studies, reduced Wave I amplitudes correlate with greater SYN risk or poorer performance on speech-in-noise tests (Bramhall et al., 2017; Burkard & Sims, 2002; Grant et al., 2020; Liberman et al., 2016; Ridley et al., 2018; Schaette & McAlpine, 2011; Skoe & Tufts, 2018; Suresh & Krishnan, 2020), but not

in others (Fulbright et al., 2017; Grinn et al., 2017; Guest et al., 2018; Prendergast et al., 2019; Spankovich et al., 2017). Additional ABR metrics, such as the SP/AP ratio and Wave V/I or IV/I ratios, have also shown mixed results (Bharadwaj et al., 2021; Liberman et al., 2016; Mepani et al., 2020; Suresh & Krishnan, 2020), suggesting that the ABR may not be the most sensitive biomarker for SYN in humans. In this vein, alternative physiological biomarkers, such as the middle-ear muscle reflex (see Chapter 8) and envelope following response (Bharadwaj et al., 2015; Bramhall et al., 2021; Keshishzadeh et al., 2020; Paul et al., 2017; Race et al., 2017; Shaheen et al., 2015; Vasilkov et al., 2021; Verhulst et al., 2018) (but see Chen et al., 2019; Prendergast et al., 2019), have shown more consistent sensitivity to SYN across rodents and humans.

Our laboratory previously established normative ABR responses in macaque monkeys (Stahl et al. submitted). Like humans (Prendergast et al., 2018), monkeys have small ABR Wave I amplitudes, likely due to larger head size and greater distance between surface electrodes and the auditory nerve compared to rodents. Preliminary data from noise-exposed macaques showed small and variable effects of noise exposure on ABR amplitudes, consistent with a species-dimorphic sensitivity of this metric. In an effort to exhaust the diagnostic possibilities of the ABR, which is already available in the clinic and thus is readily implementable, we expanded our post-exposure ABR dataset and pursued ABR paradigms that utilize masking noise. Masked ABRs are designed to saturate low threshold neurons and therefore isolate responses from high threshold neurons, which may be preferentially lost with SYN (Furman et al., 2013; Liberman et al., 2015; Schmiedt et al., 1996; but see Suthakar & Liberman, 2021). Of note, there is debate about the extent to which suprathreshold or masked ABRs actually represent the response of high threshold neurons, as opposed to the robust contributions from low threshold neurons (Bourien et al., 2014; Verhulst et al., 2018).

Masking paradigms have been described since nearly the beginning of evoked potential studies (e.g. Dewson, 1967), using both ipsilateral (e.g. Burkard & Hecox 1983a,b, 1987a,b; Owen & Burkard 1991) and contralateral noise (e.g. Humes & Ochs 1982, Rosenhamer & Holmkvist 1983, Reid et al. 1984; Hatanaka et al. 1990). The addition of ipsilateral masking reduces wave amplitudes and increases wave latencies due to a reduced number of neural components responding to the stimulus, disrupted neural synchrony, and longer latencies of high threshold neurons (Beattie et al., 1994; Boezeman et al., 1983; Burkard & Hecox, 1983). In the

presence of SYN, masked ABR amplitudes may be significantly reduced due to loss of auditory nerve fibers and therefore an even smaller pool of neurons available to respond (Burkard & Sims, 2002; Giraudet et al., 2021). Masked ABR latencies may also be affected by SYN (Burkard & Sims, 2002; Mehraei et al., 2016), but predictions regarding the direction of change are dependent upon the population of neurons lost (i.e. short vs. long onset latency, one type or multiple types and in what proportion).

There is a small but mixed literature on the effects of subclinical hearing loss on masked ABR responses in both animal models and humans at risk for SYN. Rodent studies globally indicate sensitivity of masked ABR metrics for identifying subclinical hearing pathologies. Compared to young gerbils, older gerbils with near-normal ABR thresholds in quiet showed higher ABR thresholds to signals in low-pass noise, suggesting excessive upward spread of masking (Boettcher et al., 1995). Similar results were observed for on-frequency-masked evoked potentials recorded in the inferior colliculus of aging chinchillas (McFadden et al., 1997). More recently, Giraudet et al. (2021) showed significantly reduced or absent masked ABR Wave I amplitudes in mice with histologically-verified noise-induced SYN compared to controls; latencies were not reported for masked ABR conditions. In another set of experiments investigating mice with SYN, Mehraei et al. (2016) focused on latency metrics from the more easily identifiable ABR Wave IV (in rodents, Wave V in humans). Following noise exposure, mice exhibited shallower latency by noise level slopes, which may be caused by loss of high threshold auditory nerve fibers with delayed onset responses (Bourien et al., 2014).

In contrast, studies assessing masked ABRs in humans at risk for SYN (e.g. normal hearing + history of noise exposure or older age) show mixed findings. Burkard and Sims (2002) compared masked click ABRs in young and older adults with normal hearing sensitivity. Like the animal studies described above, older normal hearing adults showed longer latencies and smaller amplitudes for Waves I and V than young adults. However, older adults actually showed enhanced ABR Wave I amplitudes in low level noise compared to in quiet, unlike the young adults. In addition to the mouse data described above, Mehraei et al. (2016) found that human click-evoked ABR Wave V latency shifts were correlated with performance on a psychophysical temporal acuity task that may be predictive of SYN (envelope interaural time difference threshold; Bharadwaj et al., 2015). A shallower Wave V latency shift was only weakly observed in the older adult data from (Burkard & Sims, 2002). Suresh and Krishnan (2020) measured

masked click ABRs in young adults with normal hearing and either little to no history of recreational or occupational noise exposure (low-risk for SYN) or a minimum of 5 years participating in marching band (high-risk for SYN). Similar to Burkard and Sims (2002), the high-risk participants showed relatively smaller decreases in Wave I amplitude with the addition of masking noise compared to the low-risk group, but no differences in Wave V amplitude reductions with noise. In contrast to (Mehraei et al., 2016), the low- and high-risk groups did not differ in noise-induced Wave V latency shifts. In sum, research suggests that SYN may cause an increase or decrease in susceptibility to masking noise as evidenced by changes in masked ABR amplitudes or latencies. These mixed findings could be due to i) differences in the masked ABR stimulus parameters used (clicks vs. tonebursts; noise levels), ii) the chronicity of synapse loss and central compensation, iii) the presence of comorbid inner ear pathologies in the different populations studied (aging, noise-exposed), and/or iv) species differences in the manifestation of SYN pathology.

In this study, we measured auditory brainstem responses to clicks in quiet and ipsilateral broadband noise in nonhuman primates before and after noise exposure intended to cause SYN. This report provides the first characterization of masked ABR responses in rhesus macaques, which are phylogenetically similar to humans and serve as a translational bridge between rodent and human research (Burton et al., 2019). We hypothesized that i) masked ABR wave amplitudes would be reduced following noise exposure due to loss of high threshold neurons, ii) masked ABR wave latencies would be increased following noise exposure due to longer latency of the remaining fibers, and iii) masked ABR amplitudes would predict the extent of cochlear synapse loss.

9.2 MATERIALS AND METHODS

9.2.1 Subjects

Eleven adult rhesus macaques (*Macaca mulatta*, 7-10 years old, four female) underwent auditory brainstem response testing. Of these, nine subjects (four female) had testing completed before and after noise exposure.

9.2.2 Auditory brainstem response (ABR) testing

ABRs were measured as described in the General Methods. In this set of experiments, suprathreshold clicks (100μs; 70, 80, 90 dB SPL) were presented in quiet or with continuous

ipsilateral broadband noise (0.4-40kHz, 30-60 dB spectrum level in 5 dB steps). Clicks and noise were analog summed using a SM5 Signal Mixer (Tucker-Davis Technologies). ABR Wave I, II, and IV amplitudes and latencies were visually identified for each stimulus and level in order to derive input-output functions for each click level and noise level. Responses were considered present if they were repeatable and larger than the recording noise floor (40 nV). ABR testing was completed prior to noise exposure and at 2 months post-exposure. Details of the noise exposure are described in the General Methods.

9.2.3 Statistical analyses

Statistical analyses were conducted using linear mixed effects models ("fitlme") in MATLAB 2018a. The dependent variable in the models was ABR wave amplitude or latency. Sex, ear laterality, click level, noise level, and noise exposure status were entered as fixed effects into the model, while intercepts for individual subjects were entered as random effects. In all cases *p*-values were obtained by likelihood ratio testing of the model with the effect in question against the model without the effect in question. A significant *p*-value was defined as $p < 0.05$. *T*-statistics are reported for each model, similar to the *F*-statistic that is often reported for such models.

9.3 RESULTS

9.3.1 Auditory brainstem responses to unmasked and masked clicks in normal hearing macaques

Exemplar ABR traces from Monkey Op in response to 90, 80, and 70 dB SPL clicks in quiet and in 30 dB spectrum level noise are shown in Figure 9.1. Waves I, II, and IV are readily identifiable on all traces and are thought to be homologous to human ABR Waves I, III, and V (Kraus et al., 1985). ABR morphology is significantly affected by the

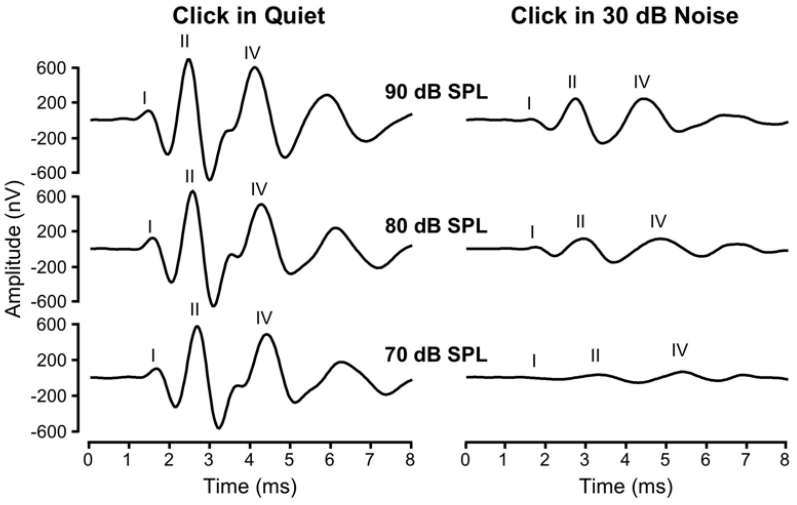

Figure 9.1 Exemplar ABR traces to 90, 80, and 70 dB SPL clicks in quiet and in 30 dB spectrum level noise.

addition of masking noise, with noticeable reductions in wave amplitudes and increases in wave latencies.

Average ABR peak-to-peak amplitudes and peak latencies for Waves I, II, and IV in response to unmasked clicks are shown in Figure 9.2 (filled circles) as a function of click level. As click level increased, wave amplitudes increased (positive slope) and wave latencies decreased (negative slope). Wave II amplitudes were largest, followed by Wave IV and then Wave I. Mean click-evoked Wave I, II, and IV amplitudes and latencies are listed in Table 9.1 (n = 20 ears). Linear mixed effects models for each wave amplitude and latency indicated a significant effect of click level (Table 9.2). Wave II and IV amplitudes differed across sexes, with significantly larger amplitudes for females than males, consistent with prior reports in monkeys (Fowler et al., 2002) and humans (McFadden et al., 2021). There were no differences in unmasked click ABR amplitudes or latencies according to ear laterality.

The addition of low level (30 dB spectrum level) masking noise reduced wave amplitudes and increased wave latencies for all click levels and wave components (open circles, Figure 9.2). Linear mixed effects models identified significant differences in Wave I and II amplitudes and latencies according to click level, as well as Wave I amplitudes and Wave I and II latencies according to sex (Table 9.3). There were no significant differences in Wave IV amplitudes or latencies according to sex, ear laterality, or click level.

Table 9.1 Mean (standard deviation) ABR wave amplitudes (nV) and latencies (ms) to clicks in quiet and in 30 dB spectrum level ipsilateral broadband noise.

Stimulus	**Wave I**		**Wave II**		**Wave IV**	
	Amplitude	**Latency**	**Amplitude**	**Latency**	**Amplitude**	**Latency**
90 dB SPL click	283.34 (126.58)	1.42 (0.10)	933.09 (239.15)	2.46 (0.09)	562.90 (343.50)	4.13 (0.27)
+ 30 dB noise	89.70 (57.44)	1.54 (0.16)	392.58 (152.97)	2.76 (0.12)	242.22 (110.98)	4.54 (0.30)
80 dB SPL click	282.04 (120.49)	1.52 (0.09)	913.69 (268.95)	2.57 (0.07)	477.55 (267.19)	4.29 (0.22)
+ 30 dB noise	66.93 (42.90)	1.68 (0.09)	251.06 (120.80)	2.89 (0.13)	196.20 (98.06)	4.93 (0.35)
70 dB SPL click	236.03 (95.86)	1.64 (0.09)	815.67 (256.48)	2.69 (0.06)	465.65 (267.00)	4.39 (0.16)
+ 30 dB noise	23.84 (9.76)	1.88 (0.14)	104.05 (50.71)	3.13 (0.31)	138.71 (83.68)	5.18 (0.41)

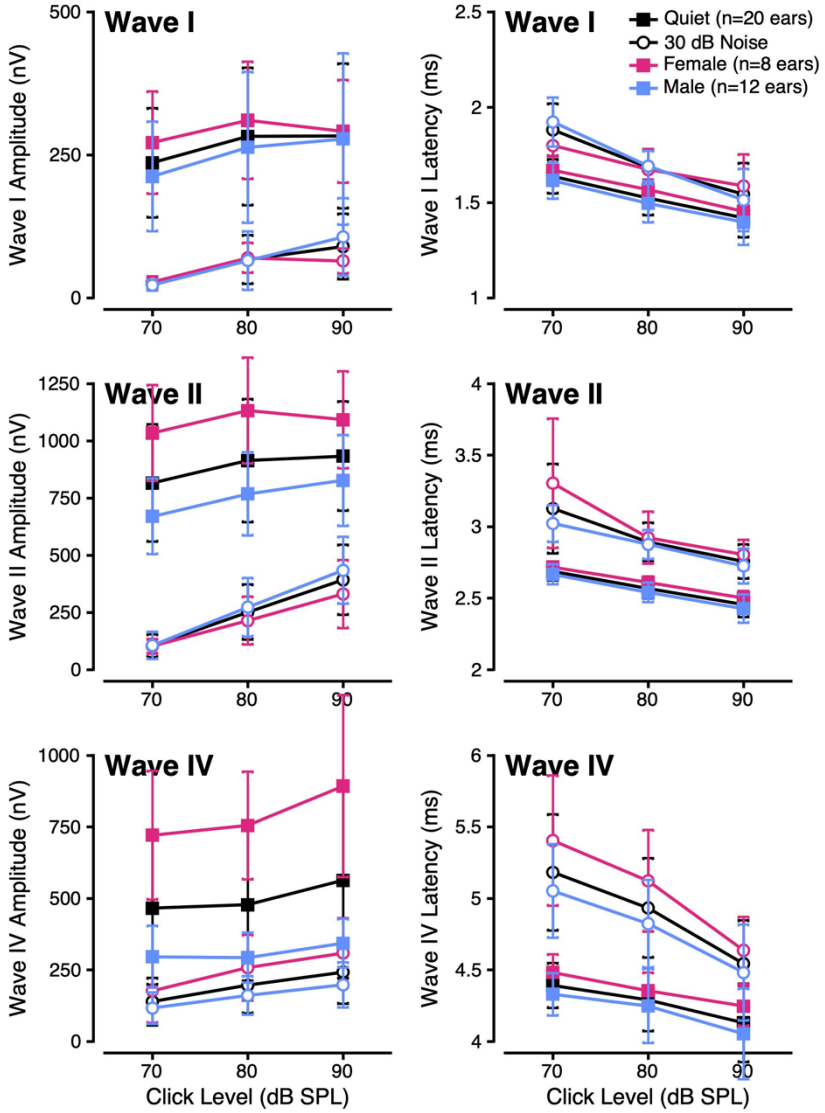

Figure 9.2 Mean input-output functions for ABR Wave I, II, and IV amplitudes and latencies as a function of click level (dB SPL) in quiet (filled symbols) or in 30 dB spectrum level noise (open symbols). Data are shown for all monkeys (black, n = 20 ears), females only (pink, n = 8 ears), and males only (n = 12 ears). Error bars illustrate ±1 standard deviation from the mean.

Table 9.2 Linear mixed effects models for normative ABR wave amplitudes and latencies to clicks in quiet.

ABR Component	***R-squared***	**Variable**	***T-statistic (df)***	***p-value***
Wave I Amplitude	0.81	Click Level	2.17 (54)	0.034
Wave I Latency	0.94	Click Level	-4.94 (54)	<0.000
Wave II Amplitude	0.95	Click Level Sex Sex*Click Level	4.25 (54) 3.83 (54) -4.98 (54)	0.001 0.000 0.018
Wave II Latency	0.93	Click Level	-5.61 (54)	<0.000
Wave IV Amplitude	0.93	Sex*Click Level	2.37 (54)	0.021
Wave IV Latency	0.67	Click Level	-2.78 (54)	0.008

Table 9.3 Linear mixed effects models for normative ABR wave amplitudes and latencies to clicks in 30 dB spectrum level ipsilateral broadband noise.

ABR Component	***R-squared***	**Variable**	***T-statistic (df)***	***p-value***
Wave I Amplitude	0.73	Sex Click Level Sex*Click Level	2.11 (48) 4.65 (48) -2.46 (48)	0.040 0.000 0.018
Wave I Latency	0.69	Sex Click Level Sex*Click Level	-2.59 (48) -3.54 (48) 2.57 (48)	0.013 0.001 0.013
Wave II Amplitude	0.85	Click Level	5.20 (52)	0.000
Wave II Latency	0.74	Sex Sex*Click Level	2.40 (52) -2.12 (52)	0.020 0.039
Wave IV Amplitude	0.77	none		
Wave IV Latency	0.79	none		

9.3.2 Auditory brainstem responses to unmasked clicks are unchanged following noise exposure

Figure 9.3 shows input-output functions for suprathreshold clicks in quiet (filled symbols) before (black) and after (red) noise exposure. Although there was still a significant effect of click level on wave latencies, there was no significant effect of noise exposure on ABR amplitude or latency for any wave component or click level (Table 9.4).

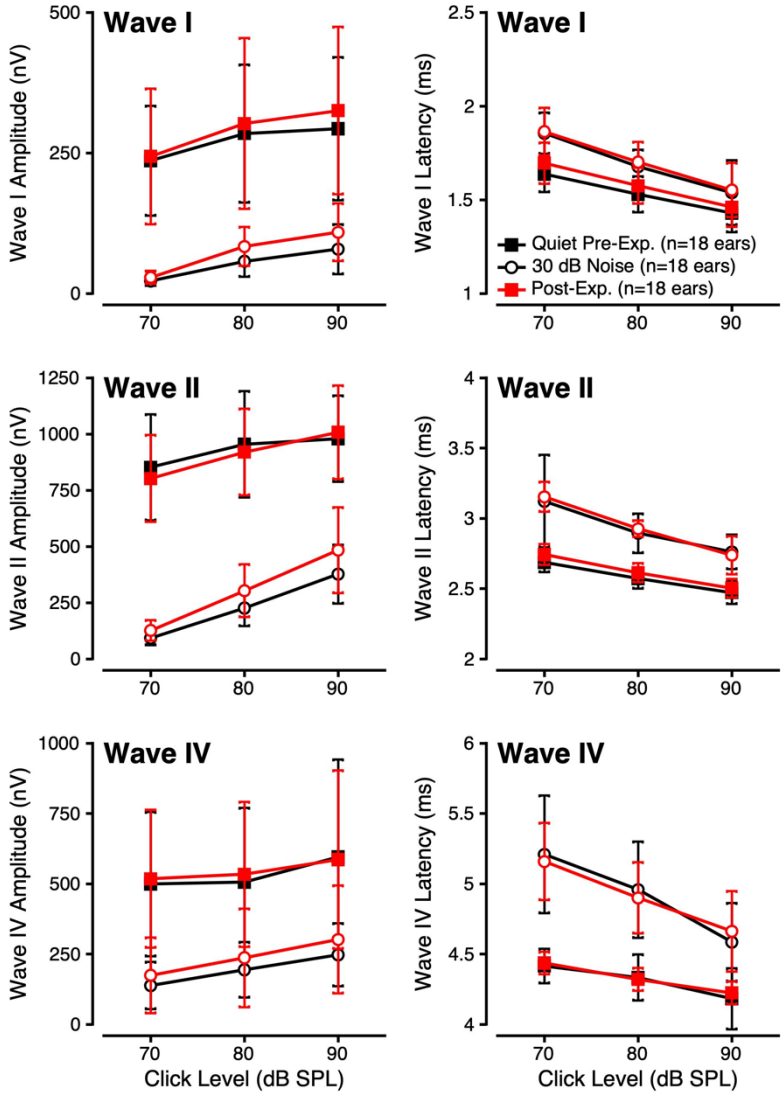

Figure 9.3 Same as Figure 9.2, except showing group data (n = 18 ears) before (black) and after (red) noise exposure.

Table 9.4 Linear mixed effects models of the effect of noise exposure on ABR wave amplitudes and latencies to clicks in quiet.

ABR Component	*R-squared*	Variable	*T-statistic (df)*	*p-value*
Wave I Amplitude	0.77	none		
Wave I Latency	0.90	Click Level	-4.41 (108)	<0.000
Wave II Amplitude	0.76	none		
Wave II Latency	0.88	Click Level	-4.81 (108)	<0.000
Wave IV Amplitude	0.90	none		
Wave IV Latency	0.65	Click Level	-2.58 (108)	0.011

9.3.3 Auditory brainstem responses to masked clicks are unchanged following noise exposure

9.3.3.1 Fixed noise level

Figure 9.3 also shows input-output functions for suprathreshold clicks in the presence of 30 dB spectrum level ipsilateral broadband noise (open symbols) pre- and post-exposure (black and red, respectively). There was no significant effect of noise exposure on wave amplitudes or latencies across all wave components and click levels (Table 9.5). These analyses were not pursued for other noise levels, since ABRs to 70 dB SPL clicks with more than 30 dB spectrum level noise were often absent or very small in amplitude. Because there was no interaction of noise exposure status and click level, analyses of amplitude and latency slopes (as a function of click level) were also not pursued.

Table 9.5 Linear mixed effects models of effect of noise exposure on ABR wave amplitudes and latencies to clicks in 30 dB spectrum level ipsilateral broadband noise.

ABR Component	*R-squared*	Variable	*T-statistic (df)*	*p-value*
Wave I Amplitude	0.65	Click Level	2.442 (96)	0.016
Wave I Latency	0.71	Click Level	-4.37 (96)	<0.000
Wave II Amplitude	0.72	Click Level	2.89 (104)	0.005
Wave II Latency	0.68	Sex Sex*Click Level	2.51 (104) -2.28 (104)	0.013 0.025
Wave IV Amplitude	0.67	none		
Wave IV Latency	0.39	none		

9.3.3.2 Fixed click level

Input-output functions were also derived for ABR responses to clicks at a fixed level (e.g. 90 dB SPL) as a function of noise level (30 to 60 dB spectrum level) as shown in Figure 9.4. Surprisingly, Wave I, II, and IV amplitudes were significantly larger post-exposure, especially at lower noise levels (Table 9.6). There was no significant effect of noise exposure on masked click ABR wave latencies. Similar trends were observed for 80 and 70 dB SPL clicks (data not shown).

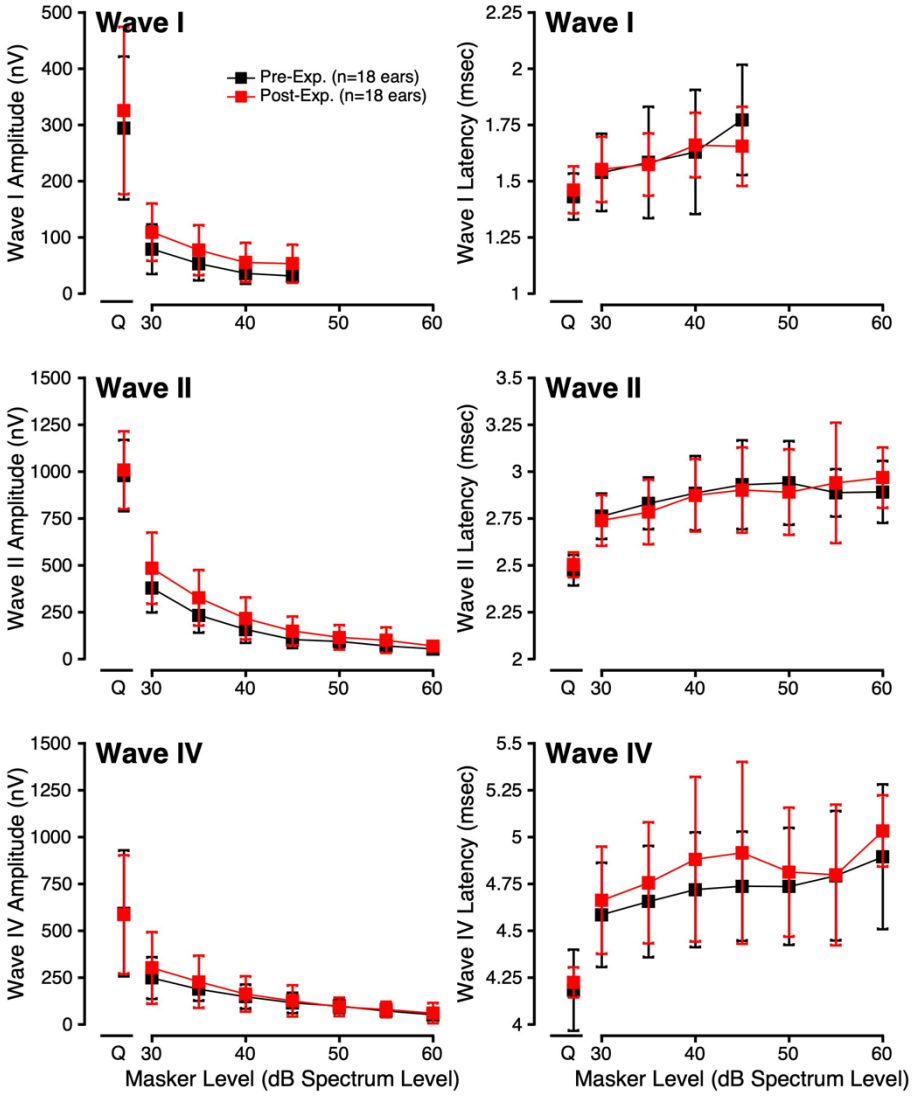

Figure 9.4 Mean (n = 18 ears) input-output functions for ABR Wave I, II, and IV amplitudes and latencies to a 90 dB SPL click as a function of noise level (dB spectrum level) before (black) and after (red) noise exposure. Q indicates response to click in quiet for reference.

Table 9.6 Linear mixed effects models of effect of noise exposure on ABR wave amplitudes and latencies to 90 dB SPL clicks in ipsilateral broadband noise.

ABR Component	*R-squared*	Variable	*T-statistic (df)*	*p-value*
Wave I Amplitude	0.53	Exposure Exposure*Noise Level	3.97 (113) -3.49 (113)	<0.000 0.001
Wave I Latency	0.57	none		
Wave II Amplitude	0.63	Exposure Exposure*Noise Level	4.03 (191) -3.25 (191)	<0.000 0.001
Wave II Latency	0.44	none		
Wave IV Amplitude	0.64	Exposure Noise Level Exposure*Noise Level Sex*Noise Level	2.68 (190) 2.60 (190) -2.35 (190) -5.90 (190)	0.008 0.010 0.020 <0.000
Wave IV Latency	0.26	Noise Level	2.02 (190)	0.045

In order to examine whether the relative reduction in wave amplitudes or latency shifts was different from pre- to post-exposure, we normalized the masked ABR data within-subject to the *pre-exposure* response in 30 dB spectrum level noise from the same click level. Wave amplitude ratios ($amplitude_X$ / $amplitude_{pre\text{-}exp\ 30\ dB\ noise}$) and latency shifts ($latency_X$ – $latency_{pre\text{-}exp\ 30\ dB\ noise}$) are plotted as a function of noise level for each wave component in Figure 9.5. In comparison to the raw data in Figure 9.4, this depiction emphasizes the increase in wave amplitudes and relative stability of wave latencies on a within-subject level (Table 9.7), though with considerable variability especially in Wave IV.

Previous studies observed changes in latency shift rates with noise level (e.g. Mehraei et al. 2016). Given this and the interactions between exposure and noise level on raw masked ABR wave amplitudes (Table 9.6), we also normalized the masked ABR data within-subject to the response in 30 dB spectrum level noise from the same click level *and same time point* (pre- or post-exposure). Wave amplitude ratios ($amplitude_X$ / $amplitude_{30\ dB\ noise}$) and latency shifts ($latency_X$ – $latency_{30\ dB\ noise}$) are plotted as a function of noise level for each wave component in Figure 9.6. There was no significant effect of noise exposure on the relative reduction of wave

amplitudes or latency shifts when comparing pre- and post-exposure data (Table 9.8). Together with the data in Figure 9.5, these findings suggest a constant increase in ABR wave amplitudes independent of stimulus level or signal-to-noise ratio, as opposed to a change in amplitude growth function slopes.

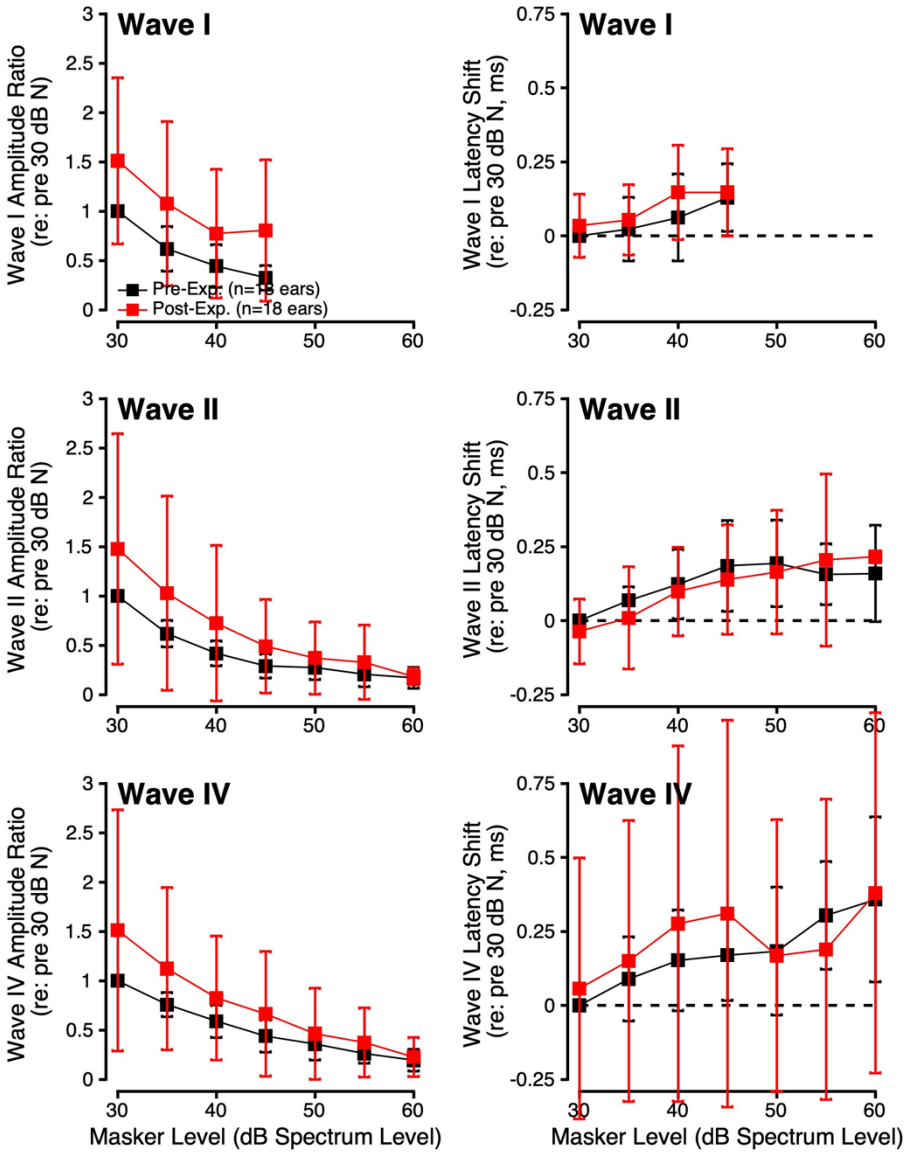

Figure 9.5 Same as Figure 9.4, except amplitude and latency values are normalized within-subject to the *pre-exposure* 90 dB SPL click in 30 dB noise response. Amplitude ratio = (amp_X / $amp_{pre\text{-}exp\ 30\ dB\ Noise}$). Latency shift = ($lat_X$ – $lat_{pre\text{-}exp\ 30\ dB\ Noise}$).

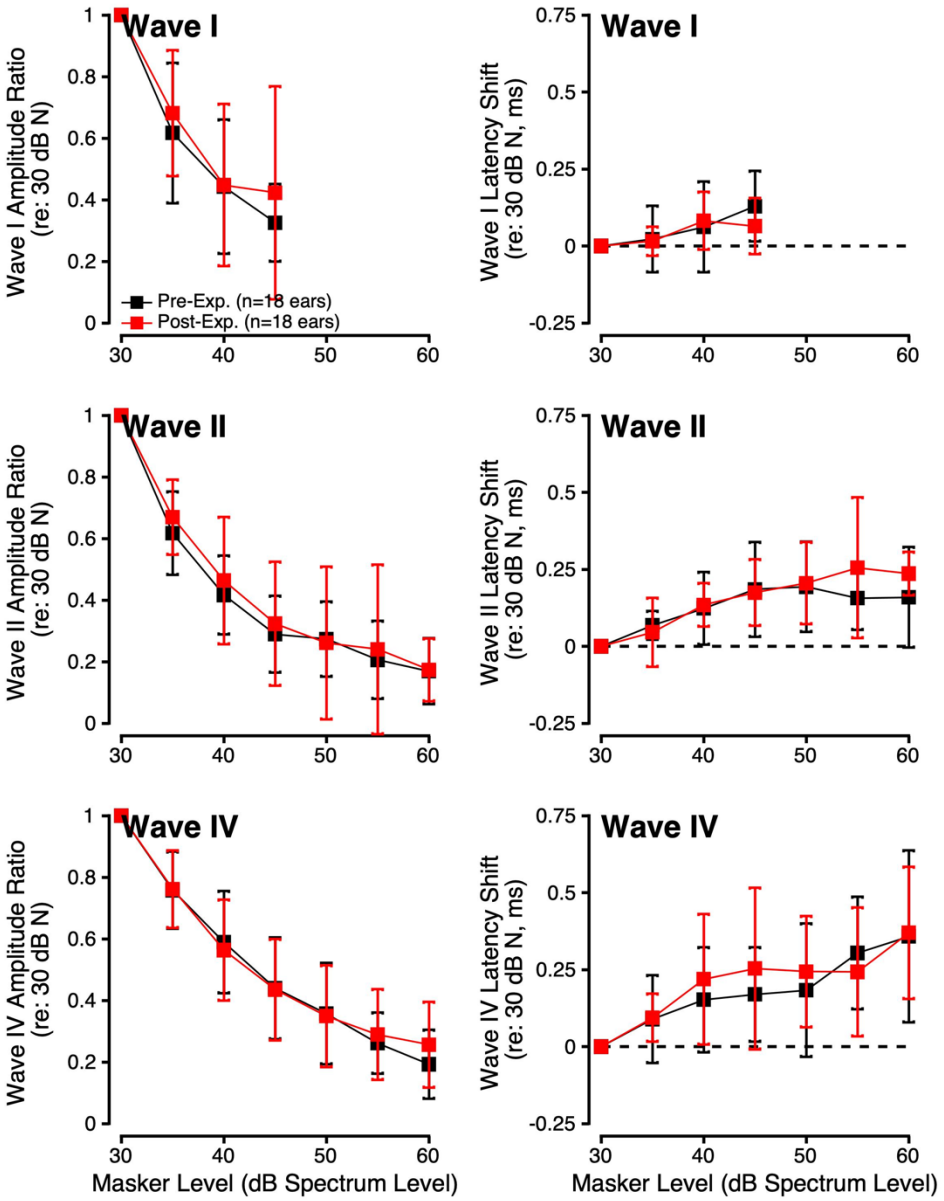

Figure 9.6 Same as Figure 9.4 and 9.5, except amplitude and latency values are normalized within-subject to the 90 dB SPL click in 30 dB noise response from the same time point. Amplitude ratio = (amp_X / $amp_{30\ dB\ Noise}$). Latency shift = (lat_X – $lat_{30\ dB\ Noise}$).

Table 9.7 Linear mixed effects models of effect of noise exposure on normalized (re: *pre-exposure* click in 30 dB noise) ABR wave amplitudes and latencies to 90 dB SPL clicks in ipsilateral broadband noise.

ABR Component	***R-squared***	**Variable**	***T-statistic (df)***	***p-value***
Wave I Amplitude	0.61	Exposure	2.60 (113)	0.010
Wave I Latency	0.24	none		
Wave II Amplitude	0.51	Sex	2.40 (191)	0.017
		Exposure	2.95 (191)	0.004
		Exposure*Noise Level	-2.11 (191)	0.036
Wave II Latency	0.22	none		
Wave IV Amplitude	0.46	Sex	3.28 (190)	0.001
		Exposure	2.76 (190)	0.006
		Sex*Noise Level	-2.36 (190)	0.019
		Exposure*Noise Level	-2.02 (190)	0.045
Wave IV Latency	0.34	Noise Level	2.24 (190)	0.027

Table 9.8 Linear mixed effects models of effect of noise exposure on normalized (re: click in 30 dB noise from same time point) ABR wave amplitudes and latencies to 90 dB SPL clicks in ipsilateral broadband noise.

ABR Component	***R-squared***	**Variable**	***T-statistic (df)***	***p-value***
Wave I Amplitude	0.63	Sex	-2.51 (113)	0.014
		Noise Level	-5.40 (113)	<0.000
		Sex*Noise Level	3.21 (113)	0.002
Wave I Latency	0.13	none		
Wave II Amplitude	0.76	Noise Level	-6.55 (191)	<0.000
		Sex*Noise Level	2.26 (191)	0.025
Wave II Latency	0.44	none		
Wave IV Amplitude	0.81	Noise Level	-6.92 (190)	<0.000
Wave IV Latency	0.42	Sex	2.04 (190)	0.043
		Noise Level	4.47 (190)	<0.000
		Sex*Noise Level	-3.31 (190)	0.001

9.4 DISCUSSION

9.4.1 Normative unmasked and masked click ABRs in macaque monkeys

In normal hearing macaques, ABR amplitudes increased and latencies decreased with increasing click level. Wave II and IV amplitudes were larger for female than male monkeys (Fowler et al., 2002) and this difference was quite large compared to humans (McFadden et al., 2021). This may be due to a greater difference in head size across sexes in macaques than humans.

Consistent with human studies (e.g. Beattie et al., 1994; Boezeman et al., 1983; Burkard & Hecox, 1983), the addition of ipsilateral masking noise reduced ABR amplitudes and increased latencies in macaques. There was a significant effect of sex on some masked ABR components, but these effects were small compared to the effect of click level.

9.4.2 Effects of noise exposure on unmasked and masked click ABRs in macaque monkeys.

Across all conditions tested and metrics assessed, unmasked click ABRs were not different in our macaque model of noise-induced SYN. These findings contrast a multitude of research demonstrating significant reductions of suprathreshold ABR Wave I amplitudes following noise-induced SYN in several rodent species (e.g. Bharadwaj et al., 2021; Furman et al., 2013; Kujawa & Liberman, 2009; Lee et al., 2020; Lin et al., 2011).

Masked click ABR amplitudes significantly increased following noise exposure, but without significant changes to wave latencies. Although these data are consistent with some studies of humans at risk for SYN (Burkard & Sims, 2002; Suresh & Krishnan, 2020) and could support the utility of masked ABR biomarkers for the clinical diagnosis of SYN, the findings contrast previous rodent studies (Giraudet et al., 2021; Mehraei et al., 2016) that showed smaller masked ABR amplitudes or increased masked ABR latencies. In the following sections, we discuss potential explanations for the divergent observations in the present study.

9.4.2.1 Macaque model of SYN

The absence of reduced suprathreshold ABR Wave I amplitudes to clicks in quiet informs the nature of our macaque model of SYN and highlights possible species differences in the manifestation of SYN pathology. Unlike rodent models of SYN, which commonly exhibit 50% ribbon loss (Bharadwaj et al., 2021; Kujawa & Liberman, 2009; Lin et al., 2011; Singer et al., 2013), our macaque model may represent a mild phenotype with an average of 20-30% ribbon

loss and a maximum of 40% loss only in some ears at 2 months post-exposure (Chapter 7, Figure 7.4A). It is possible that greater amounts of ribbon loss would lead to the expected suprathreshold ABR amplitude reductions and different changes in masked ABR responses. Additionally, the cochlear histological data in Chapter 7 and the ABR data presented here are from different subjects; histological analyses of the subjects discussed in this chapter is ongoing.

The possibility of synaptic repair or regeneration in macaques (discussed in Chapter 7) also complicates interpretation of the current data, as the precise time course of damage and recovery is unknown. (Further, we do not yet have cochlear histology for the subjects included in this Chapter.) The temporal dynamics of our macaque model of SYN afford the opportunity to examine changes in SYN pathology over time, but also complicate comparison to acute SYN models in rodents. One study in guinea pigs showed partial recovery of suprathreshold ABR Wave I amplitudes through 1 month post-exposure (Song et al., 2016), and this recovery may be nearly complete by 2 months post-exposure (Dan Tollin and colleagues, personal communication). ABR amplitude recovery may be an index of the ribbon repair or regeneration that is known to occur within 1-2 months in guinea pigs (Hickman et al., 2020, 2021; Shi et al., 2015; Song et al., 2016).

Although unmasked ABR amplitudes are apparently unaffected in macaques at 2 months post-exposure – when subjects are known to show reduced ribbon counts (Chapter 7, Figure 7.4A), we still observe changes in hearing abilities (Chapters 10 and 11). Perhaps low amounts of (and possibly transient) auditory nerve fiber loss does not noticeably impact the small ABR amplitudes of macaques. But this loss can still manifest as significant downstream changes in central auditory system encoding and perceptual deficits due to divergent connections in the ascending auditory pathway. Overall, our research emphasizes the importance of species considerations when modeling auditory pathologies.

9.4.2.2 Mechanisms contributing to suprathreshold and masked ABRs and their alteration by SYN

When interpreting findings from far-field electrophysiological assays, underlying mechanisms must be considered. Evoked potentials represent summed synchronous activity of a population of neurons. Higher sound levels recruit responses from a larger population of neurons. The addition of masking noise may saturate the responses of low threshold neurons and thus isolate responses from neurons that have high sound-evoked thresholds. A reduced neuronal

population should result in smaller evoked potentials, as demonstrated in rodent models of SYN-related deafferentation (e.g. Kujawa & Liberman, 2009). Preferential loss of high (or low) threshold neurons may alter ABR wave latencies, due to differences in first spike latencies (Heil & Peterson, 2015).

The stable unmasked ABR amplitudes reported here may indicate that not enough neurons were lost or that the remaining neuron population was sufficient to produce the suprathreshold and masked ABRs. This rationale is supported by reports that high threshold neurons contribute little to suprathreshold ABRs (Bourien et al., 2014) or that SYN may result in loss of both low and high threshold neurons (Suthakar & Liberman, 2021). Similarly, the unchanged ABR latencies may indicate that the remaining neuron population had a preserved proportion of low and high threshold neurons, thus maintaining the latency of the population response.

More perplexing is the apparent increase in masked ABR wave amplitudes. The effect of steady-state noise on auditory physiology combines mechanisms of saturation, adaptation (short, long, dynamic range), suppression and inhibition, cross-channel processing, and more among diverse populations of neurons within interacting auditory nuclei (Costalupes et al., 1984; Harris & Dallos, 1979; Heil & Peterson, 2015; Sachs et al., 1983; Smith, 1979; Wen et al., 2009). Identifying which mechanism is driving an observed effect is challenging if not impossible at the gross electrophysiological level.

One candidate mechanistic explanation comes from a recent study, which found enhanced onset responses in auditory nerve fibers of mice with noise-induced SYN (Suthakar & Liberman, 2021). This contrasts previous studies that saw no change in onset responses (Furman et al., 2013; Song et al., 2016), though species differences and the time course of synaptic damage and repair muddy the comparison of these studies. However, enhanced onset encoding following SYN may be a compensatory mechanism that could overcome neuronal loss and result in “unchanged” – or reduced but compensated – or even larger ABR Wave I amplitudes in both quiet and in noise.

The increase in masked ABR amplitudes supports our finding that tone detection performance in steady-state noise does not change following noise exposure (Chapter 10, Figure 10.6). These findings converge to suggest that the total effect of steady-state broadband noise on

auditory function following such noise exposures may be minimal, but individual components may change and compensate dynamically over time.

9.4.3 Future directions for noninvasive physiological biomarkers of SYN

Our findings are an important contribution to the literature on diagnostics for SYN. The inconsistent changes in suprathreshold and masked ABRs in noise-exposed macaques compared to rodent models of SYN may help make sense of the mixed findings in humans at risk for SYN. Humans and monkeys have small ABR Wave I amplitudes compared to rodents (Stahl et al., submitted; Prendergast et al., 2018), which may contraindicate the clinical utility of Wave I metrics for diagnosing SYN in humans. Other ABR wave components (II and IV in macaques, III and V in humans) are larger and more readily identified, and therefore may offer greater clinical utility.

Alternative ABR stimulus paradigms may be worth pursuing. For example, stimulus and masker paradigms with temporal complexity, such as forward masking, may be sensitive to SYN (Lee et al., 2020; Mehraei et al., 2017; Song et al., 2016; also see discussion of psychoacoustic masking paradigms in Chapter 11). Another candidate masking paradigm uses high-pass noise to isolate responses of auditory nerve fiber populations along the cochlear length (Burkard & Hecox, 1987; Don & Eggermont, 1978; Earl & Chertoff, 2012). By sequentially increasing the high-pass cutoff frequency, regions of deafferentation may be identified as plateaus in ABR amplitude growth functions (Earl & Chertoff, 2012).

Although our null and conflicting results are an important contribution to an already mixed literature, our findings ultimately do not provide support for a SYN diagnostic test. Unmasked and masked ABR amplitudes were highly variable across subjects before and after noise exposure. Though we were able to see group-level and within-subject changes in masked ABR amplitudes following noise exposure, it seems unlikely that any ABR metric will have the sensitivity to diagnose an individual with SYN, unless a change can be documented in the same patient over time. This work underscores the need for continued research efforts in the search for SYN biomarkers. We did observe other physiological changes and perceptual deficits in our noise-exposed macaques (see Chapters 8 and 11). Future work should draw on the findings from our parallel studies to identify novel biomarkers. Furthermore, as the literature on the physiological and perceptual consequences of SYN continues to expand, findings should be

synthesized together in order to identify common mechanisms of change, which can then be developed into targeted diagnostic tests.

CHAPTER 10

Tone detection in quiet and in steady-state noise are unchanged following noise exposure designed to cause cochlear synaptopathy

10.1 INTRODUCTION

Cochlear synaptopathy (SYN) is an inner ear pathology characterized by the selective loss of inner hair cell ribbon synapses and subsequent loss of auditory nerve fibers (Kujawa & Liberman, 2009). Physiological and modeling studies show that this deafferentation, especially loss of low spontaneous firing rate fibers, results in impaired encoding of suprathreshold sounds, such as signals in noise (Bharadwaj et al., 2014; Furman et al., 2013). These changes in suprathreshold sound encoding are hypothesized to underlie a clinical presentation called "hidden hearing loss" – difficulties hearing in background noise despite an absence of overt hearing loss. Indeed, approximately 15% of individuals seeking audiologic care have normal audiometric test results, but report hearing difficulties (Cooper & Gates, 1991; Grant et al., 2021; Hind et al., 2011; Kumar et al., 2007; Spankovich et al., 2018; Tremblay et al., 2015). SYN provides a possible site of lesion that may contribute to this clinical presentation. Many research groups have attempted to identify biomarkers that correlate with these reported perceptual deficits, but with mixed results (Bramhall et al., 2019; DiNino et al., 2021; Henry, 2022; Hickox et al., 2017).

Leading biomarkers for SYN in rodents include reduction of auditory brainstem response Wave I amplitude and middle ear muscle reflex magnitude (Bharadwaj et al., 2021; Kujawa & Liberman, 2009; Valero et al., 2016; Valero et al., 2018). These same metrics have been assessed in human populations at risk for SYN, including older adults and individuals with a significant history of noise exposure who also have normal hearing sensitivity. Some human studies have shown an association between greater SYN risk or poorer performance on speech-in-noise tests and reduced ABR Wave I amplitudes (Bramhall et al., 2017; Burkard & Sims, 2002; Grant et al., 2020; Harris et al., 2021; Liberman et al., 2016; Ridley et al., 2018; Schaette & McAlpine, 2011; Skoe & Tufts, 2018; Suresh & Krishnan, 2020) or reduced MEMR magnitude (Bharadwaj et al., 2021; Shehorn et al., 2020; Wojtczak et al., 2017), but not in others (ABR: Fulbright et al., 2017;

Grinn et al., 2017; Guest et al., 2018; Prendergast et al., 2019; Spankovich et al., 2017) (MEMR: Guest et al., 2019; Mepani et al., 2020).

An alternative approach to understanding the perceptual consequences of SYN is to psychophysically assess animals before and after experimental induction of SYN. This approach provides the advantage of histological verification of inner ear pathology, as well as paired within-subject comparisons. Despite a broad literature searching for noninvasive physiological assays of SYN, there is little evidence for perceptual deficits in the same subjects (Henry, 2022). In this and parallel reports from our laboratory, we describe the results from a comprehensive battery of psychoacoustic tone detection tasks performed by rhesus macaques before and after noise exposure known to cause SYN.

The overall aim of this work was to assess the functional consequences of SYN in nonhuman primates. In developing our behavioral test battery, we wanted to include a range of tasks to probe different facets of hearing abilities. Here, we report findings from paradigms designed to assess hearing sensitivity, growth of masking, and frequency selectivity. We previously demonstrated that these three tasks are affected by sensorineural hearing loss and correlate with the extent of cochlear damage (Hauser et al. 2018, Burton et al. 2020). Here, we investigate the same tasks in our nonhuman primate model of SYN, which has intact cochlear mechanics as evidenced by normal otoacoustic emissions (Chapter 8, Figure 8.7) and minimal loss of hair cells (Chapter 7, Figure 7.2).

10.2 MATERIALS AND METHODS

10.2.1 Subjects

Rhesus macaques (*Macaca mulatta*, $n = 9$, 4 female) were trained to perform a reaction time Go/No-Go lever release task to detect pure tone signals (200 ms, 10 ms rise/fall) in quiet and in steady-state noise under diotic, open field testing conditions.

10.2.2 Psychophysical tone detection tasks

A complete description of our psychophysical tone detection task design and analysis are described in the General Methods. Details on the stimuli and analyses specific to the tasks discussed in this chapter are provided here.

10.2.2.1 Hearing sensitivity

Tone detection was assessed in quiet to construct behavioral audiograms as previously reported (Burton et al., 2020; Dylla et al., 2013). Signal frequencies of 0.125, 0.25, 0.5, 1, 1.4, 2, 2.8, 4, 5.6, 8, 16, 24, and 32 kHz were chosen to span the audible range of macaques (Dylla et al., 2013; Pfingst et al., 1978) in octave steps with additional half-octave resolution near the noise exposure band. Audiometric thresholds were derived from psychometric functions, as described in detail in the General Methods. Audiograms were measured monthly before noise exposure while subjects were completing other psychophysical tasks. Immediately following noise exposure, audiograms were assessed daily to evaluate for temporary threshold shifts. Threshold shifts were quantified by taking the difference between the post-exposure and pre-exposure thresholds at that frequency. A full audiogram could not be completed in one day, so frequencies of interest were targeted for the first time point (24 hours post-exposure). Subjects were often less motivated to work the day following noise exposure, since they were well hydrated from IV fluids given during the procedure and may have anesthesia remaining anesthesia in the system. Audiograms were monitored for three to four weeks following exposure until all thresholds had returned to within 2 dB of pre-exposure values (no remaining threshold shifts). After the first month, post-exposure audiograms were measured monthly to monitor for changes in hearing sensitivity (see blue boxes in Figure 10.1). Since each subject typically had 5-10 thresholds for each frequency, audiometric threshold variability (standard deviation) was also compared before and after exposure.

10.2.2.2 Growth of masking

Tone detection (1, 2, 2.8, 4, 5.6, 8, and 16 kHz) was assessed in continuous, steady-state broadband noise (0.1-40 kHz). Noise level was varied across a wide range of levels (10-50 dB spectrum level) to estimate growth of masking as reported previously (Dylla et al., 2013; Hauser et al., 2018). Detection thresholds were regressed against the noise spectrum level. Threshold shift rates and intercepts were defined by the slope and y-intercept of the best linear fit of threshold vs. noise spectrum level. Growth of masking was assessed at all test frequencies before noise exposure and at 1.5-2 months post-exposure. Frequencies of interest (near the exposure band) were also probed for some monkeys at 3 (n = 3), 5-6 (n = 3), 7-8 (n = 5), and 9-10 (n = 4) months post-exposure (see green boxes in Figure 10.1).

10.2.2.3 Frequency selectivity

Modeled after Patterson and Nimmo-Smith (1980) and Glasberg et al. (1984), the notched-noise methods used here were similar to those described previously (Burton et al., 2018; Burton et al., 2020). In brief, tone detection performance was measured in the presence of spectrally-notched noise. 30 dB spectrum level noise was used to estimate symmetric auditory filters at signal frequencies (f_0) of 0.5, 1, 2, 4, 8, 16, and 32 kHz. The normalized half-notchwidths ($\Delta f/f_0$) for the symmetric noise notches were 0, 0.2, 0.4, 0.6, and 0.8. Two 50 dB spectrum level narrowband noise maskers (bandwidth = 0.4*f_0) were placed symmetrically and asymmetrically around the tone frequency to estimate asymmetric auditory filters at signal frequencies of 1, 2, 2.8, 4, 5.6, 8, and 16 kHz. In addition to the symmetric normalized half-notchwidths listed above, upward and downward shifted asymmetric notches were (f_l/f_u values re: f_0) = 0.2/0.4, 0.4/0.6, 0.4/0.2, 0.6/0.4. Estimates of filter shape were obtained from the tone detection thresholds as a function of notch width using the rounded exponential fit as reported previously (Burton et al., 2018; Burton et al., 2020). Analysis was completed using the publicly available ROEXPR (symmetric filters) and ROEX3 (asymmetric filters) programs, developed by Moore & Glasberg. Filter bandwidths were calculated using the equivalent rectangular bandwidth (ERB) according to Glasberg et al. (1984). Changes in frequency selectivity were quantified according to the ratio: $ERB_{post\text{-}exposure}$ (f_0) / $ERB_{pre\text{-}exposure}$ (f_0). Frequency selectivity was assessed at all test frequencies before noise exposure and at 2-3 months post-exposure (n = 3, males) or 7-8 months post-exposure (n = 4, females). Frequencies of interest were also probed for the male monkeys at 8-9 months post-exposure (see yellow boxes in Figure 10.1).

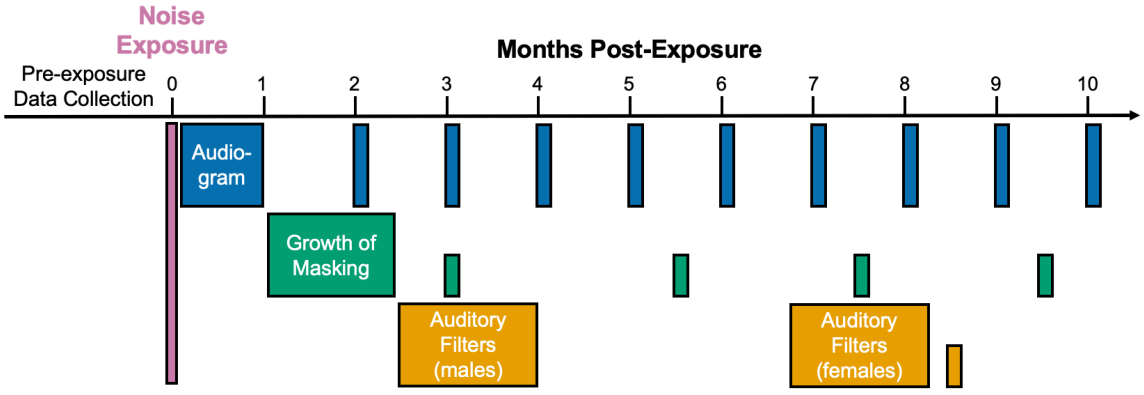

Figure 10.1 Timeline for behavioral data collection. Audiograms were collected for the first month to assess temporary threshold shifts, and then monitored monthly. Growth of masking was assessed at 1-2 months post-exposure and probed at frequencies of interest every 2 months. Auditory filters were measured at 2-3 or 7-8 months post-exposure and probed at frequencies of interest at 8-9 months post-

10.3 RESULTS

10.3.1 Audiogram reveals temporary changes in hearing sensitivity following noise exposure

Tone detection was measured in quiet to assess hearing sensitivity across the audible hearing range of the macaques. Exemplar pre- and post-exposure psychometric functions are shown in Figure 10.2A (Monkey Lu, 2 kHz). The rightward shift of the 24 hours post-exposure function (red) illustrates the temporary threshold shift induced by the noise exposure, which resolves by 1 month post-exposure (dark red).

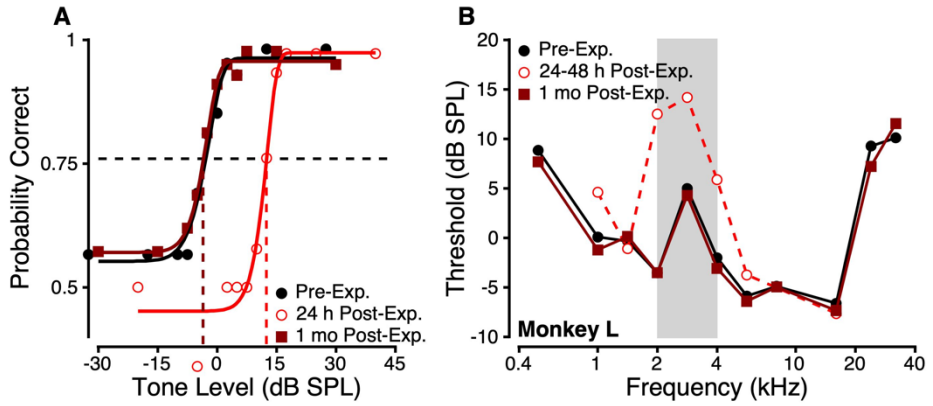

Figure 10.2 A. Psychometric functions for tone detection in quiet. Data from Monkey Lu (2 kHz tone) before (black circles), 24 hours after (red circles), and 1 month (dark red squares) after noise exposure. Symbols indicate raw data, lines illustrate Weibull fits of the data. Horizontal dashed line indicates *pc* = 0.76, and the vertical dashed lines illustrate these threshold values for each condition. B. Audiograms from Monkey Lu before (black), 24 hours after (red circles), and 1 month (dark red squares) after noise exposure, illustrating a temporary threshold shift. Gray box here and in other figures illustrates the noise exposure band.

The earliest post-exposure behavioral audiogram measurements were conducted at 24 and 48 hours after the end of the exposure to assess for temporary threshold shifts (TTS). Thresholds in quiet were measured daily for 3-4 weeks to monitor recovery from TTS. Once thresholds had recovered to pre-exposure values, one final audiogram was obtained, and then subsequent psychophysical testing was pursued. Exemplar audiograms from Monkey Lu are shown in Figure 10.2B. At 24-48 hours post-exposure, tone detection thresholds were

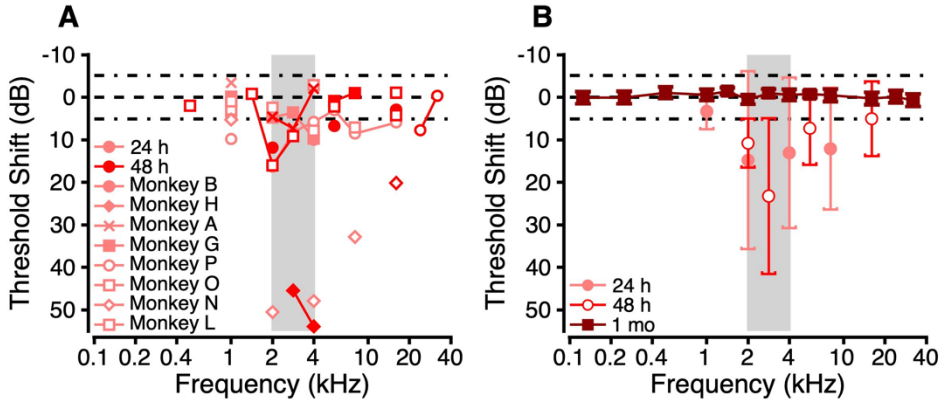

Figure 10.3 A. Temporary threshold shifts (*post-exposure – pre-exposure*) measured for individual subjects at 24 hours (pink symbols) and 48 hours (red symbols) after noise exposure. B. Mean threshold shifts plotted as a function of frequency at 24 hours (n = 3-7), 48 hours (n = 3-5), and 1 month (n = 8) post-exposure. Error bars indicate ± 1 standard deviation from the mean. Dashed lines equal 0, indicating no threshold shift. Dot-dash lines illustrate the 95% confidence interval for audiometric threshold variability (± 5.12 dB, two times the median of the pre-exposure distribution in Figure 10.4).

elevated at frequencies near the noise exposure band. All thresholds recovered by 1 month post-exposure.

Figure 10.3A illustrates threshold shifts measured for individual subjects at 24 (pink) and 48 hours (red) post-exposure. Maximum temporary threshold shifts varied from 7.1 – 53.9 dB, which exceeds the 95% confidence interval for audiometric threshold variability, and typically occurred at 2, 2.8, or 4 kHz. The noise exposure seemed to generate a bimodal distribution of TTS, with two subjects (Monkeys Ha & Ne) exhibiting much larger shifts (50.5-53.9 dB max. TTS) than the other six subjects (7.1-16.3 dB max. TTS). Mean threshold shifts are plotted as a function of frequency in Figure 10.3B for timepoints of 24 hours (n = 3-7), 48 hours (n = 3-5), and 1 month (n = 8) post-exposure. Threshold shifts were greatest for frequencies near the noise exposure band. By 1 month post-exposure, no significant threshold shifts remained for any subject or tone frequency (all < 3 dB), suggesting full recovery of hearing sensitivity. Audiometric thresholds remained stable (within ± 5 dB of pre-exposure values) throughout post-exposure data collection, including a final timepoint just prior to sacrifice.

SYN could result in less robust encoding, or stochastic undersampling, of incoming signals (Lopez-Poveda, 2014). To probe this at the behavioral level, we took advantage of the numerous audiogram measurements available for each subject pre- and post-exposure, and calculated tone detection threshold variability (one standard deviation from the mean). A linear mixed effects model revealed no significant differences in threshold variability as a function of frequency (p > 0.05), so all data were combined into a histogram of pre- (black) and post-exposure (red) audiometric threshold variability values (Figure 10.4). There was a statistically significant difference in these distributions (k = 0.28, p = 0.010), which had a pre-exposure median of 2.56 dB and a post-exposure median of 2.19 dB. In contrast to the prediction, this lower post-exposure threshold variability likely represents a practice effect on this task.

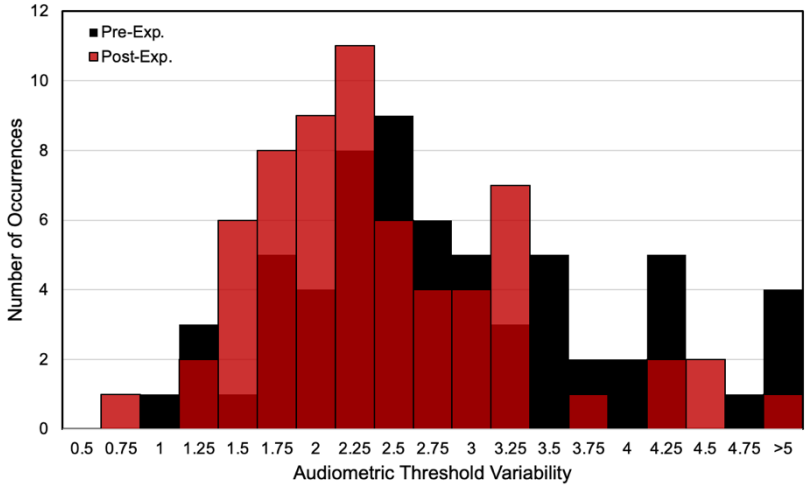

Figure 10.4 Distribution of audiometric threshold variability values pre- (black) and post-exposure (red). Data are combined across subjects (n = 8) and frequencies (1, 2, 2.8, 4, 5.6, 8, & 16 kHz).

10.3.2 Tone detection in steady-state noise is unchanged following noise exposure

Tone detection was measured in steady-state broadband noise ranging from 10 to 50 dB spectrum level to estimate threshold shift rates. Exemplar pre- and post-exposure psychometric functions are shown in Figure 10.5A (Monkey Ga, 2.8 kHz). Threshold increased as noise level increases, as illustrated by the rightward shift of the psychometric functions. Following noise exposure, there were no significant changes in tone detection thresholds, psychometric function slopes, or reaction times for any tone frequency or noise level (Mackey, personal communication). Exemplar tone detection thresholds from one subject for all tone frequencies and noise levels (Figure 10.5B; after Hawkins and Stevens (1950)) illustrate the consistency in thresholds pre- and post-exposure.

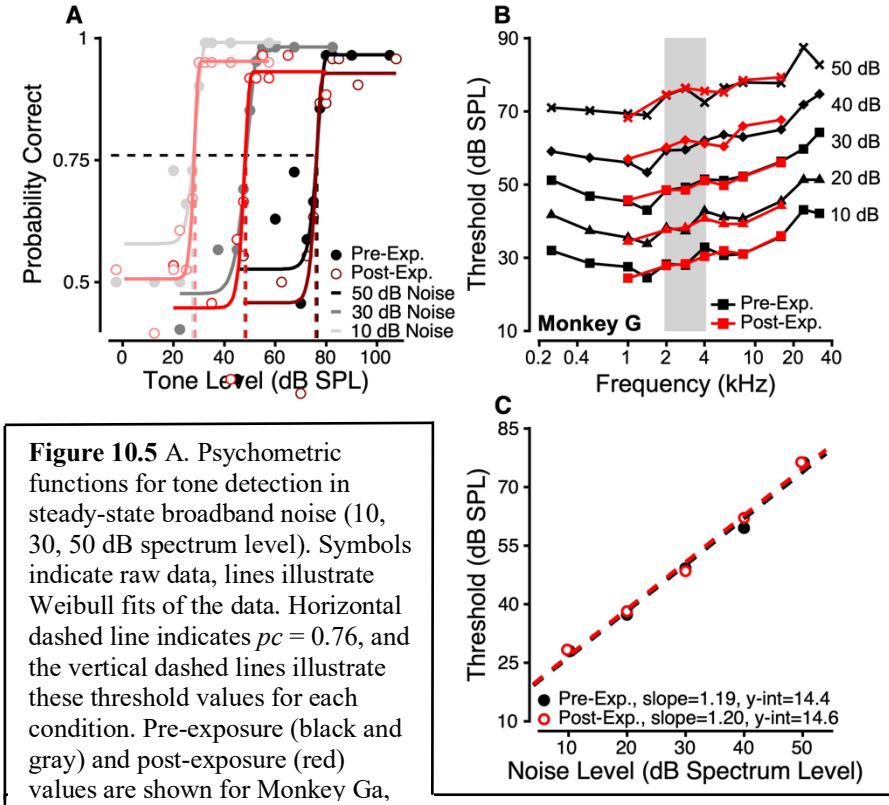

Figure 10.5 A. Psychometric functions for tone detection in steady-state broadband noise (10, 30, 50 dB spectrum level). Symbols indicate raw data, lines illustrate Weibull fits of the data. Horizontal dashed line indicates *pc* = 0.76, and the vertical dashed lines illustrate these threshold values for each condition. Pre-exposure (black and gray) and post-exposure (red) values are shown for Monkey Ga, 2.8 kHz tone. B. Tone detection thresholds from Monkey Ga plotted as a function of frequency in 10, 20, 30, 40, and 50 dB spectrum level noise. Pre-exposure thresholds in black, post-exposure thresholds in red. Gray box illustrates the noise exposure band. C. Pre- (black) and post-exposure (red) thresholds from panel A (plus additional conditions) plotted as a function of noise level.

Thresholds were plotted as a function of noise level (exemplar data in Figure 10.5C; Monkey Ga, 2.8 kHz) in order to calculate threshold shift rate slopes and y-intercepts for each tone frequency pre- and post-exposure. Slopes provide an estimate of growth of masking as noise level increases. Intercept values provide information about the absolute masked thresholds independent of slope.

Figure 10.6 illustrates mean threshold shift rate slopes (A) and y-intercepts (B) as a function of frequency. Slope values were near to 1 across frequencies, indicating a 1 dB/dB exchange rate that is well-established in the literature (Dylla et al., 2013; Gibson et al., 1985;

Hawkins & Stevens, 1950). A linear mixed effects model indicated no significant differences in threshold shift rate slopes or intercepts according to sex or exposure status (*p*-values > 0.05), and only an effect of frequency on intercepts ($t(df)$ = 3.6142(115), p = 0.000). There was a small but non-significant trend for intercept values to decrease post-exposure, which is likely a practice effect.

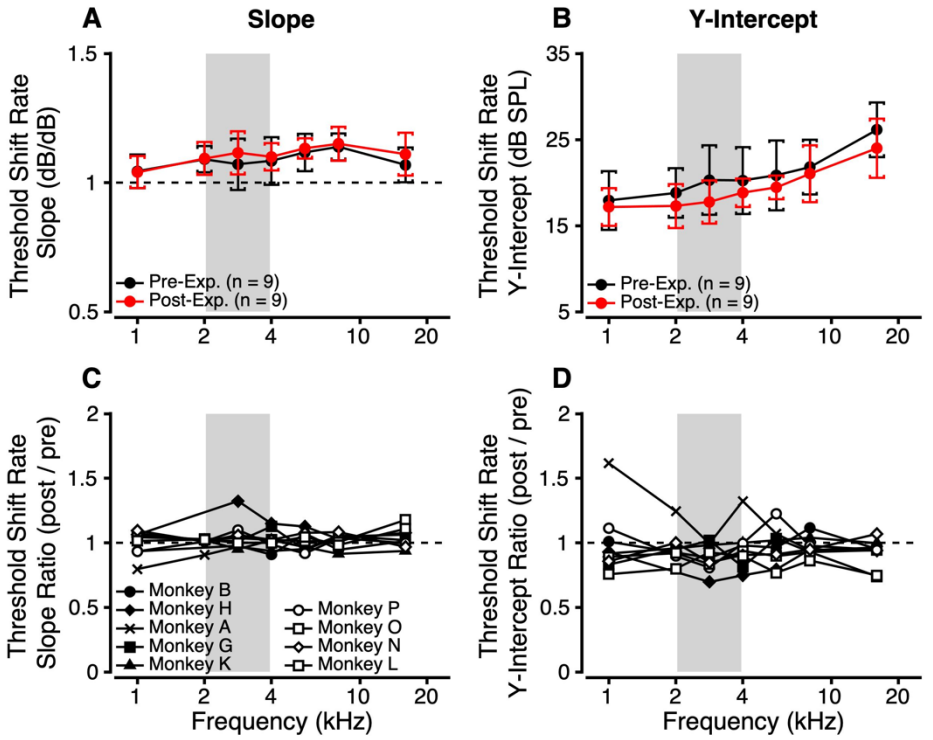

Figure 10.6 A. Mean threshold shift rates as a function of frequency before (black) and after (red) noise exposure. Error bars indicate ± 1 standard deviation from the mean. B. Same as A, but for threshold shift Y-intercepts. C. Within-subject ratio of post-exposure:pre-exposure threshold shift rates as a function of frequency. Black dashed line indicates a ratio of 1. D. Same as C, but for threshold shift Y-intercepts. Gray boxes illustrate the noise exposure band.

To increase the transparency of our data and to illustrate within-subject changes, threshold shift rate slope ratios ($slope_{pre\text{-}exposure}$ / $slope_{post\text{-}exposure}$) and intercept ratios ($intercept_{pre\text{-}exposure}$ / $intercept_{post\text{-}exposure}$) were calculated for each subject and tone frequency. These ratios are plotted as a function of frequency in Figure 10.6C and D. Ratios greater than 1 indicate steeper slopes or higher masked thresholds post-exposure, respectively; ratios less than 1 indicate shallower slopes or lower masked thresholds post-exposure. Across subjects and tone frequencies, there was no clear trend in the threshold shift rate slope and intercept ratios, confirming no effect of noise exposure on tone detection in steady-state noise.

Threshold shift rates were probed at frequencies of interest at later post-exposure time points. Raw thresholds were within ± 3 dB of pre- and 2 month post-exposure thresholds. Threshold shift rate slopes and intercepts were not significantly different from pre-exposure values at 3, 5, 7, and 9 months post-exposure (*p-values* > 0.05; data not shown).

10.3.3 Frequency selectivity is unchanged following noise exposure

Tone detection in notched noise was used to derive perceptual auditory filters to estimate frequency selectivity. Exemplar pre- and post-exposure psychometric functions and thresholds as a function of notchwidth are shown in Figure 10.7 (Monkey B, 8kHz, 50 dB noise). Threshold decreased as notchwidth increased, as illustrated by the leftward shift of the psychometric functions in Figure 10.7A and the negative sloping functions in Figure 10.7B. Following noise exposure, there were no changes in tone detection thresholds, psychometric function slopes, or reaction times across notchwidth conditions, tone frequencies, and noise levels (Mackey, personal communication). Exemplar filter banks are shown in Figure 10.8 for the 30 and 50 dB noise conditions (Monkey G). No qualitative differences in auditory filter shape were noted when comparing pre- and post-exposure filters.

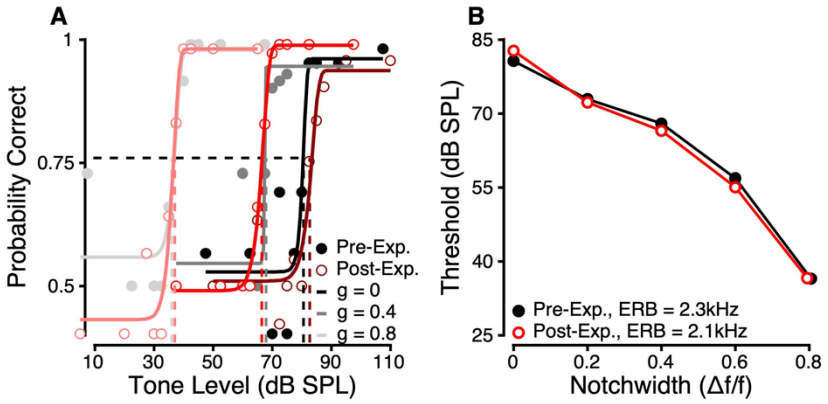

Figure 10.7 A. Psychometric functions for tone detection in notched noise with normalized half notchwidths of 0, 0.4, and 0.8. Symbols indicate raw data, lines illustrate Weibull fits of the data. Horizontal dashed line indicates *pc* = 0.76, and the vertical dashed lines illustrate these threshold values for each condition. Pre-exposure (black and gray) and post-exposure (red) values are shown for Monkey B, 8 kHz tone, 50 dB noise level. B. Pre- (black) and post-exposure (red) thresholds from panel A (plus additional conditions) plotted as a function of normalized half notchwidth.

To quantify frequency selectivity, the equivalent rectangular bandwidth (ERB) was calculated for each filter. Figure 10.9A and B illustrate mean ERB values as a function of frequency for the 30 and 50 dB noise conditions. Linear mixed effects models indicated no significant differences in ERB according to sex or exposure status (*p-values* > 0.05), but there was a significant effect of frequency on ERB for both 30 ($t(df)$ = 3.11(55), p = 0.003) and 50 dB spectrum level maskers

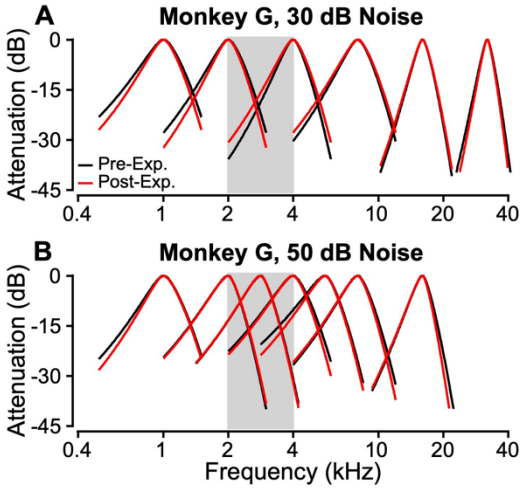

Figure 10.8 Auditory filter banks for Monkey G in 30 (A) and 50 dB noise (B). Pre-exposure filters in black, post-exposure filters in red. Gray boxes illustrate the noise exposure band.

($t(df) = 2.64(67)$, $p = 0.010$). Thus, there were no significant changes in ERB values following noise exposure.

To increase the transparency of our data and to illustrate within-subject changes, the ERB ratio ($ERB_{post\text{-}exposure}$ / $ERB_{pre\text{-}exposure}$, after Burton et al. (2020)) is plotted as a function of frequency in Figure 10.9C and D. Values greater than 1 indicate a larger ERB and broader frequency selectivity post-exposure; values less than 1 indicate a smaller ERB and narrower frequency selectivity post-exposure. Across subjects, tone frequencies, and noise levels, ERB ratios clustered around a value of 1, confirming no effect of noise exposure on auditory filter widths.

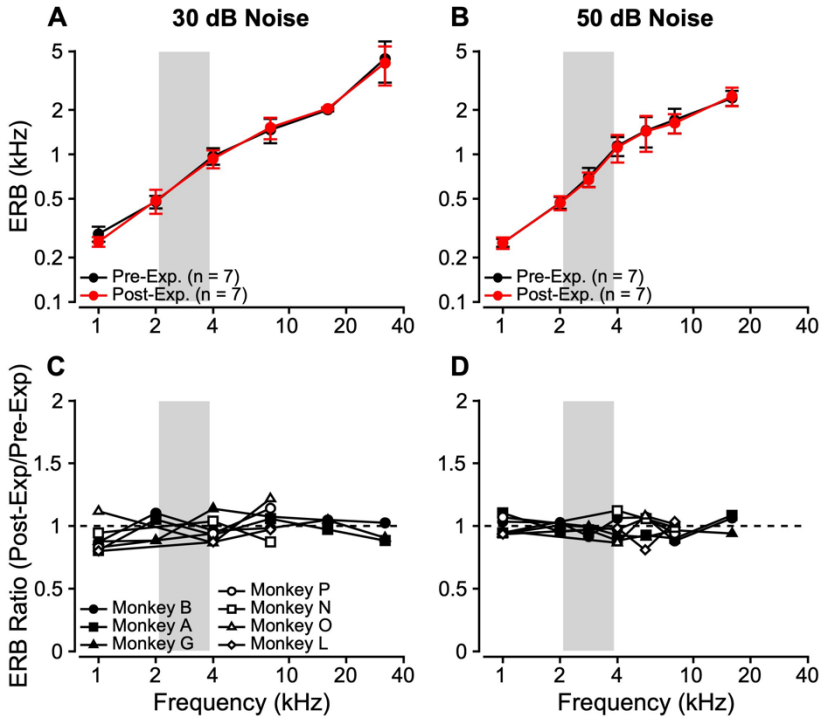

Figure 10.9 A, B. Mean ERB as a function of frequency for all subjects before (black) and after (red) noise exposure for the 30 (A) and 50 (B) dB noise conditions. Error bars indicate ± 1 standard deviation. C, D. Within-subject ERB ratio as a function of frequency for the 30 (C) and 50 (D) dB noise conditions. Black dashed line indicates an ERB ratio = 1. Gray boxes illustrate the noise exposure band.

10.4 DISCUSSION

Hearing sensitivity, growth of masking, and frequency selectivity were unchanged following recovery from noise-induced temporary threshold shifts. Across all tasks, post-exposure tone detection thresholds in quiet and in noise were not significantly different from pre-exposure thresholds up to 10-11 months post-exposure. These null observations contrast findings in parallel experiments that show deficits on other tone detection tasks (Chapter 11). Given the histopathological findings in our macaques (Chapter 7), up to 40% synapse loss (and putative synapse recovery) can occur without compromising hearing sensitivity, growth of masking, or frequency selectivity under our diotic testing conditions.

Our testing is conducted in an open sound field to mimic real-world listening conditions that utilize both ears. However, asymmetric inner ear damage (see Chapter 7) is a complicating factor in the interpretation of our findings. Consistent with previous work by our lab and others, binaural summation is thought to arise from average function across the two ears (Burton et al., 2020; Gage, 1932; Heil, 2014; Hempstock et al., 1966; Hirsh, 1948; Pollack, 1948; Shaw et al., 1947) Future analyses correlating histological and behavioral findings should adopt this approach.

10.4.1 Hearing sensitivity

It is well-documented across a variety of inner ear pathologies that behavioral hearing sensitivity is spared in the absence of outer hair cell loss, even with significant inner hair cell loss (Lobarinas et al., 2013) or auditory nerve fiber loss (Makary et al., 2011; Schuknecht & Woellner, 1955; Wong et al., 2019). Here, we demonstrate for the first time that noise exposure intended to cause SYN does not affect behavioral hearing sensitivity or day-to-day threshold variability. This finding is also consistent with reports that synapse loss does not contribute to audiometric threshold variability in sensorineural hearing loss (Burton et al., 2020; Gleich et al., 2016; Wu et al., 2021) (but see Wu et al., 2020).

Previous studies of SYN reported stable hearing sensitivity according to ABR or DPOAE threshold estimates (e.g. Kujawa & Liberman, 2009). However, behavioral measures are also important to assess, since functional hearing sensitivity is not always accurately reflected in physiological estimates. For example, individuals with auditory neuropathy spectrum disorder typically have normal OAEs and grossly abnormal or absent ABRs, accompanied by audiograms ranging from normal hearing to profound hearing loss (Starr et al., 1996). ABR and DPOAE measures typically result in higher threshold estimates than behavioral measures, even after accounting for differences in stimulus duration (e.g. Lasky et al., 1999, Stahl et al. submitted). Physiological and behavioral hearing sensitivity estimates following acoustic trauma are also weakly correlated (e.g. Burke et al., 2021; Pugh et al., 1974) and may not accurately reflect inner ear damage (reviewed in Burton et al., 2019).

10.4.2 Growth of masking

SYN is hypothesized to underlie difficulties hearing in background noise in the absence of overt hearing loss. This hypothesis is supported by previous research assessing tone in noise detection in animals with SYN-like inner ear pathologies and in humans at risk for SYN. Lobarinas and colleagues (2016) reported poorer detection of 500 ms tones in noise by chinchillas with carboplatin-induced inner hair cell loss. The same group found reduced pre-pulse inhibition of the acoustic startle to 50 ms noise bursts in continuous noise by rats following noise-induced temporary threshold shifts (Lobarinas et al., 2017). Although inner hair cell loss is a more extreme form of deafferentation than SYN, and rats were not histologically assessed for SYN, these studies support the hypothesis that SYN-like pathologies may degrade signal detection in noise. With another pharmacological deafferentation approach, ouabain-induced loss of spiral ganglion neurons impaired detection of short duration (50 ms) tones in noise (Resnik & Polley, 2021), but not longer duration (300-500 ms) tones (budgerigars: Henry & Abrams, 2021; mice: Resnik & Polley, 2021). Some studies of older adults with normal or near-normal hearing (who may be at risk for SYN) show higher thresholds for tones in noise (Margolis & Goldberg, 1980; Ralli et al., 2019; Ridley et al., 2018). However, other studies of older adults and a study in individuals with tinnitus have not observed this deficit (Bernstein & Trahiotis, 2016; Klein et al., 1990; Marmel et al., 2020; Quaranta et al., 1990). Differences in stimulus paradigm may contribute to these discrepancies. For example, Bernstein and Trahiotis (2016, 2019, 2020) did not observe tone in noise detection deficits unless binaural cues were present.

Here, we found that our macaque model of noise-induced SYN did not affect tone detection in steady-state noise. It is possible that our SYN model is less severe than the other inner ear pathologies studied and therefore does not impact growth of masking. Alternatively, more complex tone and masker combinations, such as shorter duration tones, amplitude-modulated or spatially separated noises, or gated noise maskers, may reveal the predicted hearing-in-noise deficits (see Chapter 11).

10.4.3 Frequency selectivity

Frequency selectivity is thought to be largely determined by outer hair cell function and therefore is not predicted to change with SYN. Auditory nerve fiber tuning curves are unchanged following SYN (Furman et al., 2013; Suthakar & Liberman, 2021) and inner hair cell loss (Wang et al., 1997), consistent with this prediction. Our behavioral auditory filters also indicate no

change in frequency selectivity following noise exposure intended to cause SYN. These findings contrast with previous work showing broader spectral resolution in humans with speech-in-noise deficits who may be at risk for SYN (Badri et al., 2011; Pick & Evans, 1983). Humans exposed to noise intended to cause temporary threshold shifts also show broader spectral resolution and the recovery of hearing sensitivity and perceptual tuning do not always follow the same time course (Bergman et al., 1992; Feth et al., 1979; Klein & Mills, 1981). However, contributions from differences in outer hair cell function and high frequency hearing sensitivity cannot be ruled out in these studies (see Badri et al., 2011, Figure 2). Carboplatin-induced inner hair cell loss has also been shown to broaden behavioral masking functions (Lobarinas et al., 2016), so it is possible that physiological and perceptual estimates of frequency selectivity may be differentially affected by inner ear pathology, emphasizing the importance of assessing both measurement modalities.

CHAPTER 11

Reduction of the overshoot effect, but not forward masking, in macaque monkeys following noise exposure intended to cause cochlear synaptopathy

11.1 INTRODUCTION

Listening difficulty in the presence of background noise is among the top complaints of patients seeking audiologic care (Hall, 2017; Zhao & Stephens, 1996). While hearing-in-noise difficulties commonly accompany sensorineural hearing loss, 5-20% of patients have normal hearing sensitivity (Billings et al., 2018; Cooper & Gates, 1991; Grant et al., 2021; Hannula et al., 2011; Hind et al., 2011; Koerner et al., 2020; Kumar et al., 2007; Parthasarathy et al., 2020; Spankovich et al., 2018; Tremblay et al., 2015). The etiology of this "hidden hearing loss" has been a dominating focus in hearing research over the past decade. One recently discovered inner ear pathology thought to contribute to these hidden hearing difficulties is cochlear synaptopathy (SYN), or the selective loss of inner hair cell ribbon synapses (Kujawa & Liberman, 2009). SYN results in degradation of afferent auditory nerve fibers, especially the subpopulation with low spontaneous firing rates (LSR) and high thresholds to sound stimulation (Furman et al., 2013; Liberman et al., 2015; Schmiedt et al., 1996; but see Suthakar & Liberman, 2021). Hearing sensitivity is maintained by preserved outer hair cell (OHC) function and intact high spontaneous firing rate fibers with low sound-evoked thresholds. In contrast, the more susceptible LSR fibers encode signals in noise (Costalupes, 1985), leading to the hypothesis that SYN causes impaired auditory perception in background noise (Bharadwaj et al., 2014; Oxenham, 2016; Plack et al., 2014). Evidence for SYN underlying speech perception deficits in humans is mixed (Bramhall et al., 2019; DiNino et al., 2021), and few studies have assessed behavioral hearing abilities in histologically-verified animal models of SYN (Gleich et al., 2016; Tziridis et al., 2021).

We developed a nonhuman primate model of noise-induced SYN, which shows 20-30% inner hair cell ribbon loss that recovers over the course of months (see Chapter 7). As reported in Chapter 10, tone detection in quiet and steady-state noise is unchanged following noise exposure. Here, we report the effects of noise exposure intended to cause SYN on signal detection in three gated noise paradigms: long tones in simultaneously gated noise ("*gated noise*"), short tones embedded in gated noise with varying onset asynchronies ("*overshoot*"), and short tones

preceded by gated noise with varying delays ("*forward masking*"). These alternative psychoacoustic paradigms were selected because they are designed to probe specific mechanisms hypothesized to change with SYN: adaptation, temporal resolution and evidence accumulation, and medial olivocochlear-mediated unmasking.

11.1.1 Adaptation

Adaptation refers to the reduction of neuronal responses over time, which is necessary for dynamic coding of complex stimuli. Neuronal adaptation occurs over a wide range of time scales, from rapid (<10 ms) and short-term adaptation (tens to hundreds of ms), to long-term adaptation (seconds to minutes) (Heil & Peterson, 2015; Smith & Zwislocki, 1975). Adaptation also comes in many forms, including firing rate adaptation, stimulus specific adaptation, dynamic range adaptation, and local neural inhibition (Anderson et al., 2009; Heil & Peterson, 2015; Rhode & Greenberg, 1994; Wen et al., 2009).

Ribbon synapses are specialized for efficient vesicle replenishment, allowing for continuous signaling over time with exquisite temporal fidelity (Moser et al., 2006; Nouvian et al., 2006). Loss, damage, or alteration (e.g. enlargement, see Chapter 7) of IHC ribbons with SYN could lead to changes in the readily releasable pool and therefore alter adaptation in the auditory nerve (Moser & Starr, 2016). Neuronal adaptation in single auditory nerve fibers is altered in some stimulus conditions (Shi et al., 2013; Song et al., 2016), but not others (Furman et al., 2013). Changes in synaptic transmission in the periphery will also lead to downstream compensatory changes. One study found impaired neuronal adaptation in the inferior colliculus of mice with SYN (Bakay et al., 2018). Furthermore, patients with auditory neuropathy, a more severe form of SYN, show abnormal loudness adaptation compared to normal hearing controls (Wynne et al., 2013).

Psychoacoustic tasks using gated noise bursts can probe aspects of neuronal adaptation. We assessed threshold patterns for detection of short duration tones embedded in and following gated noise bursts to estimate adaptation and recovery from adaptation in macaques following noise exposure intended to cause SYN.

11.1.2 Temporal resolution and evidence accumulation

Temporally precise neuronal encoding is essential to normal auditory system function and hearing abilities (Bharadwaj et al., 2014). IHC ribbon synapses are the rate-limiting (or, perhaps more accurately, "rate-facilitating") step for temporal coding in the auditory system

(Moser et al., 2006). IHC ribbon dysfunction desynchronizes vesicle release, therefore disrupting the precision and robustness of sound encoding over time (Moser & Starr, 2016). For example, disrupted IHC ribbon function could impair temporal precision of the onset response to a stimulus. One study of synaptopathic guinea pigs showed no change in first spike latency variance of single auditory nerve fibers compared to controls (Furman et al., 2013). In contrast, mice with SYN unexpectedly showed *decreased* variance in first spike latency, suggesting enhanced temporal precision at the level of the auditory nerve in these animals (Suthakar & Liberman, 2021). In addition, loss of IHC ribbons with SYN represents a form of deafferentation that leads to stochastic undersampling of stimuli due to fewer independent encoding channels (Lopez-Poveda & Barrios, 2013). This sparse code causes a loss of redundancy and may lead to poor representation of signals in noise (Lopez-Poveda, 2014; Lopez-Poveda & Barrios, 2013).

It follows that SYN-related IHC ribbon loss or hypertrophy may cause short duration stimuli to be encoded poorly due to a smaller opportunity for temporal integration. Animals with other forms of auditory nerve injury show impaired detection of 50 ms (but not 300 ms) tones in steady-state noise (but not in quiet) (Henry & Abrams, 2021; Resnik & Polley, 2021; Wong et al., 2019). The use of short duration tones in two of the selected detection paradigms, as well as short noise-to-tone delays in the forward masking task, provides one way of evaluating temporal resolution in our macaque model of SYN.

11.1.3 Medial olivocochlear-mediated unmasking

Auditory perception is a product of dynamic feedforward and feedback processing in the brain. Decreased afferent drive secondary to SYN could result in changes to both afferent and efferent neuronal signaling. One such pathway, the medial olivocochlear (MOC) efferent system, contributes to unmasking and protection from acoustic injury by suppressing OHC cochlear amplification (Guinan, 2018; Kawase et al., 1993; Lopez-Poveda, 2018). Importantly, the MOC system receives tonotopic input from LSR fibers (Liberman, 1988), which may be preferentially lost with SYN (Furman et al., 2013; Liberman et al., 2015; Schmiedt et al., 1996; but see Suthakar & Liberman, 2021). If MOC inputs are diminished due to synaptopathic loss of LSR fibers, the MOC pathway may also degrade (Boero et al., 2018; Boero et al., 2020; Maison et al., 2013; Qian et al., 2021), further accentuating hearing in noise difficulties. MOC projections and function also decline with age independent of outer hair cell loss and elevated hearing thresholds (Abdala et al., 2014; Fu et al., 2010; Jacobson et al., 2003; Kim et al., 2002; Liberman &

Liberman, 2019; Radtke-Schuller et al., 2015; Zhu et al., 2007), suggesting that MOC degradation may accompany age-related SYN. These converging anatomical and physiological consequences of SYN to the MOC pathway could result in difficulties hearing in noise.

In Chapter 8, we report the effects of SYN on the MOC reflex, as measured by contralateral suppression of otoacoustic emissions. Following noise exposure, macaques showed transient changes in OAE suppression that recovered within 2 months post-exposure. In the psychophysical domain, detection of short duration signals in gated noise with varying onset asynchrony (i.e. overshoot) may also probe MOC activation (Jennings et al., 2011; Jennings et al., 2009; Walsh et al., 2010) (but see Fletcher et al., 2015).

11.2 MATERIALS AND METHODS

11.2.1 Subjects

Rhesus macaques (*Macaca mulatta*, n = 8, 4 female) performed a reaction time Go/No-Go lever release task to detect pure-tone signals in gated noise under diotic, open field testing conditions. In addition to the cohort of subjects that underwent noise exposure intended to cause SYN, data from two subjects with sensorineural hearing loss – one with noise-induced permanent threshold shifts (Burton et al., 2020; Hauser et al., 2018; Mackey et al., 2021), one with likely congenital high frequency hearing loss – were included for comparison.

11.2.2 Psychophysical tone detection tasks

11.2.2.1 Gated Noise

Detection of 200 ms tones (1, 2, 2.8, 4, 5.6, 8, and 16kHz; 200 ms, 10 ms rise/fall) was measured in the presence of a simultaneously gated 200 ms broadband noise (20 or 30 dB spectrum level, 10 ms rise/fall; see Figure 11.1A). Gated noise thresholds were obtained at all frequencies before exposure and at 5-6 months post-exposure (see blue box in Figure 11.2).

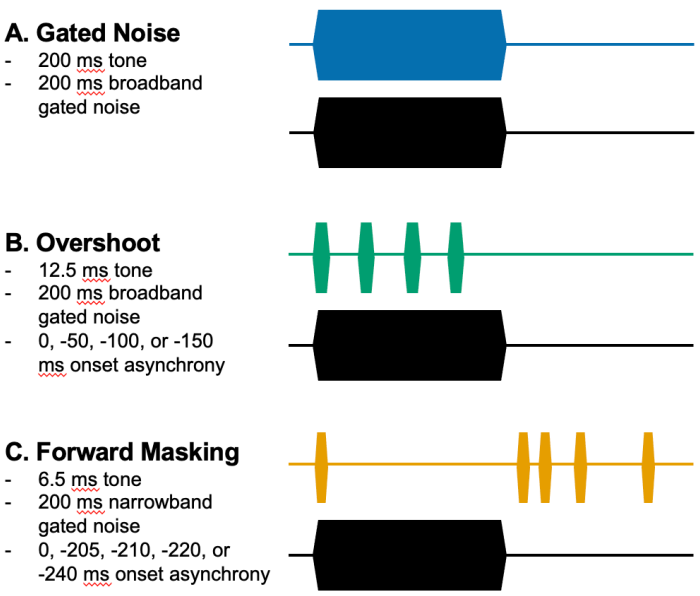

Figure 11.1 Stimulus paradigms for the gated noise (A), overshoot (B), and forward masking (C) tasks. Tones in color, gated noise in black. Schematic is a roughly accurate portrayal of relative durations and delay times.

11.2.2.2 Overshoot

Detection of short duration pure tones (0.5-32kHz; 12.5 ms, 5 ms rise/fall) was measured in the presence of a 200 ms gated broadband noise (30 dB spectrum level, 5 ms rise/fall). Stimulus parameters were chosen based on human overshoot studies (Strickland, 2001) one study of overshoot in macaques (Rocchi et al., 2017), and pilot data from two control macaques (data not shown). Tone thresholds were obtained for different signal-to-masker onset asynchronies (0, -50, -100, -150 ms; see Figure 11.1B) in order to estimate overshoot (threshold difference between 0 and non-zero onset asynchrony conditions). Overshoot was assessed at all test frequencies before noise exposure and at 5-6 months post-exposure (n = 4, females). Frequencies of interest were also probed for the female monkeys at 2, 4, 8, and 10 months post-exposure and for the male monkeys at 10 months post-exposure (see green boxes in Figure 11.2).

11.2.2.3 Forward Masking

Detection of short duration pure tones (f_0 = 1, 4, and 5.6kHz; 6.5 ms, 2.5 ms rise/fall) was measured in the presence of a 200 ms (2.5 ms rise/fall) gated narrowband noise (20, 30, and 40 dB spectrum level; bandwidth = 0.8*f_0). Stimulus parameters were modeled after forward masking studies in humans (Jesteadt et al., 1982; Kidd & Feth, 1982; Turner et al., 1994). Noise bandwidth was selected to maximize the amount of forward masking based on one study of forward masking in macaques (Rocchi et al., 2017) and pilot data from one control macaque (data not shown). Tone thresholds were obtained for different signal-to-masker onset asynchronies (0, -205, -210, -220, -240 ms; see Figure 11.1C). Forward masking functions (after Jesteadt et al., 1982) were illustrated with forward masking thresholds plotted as a function

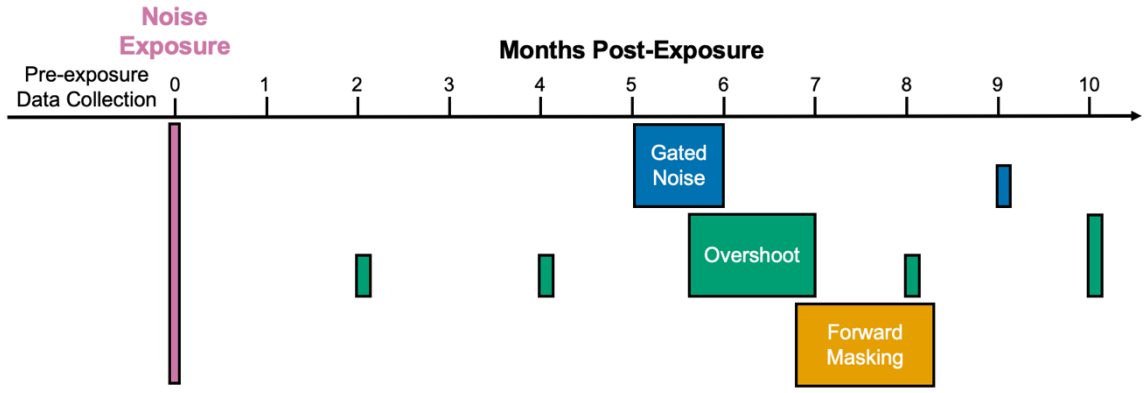

Figure 11.2 Timeline for behavioral data collection. Gated noise was measured at 5-6 months post-exposure. Overshoot was measured at 5-6 months post-exposure and 10 months post-exposure; frequencies of interest were also probed at 2, 4, and 8 months post-exposure. Forward masking was measured at 6-8 months post-exposure.

masker level or noise-to-tone delay. Forward masking was assessed before and 6-8 months post-exposure (see yellow box in Figure 11.2).

11.3 RESULTS

11.3.1 Detection of long tones in simultaneously gated noise is not impaired following noise exposure

Tone detection was measured in simultaneously gated broadband noise as a training condition for the overshoot and forward masking tasks. Exemplar pre- and post-exposure psychometric functions are shown in Figure 11.3A (Monkey A, 4 kHz), and mean gated noise thresholds are plotted as a function of frequency in Figure 11.3B for 20 and 30 dB spectrum level noise. Although there were significant main effects of frequency ($t(df) = -5.84(186)$, $p < 0.001$) and noise level ($t(df) = 9.79(186)$, $p < 0.001$), gated noise thresholds did not change following noise exposure ($t(df) = -0.40(186)$, $p = 0.691$). Thresholds in continuous noise are plotted for comparison (light gray dashed lines). Gated noise thresholds were similar or slightly higher than continuous noise thresholds, especially for higher frequency tones, consistent with previous reports in macaques and humans (Bacon & Viemeister, 1985; Campbell, 1969; Green, 1964; Rocchi et al., 2017; Wier et al., 1977). The stability of gated noise thresholds following exposure is similar to the stability of tone thresholds in continuous noise (see Chapter 10, Figure 10.6).

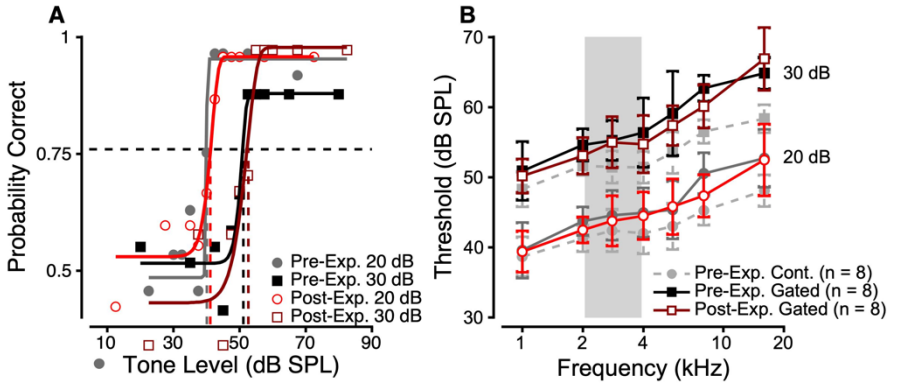

Figure 11.3 A. Psychometric functions for tone detection in 20 (circles) and 30 dB spectrum level (squares) gated noise. Data from Monkey A (4 kHz tone) before (black/gray) and after (red) noise exposure. Symbols indicate raw data, lines illustrate Weibull cdf fits of the data. Horizontal dashed line indicates *pc* = 0.76, and the vertical dashed lines illustrate the threshold values for each condition. B. Mean tone detection thresholds in 20 (circles) and 30 dB spectrum level (squares) gated noise before (black/dark gray) and after (red) noise exposure. For comparison, light gray dashed lines illustrate mean tone detection thresholds in continuous noise of the same level. Error bars indicate ± 1 standard deviation from the mean. Gray box illustrates the noise exposure band.

11.3.2 Psychophysical overshoot is impaired at late post-exposure times

Short duration tone detection was measured in a broadband gated noise with varying noise-to-tone onset asynchrony to assess psychophysical overshoot. Exemplar pre- and post-exposure psychometric functions are shown in Figure 11.4A for the 0 ms (squares) and -100 ms

(circles) onset asynchrony conditions (data from Monkey O, 8 kHz). Before noise exposure, functions from the 0 and -100 ms conditions (black and gray) were clearly separated, whereas the functions overlapped post-exposure (dark red and red). Thresholds from Figure 11.4A (and additional conditions) are plotted as a function of onset asynchrony in Figure 11.4B. Overshoot (threshold$_{0ms}$ – threshold$_{-100ms}$) was reduced and close to 0 dB at 8 kHz 6 months post-exposure.

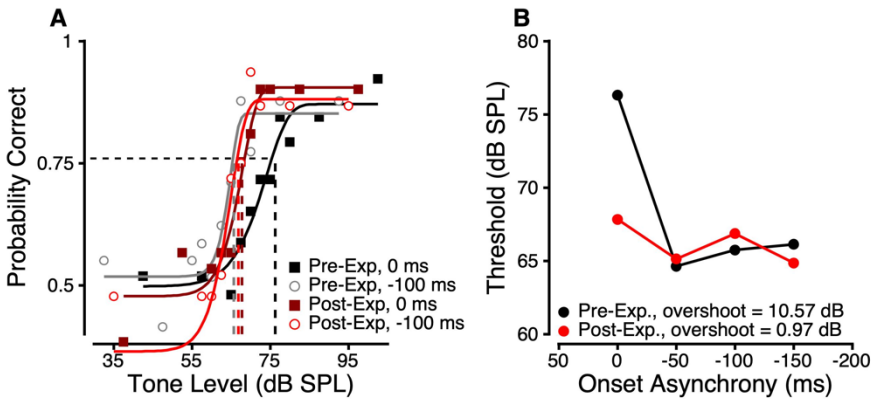

Figure 11.4 A. Psychometric functions (same as Figure 11.3A) for the 0 (squares) and -100 ms (circles) onset asynchrony overshoot conditions. Data from Monkey O (8 kHz tone) before (black/gray) and after (red) noise exposure. B. Tone detection thresholds as a function of onset asynchrony for Monkey O (8 kHz) before (black) and 6 months after (red) noise exposure. Overshoot was significantly reduced post-exposure (0.97 dB; compared to 10.57 dB pre-exposure).

Mean overshoot functions (threshold as a function of onset asynchrony; $n = 4$) are shown in Figure 11.5 for different tone frequencies before and 6 months after noise exposure. Thresholds for noise-to-tone asynchronies of -50, -100, and -150 ms were essentially unchanged after exposure. However, thresholds for the synchronous (0 ms asynchrony) condition were lower at 4, 5.6, and 8 kHz. This change indicates reduced overshoot at these frequencies following noise exposure.

Since the frequency dependence of overshoot has not been evaluated in macaques, we characterized overshoot as a function of tone frequency in a normal hearing cohort (Figure 11.6). Overshoot was greatest for mid- to high-frequency tones. Mean (standard deviation) overshoot values were 6.8 (1.6), 8.9 (4.1), and 9.0 (3.0) dB at 4, 5.6, and 8 kHz, respectively. Macaque overshoot values are comparable to previous reports in humans using similar tone and masker stimuli (Figure 11.6, open symbols; Jennings et al., 2016; McFadden et al., 2010; Strickland, 2001). Though females tended to have greater overshoot than males as reported in humans (Wright, 1994), there was no significant effect of sex on overshoot ($t(df) = 0.45(50)$, $p = 0.652$).

Overshoot was measured bi-monthly after noise exposure in a cohort of 4 female macaques and at 10 months post-exposure in 4 male macaques (Figure 11.7). Linear mixed effects models showed a significant effect of post-exposure time on overshoot from 2-8 kHz

($t(df) = -4.50(122)$, $p < 0.001$). Overshoot was essentially unchanged at 2-4 months post-exposure (Figure 11.7A). Reductions in overshoot emerged at 6, 8, and 10 months post-exposure (Figure 11.7B-C). Of note,

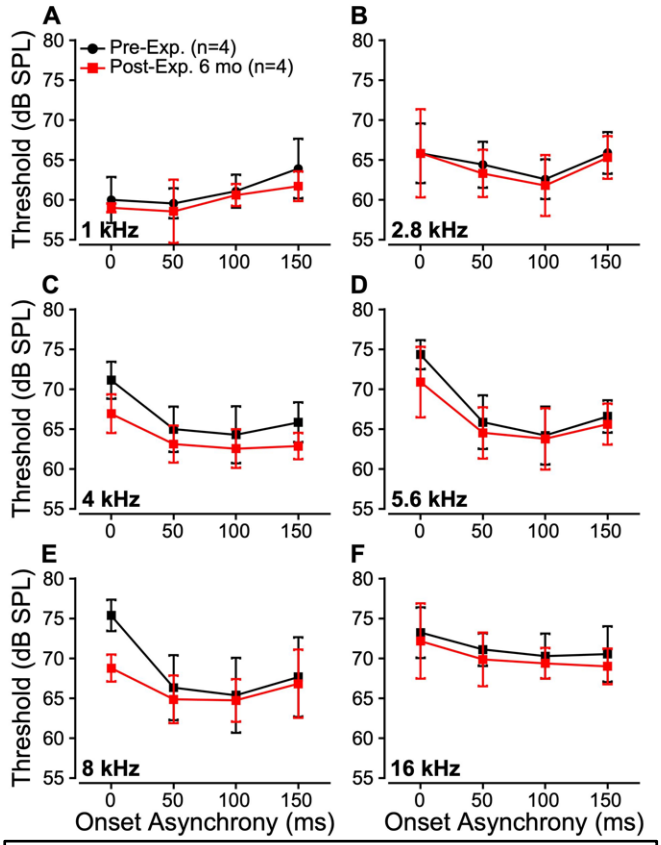

Figure 11.5 Mean overshoot functions ($n = 4$) showing threshold as a function of noise-to-tone onset asynchrony at different tone frequencies (A-F) before (black) and 6 months after (red) noise exposure. Error bars indicate ±1 standard deviation from the mean.

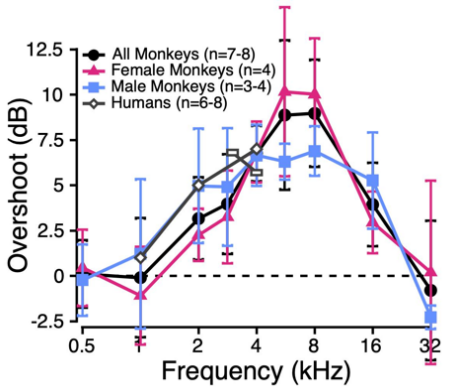

Figure 11.6 Overshoot as a function of tone frequency for normal hearing macaques (all: black; females: pink; males: blue). Error bars indicate ±1 standard deviation from the mean. Human data are plotted for comparison (diamonds: Strickland 2001, Jennings et al. 2016; rectangles: McFadden et al. 2010).

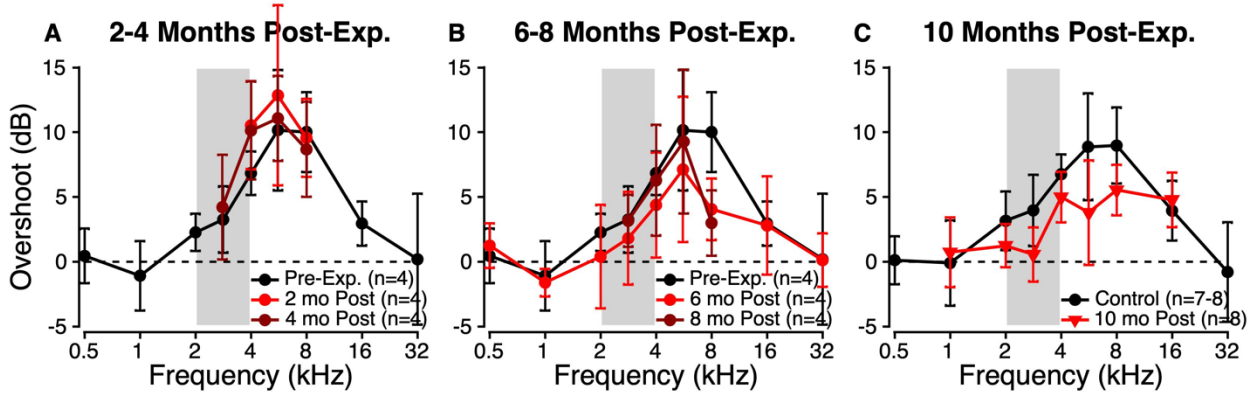

Figure 11.7 Overshoot as a function of frequency at various post-exposure timepoints. A. Overshoot in four female subjects (black) before exposure (black) and at 2 and 4 months post-exposure (red, dark red). B. Same as A, except at 6 and 8 months post-exposure (red, dark red). C. Overshoot in male and female subjects before exposure (black) and 10 months post-exposure (red).

this change in overshoot was driven by changes in the synchronous condition thresholds, as shown in Figure 11.5.

11.3.3 Forward masking is not impaired following noise exposure

Forward masking was assessed by measuring detection of short duration tones preceded by a narrowband gated noise. Exemplar psychometric functions are shown in Figure 11.8A (Monkey L, 5.6 kHz, 40 dB spectrum level noise) for the simultaneous (0 ms onset asynchrony), 5 ms delay (-205 ms onset asynchrony), and 20 ms delay (-220 ms onset asynchrony) conditions. Thresholds decreased as the delay between the noise and tone increased, as shown by the leftward shift of the psychometric functions. Thresholds were essentially the same before and after noise exposure. Thresholds for 5.6 kHz tones in 20, 30, and 40 dB spectrum level gated noise are plotted as a function of noise-to-tone delay (Figure 11.8B) to derive forward masking functions after Figure 1 in Jesteadt et al. (1982).

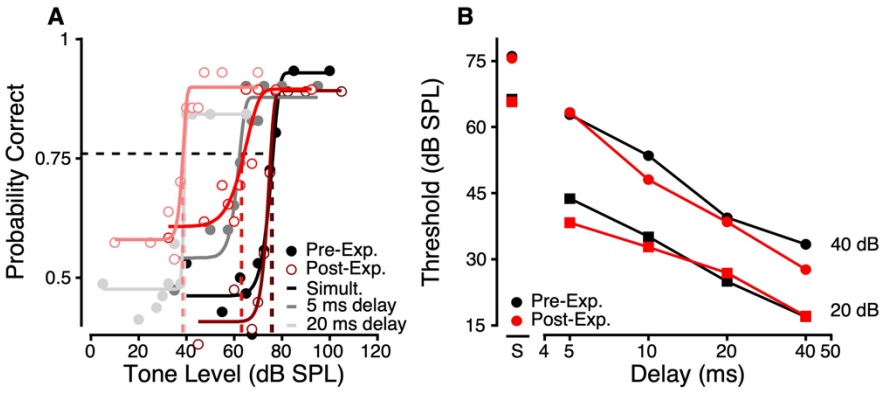

Figure 11.8 A. Psychometric functions (same as Figure 11.3A) for the simultaneous, 5 ms delay, and 20 ms delay forward masking conditions. Data from Monkey L (5.6 kHz tone, 40 dB spectrum level gated noise) before (black/gray) and after (red) noise exposure. Symbols indicate raw data, lines illustrate Weibull fits of the data. Horizontal dashed line indicates *pc* = 0.76, and the vertical dashed lines illustrate the threshold values for each condition. B. Tone detection thresholds as a function of noise-to-tone asynchrony for Monkey L (5.6 kHz) in 20 (squares) and 40 (circles) dB spectrum level gated noise before (black) and 8 months after (red) noise exposure.

Across subjects, the pre- and post-exposure forward masking functions were highly variable, possibly due to the difficulty of the task. To facilitate comparisons across subjects, thresholds for forward masking conditions were normalized to the simultaneous gated condition (normalized threshold = $\text{threshold}_{\text{simultaneous}} - \text{threshold}_{\text{delay}}$). Normalized thresholds are plotted as a function of noise-to-tone delay in Figure 11.9 for each subject and noise level at 1, 4, and 5.6 kHz (A, B, and C, respectively) before and after noise exposure. Although normalized forward masking thresholds differed significantly across tone frequencies ($t(df) = -5.58(256)$, $p < 0.001$) and delay conditions ($t(df) = -8.97(256)$, $p < 0.001$), there was no significant effect of noise exposure ($t(df) = 0.86(256)$, $p = 0.392$).

To further investigate the possibility of a change in forward masking following noise exposure, change in threshold (post-exposure – pre-exposure) was calculated for each condition and subject. Figure 11.10 illustrates this delta threshold metric as a function of noise level (A) and noise-to-tone delay (B). Although there were significant threshold differences that exceeded the test-retest variability observed for other tone detection tasks in the same subjects (see Chapter 10, Figure 10.4), these differences were not consistent across subjects, frequencies, noise levels, or delay conditions. In summary, there were no consistent changes in forward masking following noise exposure intended to cause SYN.

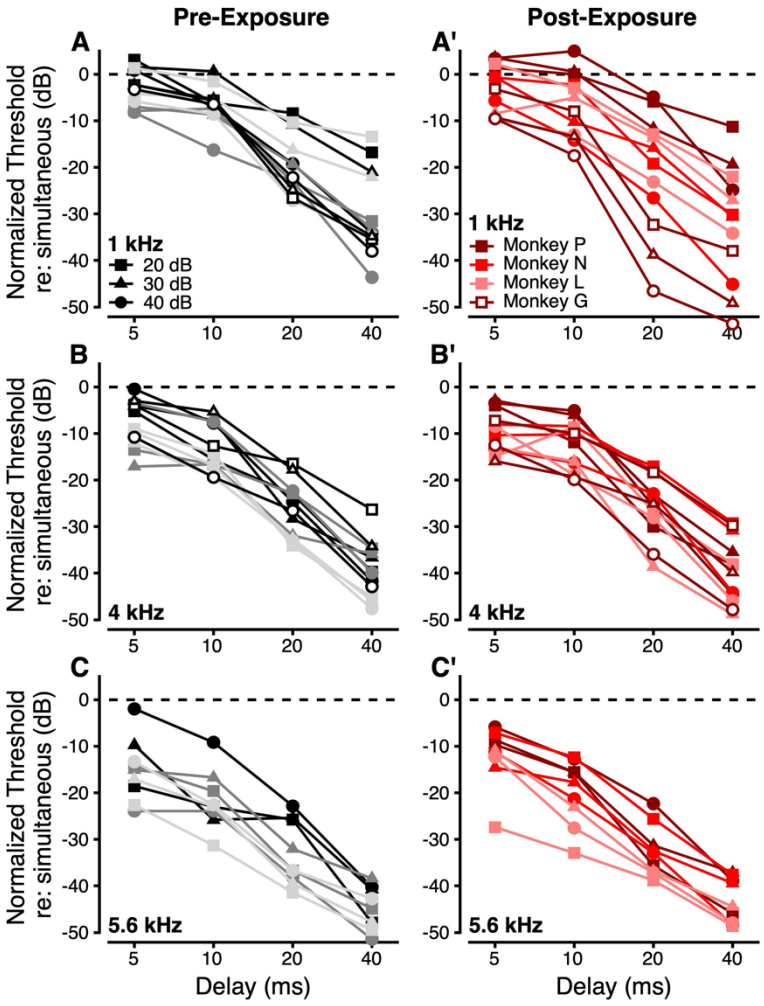

Figure 11.9 Forward masking functions with normalized thresholds ($threshold_{delay}$ – $threshold_{simultaneous}$) as a function of noise-to-tone delay. Data are shown for 1 (A, A'), 4 (B, B'), and 5.6 kHz (C, C') tones in 20 (squares), 30 (triangles), and 40 (circles) dB spectrum level noise before (A, B, C) and after (A', B', C') noise exposure.

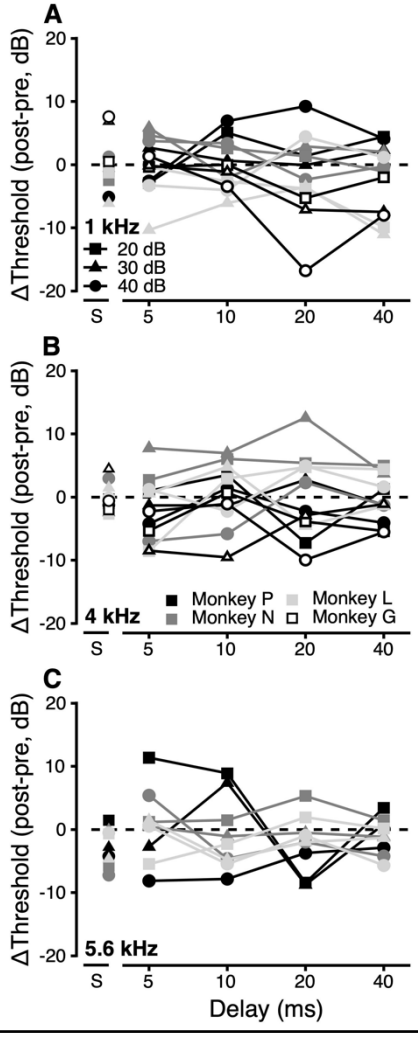

Figure 11.10 Change in forward masking thresholds (post-exposure – pre-exposure) as a function of noise-to-tone delay. Data are shown for 1 (A), 4 (B), and 5.6 kHz (C) tones in 20 (squares), 30 (triangles), and 40 (circles) dB spectrum level noise. S indicates simultaneous condition. Dashed lines indicate no threshold

Of note, thresholds for the simultaneous (0 ms onset asynchrony) condition also lacked consistent changes following exposure, unlike those observed in the overshoot task (see Figure 11.5). Additional data using different combinations of tone duration and gated noise bandwidth suggested that this was due to the use of a narrowband masker in the forward masking paradigm (data not shown). This finding is consistent with previous reports that overshoot is smaller when measured with narrowband noise than broadband noise (Wicher & Moore, 2014; Wright, 1997).

11.3.4 Overshoot and forward masking in macaques with permanent threshold shifts and outer hair cell loss

Overshoot and forward masking are known to be affected by SNHL (e.g. Bacon & Takahashi, 1992; Glasberg et al., 1987). Data from two macaques with permanent threshold shifts are included here for comparison; audiograms are shown in Figure 11.11. Monkey Fr had likely congenital high frequency hearing loss. Monkey Li underwent a 141 dB SPL noise exposure to a narrowband noise centered at 2 kHz, which resulted in permanent threshold shifts through two years post-exposure (Burton et al., 2020; Hauser et al., 2018; Mackey et al., 2021). Cochlear histological investigations revealed significant outer and some inner hair cell loss in both subjects; data from Monkey Li are shown in Burton et al. (2020). Both monkeys had absent overshoot across frequencies (Figure 11.12). Monkey Fr showed greater susceptibility to forward masking compared to controls (Figure 11.13). Although noise levels were not adjusted to equate sensation level, the maskers were intense enough to generate threshold shifts at the frequencies tested.

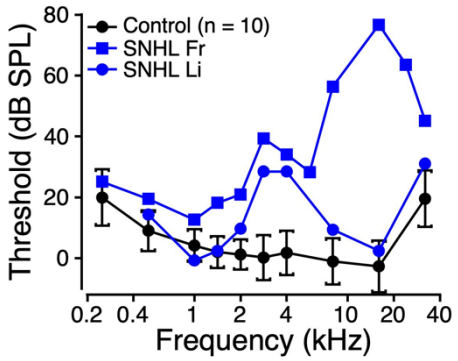

Figure 11.11 Audiograms from Monkey Fr (blue squares) and Monkey Li (blue circles). Subjects showed permanent threshold shifts compared to controls shown in black (n = 10).

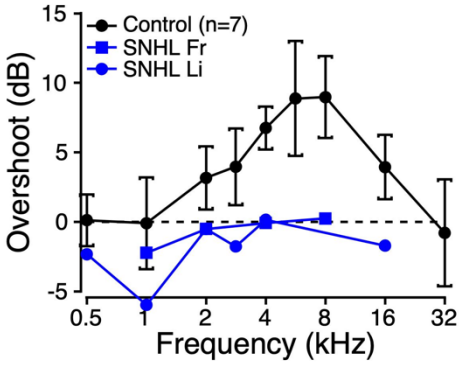

Figure 11.12 Same as Figure 11.6, but showing data from Monkeys Fr and Li (blue), who had permanent hearing loss. Mean data (± 1 standard deviation) from controls shown in black (n = 4).

11.4 DISCUSSION

Following noise exposure intended to cause SYN, macaques show normal tone detection performance in simultaneously gated noise and in a forward masking paradigm, but progressive changes in the detection of short tones in gated noise (overshoot). These behavioral data provide the first direct evidence for hearing-in-noise deficits associated with SYN pathology.

Auditory perception is the product of countless intrinsic neuronal response properties among diverse neuron populations in multiple brain areas, which interact dynamically over time and depend on stimulus characteristics and attentional state. Even a small change at one level of the auditory pathway has the potential to generate massive changes at the level of perception. Although the tasks chosen for this study were designed to probe neuronal adaptation, temporal resolution, and MOC function, other mechanisms such as excitation, facilitation, inhibition, and suppression undoubtedly contribute to the perceptual patterns observed and their changes following SYN. In the following discussion, we propose mechanistic explanations for each of our primary findings.

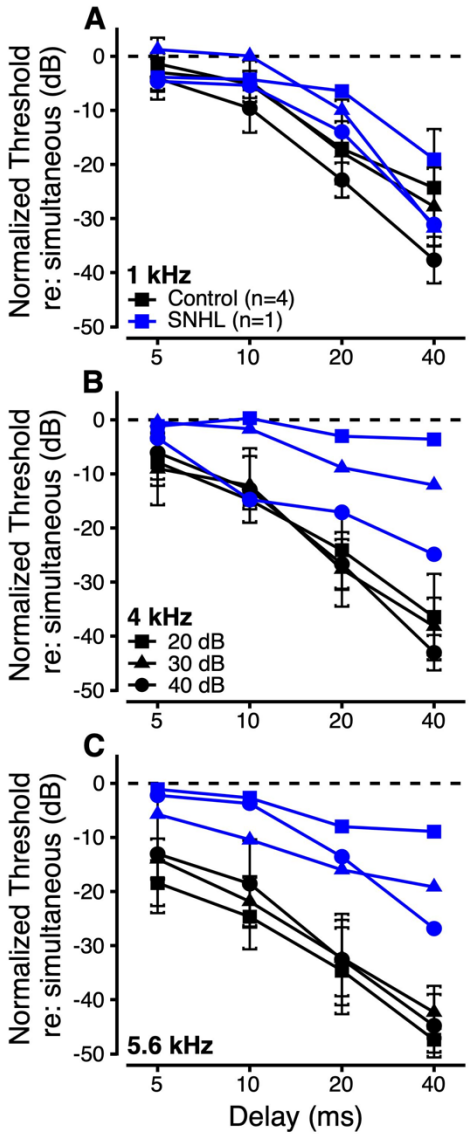

Figure 11.13 Same as Figure 11.9, but showing data from Monkey Fr (blue), who had permanent hearing loss. Mean data (± 1 standard deviation) from controls shown in black (n = 4).

11.4.1 Gated noise

Like our results for tone detection in steady-state noise (Chapter 10, Figure 10.6), we saw no effect of noise exposure on tone detection in simultaneously gated noise. These findings suggest that simultaneous masking of longer tones may be insensitive to SYN pathologies, consistent with findings in animals with chemically-induced deafferentation (Henry & Abrams, 2021; Resnik & Polley, 2021). Compared to short stimuli, encoding of longer tones is less

dependent on temporal precision and allows for evidence accumulation over time. Alternatively, our macaques may not have enough synapse loss to impair tone detection in gated noise.

11.4.2 Overshoot

Overshoot refers to the improvement in tone detection threshold when the tone occurs in the middle of a noise burst versus when it occurs at the noise onset (Elliott, 1965, 1969; Zwicker, 1965). Threshold improvement plateaus after 100 ms noise-to-tone onset asynchronies (Figure 11.5C-F; McFadden et al., 2010). The overshoot effect is greatest for mid- to high-frequency signals and moderate level broadband noise (Bacon, 1990; Strickland, 2001; Yasin et al., 2014). These characteristics suggest a possible role of the MOC system, which has a latency of 100 ms in humans and similar stimulus preferences (Backus & Guinan, 2006; Guinan, 2006). Overshoot function shapes are also reminiscent of short-term adaptation patterns in neuronal peristimulus time histograms, with peak firing rates at stimulus onset that adapt down to a firing rate plateau (Galambos & Davis, 1943; Kiang, 1965; Ruggero, 1992; Smith, 1979; Smith & Zwislocki, 1975). Adaptation of suppression through lateral inhibition in central auditory nuclei has also been proposed to underlie some aspects of overshoot (Fletcher et al., 2015). Together, forms of adaptation and MOC-mediated gain reduction are likely contributors to psychophysical overshoot (Jennings et al., 2011; Jennings et al., 2009; Keefe et al., 2009; Salloom & Strickland, 2021; Walsh et al., 2010).

We observed reduced overshoot in our noise exposed macaque at frequencies near the exposure band. We hypothesized that SYN-related impairment of adaptation or MOC function would result in elevated thresholds for the asynchronous conditions. Contrary to this prediction, changes in overshoot were driven by *reduced* thresholds in the *synchronous* condition, when the tone and noise onset were simultaneous. Although this resulted in a “deficit”, or a “loss of overshoot”, the threshold improvement is suggestive of a gain-of-function. Of note, detection thresholds in the asynchronous conditions were comparable to thresholds for the same duration tones in steady-state noise (data not shown), and temporal integration functions for short tones in steady-state noise did not change after noise exposure. Gated noise conditions must contain a unique characteristic that taps into SYN-related dysfunction.

Similar changes in overshoot (i.e. lower thresholds in the synchronous condition) have been observed in individuals with SNHL (Figure 11.12; Bacon & Takahashi, 1992; Jennings et al., 2016; Strickland & Krishnan, 2005) (but see Carlyon & Sloan, 1987), as well as during

temporary threshold shifts (Champlin & McFadden, 1989) and aspirin administration (McFadden & Champlin, 1990). Most studies have explained this phenomenon as a loss of cochlear amplification due to OHC dysfunction, damage, or loss, meaning there is less cochlear gain available to be reduced (Jennings et al., 2016). However, since we see this same psychophysical effect in our subjects with no to minimal OHC damage and no change in otoacoustic emission amplitudes, this theory fails to explain our findings. Interestingly, a few studies have reported minimal overshoot in some individuals with normal hearing sensitivity (Bacon & Takahashi, 1992), suggesting impairments independent of hearing loss. But two other studies found no change in overshoot among older adults with normal hearing sensitivity, who may be at risk for age-related SYN (Jennings et al., 2016; Wong & Cheesman, 2000).

Thus, we consider alternative explanations for improved short tone detection in simultaneous gated noise. First, the pattern of results seems inconsistent with MOC impairment, which should result in elevated thresholds in the asynchronous overshoot conditions. Physiological assessment revealed only temporary reductions of MOC function in our synaptopathic macaques (Chapter 8, Figure 8.8), which does not parallel the trajectory of changes in overshoot. However, altered adaptation of MOC activation could impact trial-to-trial encoding of the gated noise. Adaptation to rapidly changing noise backgrounds is impaired at the level of the inferior colliculus in putatively synaptopathic mice (Bakay et al., 2018). It is possible that central changes in adaptation are inherited by the MOC, which receives direct inputs from the inferior colliculus and auditory cortex (Terreros & Delano, 2015), and result in slower recovery from MOC-mediated gain reduction.

Second, auditory nerve recordings in mice with SYN show enhanced onset coding to tones in quiet and in noise (Suthakar & Liberman, 2021), which is also corroborated by our data showing increased ABR amplitudes to short duration clicks in noise (Chapter 9, Figures 9.4 and 9.5). Elevated firing rates to short duration stimuli may improve the detectability of tones in our overshoot task. However, changes to onset coding would also increase firing rates to the gated noise, so there may not be a net improvement in signal-to-noise ratio.

Finally, among the most likely explanations is that across-channel encoding is impaired. Overshoot magnitude is much smaller or absent when using narrowband noise maskers (McFadden, 1989; Wicher & Moore, 2014; Wright, 1997), implicating a role for off-frequency suppression or inhibition mechanisms in generating the threshold patterns. These mechanisms

are prevalent throughout the auditory system, occurring as early as the cochlea and auditory nerve (i.e. two tone suppression; Abbas, 1978; Delgutte, 1990) and throughout different neuron types in central auditory areas (Ramachandran et al., 1999; Rhode & Greenberg, 1994). In higher levels of the auditory pathway, integration across neurons also occurs in greater abundance, leading to transformations in neuronal response properties from peripheral to central nuclei (Joris et al., 2004). If SYN impairs off-frequency suppression or disrupts across-channel synchrony to the broadband masker, while sparing (or even enhancing) within-channel onset synchrony to the signal, the net result would be an improved signal-to-noise ratio and lower detection thresholds. This explanation is favorable, because it is parsimonious with the null findings of our forward masking experiment (see next section), which used a narrowband masker that may not elicit much across-channel processing. Other experiments that probe across-channel processing, such as comodulation masking release (Hall et al., 1984; Verhey et al., 2003), may also be sensitive to SYN (Singh et al., 2022; but see Tolnai et al., 2022).

Across-channel coding deficits are also a favorable explanation given their dependence on central processing. It is likely that the progressive manifestation of perceptual deficits following acute noise-induced SYN is due to dynamic changes in central auditory function. Central gain, or hyperactivity due to loss of inhibition, occurs in all major central auditory structures following peripheral injury (e.g. Chambers et al., 2016; Mulders et al., 2011; Schrode et al., 2018; Vogler et al., 2011). Hyperactivity emerges soon after peripheral injury (Heeringa & van Dijk, 2016) and this altered excitatory/inhibitory balance appears to be a permanent compensatory consequence (Mulders & Robertson, 2011; Salvi et al., 2000). Loss of inhibitory drive in central auditory structures may underlie disrupted across-channel cues in SYN. Beyond the confines of reductionistic psychophysical tasks, across-channel cues also contribute to hearing-in-noise abilities through auditory grouping or scene segregation (Viswanathan et al., 2022). Deficits in auditory scene analysis secondary to impaired across-channel coding could also help explain the spatial hearing deficits seen in our synaptopathic macaques (Mackey et al., in prep).

This across-channel hypothesis could imply a role of the MOC pathway in SYN deficits after all. The MOC pathway may contribute to a fluctuation-profile coding mechanism (Carney, 2018) important for signal detection in noise. According to this theory, the MOC could combine afferent inputs from the LSR population about overall sound levels with descending input from

the inferior colliculus about low-frequency fluctuations, creating a mechanistic feedback loop that could underlie signal detection in noise. Disruption of LSR inputs combined with changes in sound-evoked inferior colliculus and auditory cortex activity following noise-induced SYN (Asokan et al., 2018; Shaheen & Liberman, 2018) could contribute to impaired MOC control of fluctuation-profile coding. This model would also be consistent with a more dynamic (as opposed to reflexive) view of the MOC in controlling cochlear gain (de Boer et al., 2012).

11.4.3 Forward masking

Forward masking refers to the influence of a preceding masker on the detectability of a signal occurring later in time. As with all perceptual tasks, psychophysical forward masking patterns encompass a variety of neuronal mechanisms, including adaptation and temporal resolution. At the level of the auditory nerve, forward masking functions using different masker durations, levels, and spectral content reveal neuronal recovery from short-term adaptation (Harris & Dallos, 1979; Smith, 1977). However, discrepancies in neuronal and perceptual data (Turner et al., 1994) suggest that perceptual forward masking may be more accurately described by models of temporal integration (Oxenham, 2001), consistent with a view of this task as a form of gap detection (Glasberg et al., 1987). Varying masker bandwidth also affords estimation of suppression in forward masking paradigms (Dubno & Ahlstrom, 2001). Others find implications for MOC function in patterns of perceptual forward masking with varying masker duration and level (Wojtczak & Oxenham, 2010). Finally, contributions from central auditory structures may also be necessary to fully explain forward masking functions (Gai, 2016; Nelson et al., 2009)

Predictions of how forward masking functions could change following SYN are mixed, and the finding of a null result further complicates interpretations. On one hand, loss of ribbons opposing LSR fibers, which have slow recovery from adaptation compared to high spontaneous rate neurons (Relkin & Doucet, 1991; Shore, 1995), may not impact perceptual forward masking at all or could even lead to faster recovery from forward masking. On the other hand, damaged ribbons could have smaller readily releasable pools, impaired timing of vesicle release, and slower recovery from vesicle depletion, leading to slower recovery from forward masking. It is also possible that both of these mechanisms are occurring simultaneously, or are compensated at various levels of the auditory system, ultimately resulting in the absence of an effect on forward masking.

Previous studies of SYN or SYN-related pathologies have shown mixed effects on physiological and perceptual forward masking. Using a paired click paradigm, Wang and colleagues found prolonged recovery from forward masking in single auditory nerve fibers of synaptopathic guinea pigs (Song et al., 2016) and in compound action potentials of mice (Shi et al., 2013), although these effects recovered with post-exposure survival time, as did IHC ribbon counts. Human listeners with normal hearing show variable susceptibility to physiological and perceptual forward masking, which may index the extent of SYN effects (Mehraei et al., 2017). However, McFadden et al. (1997) found no change in evoked potential forward masking functions measured in the inferior colliculus of older chinchillas with normal hearing compared to young controls. Similar measurements conducted in chinchillas with carboplatin-induced IHC loss indicate only subtle changes in forward masking functions (McFadden et al., 1998), suggesting that central auditory system compensation may be able to overcome peripheral impairments expected to affect forward masking. Paired click ABR data from our macaque model of SYN could help to clarify these discrepant findings. In particular, it will be interesting to examine paired click responses from each ABR wave component to understand the evolution of SYN-related changes to forward masking along the auditory pathway.

In order to identify mechanisms of perceptual forward masking, it is informative to compare data from different inner ear pathologies. As shown here for one macaque (Figure 11.13), human subjects with SNHL show prolonged recovery from forward masking compared to normal hearing subjects (Glasberg et al., 1987; Kidd et al., 1984; Nelson & Freyman, 1987). In these cases, forward masking deficits may be caused by loss of compression and impaired temporal resolution secondary to OHC loss in SNHL (Glasberg et al., 1987; Heinz et al., 2002). It would follow that forward masking should not be affected in cases of isolated SYN.

Although forward masking is greatest when using narrowband noise (Turner et al., 1994), it may be useful to measure forward masking – and overshoot – using spectrally-notched gated noise in future investigations. Notched noise minimizes on-frequency suppression and adaptation while eliminating off-frequency listening (Moore & Glasberg, 1981). This approach would also help disentangle contributions from adaptation and temporal integration (Oxenham, 2001).

CHAPTER 12

General Discussion

12.1 MANIFESTATIONS OF NOISE-INDUCED TEMPORARY THRESHOLD SHIFTS IN MACAQUE MONKEYS

We previously established the first nonhuman primate model of SYN (Valero et al., 2017). Following temporary threshold shifts, macaques exhibited minimal hair cell loss, up to 30% inner hair cell ribbon loss, and ribbon enlargement. Physiological characterization with auditory brainstem responses (ABRs) and otoacoustic emissions (OAEs) revealed no permanent threshold shifts at 2 months post-exposure. Using a different noise exposure stimulus (2-4kHz, as opposed to a 50-Hz band centered at 2kHz), we observed a similar pattern of SYN histopathology in the present study. In subjects that had extended experimental timelines, inner hair cell ribbon loss seemed to recover, though enlarged ribbons remained.

Here, we strengthened our understanding of SYN manifestations in macaques with a thorough survey of putative anatomical, physiological, and perceptual biomarkers. Though suprathreshold ABR Wave I amplitudes to clicks in quiet were not reduced as in most models of SYN (e.g. Kujawa & Liberman, 2009), we did find an increase in ABR amplitudes to clicks in ipsilateral broadband noise. Medial olivocochlear reflexes (MOCRs), as measured by contralateral suppression of OAEs, were temporarily reduced following noise exposure, but recovered within a few months, consistent with the normal MOC innervation of OHCs seen at 10 months post-exposure. Middle ear muscle reflexes (MEMRs) were weak in noise-exposed macaques, suggesting sustained dysfunction of the driving low spontaneous rate fiber inputs. Behavioral hearing sensitivity showed temporary threshold shifts that recovered within 3 weeks and remained stable for the duration of the study, consistent with normal OHC counts and OAEs. Measures of hearing in steady-state noise designed to probe growth of masking and frequency selectivity showed no change following noise exposure. However, detection of short tones in gated noise improved over the extended post-exposure period.

A unique aspect of our study was the long post-exposure survival duration. Our anatomical characterization and much of the physiological characterization took place around 2 months and 10 months post-exposure, representing our early and late study time points. These

time points are much later than the time courses of most rodent studies, which often assess physiological function around 1-2 weeks (early) and occasionally at 1-2 months (late) post-exposure (Bharadwaj et al., 2021; Kujawa & Liberman, 2009; Lin et al., 2011; Shi et al., 2013). The differences in experimental timelines may account for discrepancies between our ABR results and those commonly reported in the literature. In the future, we would be interested to conduct physiological and anatomical assessments at shorter post-exposure time points to look for further evidence of recovery or regeneration. Behavioral data collection was continuous throughout the duration of the study, allowing us to look at changes in hearing abilities over time. Although most of the tasks discussed here did not change following noise exposure (audiogram, threshold shift rate, auditory filters, forward masking), we did observe delayed emergence of deficits for psychophysical overshoot. Had our behavioral studies ended at 2 months post-exposure, we may have missed this finding altogether.

To summarize, transient deafferentation caused by noise-induced temporary threshold shifts may contribute to permanent and progressive changes to afferent neural encoding (increased masked ABR amplitudes, reduced MEMRs) and some aspects of hearing-in-noise (overshoot). Heightened onset responses secondary to persistent ribbon enlargement may be one parsimonious explanation for the larger masked click ABR amplitudes and improvements in overshoot thresholds. Alterations to neural encoding appear to develop and progress over time, as the changes in overshoot are delayed relative to the time course of temporary threshold shifts and ribbon loss.

12.2 COCHLEAR SYNAPTOPATHY: REDEFINING AN INNER EAR PATHOLOGY

Given the growing evidence that IHC ribbons can regenerate (Chapter 7; Hickman et al., 2020, 2021; Kim et al., 2019; Shi et al., 2015; Shi et al., 2013; Song et al., 2016), but still result in impaired physiology and perception (Chapters 8, 9, and 11), the definition of SYN may need to be expanded. “Synaptopathy” is broadly defined as synaptic dysfunction due to structural or functional disruptions and is thought to contribute to a variety of neurodegenerative disease processes (Brose et al., 2010). Traditionally, the term “cochlear synaptopathy” was used to describe the loss of IHC ribbon synapses, swelling of postsynaptic auditory nerve fiber dendrites, and the process of primary neural degeneration (Kujawa & Liberman, 2015). Over time, it seems that this definition has been reduced to an oversimplification of SYN as the loss of IHC ribbons.

This view implies a permanency or chronicity to the cochlear synapse loss and deafferentation, which may be the case if afferent fibers do not return to regenerated ribbons. While we do see significant ribbon loss at 2 months post-exposure, it is difficult to say that macaques "have synaptopathy" at 10 months post-exposure, as their ribbon counts do not differ from unexposed controls. However, regenerated ribbons may exhibit functional differences from innate synapses (Vincent et al., 2022), so ears with normal ribbon counts may still exhibit synaptic dysfunction. As suggested by Shi et al. (2016), a revised definition of SYN could refer to the process of damage, loss, and repair or regeneration of synapses, which would encompass temporary and permanent consequences to anatomy, physiology, and perception.

SYN is typically considered a loss of function; deafferentation reduces the amount of information being transmitted to the central auditory system about incoming sounds. However, our macaques exhibited evidence for two forms of gain-of-function: increased ABR amplitudes to clicks in noise and improved thresholds for short duration tones in gated noise. While these changes are pathologic, in that the native auditory system does not function in this way, the result is larger neural responses and better sensitivity. Enhanced onset encoding and temporal precision in the auditory nerve has been reported in one study of SYN (Suthakar & Liberman, 2021). Sensorineural hearing loss (i.e. hair cell loss and loss of hearing sensitivity; SNHL) also appears to improve (Henry et al., 2014; Kale & Heinz, 2012; Scheidt et al., 2010) or not affect (Miller et al., 1997; Parida & Heinz, 2022) onset coding and temporal precision. Additionally, individuals with SNHL exhibit little to no overshoot, driven by lower thresholds to tones at noise onset (Bacon & Takahashi, 1992; Jennings et al., 2016; Strickland & Krishnan, 2005). Though these gains-of-function are seemingly paradoxical, these changes – detected in the context of simplistic experimental stimuli – may ultimately result in impaired encoding of complex signals in noise (Monaghan et al., 2020; Parida & Heinz, 2022). Because the primary findings described here are common to both SYN and SNHL pathologies, and ribbon loss and primary neural degeneration are known to both precede and accompany SNHL (Fernandez et al., 2020), SYN-related changes may underlie the variable hearing-in-noise abilities of individuals with SNHL (Figure 12.1).

SYN is a convenient pathology to study because ribbon loss and neural degeneration can be uncoupled from dysfunction of other inner ear components (OHCs, stria vascularis, etc.). Physiological and perceptual changes accompanying SYN emphasize the fact that hearing is not solely determined by the presence or absence of hair cells. Although this is well-accepted in the

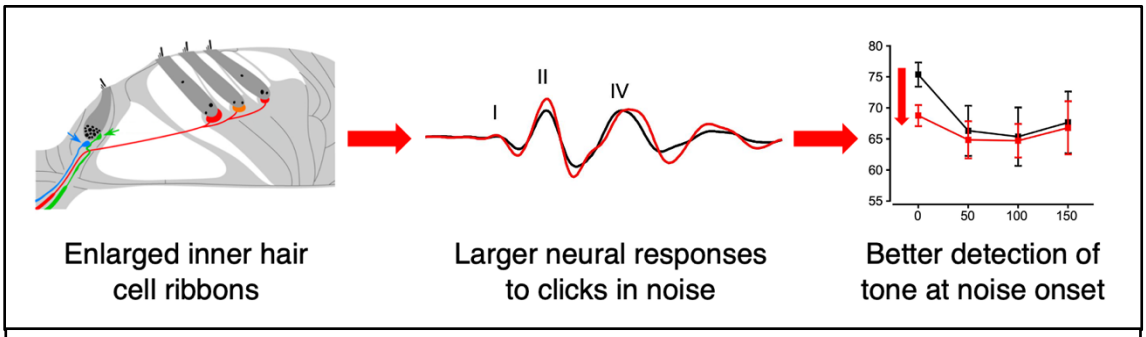

Figure 12.1 Schematic illustrating a unifying hypothesis explaining the primary features of SYN in macaques. Enlarged inner hair cell ribbons (Chapter 7) result in larger onset responses. This results in larger neural responses to signals in noise (masked click ABR, Chapter 9), which enhances sensitivity to short duration tones at noise onset (overshoot, Chapter 11).

more extreme case of auditory neuropathy (characterized by normal OAEs and grossly abnormal or absent ABRs; Starr et al., 1996), SYN research introduces the clinical relevance of uncoupled sensory and neural dysfunction to presentations of SNHL and possibly hidden hearing loss (Moser & Starr, 2016). Identifying the unique contributions and interactions of inner ear components will continue to enhance our understanding of normal and pathologic cochlear function and their role in hearing abilities.

12.3 CENTRAL COMPENSATION IN COCHLEAR SYNAPTOPATHY: THE REAL SOURCE OF HIDDEN HEARING LOSS?

Sensory deafferentation causes massive reorganization in the brain, as beautifully shown in classic somatosensory lesion studies (Lund et al., 1994; Pons et al., 1991). Cochlear ablation and ototoxic cochlear damage have been used as models of auditory deafferentation (e.g. Chambers et al., 2016; Francis & Manis, 2000; Schwaber et al., 1993), resulting in extensive topographical reorganization (Schwaber et al., 1993) and central gain (hyperactivity due to loss of inhibition; Mulders & Robertson, 2011; Salvi et al., 2000). Auditory deafferentation by SYN also does not stop in the periphery; compensatory mechanisms are pervasive throughout the auditory system, including the brainstem (Chapter 9; Mehraei et al., 2016), midbrain (Bakay et al., 2018; Mohrle et al., 2016; Shaheen & Liberman, 2018), and cortex (Asokan et al., 2018). While the act of deafferentation by lesion or acoustic overexposure is acute, peripheral and central responses are not static. Central compensation begins quickly after peripheral insult and changes over time (Asokan et al., 2018; Chambers et al., 2016; Mulders & Robertson, 2013;

Resnik & Polley, 2021). Given this, peripheral repair by intrinsic or therapeutic mechanisms does not ensure that central pathways will return to pre-insult functionality.

Compensatory mechanisms may also influence other neural pathways, such as efferent systems and non-auditory brain regions for language processing, attention, and executive function. Studies by Sharma and colleagues demonstrate massive cross-modal cortical reorganization in patients with mild hearing loss (Campbell & Sharma, 2013, 2014; Cardon & Sharma, 2018), including a shift of auditory encoding from temporal to frontal lobe regions. Impaired signal encoding accompanied by offloading of auditory processing to "non-auditory" areas may require greater listening effort from the listener. More specifically, an increase in onset responses to signals in noise may allow more signals to be passed through the auditory system for processing, thus taxing attentional resources. Listening-related fatigue is commonly reported by hearing impaired patients (Davis et al., 2021) and recalls the complaints of individuals with hidden hearing loss (Kamerer et al., 2021; Spankovich et al., 2018; Tremblay et al., 2015; Zhao & Stephens, 1996).

A broader definition of SYN that incorporates these time-varying compensatory consequences may clarify the seemingly mixed literature on hidden hearing loss in humans. Repeated acoustic injury combined with dynamic central compensation could lead to variable physiological and perceptual manifestations within and across individuals. Studies of humans "at risk for SYN" due to age, noise exposure history, tinnitus, or measured speech-in-noise deficits will be difficult to interpret since only an instantaneous view of each participant can be captured. Furthermore, difficulties hearing in background noise in the absence of overt hearing loss have been reported under the guise of many different clinical entities (e.g. hidden hearing loss, King Kopetzky syndrome, obscure auditory dysfunction, auditory processing disorder). These disorders are typically attributed to "central auditory dysfunction", with little regard for etiology and even less evidence for a specific underlying site of lesion. Central compensation following SYN may be one contributor to these clinical presentations.

12.4 DIAGNOSING COCHLEAR SYNAPTOPATHY

Hearing-in-noise difficulties in the absence of audiometric hearing loss may be caused by SYN. According to our data, we suggest that these hearing difficulties may arise from ribbon enlargement. The enlarged ribbons generate larger onset responses to signals in noise, resulting

in improved detection of signals at noise onset. In this way, the listener may be more sensitive to the many competing sounds in their environment that occur in accordance with temporal fluctuations in background noise. With competing sounds being effectively encoded in noise at more favorable signal-to-noise ratios, the auditory system is bombarded with more information than can be overcome with built-in hearing-in-noise mechanisms (such as the intact MOCR and other attentional networks). The listener is left struggling to hear out the signal of interest.

In this study, we provided further evidence for the utility of the MEMR in the diagnosis of SYN, but called into question the sensitivity of ABR metrics. We also identified psychophysical overshoot as one of the first behavioral biomarkers for the diagnosis of SYN. The WB-MEMR can be easily implemented in the clinic, and modifications to the task design could allow for relatively quick measurement of overshoot. Our collaborator, Dr. Barbara Shinn-Cunningham, is conducting parallel investigations in human subjects that will shed light on the sensitivity of overshoot to SYN pathology in humans.

We have also explored other candidate biomarkers of SYN. IHC ribbons are essential for generating onset responses and precise encoding of sounds over time (Buran et al., 2010; Jean et al., 2018). Damaged ribbons and associated changes in spike timing could disrupt the integration of binaural signals and cause spatial hearing deficits (Bharadwaj et al., 2015). Assays that probe temporal precision as it relates to binaural hearing may be useful for SYN diagnosis (Phatak et al., 2019). We previously characterized the binaural interaction component (BIC) of the ABR in macaques (Peacock et al., 2021), which is an objective measure of binaural hearing abilities. Following noise exposure, macaques show reduced BIC amplitudes and deficits in behavioral measures of spatial hearing (spatial release from masking; Mackey et al., in prep). Spatial hearing deficits may result from loss of sensitivity to interaural timing or level difference cues that are encoded in the lateral and medial superior olives in the auditory brainstem. These observations could also implicate changes in the olivocochlear system, which resides near the binaural auditory structures in the superior olivary complex and is thought to play a role in spatial hearing (Clause et al., 2017; Irving et al., 2011; Lauer et al., 2021).

Assays that probe auditory attention may also prove sensitive to central compensation following SYN. Selective attention can modulate peripheral and central representations of sound (Delano et al., 2007; Fritz et al., 2007; Ikeda et al., 2008; Smith et al., 2012; Wittekindt et al., 2014). High fidelity neuronal encoding is necessary to guide selective attention (Viswanathan et

al., 2022), so alterations to the neural representations of suprathreshold signals could impair scene analysis (Bharadwaj et al., 2014; Shinn-Cunningham, 2017). As an example, the MOC system can be modulated by attention (Bowen et al., 2020; Marcenaro et al., 2021; Srinivasan et al., 2012) (reviewed in Lauer et al., 2021), highlighting a dynamic (as opposed to purely reflexive) role of this pathway (de Boer et al., 2012). Attending to a stimulus can enhance cochlear gain for that signal and reduce cochlear gain for unattended stimuli through MOC-mediated control of OHC motility. Selective attention is impaired in transgenic mice that lack α9 nicotinic acetylcholine receptors (Terreros et al., 2016), which oppose MOC neuron terminals on OHCs (Kujawa et al., 1994). Altered signal encoding with SYN could disrupt attentional control of MOC function and the mediation of cochlear gain, resulting in poorer signal-to-noise ratios and impaired hearing-in-noise. This type of MOC dysfunction would not be captured in our MOCR test, which is conducted under passive listening conditions. Interestingly, case studies in patients with severed olivocochlear bundles actually showed better detection of unexpected signals compared to controls (Scharf et al., 1997; Scharf et al., 1994). The authors suggested that this apparent gain-of-function may have resulted from impaired selective attention. This line of evidence provides an intriguing alternative explanation for our overshoot findings and may imply the presence of selective attention deficits in SYN pathology (Bharadwaj et al., 2014; Shinn-Cunningham, 2017).

When discussing the diagnosis of SYN with clinicians, it is important to emphasize the difference between SYN and hidden hearing loss. SYN refers to a specific pathological mechanism and process (see Section 12.2). Terms like hidden hearing loss and auditory processing disorder are merely descriptive labels for a constellation of symptoms, such as difficulty hearing in background noise. Due to their descriptive nature, these labels are considered diagnoses of exclusion and are only used after eliminating other explanations for the symptoms (e.g. hearing loss, cognitive delay or degeneration, language impairment, attention deficit disorders, traumatic brain injury, psychiatric disease, etc.). However, hearing-in-noise and selective attention deficits probably always accompany hearing loss, and these symptoms are comorbid with other disorders, such as dementia (Armstrong et al., 2020) and traumatic brain injury (Bressler et al., 2017; Han et al., 2021). Although further research is needed to elucidate the causal relationships among these disorders, SYN, SNHL, and other disorders share common

clinical features and may also share common neuropathological substrates. Diagnostic tests for SYN will require excellent sensitivity and specificity before their implementation in the clinic.

Despite growing evidence of SYN in humans and advances in the search for SYN biomarkers, many clinicians remain skeptical and struggle to see how SYN diagnosis will change their clinical practice. Evidence-based conversations about the efficacy and limitations of current rehabilitative options may enlighten the clinical relevance of SYN. For example, cross-modal reorganization caused by mild hearing loss appears at least partially reversible with the use of hearing aids (Glick & Sharma, 2020). However, aided speech-in-noise perception is still highly variable among hearing impaired listeners (Humes et al., 2013; Humes et al., 2002). Implementation science is recently developed field dedicated to the effective translation of scientific findings into clinical practice (Douglas & Burshnic, 2019; Peters et al., 2014). These efforts aim to improve the dissemination of scientific advances and facilitate their successful and timely application into evidence-based practices. Collaborative studies conducted by researchers alongside practicing clinicians can be used to assess the utility and feasibility of implementing a new test or treatment into a clinical setting. Special interest groups of the American Speech-Language-Hearing Association (ASHA) have recently pledged their support of implementation science within communication sciences and disorders research (Finn et al., 2019). Implementation science efforts among audiologists, otolaryngologists, and hearing scientists will be increasingly important as therapeutic treatments for hearing disorders become available.

12.5 FUTURE DIRECTIONS

12.5.1 Large-scale analyses integrating anatomical, physiological, and behavioral data

As our large-scale and long-term studies come to a close, we look ahead to synthesizing our results as a whole. In the future, we plan to do large-scale analyses across all measures included in our study in order to tease out relationships among anatomical, physiological, and perceptual biomarkers. For example, previous studies indicate weak relationships between the magnitude of temporary threshold shifts and the severity of OHC loss (reviewed in Chapter 1). We aim to expand on these findings by assessing the relationship between temporary threshold shifts as measured by OAEs and behavioral audiograms, and relating these shifts to the amount of OHC loss or ribbon enlargement at corresponding frequencies. Another avenue of interest is using pre-exposure indices to predict susceptibility to noise exposure or post-exposure outcomes.

Several studies suggest that MOCR strength predicts susceptibility to acoustic injury, with stronger MOCRs being protective (Maison & Liberman 2000, Luebke & Foster 2002; Maison 2013, Liberman 2014). Here, we can compare pre-exposure TEOAE suppression (our measure of MOCR strength) with the magnitude of temporary threshold shifts, severity of histopathology, and post-exposure physiological or perceptual changes to assess whether this metric indexes inter-subject variability in susceptibility to noise exposure in our macaques.

12.5.2 Chronic noise exposures: Accumulation vs. protection

The acute noise exposure used in our study may not be representative of the conditions causing SYN in humans (Dobie & Humes, 2017). Chronic, low level noise exposures may also cause SYN and accumulate to produce "age-related" decline. However, one study implementing this type of exposure (80 dB SPL, 8 hours per day) did not observe ribbon loss at any time point examined (Occelli et al., 2022). Alternatively, low level noise exposures may protect against more severe acoustic insults, as shown in studies of noise conditioning (Brown et al., 1998; Canlon et al., 1999; Peng et al., 2007; Yin et al., 2020). It is unclear how or under what conditions noise exposures result in toughening as opposed to injury, but this delineation is of great relevance to our understanding of SYN pathology. Knowing the normal acoustic environments of research animals and humans will also be relevant to these types of investigations. We used an environmental monitoring device (Turner Scientific) to measure sound levels in our macaque housing rooms (McLeod et al., re-submitted). Mean sound levels were 58-62 dB SPL, with transients peaks up to 109 dB SPL. These ambient noise conditions form a baseline for future studies of chronic noise exposure in macaques.

12.5.3 Investigating cellular and molecular consequences of cochlear synaptopathy to identify treatment strategies

Further characterization of noise-induced changes in neuronal circuitry and response properties will be important for advancing our understanding of SYN. Investigations throughout the primary and non-primary auditory pathway, as well as multisensory and higher order brain areas, will generate a holistic picture of the gross changes in brain function accompanying hearing loss. As the literature on the central consequences of SYN (Asokan et al., 2018; Bakay et al., 2018; Shaheen & Liberman, 2018) and related pathologies (Bauer et al., 2008; Chambers et al., 2016; McFadden et al., 1998; Resnik & Polley, 2021; Wang et al., 2021; Wong & Xu-Friedman, 2022) continues to grow, studies that consider post-exposure time as a variable will

help decipher the course of pathology. These approaches will be particularly informative for the development of therapeutic and rehabilitation strategies for SYN.

Perhaps the first question to answer is whether recovered and/or regenerated synapses share similar function to native synapses. The presence of a presynaptic ribbon by CtBP2 staining does not imply that the ribbon is structurally or functionally intact compared to non-pathologic ribbons. Initial *in vitro* studies of regenerated inner hair cell to auditory nerve fiber synapses suggest that some functions are similar, while other aspects are functionally distinct from mature native synapses (Vincent et al., 2022). Although these studies are quite technically challenging to complete, the data are invaluable for understanding SYN pathology and the capabilities and limitations of therapeutic treatments that could recover presynaptic ribbons.

One neuronal circuit of interest is that of the small cell cap of the cochlear nucleus. These neurons receive innervation from LSR fibers (Liberman, 1991), Type II afferents (Hurd et al., 1999), and MOC collaterals (Hockley et al., 2021). Unsurprisingly, given the response properties of their neuronal inputs, encoding of signals in noise is a specialty of cochlear nucleus small cells (Hockley et al., 2021). These neurons also exhibit superior encoding of sound intensity, which is sharpened by the MOC inputs (Hockley et al., 2022). This circuit seems ripe with opportunities to change following SYN and manifest as deficits in suprathreshold sound processing and hearing-in-noise.

The molecular mechanisms underlying ribbon loss, primary neural degeneration, and ongoing plasticity are also poorly understood (Hu et al., 2020), limiting progress toward therapeutic strategies for the prevention and treatment of hearing loss. Neurotrophic support is effective at preventing and reversing SYN (Chen et al., 2018; Sly et al., 2016; Suzuki et al., 2016), but may only be useful in cases of acute noise-induced SYN and within a small treatment window. Research from other sensory systems may provide further insight about the molecular substrates of SYN pathology and approaches to treatment. For example, retinal ganglion cells can be damaged by blunt ocular trauma (Bricker-Anthony & Rex, 2015) and increased intraocular pressure in glaucoma (Crish et al., 2010). Investigations of the molecular consequences of ocular injury and neuronal degeneration as well as the time course of these changes are emerging (Bernardo-Colón et al., 2019; Naguib et al., 2021). Markers of inflammation and oxidative stress are key molecular players that show parallels to molecular

changes in cochlear hearing loss (Honkura et al., 2016; Tan et al., 2016) and may be useful targets for therapeutic interventions (Koleilat et al., 2020; Sha & Schacht, 2017).

REFERENCES

Abbas, P. J. (1978). Effects of stimulus frequency on two-tone suppression: a comparison of physiological and psychophysical results. *J Acoust Soc Am*, *63*(6), 1878-1886. https://doi.org/10.1121/1.381929

Abdala, C., Dhar, S., Ahmadi, M., & Luo, P. (2014). Aging of the medial olivocochlear reflex and associations with speech perception. *J Acoust Soc Am*, *135*(2), 754-765. https://doi.org/10.1121/1.4861841

Abdala, C., Sininger, Y. S., & Starr, A. (2000). Distortion product otoacoustic emission suppression in subjects with auditory neuropathy. *Ear Hear*, *21*(6), 542-553. https://doi.org/10.1097/00003446-200012000-00002

Anderson, L. A., Christianson, G. B., & Linden, J. F. (2009). Stimulus-specific adaptation occurs in the auditory thalamus. *J Neurosci*, *29*(22), 7359-7363. https://doi.org/10.1523/JNEUROSCI.0793-09.2009

Armstrong, N. M., An, Y., Ferrucci, L., Deal, J. A., Lin, F. R., & Resnick, S. M. (2020). Temporal Sequence of Hearing Impairment and Cognition in the Baltimore Longitudinal Study of Aging. *J Gerontol A Biol Sci Med Sci*, *75*(3), 574-580. https://doi.org/10.1093/gerona/gly268

Asokan, M. M., Williamson, R. S., Hancock, K. E., & Polley, D. B. (2018). Sensory overamplification in layer 5 auditory corticofugal projection neurons following cochlear nerve synaptic damage. *Nat Commun*, *9*(1), 2468. https://doi.org/10.1038/s41467-018-04852-y

Backus, B. C., & Guinan, J. J., Jr. (2006). Time-course of the human medial olivocochlear reflex. *J Acoust Soc Am*, *119*(5 Pt 1), 2889-2904. https://doi.org/10.1121/1.2169918

Backus, B. C., & Guinan, J. J., Jr. (2007). Measurement of the distribution of medial olivocochlear acoustic reflex strengths across normal-hearing individuals via otoacoustic emissions. *J Assoc Res Otolaryngol*, *8*(4), 484-496. https://doi.org/10.1007/s10162-007-0100-0

Bacon, S. P. (1990). Effect of masker level on overshoot. *J Acoust Soc Am*, *88*(2), 698-702. https://doi.org/10.1121/1.399773

Bacon, S. P., & Takahashi, G. A. (1992). Overshoot in normal-hearing and hearing-impaired subjects. *J Acoust Soc Am*, *91*(5), 2865-2871. https://doi.org/10.1121/1.402967

Bacon, S. P., & Viemeister, N. F. (1985). Simultaneous masking by gated and continuous sinusoidal maskers. *J Acoust Soc Am*, *78*(4), 1220-1230. https://doi.org/10.1121/1.392890

Badri, R., Siegel, J. H., & Wright, B. A. (2011). Auditory filter shapes and high-frequency hearing in adults who have impaired speech in noise performance despite clinically normal audiograms. *J Acoust Soc Am*, *129*(2), 852-863. https://doi.org/10.1121/1.3523476

Bakay, W. M. H., Anderson, L. A., Garcia-Lazaro, J. A., McAlpine, D., & Schaette, R. (2018). Hidden hearing loss selectively impairs neural adaptation to loud sound environments. *Nat Commun*, *9*(1), 4298. https://doi.org/10.1038/s41467-018-06777-y

Bauer, C. A., Turner, J. G., Caspary, D. M., Myers, K. S., & Brozoski, T. J. (2008). Tinnitus and inferior colliculus activity in chinchillas related to three distinct patterns of cochlear trauma. *J Neurosci Res*, *86*(11), 2564-2578. https://doi.org/10.1002/jnr.21699

Beattie, R. C., Thielen, K. M., & Franzone, D. L. (1994). Effects of signal-to-noise ratio on the auditory brainstem response to tone bursts in notch noise and broadband noise. *Scand Audiol*, *23*(1), 47-56. https://doi.org/10.3109/01050399409047485

Becker, L., Schnee, M. E., Niwa, M., Sun, W., Maxeiner, S., Talaei, S., Kachar, B., Rutherford, M. A., & Ricci, A. J. (2018). The presynaptic ribbon maintains vesicle populations at the hair cell afferent fiber synapse. *Elife*, *7*. https://doi.org/10.7554/eLife.30241

Bergman, M., Najenson, T., Korn, C., Harel, N., Erenthal, P., & Sachartov, E. (1992). Frequency selectivity as a potential measure of noise damage susceptibility. *Br J Audiol*, *26*(1), 15-22. https://doi.org/10.3109/03005369209077867

Berlin, C. I., Hood, L. J., Cecola, R. P., Jackson, D. F., & Szabo, P. (1993). Does type I afferent neuron dysfunction reveal itself through lack of efferent suppression? *Hear Res*, *65*(1-2), 40-50. https://doi.org/10.1016/0378-5955(93)90199-b

Berlin, C. I., Hood, L. J., Hurley, A. E., Wen, H., & Kemp, D. T. (1995). Binaural noise suppresses linear click-evoked otoacoustic emissions more than ipsilateral or contralateral noise. *Hear Res*, *87*(1-2), 96-103. https://doi.org/10.1016/0378-5955(95)00082-f

Berlin, C. I., Hood, L. J., Morlet, T., Wilensky, D., St John, P., Montgomery, E., & Thibodaux, M. (2005). Absent or elevated middle ear muscle reflexes in the presence of normal

otoacoustic emissions: a universal finding in 136 cases of auditory neuropathy/dys-synchrony. *J Am Acad Audiol*, *16*(8), 546-553. https://doi.org/10.3766/jaaa.16.8.3

Berlin, C. I., Hood, L. J., Wen, H., Szabo, P., Cecola, R. P., Rigby, P., & Jackson, D. F. (1993). Contralateral suppression of non-linear click-evoked otoacoustic emissions. *Hear Res*, *71*(1-2), 1-11. https://doi.org/10.1016/0378-5955(93)90015-s

Bernardo-Colón, A., Vest, V., Cooper, M. L., Naguib, S. A., Calkins, D. J., & Rex, T. S. (2019). Progression and Pathology of Traumatic Optic Neuropathy From Repeated Primary Blast Exposure. *Front Neurosci*, *13*, 719. https://doi.org/10.3389/fnins.2019.00719

Bernstein, L. R., & Trahiotis, C. (2016). Behavioral manifestations of audiometrically-defined "slight" or "hidden" hearing loss revealed by measures of binaural detection. *J Acoust Soc Am*, *140*(5), 3540. https://doi.org/10.1121/1.4966113

Bernstein, L. R., & Trahiotis, C. (2019). No more than "slight" hearing loss and degradations in binaural processing. *J Acoust Soc Am*, *145*(4), 2094. https://doi.org/10.1121/1.5096652

Bernstein, L. R., & Trahiotis, C. (2020). A crew of listeners with no more than "slight" hearing loss who exhibit binaural deficits also exhibit higher levels of stimulus-independent internal noise. *J Acoust Soc Am*, *147*(5), 3188. https://doi.org/10.1121/10.0001207

Bharadwaj, H. M., Hustedt-Mai, A. R., Ginsberg, H. M., Dougherty, K. M., Muthaiah, V. P. K., Hagedorn, A., Simpson, J. M., & Heinz, M. G. (2021). Cross-Species Experiments Reveal Widespread Cochlear Neural Damage in Normal Hearing. *biorxiv*. https://doi.org/10.1101/2021.03.17.435900

Bharadwaj, H. M., Mai, A. R., Simpson, J. M., Choi, I., Heinz, M. G., & Shinn-Cunningham, B. G. (2019). Non-Invasive Assays of Cochlear Synaptopathy - Candidates and Considerations. *Neuroscience*, *407*, 53-66. https://doi.org/10.1016/j.neuroscience.2019.02.031

Bharadwaj, H. M., Masud, S., Mehraei, G., Verhulst, S., & Shinn-Cunningham, B. G. (2015). Individual differences reveal correlates of hidden hearing deficits. *J Neurosci*, *35*(5), 2161-2172. https://doi.org/10.1523/JNEUROSCI.3915-14.2015

Bharadwaj, H. M., Verhulst, S., Shaheen, L., Liberman, M. C., & Shinn-Cunningham, B. G. (2014). Cochlear neuropathy and the coding of supra-threshold sound. *Front Syst Neurosci*, *8*, 26. https://doi.org/10.3389/fnsys.2014.00026

Bidelman, G. M., & Bhagat, S. P. (2015). Right-ear advantage drives the link between olivocochlear efferent 'antimasking' and speech-in-noise listening benefits. *Neuroreport*, *26*(8), 483-487. https://doi.org/10.1097/WNR.0000000000000376

Billings, C. J., Dillard, L. K., Hoskins, Z. B., Penman, T. M., & Reavis, K. M. (2018). A Large-Scale Examination of Veterans with Normal Pure-Tone Hearing Thresholds within the Department of Veterans Affairs. *J Am Acad Audiol*, *29*(10), 928-935. https://doi.org/10.3766/jaaa.17091

Boero, L. E., Castagna, V. C., Di Guilmi, M. N., Goutman, J. D., Elgoyhen, A. B., & Gomez-Casati, M. E. (2018). Enhancement of the Medial Olivocochlear System Prevents Hidden Hearing Loss. *J Neurosci*, *38*(34), 7440-7451. https://doi.org/10.1523/JNEUROSCI.0363-18.2018

Boero, L. E., Castagna, V. C., Terreros, G., Moglie, M. J., Silva, S., Maass, J. C., Fuchs, P. A., Delano, P. H., Elgoyhen, A. B., & Gomez-Casati, M. E. (2020). Preventing presbycusis in mice with enhanced medial olivocochlear feedback. *Proc Natl Acad Sci U S A*, *117*(21), 11811-11819. https://doi.org/10.1073/pnas.2000760117

Boettcher, F. A., Mills, J. H., Dubno, J. R., & Schmiedt, R. A. (1995). Masking of auditory brainstem responses in young and aged gerbils. *Hear Res*, *89*(1-2), 1-13. https://doi.org/10.1016/0378-5955(95)00116-x

Boezeman, E. H., Kapteyn, T. S., Visser, S. L., & Snel, A. M. (1983). Effect of contralateral and ipsilateral masking of acoustic stimulation on the latencies of auditory evoked potentials from cochlea and brain stem. *Electroencephalogr Clin Neurophysiol*, *55*(6), 710-713. https://doi.org/10.1016/0013-4694(83)90281-x

Bohlen, P., Dylla, M., Timms, C., & Ramachandran, R. (2014). Detection of modulated tones in modulated noise by non-human primates. *J Assoc Res Otolaryngol*, *15*(5), 801-821. https://doi.org/10.1007/s10162-014-0467-7

Borg, E., & Moller, A. R. (1968). The Acoustic Middle Ear Reflex In Unanesthetized Rabbits. *Acta Oto-Laryngologica*, *65*(1-6), 575-585. https://doi.org/10.3109/00016486809121001

Bourien, J., Tang, Y., Batrel, C., Huet, A., Lenoir, M., Ladrech, S., Desmadryl, G., Nouvian, R., Puel, J. L., & Wang, J. (2014). Contribution of auditory nerve fibers to compound action potential of the auditory nerve. *J Neurophysiol*, *112*(5), 1025-1039. https://doi.org/10.1152/jn.00738.2013

Bowen, M., Terreros, G., Moreno-Gomez, F. N., Ipinza, M., Vicencio, S., Robles, L., & Delano, P. H. (2020). The olivocochlear reflex strength in awake chinchillas is relevant for behavioural performance during visual selective attention with auditory distractors. *Sci Rep*, *10*(1), 14894. https://doi.org/10.1038/s41598-020-71399-8

Boyev, K. P., Liberman, M. C., & Brown, M. C. (2002). Effects of anesthesia on efferent-mediated adaptation of the DPOAE. *J Assoc Res Otolaryngol*, *3*(3), 362-373. https://doi.org/10.1007/s101620020044

Bramhall, N., Beach, E. F., Epp, B., Le Prell, C. G., Lopez-Poveda, E. A., Plack, C. J., Schaette, R., Verhulst, S., & Canlon, B. (2019). The search for noise-induced cochlear synaptopathy in humans: Mission impossible? *Hear Res*, *377*, 88-103. https://doi.org/10.1016/j.heares.2019.02.016

Bramhall, N. F., Konrad-Martin, D., McMillan, G. P., & Griest, S. E. (2017). Auditory Brainstem Response Altered in Humans With Noise Exposure Despite Normal Outer Hair Cell Function. *Ear Hear*, *38*(1), e1-e12. https://doi.org/10.1097/AUD.0000000000000370

Bramhall, N. F., McMillan, G. P., & Kampel, S. D. (2021). Envelope following response measurements in young veterans are consistent with noise-induced cochlear synaptopathy. *Hear Res*, *408*, 108310. https://doi.org/10.1016/j.heares.2021.108310

Bramhall, N. F., Reavis, K. M., Feeney, M. P., & Kampel, S. D. (2022). The Impacts of Noise Exposure on the Middle Ear Muscle Reflex in a Veteran Population. *Am J Audiol*, *31*(1), 126-142. https://doi.org/10.1044/2021_AJA-21-00133

Bredberg, G. (1968). Cellular pattern and nerve supply of the human organ of Corti. *Acta Otolaryngol*(Suppl 236), 1-135.

Bressler, S., Goldberg, H., & Shinn-Cunningham, B. (2017). Sensory coding and cognitive processing of sound in Veterans with blast exposure. *Hear Res*, *349*, 98-110. https://doi.org/10.1016/j.heares.2016.10.018

Bricker-Anthony, C., & Rex, T. S. (2015). Neurodegeneration and Vision Loss after Mild Blunt Trauma in the C57Bl/6 and DBA/2J Mouse. *PLoS One*, *10*(7), e0131921. https://doi.org/10.1371/journal.pone.0131921

Brose, N., O'Connor, V., & Skehel, P. (2010). Synaptopathy: dysfunction of synaptic function? *Biochem Soc Trans*, *38*(2), 443-444. https://doi.org/10.1042/BST0380443

Brown, M. C. (2016). Recording and labeling at a site along the cochlea shows alignment of medial olivocochlear and auditory nerve tonotopic mappings. *J Neurophysiol*, *115*(3), 1644-1653. https://doi.org/10.1152/jn.00842.2015

Brown, M. C., Kujawa, S. G., & Liberman, M. C. (1998). Single olivocochlear neurons in the guinea pig. II. Response plasticity due to noise conditioning. *J Neurophysiol*, *79*(6), 3088-3097. https://doi.org/10.1152/jn.1998.79.6.3088

Buran, B. N., Strenzke, N., Neef, A., Gundelfinger, E. D., Moser, T., & Liberman, M. C. (2010). Onset coding is degraded in auditory nerve fibers from mutant mice lacking synaptic ribbons. *J Neurosci*, *30*(22), 7587-7597. https://doi.org/10.1523/JNEUROSCI.0389-10.2010

Burkard, R., & Hecox, K. (1983). The effect of broadband noise on the human brainstem auditory evoked response. I. Rate and intensity effects. *J Acoust Soc Am*, *74*(4), 1204-1213. https://doi.org/10.1121/1.390024

Burkard, R., & Hecox, K. E. (1987). The effect of broadband noise on the human brain-stem auditory evoked response. III. Anatomic locus. *J Acoust Soc Am*, *81*(4), 1050-1063. https://doi.org/10.1121/1.394677

Burkard, R. F., & Sims, D. (2002). A comparison of the effects of broadband noise on the auditory brainstem response in young and older adults. *Am J Audiol*, *11*, 13-22.

Burke, K., Manohar, S., & Dent, M. L. (2021). Long term changes to auditory sensitivity following blast trauma in mice. *Hear Res*, *403*, 108201. https://doi.org/10.1016/j.heares.2021.108201

Burton, J. A., Dylla, M. E., & Ramachandran, R. (2018). Frequency selectivity in macaque monkeys measured using a notched-noise method. *Hear Res*, *357*, 73-80. https://doi.org/10.1016/j.heares.2017.11.012

Burton, J. A., Mackey, C. A., MacDonald, K. S., Hackett, T. A., & Ramachandran, R. (2020). Changes in audiometric threshold and frequency selectivity correlate with cochlear histopathology in macaque monkeys with permanent noise-induced hearing loss. *Hear Res*, *398*, 108082. https://doi.org/10.1016/j.heares.2020.108082

Burton, J. A., Tarabillo, A. L., Finnie, K. R., Shuster, K. A., Mackey, C. A., Hackett, T. A., & Ramachandran, R. (2022). Chronic Otitis Externa Secondary to Tympanic Membrane

Electrode Placement in Rhesus Macaques (Macaca mulatta). *Comp Med*. https://doi.org/10.30802/aalas-cm-21-000071

Burton, J. A., Valero, M. D., Hackett, T. A., & Ramachandran, R. (2019). The use of nonhuman primates in studies of noise injury and treatment. *J Acoust Soc Am*, *146*(5), 3770. https://doi.org/10.1121/1.5132709

Campbell, J., & Sharma, A. (2013). Compensatory changes in cortical resource allocation in adults with hearing loss. *Front Syst Neurosci*, *7*, 71. https://doi.org/10.3389/fnsys.2013.00071

Campbell, J., & Sharma, A. (2014). Cross-modal re-organization in adults with early stage hearing loss. *PLoS One*, *9*(2), e90594. https://doi.org/10.1371/journal.pone.0090594

Campbell, R. A. (1969). Thresholds re duration and levels of a continuous or gated masker. *J Acoust Soc Am*, *46*(4), 895-897. https://doi.org/10.1121/1.1911807

Canlon, B., Fransson, A., & Viberg, A. (1999). Medial olivocochlear efferent terminals are protected by sound conditioning. *Brain Res*, *850*(1-2), 253-260. https://doi.org/10.1016/s0006-8993(99)02091-0

Cardon, G., & Sharma, A. (2018). Somatosensory Cross-Modal Reorganization in Adults With Age-Related, Early-Stage Hearing Loss. *Front Hum Neurosci*, *12*, 172. https://doi.org/10.3389/fnhum.2018.00172

Carlyon, R. P., & Sloan, E. P. (1987). The "overshoot" effect and sensory hearing impairment. *J Acoust Soc Am*, *82*(3), 1078-1081. https://doi.org/10.1121/1.395329

Carney, L. H. (2018). Supra-Threshold Hearing and Fluctuation Profiles: Implications for Sensorineural and Hidden Hearing Loss. *J Assoc Res Otolaryngol*, *19*(4), 331-352. https://doi.org/10.1007/s10162-018-0669-5

Causon, A., Munro, K. J., Plack, C. J., & Prendergast, G. (2020). The Role of the Clinically Obtained Acoustic Reflex as a Research Tool for Subclinical Hearing Pathologies. *Trends Hear*, *24*, 2331216520972860. https://doi.org/10.1177/2331216520972860

Cederholm, J. M., Froud, K. E., Wong, A. C., Ko, M., Ryan, A. F., & Housley, G. D. (2012). Differential actions of isoflurane and ketamine-based anaesthetics on cochlear function in the mouse. *Hear Res*, *292*(1-2), 71-79. https://doi.org/10.1016/j.heares.2012.08.010

Chambers, A. R., Hancock, K. E., Maison, S. F., Liberman, M. C., & Polley, D. B. (2012). Sound-evoked olivocochlear activation in unanesthetized mice. *J Assoc Res Otolaryngol*, *13*(2), 209-217. https://doi.org/10.1007/s10162-011-0306-z

Chambers, A. R., Resnik, J., Yuan, Y., Whitton, J. P., Edge, A. S., Liberman, M. C., & Polley, D. B. (2016). Central Gain Restores Auditory Processing following Near-Complete Cochlear Denervation. *Neuron*, *89*(4), 867-879. https://doi.org/10.1016/j.neuron.2015.12.041

Champlin, C. A., & McFadden, D. (1989). Reductions in overshoot following intense sound exposures. *J Acoust Soc Am*, *85*(5), 2005-2011. https://doi.org/10.1121/1.397853

Chen, H., Shi, L., Liu, L., Yin, S., Aiken, S., & Wang, J. (2019). Noise-induced Cochlear Synaptopathy and Signal Processing Disorders. *Neuroscience*, *407*, 41-52. https://doi.org/10.1016/j.neuroscience.2018.09.026

Chen, H., Xing, Y., Xia, L., Chen, Z., Yin, S., & Wang, J. (2018). AAV-mediated NT-3 overexpression protects cochleae against noise-induced synaptopathy. *Gene Ther*, *25*(4), 251-259. https://doi.org/10.1038/s41434-018-0012-0

Clause, A., Lauer, A. M., & Kandler, K. (2017). Mice Lacking the Alpha9 Subunit of the Nicotinic Acetylcholine Receptor Exhibit Deficits in Frequency Difference Limens and Sound Localization. *Front Cell Neurosci*, *11*, 167. https://doi.org/10.3389/fncel.2017.00167

Collet, L., Veuillet, E., Bene, J., & Morgon, A. (1992). Effects of contralateral white noise on click-evoked emissions in normal and sensorineural ears: towards an exploration of the medial olivocochlear system. *Audiology*, *31*(1), 1-7. https://doi.org/10.3109/00206099209072897

Cooper, J. C., & Gates, G. A. (1991). Hearing in the elderly- The Framingham cohort, 1983-1985: Part II. Prevalence of central auditory processing disorders. *Ear Hear*, *12*(5), 304-311.

Costalupes, J. A. (1985). Representation of tones in noise in the responses of auditory nerve fibers in cats. I. Comparison with detection thresholds. *J Neurosci*, *5*(12), 3261-3269. https://doi.org/10.1523/jneurosci.05-12-03261.1985

Costalupes, J. A., Young, E. D., & Gibson, D. J. (1984). Effects of continuous noise backgrounds on rate response of auditory nerve fibers in cat. *J Neurophysiol*, *51*(6), 1326-1344. https://doi.org/10.1152/jn.1984.51.6.1326

Crish, S. D., Sappington, R. M., Inman, D. M., Horner, P. J., & Calkins, D. J. (2010). Distal axonopathy with structural persistence in glaucomatous neurodegeneration. *Proc Natl Acad Sci U S A*, *107*(11), 5196-5201. https://doi.org/10.1073/pnas.0913141107

Dallos, P. (1964). Dynamics of the Acoustic Reflex: Phenomenological Aspects. *J Acoust Soc Am*, *36*(11), 2175-2183. https://doi.org/10.1121/1.1919340

Davis, H., Schlundt, D., Bonnet, K., Camarata, S., Bess, F. H., & Hornsby, B. (2021). Understanding Listening-Related Fatigue: Perspectives of Adults with Hearing Loss. *Int J Audiol*, *60*(6), 458-468. https://doi.org/10.1080/14992027.2020.1834631

de Andrade, K. C., Camboim, E. D., Soares Ido, A., Peixoto, M. V., Neto, S. C., & Menezes Pde, L. (2011). The importance of acoustic reflex for communication. *Am J Otolaryngol*, *32*(3), 221-227. https://doi.org/10.1016/j.amjoto.2010.02.002

de Boer, J., & Thornton, A. R. (2008). Neural correlates of perceptual learning in the auditory brainstem: efferent activity predicts and reflects improvement at a speech-in-noise discrimination task. *J Neurosci*, *28*(19), 4929-4937. https://doi.org/10.1523/JNEUROSCI.0902-08.2008

de Boer, J., Thornton, A. R., & Krumbholz, K. (2012). What is the role of the medial olivocochlear system in speech-in-noise processing? *J Neurophysiol*, *107*(5), 1301-1312. https://doi.org/10.1152/jn.00222.2011

Delano, P. H., Elgueda, D., Hamame, C. M., & Robles, L. (2007). Selective attention to visual stimuli reduces cochlear sensitivity in chinchillas. *J Neurosci*, *27*(15), 4146-4153. https://doi.org/10.1523/JNEUROSCI.3702-06.2007

Delgutte, B. (1990). Two-tone rate suppression in auditory-nerve fibers: Dependence on suppressor frequency and level. *Hearing Research*, *49*(1), 225-246. https://doi.org/https://doi.org/10.1016/0378-5955(90)90106-Y

Dewson, J. H., 3rd. (1967). Efferent olivocochlear bundle: some relationships to noise masking and to stimulus attenuation. *J Neurophysiol*, *30*(4), 817-832. https://doi.org/10.1152/jn.1967.30.4.817

Dhar, S., Long, G. R., & Culpepper, N. B. (1998). The dependence of the distortion product 2f1-f2 on primary levels in non-impaired human ears. *J Speech Lang Hear Res*, *41*(6), 1307-1318. https://doi.org/10.1044/jslhr.4106.1307

DiNino, M., Holt, L. L., & Shinn-Cunningham, B. G. (2021). Cutting Through the Noise: Noise-Induced Cochlear Synaptopathy and Individual Differences in Speech Understanding Among Listeners With Normal Audiograms. *Ear Hear*, *43*(1), 9-22. https://doi.org/10.1097/AUD.0000000000001147

Dobie, R. A., & Humes, L. E. (2017). Commentary on the regulatory implications of noise-induced cochlear neuropathy. *Int J Audiol*, *56*(sup1), 74-78. https://doi.org/10.1080/14992027.2016.1255359

Don, M., & Eggermont, J. J. (1978). Analysis of the click-evoked brainstem potentials in man unsing high-pass noise masking. *J Acoust Soc Am*, *63*(4), 1084-1092. https://doi.org/10.1121/1.381816

Douglas, N. F., & Burshnic, V. L. (2019). Implementation Science: Tackling the Research to Practice Gap in Communication Sciences and Disorders. *Perspectives of the ASHA Special Interest Groups*, *4*(1), 3-7. https://doi.org/10.1044/2018_pers-st-2018-0000

Dubno, J. R., & Ahlstrom, J. B. (2001). Forward- and simultaneous-masked thresholds in bandlimited maskers in subjects with normal hearing and cochlear hearing loss. *J Acoust Soc Am*, *110*(2), 1049-1057. https://doi.org/10.1121/1.1381023

Dylla, M., Hrnicek, A., Rice, C., & Ramachandran, R. (2013). Detection of tones and their modification by noise in nonhuman primates. *J Assoc Res Otolaryngol*, *14*(4), 547-560. https://doi.org/10.1007/s10162-013-0384-1

Earl, B. R., & Chertoff, M. E. (2012). Mapping auditory nerve firing density using high-level compound action potentials and high-pass noise masking. *J Acoust Soc Am*, *131*(1), 337-352. https://doi.org/10.1121/1.3664052

Elliott, L. L. (1965). Changes in the simultaneous masked threshold of brief tones. *J Acoust Soc Am*, *38*(5), 738-746. https://doi.org/10.1121/1.1909798

Elliott, L. L. (1969). Masking of tones before, during, and after brief silent periods in noise. *J Acoust Soc Am*, *45*(5), 1277-1279. https://doi.org/10.1121/1.1911600

Engle, J. R., Tinling, S., & Recanzone, G. H. (2013). Age-related hearing loss in rhesus monkeys is correlated with cochlear histopathologies. *PLoS One*, *8*(2), e55092. https://doi.org/10.1371/journal.pone.0055092

Engstrom, B. (1984). Fusion of stereocilia on inner hair cells in man and in the rabbit, rat and guinea pig. *Scand Audiol*, *13*(2), 87-92. https://doi.org/10.3109/01050398409043045

Feeney, M. P., Keefe, D. H., Hunter, L. L., Fitzpatrick, D. F., Garinis, A. C., Putterman, D. B., & McMillan, G. P. (2017). Normative Wideband Reflectance, Equivalent Admittance at the Tympanic Membrane, and Acoustic Stapedius Reflex Threshold in Adults. *Ear Hear*, *38*(3), e142-e160. https://doi.org/10.1097/AUD.0000000000000399

Ferber-Viart, C., Preckel, M. P., Dubreuil, C., Banssillon, V., & Duclaux, R. (1998). Effect of anesthesia on transient evoked otoacoustic emissions in humans: a comparison between propofol and isoflurane. *Hear Res*, *121*(1-2), 53-61. https://doi.org/10.1016/s0378-5955(98)00064-1

Fernandez, K. A., Guo, D., Micucci, S., De Gruttola, V., Liberman, M. C., & Kujawa, S. G. (2020). Noise-induced Cochlear Synaptopathy with and Without Sensory Cell Loss. *Neuroscience*, *427*, 43-57. https://doi.org/10.1016/j.neuroscience.2019.11.051

Fernandez, K. A., Jeffers, P. W., Lall, K., Liberman, M. C., & Kujawa, S. G. (2015). Aging after noise exposure: acceleration of cochlear synaptopathy in "recovered" ears. *J Neurosci*, *35*(19), 7509-7520. https://doi.org/10.1523/JNEUROSCI.5138-14.2015

Feth, L. L., Oesterle, E. C., & Kidd, G. (1979). Frequency selectivity after noise exposure. *The Journal of the Acoustical Society of America*, *65*(S1), S118-S118. https://doi.org/10.1121/1.2016981

Finn, P., Beverly, B. L., Ciccia, A., & Cone, B. (2019). Bridging Knowledge Between Research and Practice. *Perspectives of the ASHA Special Interest Groups*, *4*(1), 1-2. https://doi.org/doi:10.1044/2018_PERS-ST-2018-0014

Fletcher, M., de Boer, J., & Krumbholz, K. (2015). Is off-frequency overshoot caused by adaptation of suppression? *J Assoc Res Otolaryngol*, *16*(2), 241-253. https://doi.org/10.1007/s10162-014-0498-0

Fowler, C. G., Chiasson, K. B., Leslie, T. H., Thomas, D., Beasley, T. M., Kemnitz, J. W., & Weindruch, R. (2010). Auditory function in rhesus monkeys: effects of aging and caloric

restriction in the Wisconsin monkeys five years later. *Hear Res*, *261*(1-2), 75-81. https://doi.org/10.1016/j.heares.2010.01.006

Fowler, C. G., Torre, P., 3rd, & Kemnitz, J. W. (2002). Effects of caloric restriction and aging on the auditory function of rhesus monkeys (Macaca mulatta): The University of Wisconsin Study. *Hear Res*, *169*(1-2), 24-35. https://doi.org/10.1016/s0378-5955(02)00335-0

Francis, H. W., & Manis, P. B. (2000). Effects of deafferentation on the electrophysiology of ventral cochlear nucleus neurons. *Hear Res*, *149*(1-2), 91-105. https://doi.org/10.1016/s0378-5955(00)00165-9

Fria, T., LeBlanc, J., Kristensen, R., & Alberti, P. W. (1975). Ipsilateral acoustic reflex stimulation in normal and sensorineural impaired ears: a preliminary report. *Canadian journal of otolaryngology*, *4*(4), 695-703. http://europepmc.org/abstract/MED/1192288

Fritz, J. B., Elhilali, M., & Shamma, S. A. (2007). Adaptive changes in cortical receptive fields induced by attention to complex sounds. *J Neurophysiol*, *98*(4), 2337-2346. https://doi.org/10.1152/jn.00552.2007

Fu, B., Le Prell, C., Simmons, D., Lei, D., Schrader, A., Chen, A. B., & Bao, J. (2010). Age-related synaptic loss of the medial olivocochlear efferent innervation. *Mol Neurodegener*, *5*, 53. https://doi.org/10.1186/1750-1326-5-53

Fuente, A. (2015). The olivocochlear system and protection from acoustic trauma: a mini literature review. *Front Syst Neurosci*, *9*, 94. https://doi.org/10.3389/fnsys.2015.00094

Fulbright, A. N. C., Le Prell, C. G., Griffiths, S. K., & Lobarinas, E. (2017). Effects of Recreational Noise on Threshold and Suprathreshold Measures of Auditory Function. *Seminars in hearing*, *38*(4), 298-318. https://doi.org/10.1055/s-0037-1606325

Furman, A. C., Kujawa, S. G., & Liberman, M. C. (2013). Noise-induced cochlear neuropathy is selective for fibers with low spontaneous rates. *J Neurophysiol*, *110*(3), 577-586. https://doi.org/10.1152/jn.00164.2013

Gage, F. H. (1932). A Note on the "Binaural Threshold". *British Journal of Psychology*, *23*(2), 148-151. https://doi.org/https://doi.org/10.1111/j.2044-8295.1932.tb00656.x

Gai, Y. (2016). ON and OFF inhibition as mechanisms for forward masking in the inferior colliculus: a modeling study. *J Neurophysiol*, *115*(5), 2485-2500. https://doi.org/10.1152/jn.00892.2015

Galambos, R., & Davis, H. (1943). The response of single auditory-nerve fibers to acoustic stimulation. *J Neurophysiol*, *6*(1), 39-57.

Gelfand, S. A., & Piper, N. (1981). Acoustic reflex thresholds in young and elderly subjects with normal hearing. *J Acoust Soc Am*, *69*(1), 295-297. https://doi.org/10.1121/1.385352

Gibson, D. J., Young, E. D., & Costalupes, J. A. (1985). Similarity of dynamic range adjustment in auditory nerve and cochlear nuclei. *Journal of Neurophysiology*, *53*(4), 940-958. https://doi.org/10.1152/jn.1985.53.4.940

Giraud, A. L., Garnier, S., Micheyl, C., Lina, G., Chays, A., & Chéry-Croze, S. (1997). Auditory efferents involved in speech-in-noise intelligibility. *Neuroreport*, *8*(7), 1779-1783. https://doi.org/10.1097/00001756-199705060-00042

Giraudet, F., Labanca, L., Souchal, M., & Avan, P. (2021). Decreased Reemerging Auditory Brainstem Responses Under Ipsilateral Broadband Masking as a Marker of Noise-Induced Cochlear Synaptopathy. *Ear Hear*, *42*(4), 1062-1071. https://doi.org/10.1097/AUD.0000000000001009

Glasberg, B. R., Moore, B. C., & Bacon, S. P. (1987). Gap detection and masking in hearing-impaired and normal-hearing subjects. *J Acoust Soc Am*, *81*(5), 1546-1556. https://doi.org/10.1121/1.394507

Glasberg, B. R., Moore, B. C., Patterson, R. D., & Nimmo-Smith, I. (1984). Dynamic range and asymmetry of the auditory filter. *J Acoust Soc Am*, *76*(2), 419-427. https://doi.org/10.1121/1.391584

Gleich, O., Semmler, P., & Strutz, J. (2016). Behavioral auditory thresholds and loss of ribbon synapses at inner hair cells in aged gerbils. *Exp Gerontol*, *84*, 61-70. https://doi.org/10.1016/j.exger.2016.08.011

Glick, H. A., & Sharma, A. (2020). Cortical Neuroplasticity and Cognitive Function in Early-Stage, Mild-Moderate Hearing Loss: Evidence of Neurocognitive Benefit From Hearing Aid Use. *Front Neurosci*, *14*, 93. https://doi.org/10.3389/fnins.2020.00093

Goman, A. M., & Lin, F. R. (2016). Prevalence of Hearing Loss by Severity in the United States. *Am J Public Health*, *106*(10), 1820-1822. https://doi.org/10.2105/AJPH.2016.303299

Gorga, M. P., Neely, S. T., Bergman, B. M., Beauchaine, K. L., Kaminski, J. R., Peters, J., Schulte, L., & Jesteadt, W. (1993). A comparison of transient-evoked and distortion

product otoacoustic emissions in normal-hearing and hearing-impaired subjects. *J Acoust Soc Am*, *94*(5), 2639-2648. https://doi.org/10.1121/1.407348

Grant, K. J., Mepani, A. M., Wu, P., Hancock, K. E., de Gruttola, V., Liberman, M. C., & Maison, S. F. (2020). Electrophysiological markers of cochlear function correlate with hearing-in-noise performance among audiometrically normal subjects. *J Neurophysiol*, *124*(2), 418-431. https://doi.org/10.1152/jn.00016.2020

Grant, K. W., Kubli, L. R., Phatak, S. A., Galloza, H., & Brungart, D. S. (2021). Estimated Prevalence of Functional Hearing Difficulties in Blast-Exposed Service Members With Normal to Near-Normal-Hearing Thresholds. *Ear Hear*, *42*(6), 1615-1626. https://doi.org/10.1097/AUD.0000000000001067

Green, D. M. (1964). Continuous versus Gated Masking for Noise and Sinusoidal Maskers. *The Journal of the Acoustical Society of America*, *36*(10), 2009-2009. https://doi.org/10.1121/1.1939318

Greenwood, D. D. (1990). A cochlear frequency-position function for several species--29 years later. *J Acoust Soc Am*, *87*(6), 2592-2605. https://doi.org/10.1121/1.399052

Grierson, K., Hickman, T. T., & Liberman, M. C. (2022). Noise-induced and age-related changes in the olivocochlear innervation in mice. Association for Research in Otolaryngology 45th Midwinter Meeting, Virtual.

Grinn, S. K., Wiseman, K. B., Baker, J. A., & Le Prell, C. G. (2017). Hidden Hearing Loss? No Effect of Common Recreational Noise Exposure on Cochlear Nerve Response Amplitude in Humans. *Front Neurosci*, *11*, 465. https://doi.org/10.3389/fnins.2017.00465

Guest, H., Munro, K. J., & Plack, C. J. (2019). Acoustic Middle-Ear-Muscle-Reflex Thresholds in Humans with Normal Audiograms: No Relations to Tinnitus, Speech Perception in Noise, or Noise Exposure. *Neuroscience*, *407*, 75-82. https://doi.org/10.1016/j.neuroscience.2018.12.019

Guest, H., Munro, K. J., Prendergast, G., Millman, R. E., & Plack, C. J. (2018). Impaired speech perception in noise with a normal audiogram: No evidence for cochlear synaptopathy and no relation to lifetime noise exposure. *Hear Res*, *364*, 142-151. https://doi.org/10.1016/j.heares.2018.03.008

Guinan, J. J., Jr. (2006). Olivocochlear efferents: anatomy, physiology, function, and the measurement of efferent effects in humans. *Ear Hear*, *27*(6), 589-607. https://doi.org/10.1097/01.aud.0000240507.83072.e7

Guinan, J. J., Jr. (2018). Olivocochlear efferents: Their action, effects, measurement and uses, and the impact of the new conception of cochlear mechanical responses. *Hear Res*, *362*, 38-47. https://doi.org/10.1016/j.heares.2017.12.012

Guinan, J. J., Jr., & McCue, M. P. (1987). Asymmetries in the acoustic reflexes of the cat stapedius muscle. *Hear Res*, *26*(1), 1-10. https://doi.org/10.1016/0378-5955(87)90031-1

Guitton, M. J., Avan, P., Puel, J. L., & Bonfils, P. (2004). Medial olivocochlear efferent activity in awake guinea pigs. *Neuroreport*, *15*(9), 1379-1382. https://doi.org/10.1097/01.wnr.0000131672.15566.64

Guven, S., Tas, A., Adali, M. K., Yagiz, R., Alagol, A., Uzun, C., Koten, M., & Karasalihoglu, A. R. (2006). Influence of anaesthetic agents on transient evoked otoacoustic emissions and stapedius reflex thresholds. *J Laryngol Otol*, *120*(1), 10-15. https://doi.org/10.1017/s0022215105004810

Hall, J. W. (2017). Hidden Hearing Loss: An Audiologist's Perspective. *The Hearing Journal*, *70*(1), 6.

Hall, J. W., Haggard, M. P., & Fernandes, M. A. (1984). Detection in noise by spectro-temporal pattern analysis. *J Acoust Soc Am*, *76*(1), 50-56. https://doi.org/10.1121/1.391005

Han, E. X., Fernandez, J. M., Swanberg, C., Shi, R., & Bartlett, E. L. (2021). Longitudinal auditory pathophysiology following mild blast-induced trauma. *J Neurophysiol*, *126*(4), 1172-1189. https://doi.org/10.1152/jn.00039.2021

Hannula, S., Bloigu, R., Majamaa, K., Sorri, M., & Maki-Torkko, E. (2011). Self-reported hearing problems among older adults: prevalence and comparison to measured hearing impairment. *J Am Acad Audiol*, *22*(8), 550-559. https://doi.org/10.3766/jaaa.22.8.7

Harel, N., Kakigi, A., Hirakawa, H., Mount, R. J., & Harrison, R. V. (1997). The effects of anesthesia on otoacoustic emissions. *Hear Res*, *110*(1-2), 25-33. https://doi.org/10.1016/s0378-5955(97)00061-0

Harris, D. M., & Dallos, P. (1979). Forward masking of auditory nerve fiber responses. *J Neurophysiol*, *42*(4), 1083-1107. https://doi.org/10.1152/jn.1979.42.4.1083

Harris, K. C., Ahlstrom, J. B., Dias, J. W., Kerouac, L. B., McClaskey, C. M., Dubno, J. R., & Eckert, M. A. (2021). Neural Presbyacusis in Humans Inferred from Age-Related Differences in Auditory Nerve Function and Structure. *J Neurosci*, *41*(50), 10293-10304. https://doi.org/10.1523/JNEUROSCI.1747-21.2021

Hauser, S. N., Burton, J. A., Mercer, E. T., & Ramachandran, R. (2018). Effects of noise overexposure on tone detection in noise in nonhuman primates. *Hear Res*, *357*, 33-45. https://doi.org/10.1016/j.heares.2017.11.004

Hawkins, J. E., Jr., Johnsson, L. G., Stebbins, W. C., Moody, D. B., & Coombs, S. L. (1976). Hearing loss and cochlear pathology in monkeys after noise exposure. *Acta Otolaryngol*, *81*(3-4), 337-343. https://doi.org/10.3109/00016487609119971

Hawkins, J. E., Jr., & Stevens, S. S. (1950). The masking of pure tones and of speech by white noise. *J Acoust Soc Am*, *22*(1), 6-13.

Heeringa, A. N., & van Dijk, P. (2016). The immediate effects of acoustic trauma on excitation and inhibition in the inferior colliculus: A Wiener-kernel analysis. *Hear Res*, *331*, 47-56. https://doi.org/10.1016/j.heares.2015.10.007

Heil, P. (2014). Towards a unifying basis of auditory thresholds: binaural summation. *J Assoc Res Otolaryngol*, *15*(2), 219-234. https://doi.org/10.1007/s10162-013-0432-x

Heil, P., & Peterson, A. J. (2015). Basic response properties of auditory nerve fibers: a review. *Cell Tissue Res*, *361*(1), 129-158. https://doi.org/10.1007/s00441-015-2177-9

Heinz, M. G., Colburn, H. S., & Carney, L. H. (2002). Quantifying the implications of nonlinear cochlear tuning for auditory-filter estimates. *J Acoust Soc Am*, *111*(2), 996-1011. https://doi.org/10.1121/1.1436071

Hempstock, T. I., Bryan, M. E., & Webster, J. B. C. (1966). Free field threshold variance. *Journal of Sound and Vibration*, *4*(1), 33-44. https://doi.org/https://doi.org/10.1016/0022-460X(66)90151-9

Henry, K. S. (2022). Animal models of hidden hearing loss: Does auditory-nerve-fiber loss cause real-world listening difficulties? *Mol Cell Neurosci*, *118*, 103692. https://doi.org/10.1016/j.mcn.2021.103692

Henry, K. S., & Abrams, K. S. (2021). Normal Tone-In-Noise Sensitivity in Trained Budgerigars despite Substantial Auditory-Nerve Injury: No Evidence of Hidden Hearing Loss. *J Neurosci*, *41*(1), 118-129. https://doi.org/10.1523/JNEUROSCI.2104-20.2020

Henry, K. S., Kale, S., & Heinz, M. G. (2014). Noise-induced hearing loss increases the temporal precision of complex envelope coding by auditory-nerve fibers. *Front Syst Neurosci*, *8*, 20. https://doi.org/10.3389/fnsys.2014.00020

Hickman, T. T., Hashimoto, K., Liberman, L. D., & Liberman, M. C. (2020). Synaptic migration and reorganization after noise exposure suggests regeneration in a mature mammalian cochlea. *Sci Rep*, *10*(1), 19945. https://doi.org/10.1038/s41598-020-76553-w

Hickman, T. T., Hashimoto, K., Liberman, L. D., & Liberman, M. C. (2021). Cochlear Synaptic Degeneration and Regeneration After Noise: Effects of Age and Neuronal Subgroup. *Front Cell Neurosci*, *15*, 684706. https://doi.org/10.3389/fncel.2021.684706

Hickman, T. T., Smalt, C., Bobrow, J., Quatieri, T., & Liberman, M. C. (2018). Blast-induced cochlear synaptopathy in chinchillas. *Sci Rep*, *8*(1), 10740. https://doi.org/10.1038/s41598-018-28924-7

Hickox, A. E., Larsen, E., Heinz, M. G., Shinobu, L., & Whitton, J. P. (2017). Translational issues in cochlear synaptopathy. *Hear Res*, *349*, 164-171. https://doi.org/10.1016/j.heares.2016.12.010

Higson, J. M., Morgan, N., Stephenson, H., & Haggard, M. P. (1996). Auditory performance and acoustic reflexes in young adults reporting listening difficulties. *Br J Audiol*, *30*(6), 381-387. https://doi.org/10.3109/03005369609078425

Higson, J. M., Stephenson, H., & Haggard, M. P. (1996). Binaural summation of the acoustic reflex. *Ear Hear*, *17*(4), 334-340. https://doi.org/10.1097/00003446-199608000-00005

Hind, S. E., Haines-Bazrafshan, R., Benton, C. L., Brassington, W., Towle, B., & Moore, D. R. (2011). Prevalence of clinical referrals having hearing thresholds within normal limits. *Int J Audiol*, *50*(10), 708-716. https://doi.org/10.3109/14992027.2011.582049

Hirsh, I. J. (1948). Binaural summation- a century of investigation. *Psychological Bulletin*, *45*(3), 193-206. https://doi.org/10.1037/h0059461

Hockley, A., Wu, C., & Shore, S. E. (2021). Cochlear nucleus small cells use olivocochlear collaterals to encode sounds in noise. *biorxiv*. https://doi.org/10.1101/2021.05.20.444983

Hockley, A., Wu, C., & Shore, S. E. (2022). Olivocochlear projections contribute to superior intensity coding in cochlear nucleus small cells. *J Physiol*, *600*(1), 61-73. https://doi.org/10.1113/JP282262

Hoffman, H. J., Dobie, R. A., Losonczy, K. G., Themann, C. L., & Flamme, G. A. (2017). Declining Prevalence of Hearing Loss in US Adults Aged 20 to 69 Years. *JAMA Otolaryngol Head Neck Surg*, *143*(3), 274-285. https://doi.org/10.1001/jamaoto.2016.3527

Honkura, Y., Matsuo, H., Murakami, S., Sakiyama, M., Mizutari, K., Shiotani, A., Yamamoto, M., Morita, I., Shinomiya, N., Kawase, T., Katori, Y., & Motohashi, H. (2016). NRF2 Is a Key Target for Prevention of Noise-Induced Hearing Loss by Reducing Oxidative Damage of Cochlea. *Sci Rep*, *6*, 19329. https://doi.org/10.1038/srep19329

Hood, L. J., Berlin, C. I., Bordelon, J., & Rose, K. (2003). Patients with auditory neuropathy/dys-synchrony lack efferent suppression of transient evoked otoacoustic emissions. *J Am Acad Audiol*, *14*(6), 302-313.

Hood, L. J., Berlin, C. I., Hurley, A., Cecola, R. P., & Bell, B. (1996). Contralateral suppression of transient-evoked otoacoustic emissions in humans: intensity effects. *Hear Res*, *101*(1-2), 113-118. https://doi.org/10.1016/s0378-5955(96)00138-4

Hu, N., Rutherford, M. A., & Green, S. H. (2020). Protection of cochlear synapses from noise-induced excitotoxic trauma by blockade of Ca(2+)-permeable AMPA receptors. *Proc Natl Acad Sci U S A*, *117*(7), 3828-3838. https://doi.org/10.1073/pnas.1914247117

Humes, L. E., Kidd, G. R., & Lentz, J. J. (2013). Auditory and cognitive factors underlying individual differences in aided speech-understanding among older adults. *Front Syst Neurosci*, *7*, 55. https://doi.org/10.3389/fnsys.2013.00055

Humes, L. E., Wilson, D. L., Barlow, N. N., & Garner, C. (2002). Changes in hearing-aid benefit following 1 or 2 years of hearing-aid use by older adults. *J Speech Lang Hear Res*, *45*(4), 772-782. https://doi.org/10.1044/1092-4388(2002/062)

Hunter-Duvar, I. M., & Elliott, D. N. (1973). Effects of intense auditory stimulation: hearing losses and inner ear changes in the squirrel monkey. II. *J Acoust Soc Am*, *54*(5), 1179-1183. https://doi.org/10.1121/1.1914364

Hurd, L. B., Hutson, K. A., & Morest, D. K. (1999). Cochlear nerve projections to the small cell shell of the cochlear nucleus: the neuroanatomy of extremely thin sensory axons. *Synapse*, *33*(2), 83-117. https://doi.org/10.1002/(sici)1098-2396(199908)33:2<83::Aid-syn1>3.0.Co;2-9

Ikeda, K., Sekiguchi, T., & Hayashi, A. (2008). Attention-related modulation of auditory brainstem responses during contralateral noise exposure. *Neuroreport*, *19*(16), 1593-1599. https://doi.org/10.1097/WNR.0b013e32831269be

Irving, S., Moore, D. R., Liberman, M. C., & Sumner, C. J. (2011). Olivocochlear efferent control in sound localization and experience-dependent learning. *J Neurosci*, *31*(7), 2493-2501. https://doi.org/10.1523/JNEUROSCI.2679-10.2011

Jacobson, M., Kim, S., Romney, J., Zhu, X., & Frisina, R. D. (2003). Contralateral suppression of distortion-product otoacoustic emissions declines with age: a comparison of findings in CBA mice with human listeners. *Laryngoscope*, *113*(10), 1707-1713. https://doi.org/10.1097/00005537-200310000-00009

Jean, P., Lopez de la Morena, D., Michanski, S., Jaime Tobon, L. M., Chakrabarti, R., Picher, M. M., Neef, J., Jung, S., Gultas, M., Maxeiner, S., Neef, A., Wichmann, C., Strenzke, N., Grabner, C., & Moser, T. (2018). The synaptic ribbon is critical for sound encoding at high rates and with temporal precision. *Elife*, *7*. https://doi.org/10.7554/eLife.29275

Jennings, S. G., Ahlstrom, J. B., & Dubno, J. R. (2016). Effects of age and hearing loss on overshoot. *J Acoust Soc Am*, *140*(4), 2481. https://doi.org/10.1121/1.4964267

Jennings, S. G., Heinz, M. G., & Strickland, E. A. (2011). Evaluating adaptation and olivocochlear efferent feedback as potential explanations of psychophysical overshoot. *J Assoc Res Otolaryngol*, *12*(3), 345-360. https://doi.org/10.1007/s10162-011-0256-5

Jennings, S. G., Strickland, E. A., & Heinz, M. G. (2009). Precursor effects on behavioral estimates of frequency selectivity and gain in forward masking. *J Acoust Soc Am*, *125*(4), 2172-2181. https://doi.org/10.1121/1.3081383

Jerger, J., Mauldin, L., & Igarashi, M. (1978a). Impedance audiometry in the squirrel monkey. Effect of middle ear surgery. *Arch Otolaryngol*, *104*(4), 214-224. https://doi.org/10.1001/archotol.1978.00790040036008

Jerger, J., Mauldin, L., & Igarashi, M. (1978b). Impedance audiometry in the squirrel monkey. Sensorineural losses. *Arch Otolaryngol*, *104*(10), 559-563. https://doi.org/10.1001/archotol.1978.00790100013003

Jesteadt, W., Bacon, S. P., & Lehman, J. R. (1982). Forward masking as a function of frequency, masker level, and signal delay. *J Acoust Soc Am*, *71*(4), 950-962. https://doi.org/10.1121/1.387576

Johnsson, L. G., & Hawkins, J. E., Jr. (1967). A direct approach to cochlear anatomy and pathology in man. *Arch Otolaryngol*, *85*(6), 599-613. https://doi.org/10.1001/archotol.1967.00760040601005

Joris, P. X., Schreiner, C. E., & Rees, A. (2004). Neural processing of amplitude-modulated sounds. *Physiol Rev*, *84*(2), 541-577. https://doi.org/10.1152/physrev.00029.2003

Kale, S., & Heinz, M. G. (2012). Temporal modulation transfer functions measured from auditory-nerve responses following sensorineural hearing loss. *Hear Res*, *286*(1-2), 64-75. https://doi.org/10.1016/j.heares.2012.02.004

Kamerer, A. M., Harris, S. E., Kopun, J. G., Neely, S. T., & Rasetshwane, D. M. (2021). Understanding Self-reported Hearing Disability in Adults With Normal Hearing. *Ear Hear*. https://doi.org/10.1097/AUD.0000000000001161

Kawase, T., Delgutte, B., & Liberman, M. C. (1993). Antimasking effects of the olivocochlear reflex. II. Enhancement of auditory-nerve response to masked tones. *J Neurophysiol*, *70*(6), 2533-2549. https://doi.org/10.1152/jn.1993.70.6.2533

Keefe, D. H., Feeney, M. P., Hunter, L. L., & Fitzpatrick, D. F. (2017). Aural Acoustic Stapedius-Muscle Reflex Threshold Procedures to Test Human Infants and Adults. *J Assoc Res Otolaryngol*, *18*(1), 65-88. https://doi.org/10.1007/s10162-016-0599-z

Keefe, D. H., Schairer, K. S., Ellison, J. C., Fitzpatrick, D. F., & Jesteadt, W. (2009). Use of stimulus-frequency otoacoustic emissions to investigate efferent and cochlear contributions to temporal overshoot. *J Acoust Soc Am*, *125*(3), 1595-1604. https://doi.org/10.1121/1.3068443

Kemp, D. T. (1978). Stimulated acoustic emissions from within the human auditory system. *J Acoust Soc Am*, *64*(5), 1386-1391. https://doi.org/10.1121/1.382104

Keppler, H., Dhooge, I., Corthals, P., Maes, L., D'Haenens, W., Bockstael, A., Philips, B., Swinnen, F., & Vinck, B. (2010). The effects of aging on evoked otoacoustic emissions and efferent suppression of transient evoked otoacoustic emissions. *Clin Neurophysiol*, *121*(3), 359-365. https://doi.org/10.1016/j.clinph.2009.11.003

Keshishzadeh, S., Garrett, M., Vasilkov, V., & Verhulst, S. (2020). The derived-band envelope following response and its sensitivity to sensorineural hearing deficits. *Hear Res*, *392*, 107979. https://doi.org/10.1016/j.heares.2020.107979

Kiang, N. Y. (1965). Discharge patterns of single fibers in the cat's auditory nerve. In *Vol Research Monograph No. 35*. The M.I.T. Press.

Kidd, G., Jr., & Feth, L. L. (1982). Effects of masker duration in pure-tone forward masking. *J Acoust Soc Am*, *72*(5), 1384-1386. https://doi.org/10.1121/1.388443

Kidd, G., Jr., Mason, C. R., & Feth, L. L. (1984). Temporal integration of forward masking in listeners having sensorineural hearing loss. *J Acoust Soc Am*, *75*(3), 937-944. https://doi.org/10.1121/1.390558

Kim, J. U., Ahn, Y. S., Suh, J. K., & Chung, J. W. (2012). Effect of isoflurane on the hearing in mice. *Korean J Audiol*, *16*(1), 14-17. https://doi.org/10.7874/kja.2012.16.1.14

Kim, K. X., Payne, S., Yang-Hood, A., Li, S. Z., Davis, B., Carlquist, J., B, V. G., Gantz, J. A., Kallogjeri, D., Fitzpatrick, J. A. J., Ohlemiller, K. K., Hirose, K., & Rutherford, M. A. (2019). Vesicular Glutamatergic Transmission in Noise-Induced Loss and Repair of Cochlear Ribbon Synapses. *J Neurosci*, *39*(23), 4434-4447. https://doi.org/10.1523/JNEUROSCI.2228-18.2019

Kim, S., Frisina, D. R., & Frisina, R. D. (2002). Effects of age on contralateral suppression of distortion product otoacoustic emissions in human listeners with normal hearing. *Audiol Neurootol*, *7*(6), 348-357. https://doi.org/10.1159/000066159

Klein, A. J., & Mills, J. H. (1981). Physiological and psychophysical measures from humans with temporary threshold shift. *J Acoust Soc Am*, *70*(4), 1045-1053. https://doi.org/10.1121/1.386955

Klein, A. J., Mills, J. H., & Adkins, W. Y. (1990). Upward spread of masking, hearing loss, and speech recognition in young and elderly listeners. *J Acoust Soc Am*, *87*(3), 1266-1271. https://doi.org/10.1121/1.398802

Knudson, I. M., Shera, C. A., & Melcher, J. R. (2014). Increased contralateral suppression of otoacoustic emissions indicates a hyperresponsive medial olivocochlear system in humans with tinnitus and hyperacusis. *J Neurophysiol*, *112*(12), 3197-3208. https://doi.org/10.1152/jn.00576.2014

Kobler, J. B., Guinan, J. J., Jr., Vacher, S. R., & Norris, B. E. (1992). Acoustic reflex frequency selectivity in single stapedius motoneurons of the cat. *J Neurophysiol*, *68*(3), 807-817. https://doi.org/10.1152/jn.1992.68.3.807

Kobrina, A., Schrode, K. M., Screven, L. A., Javaid, H., Weinberg, M. M., Brown, G., Board, R., Villavisanis, D. F., Dent, M. L., & Lauer, A. M. (2020). Linking anatomical and physiological markers of auditory system degeneration with behavioral hearing assessments in a mouse (Mus musculus) model of age-related hearing loss. *Neurobiol Aging*, *96*, 87-103. https://doi.org/10.1016/j.neurobiolaging.2020.08.012

Koerner, T. K., M, A. P., & Gallun, F. J. (2020). A Questionnaire Survey of Current Rehabilitation Practices for Adults With Normal Hearing Sensitivity Who Experience Auditory Difficulties. *Am J Audiol*, *29*(4), 738-761. https://doi.org/10.1044/2020_AJA-20-00027

Kohrman, D. C., Wan, G., Cassinotti, L., & Corfas, G. (2020). Hidden Hearing Loss: A Disorder with Multiple Etiologies and Mechanisms. *Cold Spring Harb Perspect Med*, *10*(1). https://doi.org/10.1101/cshperspect.a035493

Koleilat, A., Driscoll, C. L. W., Schimmenti, L. A., & Poling, G. L. (2020). Emerging Therapies and Approaches to Treat and Prevent Hearing Loss. *Perspectives of the ASHA Special Interest Groups*, *5*(5), 1147-1165. https://doi.org/10.1044/2020_persp-20-00072

Kraus, N., Smith, D. I., Reed, N. L., Willott, J., & Erwin, J. (1985). Auditory brainstem and middle latency responses in non-human primates. *Hear Res*, *17*(3), 219-226. https://doi.org/10.1016/0378-5955(85)90066-8

Kujawa, S. G., Glattke, T. J., Fallon, M., & Bobbin, R. P. (1993). Contralateral sound suppresses distortion product otoacoustic emissions through cholinergic mechanisms. *Hear Res*, *68*(1), 97-106. https://doi.org/10.1016/0378-5955(93)90068-c

Kujawa, S. G., Glattke, T. J., Fallon, M., & Bobbin, R. P. (1994). A nicotinic-like receptor mediates suppression of distortion product otoacoustic emissions by contralateral sound. *Hear Res*, *74*(1-2), 122-134. https://doi.org/10.1016/0378-5955(94)90181-3

Kujawa, S. G., & Liberman, M. C. (2006). Acceleration of age-related hearing loss by early noise exposure: evidence of a misspent youth. *J Neurosci*, *26*(7), 2115-2123. https://doi.org/10.1523/JNEUROSCI.4985-05.2006

Kujawa, S. G., & Liberman, M. C. (2009). Adding insult to injury: cochlear nerve degeneration after "temporary" noise-induced hearing loss. *J Neurosci*, *29*(45), 14077-14085. https://doi.org/10.1523/JNEUROSCI.2845-09.2009

Kujawa, S. G., & Liberman, M. C. (2015). Synaptopathy in the noise-exposed and aging cochlea: Primary neural degeneration in acquired sensorineural hearing loss. *Hear Res*, *330*(Pt B), 191-199. https://doi.org/10.1016/j.heares.2015.02.009

Kumar, G., Amen, F., & Roy, D. (2007). Normal hearing tests: is a further appointment really necessary? *J R Soc Med*, *100*(2), 66. https://doi.org/10.1177/014107680710000212

Kumar, U. A., Methi, R., & Avinash, M. C. (2013). Test/retest repeatability of effect contralateral acoustic stimulation on the magnitudes of distortion product otoacoustic emissions. *Laryngoscope*, *123*, 463-471.

Landegger, L. D., Psaltis, D., & Stankovic, K. M. (2016). Human audiometric thresholds do not predict specific cellular damage in the inner ear. *Hear Res*, *335*, 83-93. https://doi.org/10.1016/j.heares.2016.02.018

Lasky, R. E., Beach, K. E., & Laughlin, N. K. (2000). Immittance and otoacoustic emissions in rhesus monkeys and humans. *Audiology*, *39*(2), 61-69. https://doi.org/10.3109/00206090009073055

Lasky, R. E., Snodgrass, E. B., Laughlin, N. K., & Hecox, K. E. (1995). Distortion product otoacoustic emissions in Macaca mulatta and humans. *Hear Res*, *89*(1-2), 35-51. https://doi.org/10.1016/0378-5955(95)00120-1

Lasky, R. E., Soto, A. A., Luck, M. L., & Laughlin, N. K. (1999). Otoacoustic emission, evoked potential, and behavioral auditory thresholds in the rhesus monkey (Macaca mulatta). *Hear Res*, *136*(1-2), 35-43. https://doi.org/10.1016/s0378-5955(99)00100-8

Lauer, A. M., Fuchs, P. A., Ryugo, D. K., & Francis, H. W. (2012). Efferent synapses return to inner hair cells in the aging cochlea. *Neurobiol Aging*, *33*(12), 2892-2902. https://doi.org/10.1016/j.neurobiolaging.2012.02.007

Lauer, A. M., Jimenez, S. V., & Delano, P. H. (2021). Olivocochlear efferent effects on perception and behavior. *Hear Res*, 108207. https://doi.org/10.1016/j.heares.2021.108207

Le Prell, C. G., Yagi, M., Kawamoto, K., Beyer, L. A., Atkin, G., Raphael, Y., Dolan, D. F., Bledsoe, S. C., Jr., & Moody, D. B. (2004). Chronic excitotoxicity in the guinea pig cochlea induces temporary functional deficits without disrupting otoacoustic emissions. *J Acoust Soc Am*, *116*(2), 1044-1056. https://doi.org/10.1121/1.1772395

Lee, J. H., Lee, M. Y., Choi, J. E., & Jung, J. Y. (2020). Auditory Brainstem Response to Paired Click Stimulation as an Indicator of Peripheral Synaptic Health in Noise-Induced

Cochlear Synaptopathy. *Front Neurosci*, *14*, 596670. https://doi.org/10.3389/fnins.2020.596670

Lefebvre, P. P., Malgrange, B., Thiry, M., Breuskin, I., Van De Water, T. R., & Moonen, G. (2001). Supernumerary outer hair cells arise external to the last row of sensory cells in the organ of corti. *Acta Otolaryngol*, *121*(2), 164-168. https://doi.org/10.1080/000164801300043325

Letien, W. C., & Bess, F. H. (1975). Acoustic reflex relaxation in sensorineural hearing loss. *Arch Otolaryngol*, *101*(10), 617-621. https://doi.org/10.1001/archotol.1975.00780390031008

Liberman, L. D., & Liberman, M. C. (2016). Postnatal maturation of auditory-nerve heterogeneity, as seen in spatial gradients of synapse morphology in the inner hair cell area. *Hear Res*, *339*, 12-22. https://doi.org/10.1016/j.heares.2016.06.002

Liberman, L. D., & Liberman, M. C. (2019). Cochlear Efferent Innervation Is Sparse in Humans and Decreases with Age. *J Neurosci*, *39*(48), 9560-9569. https://doi.org/10.1523/JNEUROSCI.3004-18.2019

Liberman, L. D., Suzuki, J., & Liberman, M. C. (2015). Dynamics of cochlear synaptopathy after acoustic overexposure. *J Assoc Res Otolaryngol*, *16*(2), 205-219. https://doi.org/10.1007/s10162-015-0510-3

Liberman, L. D., Wang, H., & Liberman, M. C. (2011). Opposing gradients of ribbon size and AMPA receptor expression underlie sensitivity differences among cochlear-nerve/hair-cell synapses. *J Neurosci*, *31*(3), 801-808. https://doi.org/10.1523/JNEUROSCI.3389-10.2011

Liberman, M. C. (1988). Physiology of cochlear efferent and afferent neurons: direct comparisons in the same animal. *Hear Res*, *34*(2), 179-191. https://doi.org/10.1016/0378-5955(88)90105-0

Liberman, M. C. (1991). Central projections of auditory-nerve fibers of differing spontaneous rate. I. Anteroventral cochlear nucleus. *J Comp Neurol*, *313*(2), 240-258. https://doi.org/10.1002/cne.903130205

Liberman, M. C., & Dodds, L. W. (1984a). Single-neuron labeling and chronic cochlear pathology. II. Stereocilia damage and alterations of spontaneous discharge rates. *Hear Res*, *16*(1), 43-53. https://doi.org/10.1016/0378-5955(84)90024-8

Liberman, M. C., & Dodds, L. W. (1984b). Single-neuron labeling and chronic cochlear pathology. III. Stereocilia damage and alterations of threshold tuning curves. *Hear Res*, *16*(1), 55-74. https://doi.org/10.1016/0378-5955(84)90025-x

Liberman, M. C., Dodds, L. W., & Pierce, S. (1990). Afferent and efferent innervation of the cat cochlea: quantitative analysis with light and electron microscopy. *J Comp Neurol*, *301*(3), 443-460. https://doi.org/10.1002/cne.903010309

Liberman, M. C., Epstein, M. J., Cleveland, S. S., Wang, H., & Maison, S. F. (2016). Toward a Differential Diagnosis of Hidden Hearing Loss in Humans. *PLoS One*, *11*(9), e0162726. https://doi.org/10.1371/journal.pone.0162726

Liberman, M. C., & Guinan, J. J., Jr. (1998). Feedback control of the auditory periphery: anti-masking effects of middle ear muscles vs. olivocochlear efferents. *J Commun Disord*, *31*(6), 471-482; quiz 483; 553. https://doi.org/10.1016/s0021-9924(98)00019-7

Liberman, M. C., & Kiang, N. Y. (1984). Single-neuron labeling and chronic cochlear pathology. IV. Stereocilia damage and alterations in rate- and phase-level functions. *Hear Res*, *16*(1), 75-90. https://doi.org/10.1016/0378-5955(84)90026-1

Liberman, M. C., & Kiang, N. Y. S. (1978). Acoustic trauma in cats: Cochlear pathology and auditory nerve activity. *Acta Oto-Laryngologica*, *86*(Suppl. 358), 1-63. https://doi.org/10.3109/00016487809127889

Liberman, M. C., & Simmons, D. D. (1985). Applications of neuronal labeling techniques to the study of the peripheral auditory system. *J Acoust Soc Am*, *78*(1 Pt 2), 312-319. https://doi.org/10.1121/1.392492

Lin, H. W., Furman, A. C., Kujawa, S. G., & Liberman, M. C. (2011). Primary neural degeneration in the Guinea pig cochlea after reversible noise-induced threshold shift. *J Assoc Res Otolaryngol*, *12*(5), 605-616. https://doi.org/10.1007/s10162-011-0277-0

Lindgren, F., Nilsson, R., & Axelsson, A. (1983). The acoustic reflex threshold in relation to noise-induced hearing loss. *Scand Audiol*, *12*(1), 49-55. https://doi.org/10.3109/01050398309076224

Liu, C., Glowatzki, E., & Fuchs, P. A. (2015). Unmyelinated type II afferent neurons report cochlear damage. *Proc Natl Acad Sci U S A*, *112*(47), 14723-14727. https://doi.org/10.1073/pnas.1515228112

Liu, L., Wang, H., Shi, L., Almuklass, A., He, T., Aiken, S., Bance, M., Yin, S., & Wang, J. (2012). Silent damage of noise on cochlear afferent innervation in guinea pigs and the impact on temporal processing. *PLoS One*, *7*(11), e49550. https://doi.org/10.1371/journal.pone.0049550

Lobarinas, E., Salvi, R., & Ding, D. (2013). Insensitivity of the audiogram to carboplatin induced inner hair cell loss in chinchillas. *Hear Res*, *302*, 113-120. https://doi.org/10.1016/j.heares.2013.03.012

Lobarinas, E., Salvi, R., & Ding, D. (2016). Selective Inner Hair Cell Dysfunction in Chinchillas Impairs Hearing-in-Noise in the Absence of Outer Hair Cell Loss. *J Assoc Res Otolaryngol*, *17*(2), 89-101. https://doi.org/10.1007/s10162-015-0550-8

Lobarinas, E., Spankovich, C., & Le Prell, C. G. (2017). Evidence of "hidden hearing loss" following noise exposures that produce robust TTS and ABR wave-I amplitude reductions. *Hear Res*, *349*, 155-163. https://doi.org/10.1016/j.heares.2016.12.009

Lonsbury-Martin, B. L., Martin, G. K., Probst, R., & Coats, A. C. (1988). Spontaneous otoacoustic emissions in a nonhuman primate. II. Cochlear anatomy. *Hear Res*, *33*(1), 69-93. https://doi.org/10.1016/0378-5955(88)90021-4

Lopez-Poveda, E. A. (2014). Why do I hear but not understand? Stochastic undersampling as a model of degraded neural encoding of speech. *Front Neurosci*, *8*, 348. https://doi.org/10.3389/fnins.2014.00348

Lopez-Poveda, E. A. (2018). Olivocochlear Efferents in Animals and Humans: From Anatomy to Clinical Relevance. *Front Neurol*, *9*, 197. https://doi.org/10.3389/fneur.2018.00197

Lopez-Poveda, E. A., & Barrios, P. (2013). Perception of stochastically undersampled sound waveforms: a model of auditory deafferentation. *Front Neurosci*, *7*, 124. https://doi.org/10.3389/fnins.2013.00124

Lund, J. P., Sun, G. D., & Lamarre, Y. (1994). Cortical reorganization and deafferentation in adult macaques. *Science*, *265*(5171), 546-548. https://doi.org/10.1126/science.8036500

Lurie, M. H., Davis, H., & Hawkins Jr., J. E. (1944). Acoustic trauma of the organ of corti in the guinea pig. *The Laryngoscope*, *54*(8), 375-386. https://doi.org/https://doi.org/10.1288/00005537-194408000-00001

Mackey, C. A., McCrate, J., MacDonald, K. S., Feller, J., Liberman, L., Liberman, M. C., Hackett, T. A., & Ramachandran, R. (2021). Correlations between cochlear

pathophysiology and behavioral measures of temporal and spatial processing in noise exposed macaques. *Hear Res*, *401*, 108156. https://doi.org/10.1016/j.heares.2020.108156

Mahoney, T., Vernon, J., & Meikle, M. (1979). Function of the Acoustic Reflex in Discrimination of Intense Speech. *Archives of Otolaryngology*, *105*(3), 119-123. https://doi.org/10.1001/archotol.1979.00790150009003

Maison, S., Liberman, L. D., & Liberman, M. C. (2016). Type II Cochlear Ganglion Neurons Do Not Drive the Olivocochlear Reflex: Re-Examination of the Cochlear Phenotype in Peripherin Knock-Out Mice. *eNeuro*, *3*(4). https://doi.org/10.1523/ENEURO.0207-16.2016

Maison, S. F., & Liberman, M. C. (2000). Predicting vulnerability to acoustic injury with a noninvasive assay of olivocochlear reflex strength. *J Neurosci*, *20*(12), 4701-4707. https://doi.org/10.1523/jneurosci.20-12-04701.2000

Maison, S. F., Usubuchi, H., & Liberman, M. C. (2013). Efferent feedback minimizes cochlear neuropathy from moderate noise exposure. *J Neurosci*, *33*(13), 5542-5552. https://doi.org/10.1523/JNEUROSCI.5027-12.2013

Makary, C. A., Shin, J., Kujawa, S. G., Liberman, M. C., & Merchant, S. N. (2011). Age-related primary cochlear neuronal degeneration in human temporal bones. *J Assoc Res Otolaryngol*, *12*(6), 711-717. https://doi.org/10.1007/s10162-011-0283-2

Mangham, C. A., Jr., Burnett, P. A., & Lindeman, R. C. (1982). Standardization of acoustic reflex latency: a study in humans and nonhuman primates. *Ann Otol Rhinol Laryngol*, *91*(2 Pt 1), 169-174. https://doi.org/10.1177/000348948209100211

Marcenaro, B., Leiva, A., Dragicevic, C., Lopez, V., & Delano, P. H. (2021). The medial olivocochlear reflex strength is modulated during a visual working memory task. *J Neurophysiol*, *125*(6), 2309-2321. https://doi.org/10.1152/jn.00032.2020

Margolis, R. H. (1993). Detection of hearing impairment with the acoustic stapedius reflex. *Ear Hear*, *14*(1), 3-10. https://doi.org/10.1097/00003446-199302000-00002

Margolis, R. H., Dubno, J. R., & Wilson, R. H. (1980). Acoustic-reflex thresholds for noise stimuli. *J Acoust Soc Am*, *68*(3), 892-895. https://doi.org/10.1121/1.384828

Margolis, R. H., & Goldberg, S. M. (1980). Auditory frequency selectivity in normal and presbycusic subjects. *J Speech Lang Hear Res*, *23*, 603-613.

Marks, K. L., & Siegel, J. H. (2017). Differentiating Middle Ear and Medial Olivocochlear Effects on Transient-Evoked Otoacoustic Emissions. *J Assoc Res Otolaryngol*, *18*(4), 529-542. https://doi.org/10.1007/s10162-017-0621-0

Marmel, F., Cortese, D., & Kluk, K. (2020). The ongoing search for cochlear synaptopathy in humans: Masked thresholds for brief tones in Threshold Equalizing Noise. *Hear Res*, *392*, 107960. https://doi.org/10.1016/j.heares.2020.107960

Matthews, G., & Fuchs, P. (2010). The diverse roles of ribbon synapses in sensory neurotransmission. *Nat Rev Neurosci*, *11*(12), 812-822. https://doi.org/10.1038/nrn2924

McFadden, D. (1989). Spectral differences in the ability of temporal gaps to reset the mechanisms underlying overshoot. *J Acoust Soc Am*, *85*(1), 254-261. https://doi.org/10.1121/1.397732

McFadden, D., & Champlin, C. A. (1990). Reductions in overshoot during aspirin use. *J Acoust Soc Am*, *87*(6), 2634-2642. https://doi.org/10.1121/1.399056

McFadden, D., Champlin, C. A., Pho, M. H., Pasanen, E. G., Maloney, M. M., & Leshikar, E. M. (2021). Auditory evoked potentials: Differences by sex, race, and menstrual cycle and correlations with common psychoacoustical tasks. *PLoS One*, *16*(5), e0251363. https://doi.org/10.1371/journal.pone.0251363

McFadden, D., Martin, G. K., Stagner, B. B., & Maloney, M. M. (2009). Sex differences in distortion-product and transient-evoked otoacoustic emissions compared. *J Acoust Soc Am*, *125*(1), 239-246. https://doi.org/10.1121/1.3037231

McFadden, D., & Pasanen, E. G. (1998). Comparison of the auditory systems of heterosexuals and homosexuals: click-evoked otoacoustic emissions. *Proc Natl Acad Sci U S A*, *95*(5), 2709-2713. https://doi.org/10.1073/pnas.95.5.2709

McFadden, D., Pasanen, E. G., Raper, J., Lange, H. S., & Wallen, K. (2006). Sex differences in otoacoustic emissions measured in rhesus monkeys (Macaca mulatta). *Horm Behav*, *50*(2), 274-284. https://doi.org/10.1016/j.yhbeh.2006.03.012

McFadden, D., Walsh, K. P., Pasanen, E. G., & Grenwelge, E. M. (2010). Overshoot using very short signal delays. *J Acoust Soc Am*, *128*(4), 1915-1921. https://doi.org/10.1121/1.3480568

McFadden, S. L., Kasper, C., Ostrowski, J., Ding, D., & Salvi, R. J. (1998). Effects of inner hair cell loss on inferior colliculus evoked potential thresholds, amplitudes and forward

masking functions in chinchillas. *Hear Res*, *120*(1-2), 121-132. https://doi.org/10.1016/s0378-5955(98)00052-5

McFadden, S. L., Quaranta, N., & Henderson, D. (1997). Suprathreshold measures of auditory function in the aging chinchilla. *Hearing Research*, *111*(1-2), 127-135. https://doi.org/10.1016/s0378-5955(97)00100-7

McLeod, A., Burton, J. A., Mackey, C. A., & Ramachandran, R. (re-submitted). *An assessment of ambient noise conditions in a non-human primate facility*.

Mehraei, G., Gallardo, A. P., Shinn-Cunningham, B. G., & Dau, T. (2017). Auditory brainstem response latency in forward masking, a marker of sensory deficits in listeners with normal hearing thresholds. *Hear Res*, *346*, 34-44. https://doi.org/10.1016/j.heares.2017.01.016

Mehraei, G., Hickox, A. E., Bharadwaj, H. M., Goldberg, H., Verhulst, S., Liberman, M. C., & Shinn-Cunningham, B. G. (2016). Auditory Brainstem Response Latency in Noise as a Marker of Cochlear Synaptopathy. *J Neurosci*, *36*(13), 3755-3764. https://doi.org/10.1523/JNEUROSCI.4460-15.2016

Mepani, A. M., Kirk, S. A., Hancock, K. E., Bennett, K., de Gruttola, V., Liberman, M. C., & Maison, S. F. (2020). Middle Ear Muscle Reflex and Word Recognition in "Normal-Hearing" Adults: Evidence for Cochlear Synaptopathy? *Ear Hear*, *41*(1), 25-38. https://doi.org/10.1097/AUD.0000000000000804

Mertes, I. B. (2020). Establishing critical differences in ear-canal stimulus amplitude for detecting middle ear muscle reflex activation during olivocochlear efferent measurements. *Int J Audiol*, *59*(2), 140-147. https://doi.org/10.1080/14992027.2019.1673491

Mertes, I. B., Johnson, K. M., & Dinger, Z. A. (2019). Olivocochlear efferent contributions to speech-in-noise recognition across signal-to-noise ratios. *J Acoust Soc Am*, *145*(3), 1529. https://doi.org/10.1121/1.5094766

Mertes, I. B., & Leek, M. R. (2016). Concurrent measures of contralateral suppression of transient-evoked otoacoustic emissions and of auditory steady-state responses. *J Acoust Soc Am*, *140*(3), 2027. https://doi.org/10.1121/1.4962666

Miller, R. L., Schilling, J. R., Franck, K. R., & Young, E. D. (1997). Effects of acoustic trauma on the representation of the vowel "eh" in cat auditory nerve fibers. *J Acoust Soc Am*, *101*(6), 3602-3616. https://doi.org/10.1121/1.418321

Mohrle, D., Ni, K., Varakina, K., Bing, D., Lee, S. C., Zimmermann, U., Knipper, M., & Ruttiger, L. (2016). Loss of auditory sensitivity from inner hair cell synaptopathy can be centrally compensated in the young but not old brain. *Neurobiol Aging*, *44*, 173-184. https://doi.org/10.1016/j.neurobiolaging.2016.05.001

Moller, A. R. (1962). Acoustic reflex in man. *J Acoust Soc Am*, *34*(8, Pt. II), 1524-1534. https://doi.org/10.1121/1.1918384

Monaghan, J. J. M., Garcia-Lazaro, J. A., McAlpine, D., & Schaette, R. (2020). Hidden Hearing Loss Impacts the Neural Representation of Speech in Background Noise. *Curr Biol*, *30*(23), 4710-4721 e4714. https://doi.org/10.1016/j.cub.2020.09.046

Moore, B. C., & Glasberg, B. R. (1981). Auditory filter shapes derived in simultaneous and forward masking. *J Acoust Soc Am*, *70*(4), 1003-1014. https://doi.org/10.1121/1.386950

Moser, T., Grabner, C. P., & Schmitz, F. (2020). Sensory Processing at Ribbon Synapses in the Retina and the Cochlea. *Physiol Rev*, *100*(1), 103-144. https://doi.org/10.1152/physrev.00026.2018

Moser, T., Neef, A., & Khimich, D. (2006). Mechanisms underlying the temporal precision of sound coding at the inner hair cell ribbon synapse. *J Physiol*, *576*(Pt 1), 55-62. https://doi.org/10.1113/jphysiol.2006.114835

Moser, T., & Starr, A. (2016). Auditory neuropathy--neural and synaptic mechanisms. *Nat Rev Neurol*, *12*(3), 135-149. https://doi.org/10.1038/nrneurol.2016.10

Moulin, A., Collet, L., Veuillet, E., & Morgon, A. (1993). Interrelations between transiently evoked otoacoustic emissions, spontaneous otoacoustic emissions and acoustic distortion products in normally hearing subjects. *Hear Res*, *65*(1-2), 216-233. https://doi.org/10.1016/0378-5955(93)90215-m

Mulders, W. H., Ding, D., Salvi, R., & Robertson, D. (2011). Relationship between auditory thresholds, central spontaneous activity, and hair cell loss after acoustic trauma. *J Comp Neurol*, *519*(13), 2637-2647. https://doi.org/10.1002/cne.22644

Mulders, W. H., & Robertson, D. (2011). Progressive centralization of midbrain hyperactivity after acoustic trauma. *Neuroscience*, *192*, 753-760. https://doi.org/10.1016/j.neuroscience.2011.06.046

Mulders, W. H., & Robertson, D. (2013). Development of hyperactivity after acoustic trauma in the guinea pig inferior colliculus. *Hear Res*, *298*, 104-108. https://doi.org/10.1016/j.heares.2012.12.008

Musiek, F. E., Chermak, G. D., Bamiou, D.-E., & Shinn, J. (2018). CAPD: The Most Common 'Hidden Hearing Loss'. *The ASHA Leader*, *23*(3), 6-9. https://doi.org/10.1044/leader.FMP.23032018.6

Naguib, S., Backstrom, J. R., Gil, M., Calkins, D. J., & Rex, T. S. (2021). Retinal oxidative stress activates the NRF2/ARE pathway: An early endogenous protective response to ocular hypertension. *Redox Biol*, *42*, 101883. https://doi.org/10.1016/j.redox.2021.101883

Nelson, D. A., & Freyman, R. L. (1987). Temporal resolution in sensorineural hearing-impaired listeners. *J Acoust Soc Am*, *81*(3), 709-720. https://doi.org/10.1121/1.395131

Nelson, P. C., Smith, Z. M., & Young, E. D. (2009). Wide-dynamic-range forward suppression in marmoset inferior colliculus neurons is generated centrally and accounts for perceptual masking. *J Neurosci*, *29*(8), 2553-2562. https://doi.org/10.1523/JNEUROSCI.5359-08.2009

Ng, C. W., Navarro, X., Engle, J. R., & Recanzone, G. H. (2015). Age-related changes of auditory brainstem responses in nonhuman primates. *J Neurophysiol*, *114*(1), 455-467. https://doi.org/10.1152/jn.00663.2014

Nouvian, R., Beutner, D., Parsons, T. D., & Moser, T. (2006). Structure and function of the hair cell ribbon synapse. *J Membr Biol*, *209*(2-3), 153-165. https://doi.org/10.1007/s00232-005-0854-4

Occelli, F., Hasselmann, F., Bourien, J., Puel, J. L., Desvignes, N., Wiszniowski, B., Edeline, J. M., & Gourevitch, B. (2022). Temporal Alterations to Central Auditory Processing without Synaptopathy after Lifetime Exposure to Environmental Noise. *Cereb Cortex*, *32*(8), 1737-1754. https://doi.org/10.1093/cercor/bhab310

Oxenham, A. J. (2001). Forward masking: adaptation or integration? *J Acoust Soc Am*, *109*(2), 732-741. https://doi.org/10.1121/1.1336501

Oxenham, A. J. (2016). Predicting the Perceptual Consequences of Hidden Hearing Loss. *Trends Hear*, *20*, 2331216516686768. https://doi.org/10.1177/2331216516686768

Parida, S., & Heinz, M. G. (2022). Distorted Tonotopy Severely Degrades Neural Representations of Connected Speech in Noise following Acoustic Trauma. *J Neurosci*, *42*(8), 1477-1490. https://doi.org/10.1523/JNEUROSCI.1268-21.2021

Park, J. Y., Clark, W. W., Coticchia, J. M., Esselman, G. H., & Fredrickson, J. M. (1995). Distortion product otoacoustic emissions in rhesus (Macaca mulatta) monkey ears: normative findings. *Hear Res*, *86*(1-2), 147-162. https://doi.org/10.1016/0378-5955(95)00065-c

Parthasarathy, A., Hancock, K. E., Bennett, K., DeGruttola, V., & Polley, D. B. (2020). Bottom-up and top-down neural signatures of disordered multi-talker speech perception in adults with normal hearing. *Elife*, *9*. https://doi.org/10.7554/eLife.51419

Patterson, R. D., & Nimmo-Smith, I. (1980). Off-frequency listening and auditory-filter asymmetry. *J Acoust Soc Am*, *67*(1), 229-245. https://doi.org/10.1121/1.383732

Paul, B. T., Bruce, I. C., & Roberts, L. E. (2017). Evidence that hidden hearing loss underlies amplitude modulation encoding deficits in individuals with and without tinnitus. *Hear Res*, *344*, 170-182. https://doi.org/10.1016/j.heares.2016.11.010

Peacock, J., Mackey, C. A., Benson, M. A., Burton, J. A., Greene, N. T., Ramachandran, R., & Tollin, D. J. (2021). The Binaural Interaction Component in Rhesus Macaques (Macaca mulatta). *eNeuro*, *8*(6). https://doi.org/10.1523/ENEURO.0402-21.2021

Peng, J.-H., Tao, Z.-Z., & Huang, Z.-W. (2007). Long-term sound conditioning increases distortion product otoacoustic emission amplitudes and decreases olivocochlear efferent reflex strength. *Neuroreport*, *18*(11), 1167-1170. https://doi.org/10.1097/WNR.0b013e32820049a8

Peters, D. H., Adam, T., Alonge, O., Agyepong, I. A., & Tran, N. (2014). Republished research: Implementation research: what it is and how to do it. *British Journal of Sports Medicine*, *48*(8), 731-736. https://doi.org/10.1136/bmj.f6753

Pfingst, B. E., Laycock, J., Flammino, F., Lonsbury-Martin, B., & Martin, G. (1978). Pure tone thresholds for the rhesus monkey. *Hear Res*, *1*(1), 43-47. https://doi.org/10.1016/0378-5955(78)90008-4

Phatak, S. A., Brungart, D. S., Zion, D. J., & Grant, K. W. (2019). Clinical Assessment of Functional Hearing Deficits: Speech-in-Noise Performance. *Ear Hear*, *40*(2), 426-436. https://doi.org/10.1097/AUD.0000000000000635

Pick, G. F., & Evans, E. F. (1983). Dissociation between frequency resolution and hearing threshold. In R. Klinke & R. Hartmann (Eds.), *HEARING — Physiological Bases and Psychophysics* (pp. 393-398). Springer. https://doi.org/10.1007/978-3-642-69257-4_57

Plack, C. J., Barker, D., & Prendergast, G. (2014). Perceptual consequences of "hidden" hearing loss. *Trends Hear*, *18*. https://doi.org/10.1177/2331216514550621

Pollack, I. (1948). Monaural and Binaural Threshold Sensitivity for Tones and for White Noise. *J Acoust Soc Am*, *20*(1), 52-57. https://doi.org/10.1121/1.1906347

Pons, T. P., Garraghty, P. E., Ommaya, A. K., Kaas, J. H., Taub, E., & Mishkin, M. (1991). Massive cortical reorganization after sensory deafferentation in adult macaques. *Science*, *252*(5014), 1857-1860. https://doi.org/10.1126/science.1843843

Prendergast, G., Couth, S., Millman, R. E., Guest, H., Kluk, K., Munro, K. J., & Plack, C. J. (2019). Effects of Age and Noise Exposure on Proxy Measures of Cochlear Synaptopathy. *Trends Hear*, *23*, 2331216519877301. https://doi.org/10.1177/2331216519877301

Prendergast, G., Tu, W., Guest, H., Millman, R. E., Kluk, K., Couth, S., Munro, K. J., & Plack, C. J. (2018). Supra-threshold auditory brainstem response amplitudes in humans: Test-retest reliability, electrode montage and noise exposure. *Hear Res*, *364*, 38-47. https://doi.org/10.1016/j.heares.2018.04.002

Puel, J. L., Ruel, J., Gervais d'Aldin, C., & Pujol, R. (1998). Excitotoxicity and repair of cochlear synapses after noise-trauma induced hearing loss. *Neuroreport*, *9*, 2109-2114.

Pugh, J. E., Jr., Horwitz, M. R., & Anderson, D. J. (1974). Cochlear electrical activity in noise-induced hearing loss: Behavioral and electrophysiological studies in primates. *Arch Otolaryngol*, *100*(1), 36-40. https://doi.org/10.1001/archotol.1974.00780040040008

Puria, S., Guinan, J. J., Jr., & Liberman, M. C. (1996). Olivocochlear reflex assays: effects of contralateral sound on compound action potentials versus ear-canal distortion products. *J Acoust Soc Am*, *99*(1), 500-507. https://doi.org/10.1121/1.414508

Qian, M., Wang, Q., Wang, Z., Ma, Q., Wang, X., Han, K., Wu, H., & Huang, Z. (2021). Dose-Dependent Pattern of Cochlear Synaptic Degeneration in C57BL/6J Mice Induced by

Repeated Noise Exposure. *Neural Plasticity*, *2021*, 9919977. https://doi.org/10.1155/2021/9919977

Quaranta, A., Salonna, I., & Longo, G. (1990). Subclinical changes of auditory function in the aged. *Acta Otolaryngol Suppl*, *476*, 91-95; discussion 96. https://doi.org/10.3109/00016489109127260

Race, N., Lai, J., Shi, R., & Bartlett, E. L. (2017). Differences in postinjury auditory system pathophysiology after mild blast and nonblast acute acoustic trauma. *J Neurophysiol*, *118*(2), 782-799. https://doi.org/10.1152/jn.00710.2016

Radtke-Schuller, S., Seeler, S., & Grothe, B. (2015). Restricted loss of olivocochlear but not vestibular efferent neurons in the senescent gerbil (Meriones unguiculatus). *Front Aging Neurosci*, *7*, 4. https://doi.org/10.3389/fnagi.2015.00004

Ralli, M., Greco, A., De Vincentiis, M., Sheppard, A., Cappelli, G., Neri, I., & Salvi, R. (2019). Tone-in-noise detection deficits in elderly patients with clinically normal hearing. *Am J Otolaryngol*, *40*(1), 1-9. https://doi.org/10.1016/j.amjoto.2018.09.012

Ramachandran, R., Davis, K. A., & May, B. J. (1999). Single-Unit Responses in the Inferior Colliculus of Decerebrate Cats I. Classification Based on Frequency Response Maps. *Journal of Neurophysiology*, *82*(1), 152-163. https://doi.org/10.1152/jn.1999.82.1.152

Rask-Andersen, H., Li, H., Lowenheim, H., Muller, M., Pfaller, K., Schrott-Fischer, A., & Glueckert, R. (2017). Supernumerary human hair cells-signs of regeneration or impaired development? A field emission scanning electron microscopy study. *Ups J Med Sci*, *122*(1), 11-19. https://doi.org/10.1080/03009734.2016.1271843

Relkin, E. M., & Doucet, J. R. (1991). Recovery from prior stimulation. I: Relationship to spontaneous firing rates of primary auditory neurons. *Hear Res*, *55*(2), 215-222. https://doi.org/10.1016/0378-5955(91)90106-j

Resnik, J., & Polley, D. B. (2021). Cochlear neural degeneration disrupts hearing in background noise by increasing auditory cortex internal noise. *Neuron*, *109*(6), 984-996 e984. https://doi.org/10.1016/j.neuron.2021.01.015

Rhode, W. S., & Greenberg, S. (1994). Lateral suppression and inhibition in the cochlear nucleus of the cat. *Journal of Neurophysiology*, *71*(2), 493-514. https://doi.org/10.1152/jn.1994.71.2.493

Ridley, C. L., Kopun, J. G., Neely, S. T., Gorga, M. P., & Rasetshwane, D. M. (2018). Using Thresholds in Noise to Identify Hidden Hearing Loss in Humans. *Ear Hear*, *39*(5), 829-844. https://doi.org/10.1097/AUD.0000000000000543

Rocchi, F., Dylla, M. E., Bohlen, P. A., & Ramachandran, R. (2017). Spatial and temporal disparity in signals and maskers affects signal detection in non-human primates. *Hear Res*, *344*, 1-12. https://doi.org/10.1016/j.heares.2016.10.013

Ruggero, M. A. (1992). Physiology and coding of sound in the auditory nerve. In R. R. Fay (Ed.), *The Mammalian Auditory Pathway: Neurophysiology* (Vol. 2, pp. 34-93). Springer-Verlag.

Sachs, M. B., Voigt, H. F., & Young, E. D. (1983). Auditory nerve representation of vowels in background noise. *J Neurophysiol*, *50*(1), 27-45. https://doi.org/10.1152/jn.1983.50.1.27

Sagers, J. E., Landegger, L. D., Worthington, S., Nadol, J. B., & Stankovic, K. M. (2017). Human Cochlear Histopathology Reflects Clinical Signatures of Primary Neural Degeneration. *Sci Rep*, *7*(1), 4884. https://doi.org/10.1038/s41598-017-04899-9

Salanger, M., & Parker, M. A. (2018). Synaptopathy in humans? Not so fast. *The Hearing Journal*, *71*(6), 8-9. https://doi.org/10.1097/01.HJ.0000538927.35055.48

Salloom, W. B., & Strickland, E. A. (2021). The effect of broadband elicitor laterality on psychoacoustic gain reduction across signal frequency. *J Acoust Soc Am*, *150*(4), 2817. https://doi.org/10.1121/10.0006662

Salvi, R. J., Wang, J., & Ding, D. (2000). Auditory plasticity and hyperactivity following cochlear damage. *Hear Res*, *147*(1-2), 261-274. https://doi.org/10.1016/s0378-5955(00)00136-2

Schaette, R., & McAlpine, D. (2011). Tinnitus with a normal audiogram: physiological evidence for hidden hearing loss and computational model. *J Neurosci*, *31*(38), 13452-13457. https://doi.org/10.1523/JNEUROSCI.2156-11.2011

Schairer, K. S., Feeney, M. P., & Sanford, C. A. (2013). Acoustic reflex measurement. *Ear Hear*, *34 Suppl 1*, 43s-47s. https://doi.org/10.1097/AUD.0b013e31829c70d9

Scharf, B., Magnan, J., & Chays, A. (1997). On the role of the olivocochlear bundle in hearing: 16 case studies. *Hearing Research*, *103*(1-2), 101-122. https://doi.org/10.1016/s0378-5955(96)00168-2

Scharf, B., Magnan, J., Collet, L., Ulmer, E., & Chays, A. (1994). On the role of the olivocochlear bundle in hearing: a case study. *Hear Res*, *75*(1-2), 11-26. https://doi.org/10.1016/0378-5955(94)90051-5

Scheidt, R. E., Kale, S., & Heinz, M. G. (2010). Noise-induced hearing loss alters the temporal dynamics of auditory-nerve responses. *Hear Res*, *269*(1-2), 23-33. https://doi.org/10.1016/j.heares.2010.07.009

Schmiedt, R. A., Mills, J. H., & Boettcher, F. A. (1996). Age-related loss of activity of auditory-nerve fibers. *J Neurophysiol*, *76*(4), 2799-2803. https://doi.org/10.1152/jn.1996.76.4.2799

Schrode, K. M., Muniak, M. A., Kim, Y. H., & Lauer, A. M. (2018). Central Compensation in Auditory Brainstem after Damaging Noise Exposure. *eNeuro*, *5*(4). https://doi.org/10.1523/ENEURO.0250-18.2018

Schuknecht, H. F., & Gacek, M. R. (1993). Cochlear pathology in presbycusis. *Ann Otol Rhinol Laryngol*, *102*(1 Pt 2), 1-16. https://doi.org/10.1177/00034894931020s101

Schuknecht, H. F., & Woellner, R. C. (1955). Hearing loss from lesions of the cochlear nerve: an experimental and clinical study. *Trans Am Acad Ophthalmol Otolaryngol*, *59*(2), 147-149.

Schwaber, M. K., Garraghty, P. E., & Kaas, J. H. (1993). Neuroplasticity of the adult primate auditory cortex following cochlear hearing loss. *Am J Otol*, *14*(3), 252-258.

Sergeyenko, Y., Lall, K., Liberman, M. C., & Kujawa, S. G. (2013). Age-related cochlear synaptopathy: an early-onset contributor to auditory functional decline. *J Neurosci*, *33*(34), 13686-13694. https://doi.org/10.1523/JNEUROSCI.1783-13.2013

Sha, S. H., & Schacht, J. (2017). Emerging therapeutic interventions against noise-induced hearing loss. *Expert Opin Investig Drugs*, *26*(1), 85-96. https://doi.org/10.1080/13543784.2017.1269171

Shaheen, L. A., & Liberman, M. C. (2018). Cochlear Synaptopathy Changes Sound-Evoked Activity Without Changing Spontaneous Discharge in the Mouse Inferior Colliculus. *Front Syst Neurosci*, *12*, 59. https://doi.org/10.3389/fnsys.2018.00059

Shaheen, L. A., Valero, M. D., & Liberman, M. C. (2015). Towards a Diagnosis of Cochlear Neuropathy with Envelope Following Responses. *J Assoc Res Otolaryngol*, *16*(6), 727-745. https://doi.org/10.1007/s10162-015-0539-3

Shaw, W. A., Newman, E. B., & Hirsh, I. J. (1947). The difference between monaural and binaural thresholds. *Journal of Experimental Psychology*, *37*(3), 229–242. https://doi.org/https://doi.org/10.1037/h0055386

Shehorn, J., Strelcyk, O., & Zahorik, P. (2020). Associations between speech recognition at high levels, the middle ear muscle reflex and noise exposure in individuals with normal audiograms. *Hear Res*, *392*, 107982. https://doi.org/10.1016/j.heares.2020.107982

Sheppard, A. M., Zhao, D. L., & Salvi, R. (2018). Isoflurane anesthesia suppresses distortion product otoacoustic emissions in rats. *J Otol*, *13*(2), 59-64. https://doi.org/10.1016/j.joto.2018.03.002

Shera, C. A., & Guinan, J. J., Jr. (1999). Evoked otoacoustic emissions arise by two fundamentally different mechanisms: a taxonomy for mammalian OAEs. *J Acoust Soc Am*, *105*(2 Pt 1), 782-798. https://doi.org/10.1121/1.426948

Shi, L., Chang, Y., Li, X., Aiken, S., Liu, L., & Wang, J. (2016). Cochlear Synaptopathy and Noise-Induced Hidden Hearing Loss. *Neural Plast*, *2016*, 6143164. https://doi.org/10.1155/2016/6143164

Shi, L., Liu, K., Wang, H., Zhang, Y., Hong, Z., Wang, M., Wang, X., Jiang, X., & Yang, S. (2015). Noise induced reversible changes of cochlear ribbon synapses contribute to temporary hearing loss in mice. *Acta Otolaryngol*, *135*(11), 1093-1102. https://doi.org/10.3109/00016489.2015.1061699

Shi, L., Liu, L., He, T., Guo, X., Yu, Z., Yin, S., & Wang, J. (2013). Ribbon synapse plasticity in the cochleae of Guinea pigs after noise-induced silent damage. *PLoS One*, *8*(12), e81566. https://doi.org/10.1371/journal.pone.0081566

Shinn-Cunningham, B. (2017). Cortical and Sensory Causes of Individual Differences in Selective Attention Ability Among Listeners With Normal Hearing Thresholds. *J Speech Lang Hear Res*, *60*(10), 2976-2988. https://doi.org/10.1044/2017_JSLHR-H-17-0080

Shore, S. E. (1995). Recovery of forward-masked responses in ventral cochlear nucleus neurons. *Hear Res*, *82*(1), 31-43. https://doi.org/10.1016/0378-5955(94)00160-r

Silman, S. (1979). The effects of aging on the stapedius reflex thresholds. *J Acoust Soc Am*, *66*(3), 735-738. https://doi.org/10.1121/1.383675

Silman, S., Popelka, G. R., & Gelfand, S. A. (1978). Effect of sensorineural hearing loss on acoustic stapedius reflex growth functions. *J Acoust Soc Am*, *64*(5), 1406-1411. https://doi.org/10.1121/1.382107

Silverman, C. A., Silman, S., & Miller, M. H. (1983). The acoustic reflex threshold in aging ears. *J Acoust Soc Am*, *73*(1), 248-255. https://doi.org/10.1121/1.388856

Singer, W., Zuccotti, A., Jaumann, M., Lee, S. C., Panford-Walsh, R., Xiong, H., Zimmermann, U., Franz, C., Geisler, H. S., Kopschall, I., Rohbock, K., Varakina, K., Verpoorten, S., Reinbothe, T., Schimmang, T., Ruttiger, L., & Knipper, M. (2013). Noise-induced inner hair cell ribbon loss disturbs central arc mobilization: a novel molecular paradigm for understanding tinnitus. *Mol Neurobiol*, *47*(1), 261-279. https://doi.org/10.1007/s12035-012-8372-8

Singh, R., Arthreya, V. M., & Bharadwaj, H. M. (2022). Relationships between co-modulation masking release, speech-in-noise perception, and EEG measures of temporal-coherence processing. Association for Research in Otolaryngology 45th Midwinter Meeting, Virtual.

Skoe, E., & Tufts, J. (2018). Evidence of noise-induced subclinical hearing loss using auditory brainstem responses and objective measures of noise exposure in humans. *Hear Res*, *361*, 80-91. https://doi.org/10.1016/j.heares.2018.01.005

Sly, D. J., Campbell, L., Uschakov, A., Saief, S. T., Lam, M., & O'Leary, S. J. (2016). Applying Neurotrophins to the Round Window Rescues Auditory Function and Reduces Inner Hair Cell Synaptopathy After Noise-induced Hearing Loss. *Otol Neurotol*, *37*(9), 1223-1230. https://doi.org/10.1097/MAO.0000000000001191

Smart, J. L., Kuruvilla-Mathew, A., Kelly, A. S., & Purdy, S. C. (2019). Assessment of the efferent auditory system in children with suspected auditory processing disorder: the Middle ear muscle reflex and contralateral inhibition of OAEs. *Int J Audiol*, *58*(1), 37-44. https://doi.org/10.1080/14992027.2018.1523578

Smith, D. W., Aouad, R. K., & Keil, A. (2012). Cognitive task demands modulate the sensitivity of the human cochlea. *Front Psychol*, *3*, 30. https://doi.org/10.3389/fpsyg.2012.00030

Smith, D. W., & Keil, A. (2015). The biological role of the medial olivocochlear efferents in hearing: separating evolved function from exaptation. *Front Syst Neurosci*, *9*, 12. https://doi.org/10.3389/fnsys.2015.00012

Smith, R. L. (1977). Short-term adaptation in single auditory nerve fibers: some poststimulatory effects. *J Neurophysiol*, *40*(5), 1098-1111. https://doi.org/10.1152/jn.1977.40.5.1098

Smith, R. L. (1979). Adaptation, saturation, and physiological masking in single auditory-nerve fibers. *J Acoust Soc Am*, *65*(1), 166-178. https://doi.org/10.1121/1.382260

Smith, R. L., & Zwislocki, J. J. (1975). Short-term adaptation and incremental responses of single auditory-nerve fibers. *Biol Cybern*, *17*(3), 169-182. https://doi.org/10.1007/bf00364166

Sobkowicz, H. M., Rose, J. E., Scott, G. L., & Levenick, C. V. (1986). Distribution of synaptic ribbons in the developing organ of Corti. *J Neurocytol*, *15*(6), 693-714. https://doi.org/10.1007/bf01625188

Song, Q., Shen, P., Li, X., Shi, L., Liu, L., Wang, J., Yu, Z., Stephen, K., Aiken, S., Yin, S., & Wang, J. (2016). Coding deficits in hidden hearing loss induced by noise: the nature and impacts. *Sci Rep*, *6*, 25200. https://doi.org/10.1038/srep25200

Spankovich, C., Gonzalez, V. B., Su, D., & Bishop, C. E. (2018). Self reported hearing difficulty, tinnitus, and normal audiometric thresholds, the National Health and Nutrition Examination Survey 1999-2002. *Hear Res*, *358*, 30-36. https://doi.org/10.1016/j.heares.2017.12.001

Spankovich, C., Le Prell, C. G., Lobarinas, E., & Hood, L. J. (2017). Noise History and Auditory Function in Young Adults With and Without Type 1 Diabetes Mellitus. *Ear Hear*, *38*(6), 724-735. https://doi.org/10.1097/AUD.0000000000000457

Spoendlin, H., & Brun, J. P. (1973). Relation of structural damage to exposure time and intensity in acoustic trauma. *Acta Otolaryngol*, *75*(2), 220-226. https://doi.org/10.3109/00016487309139699

Srinivasan, S., Keil, A., Stratis, K., Woodruff Carr, K. L., & Smith, D. W. (2012). Effects of cross-modal selective attention on the sensory periphery: cochlear sensitivity is altered by selective attention. *Neuroscience*, *223*, 325-332. https://doi.org/10.1016/j.neuroscience.2012.07.062

Stahl, A. N., Mondul, J. A., Alek, C. A., Hackett, T. A., & Ramachandran, R. (submitted). *Audiologic characterization using clinical physiological measures: Normative data from macaque monkeys*.

Stamataki, S., Francis, H. W., Lehar, M., May, B. J., & Ryugo, D. K. (2006). Synaptic alterations at inner hair cells precede spiral ganglion cell loss in aging C57BL/6J mice. *Hear Res*, *221*(1-2), 104-118. https://doi.org/10.1016/j.heares.2006.07.014

Starr, A., Picton, T. W., Sininger, Y., Hood, L. J., & Berlin, C. I. (1996). Auditory neuropathy. *Brain*, *119 (Pt 3)*, 741-753. https://doi.org/10.1093/brain/119.3.741

Steenken, F., Heeringa, A. N., Beutelmann, R., Zhang, L., Bovee, S., Klump, G. M., & Koppl, C. (2021). Age-related decline in cochlear ribbon synapses and its relation to different metrics of auditory-nerve activity. *Neurobiol Aging*, *108*, 133-145. https://doi.org/10.1016/j.neurobiolaging.2021.08.019

Strickland, E. A. (2001). The relationship between frequency selectivity and overshoot. *J Acoust Soc Am*, *109*(5 Pt 1), 2062-2073. https://doi.org/10.1121/1.1357811

Strickland, E. A., & Krishnan, L. A. (2005). The temporal effect in listeners with mild to moderate cochlear hearing impairment. *J Acoust Soc Am*, *118*(5), 3211-3217. https://doi.org/10.1121/1.2074787

Stuart, A., & Daughtrey, E. R. (2016). On the Relationship Between Musicianship and Contralateral Suppression of Transient-Evoked Otoacoustic Emissions. *J Am Acad Audiol*, *27*(4), 333-344. https://doi.org/10.3766/jaaa.15057

Sugawara, M., Corfas, G., & Liberman, M. C. (2005). Influence of supporting cells on neuronal degeneration after hair cell loss. *J Assoc Res Otolaryngol*, *6*(2), 136-147. https://doi.org/10.1007/s10162-004-5050-1

Suresh, C. H., & Krishnan, A. (2020). Search for Electrophysiological Indices of Hidden Hearing Loss in Humans: Click Auditory Brainstem Response Across Sound Levels and in Background Noise. *Ear Hear*, *42*(1), 53-67. https://doi.org/10.1097/AUD.0000000000000905

Suthakar, K., & Liberman, M. C. (2021). Auditory-nerve responses in mice with noise-induced cochlear synaptopathy. *J Neurophysiol*, *126*(6), 2027-2038. https://doi.org/10.1152/jn.00342.2021

Suzuki, J., Corfas, G., & Liberman, M. C. (2016). Round-window delivery of neurotrophin 3 regenerates cochlear synapses after acoustic overexposure. *Sci Rep*, *6*, 24907. https://doi.org/10.1038/srep24907

Tan, W. J., Thorne, P. R., & Vlajkovic, S. M. (2016). Characterisation of cochlear inflammation in mice following acute and chronic noise exposure. *Histochem Cell Biol*, *146*(2), 219-230. https://doi.org/10.1007/s00418-016-1436-5

Terreros, G., & Delano, P. H. (2015). Corticofugal modulation of peripheral auditory responses. *Front Syst Neurosci*, *9*, 134. https://doi.org/10.3389/fnsys.2015.00134

Terreros, G., Jorratt, P., Aedo, C., Elgoyhen, A. B., & Delano, P. H. (2016). Selective Attention to Visual Stimuli Using Auditory Distractors Is Altered in Alpha-9 Nicotinic Receptor Subunit Knock-Out Mice. *J Neurosci*, *36*(27), 7198-7209. https://doi.org/10.1523/JNEUROSCI.4031-15.2016

Tolnai, S., Ippen, F., Muller, J., Beutelmann, R., & Klump, G. M. (2022). Comodulation masking release in young and old Mongolian gerbils. Association for Research in Otolaryngology 45th Midwinter Meeting, Virtual.

Torre, P., 3rd, Mattison, J. A., Fowler, C. G., Lane, M. A., Roth, G. S., & Ingram, D. K. (2004). Assessment of auditory function in rhesus monkeys (Macaca mulatta): effects of age and calorie restriction. *Neurobiol Aging*, *25*(7), 945-954. https://doi.org/10.1016/j.neurobiolaging.2003.09.006

Tremblay, K. L., Pinto, A., Fischer, M. E., Klein, B. E., Klein, R., Levy, S., Tweed, T. S., & Cruickshanks, K. J. (2015). Self-Reported Hearing Difficulties Among Adults With Normal Audiograms: The Beaver Dam Offspring Study. *Ear Hear*, *36*(6), e290-299. https://doi.org/10.1097/aud.0000000000000195

Tumolo, J. (2020). New data demystify hidden hearing loss. *The Hearing Journal*, *73*(4), 28,30-31.

Turner, C. W., Relkin, E. M., & Doucet, J. (1994). Psychophysical and physiological forward masking studies: probe duration and rise-time effects. *J Acoust Soc Am*, *96*(2 Pt 1), 795-800. https://doi.org/10.1121/1.410317

Tziridis, K., Forster, J., Buchheidt-Dorfler, I., Krauss, P., Schilling, A., Wendler, O., Sterna, E., & Schulze, H. (2021). Tinnitus development is associated with synaptopathy of inner hair cells in Mongolian gerbils. *Eur J Neurosci*, *54*(3), 4768-4780. https://doi.org/10.1111/ejn.15334

Valero, M. D., Burton, J. A., Hauser, S. N., Hackett, T. A., Ramachandran, R., & Liberman, M. C. (2017). Noise-induced cochlear synaptopathy in rhesus monkeys (Macaca mulatta). *Hear Res*, *353*, 213-223. https://doi.org/10.1016/j.heares.2017.07.003

Valero, M. D., Hancock, K. E., & Liberman, M. C. (2016). The middle ear muscle reflex in the diagnosis of cochlear neuropathy. *Hear Res*, *332*, 29-38. https://doi.org/10.1016/j.heares.2015.11.005

Valero, M. D., Hancock, K. E., Maison, S. F., & Liberman, M. C. (2018). Effects of cochlear synaptopathy on middle-ear muscle reflexes in unanesthetized mice. *Hear Res*, *363*, 109-118. https://doi.org/10.1016/j.heares.2018.03.012

Vasilkov, V., Garrett, M., Mauermann, M., & Verhulst, S. (2021). Enhancing the sensitivity of the envelope-following response for cochlear synaptopathy screening in humans: The role of stimulus envelope. *Hear Res*, *400*, 108132. https://doi.org/10.1016/j.heares.2020.108132

Verhey, J. L., Pressnitzer, D., & Winter, I. M. (2003). The psychophysics and physiology of comodulation masking release. *Exp Brain Res*, *153*(4), 405-417. https://doi.org/10.1007/s00221-003-1607-1

Verhulst, S., Altoe, A., & Vasilkov, V. (2018). Computational modeling of the human auditory periphery: Auditory-nerve responses, evoked potentials and hearing loss. *Hear Res*, *360*, 55-75. https://doi.org/10.1016/j.heares.2017.12.018

Veuillet, E., Martin, V., Suc, B., Vesson, J. F., Morgon, A., & Collet, L. (2001). Otoacoustic emissions and medial olivocochlear suppression during auditory recovery from acoustic trauma in humans. *Acta Otolaryngol*, *121*(2), 278-283. https://doi.org/10.1080/00016480130004384 8

Viana, L. M., O'Malley, J. T., Burgess, B. J., Jones, D. D., Oliveira, C. A., Santos, F., Merchant, S. N., Liberman, L. D., & Liberman, M. C. (2015). Cochlear neuropathy in human presbycusis: Confocal analysis of hidden hearing loss in post-mortem tissue. *Hear Res*, *327*, 78-88. https://doi.org/10.1016/j.heares.2015.04.014

Vincent, P. F. Y., Young, E., Edge, A. S. B., & Glowatzki, E. (2022). Functional properties of regenerated synapses between hair cells and auditory nerve fibers in vitro. Association for Research in Otolaryngology 45th Midwinter Meeting, Virtual.

Viswanathan, V., Shinn-Cunningham, B. G., & Heinz, M. G. (2022). Speech Categorization Reveals the Role of Early-Stage Temporal-Coherence Processing in Auditory Scene Analysis. *J Neurosci*, *42*(2), 240-254. https://doi.org/10.1523/JNEUROSCI.1610-21.2021

Vogler, D. P., Robertson, D., & Mulders, W. H. (2011). Hyperactivity in the ventral cochlear nucleus after cochlear trauma. *J Neurosci*, *31*(18), 6639-6645. https://doi.org/10.1523/JNEUROSCI.6538-10.2011

Wagner, W., Heppelmann, G., Muller, J., Janssen, T., & Zenner, H. P. (2007). Olivocochlear reflex effect on human distortion product otoacoustic emissions is largest at frequencies with distinct fine structure dips. *Hear Res*, *223*(1-2), 83-92. https://doi.org/10.1016/j.heares.2006.10.001

Walsh, K. P., Pasanen, E. G., & McFadden, D. (2010). Overshoot measured physiologically and psychophysically in the same human ears. *Hear Res*, *268*(1-2), 22-37. https://doi.org/10.1016/j.heares.2010.04.007

Wan, G., Corfas, G., & Stone, J. S. (2013). Inner ear supporting cells: rethinking the silent majority. *Semin Cell Dev Biol*, *24*(5), 448-459. https://doi.org/10.1016/j.semcdb.2013.03.009

Wan, G., Gomez-Casati, M. E., Gigliello, A. R., Liberman, M. C., & Corfas, G. (2014). Neurotrophin-3 regulates ribbon synapse density in the cochlea and induces synapse regeneration after acoustic trauma. *Elife*, *3*. https://doi.org/10.7554/eLife.03564

Wang, J., Powers, N. L., Hofstetter, P., Trautwein, P., Ding, D., & Salvi, R. (1997). Effects of selective inner hair cell loss on auditory nerve fiber threshold, tuning and spontaneous and driven discharge rate. *Hearing Research*, *107*(1-2), 67-82. https://doi.org/10.1016/s0378-5955(97)00020-8

Wang, M., Zhang, C., Lin, S., Wang, Y., Seicol, B. J., Ariss, R. W., & Xie, R. (2021). Biased auditory nerve central synaptopathy is associated with age-related hearing loss. *J Physiol*, *599*(6), 1833-1854. https://doi.org/10.1113/JP281014

Wang, Y., Hirose, K., & Liberman, M. C. (2002). Dynamics of noise-induced cellular injury and repair in the mouse cochlea. *J Assoc Res Otolaryngol*, *3*(3), 248-268. https://doi.org/10.1007/s101620020028

Weisz, C. J., Lehar, M., Hiel, H., Glowatzki, E., & Fuchs, P. A. (2012). Synaptic transfer from outer hair cells to type II afferent fibers in the rat cochlea. *J Neurosci*, *32*(28), 9528-9536. https://doi.org/10.1523/JNEUROSCI.6194-11.2012

Wen, B., Wang, G. I., Dean, I., & Delgutte, B. (2009). Dynamic range adaptation to sound level statistics in the auditory nerve. *J Neurosci*, *29*(44), 13797-13808. https://doi.org/10.1523/JNEUROSCI.5610-08.2009

Whitehead, M. L., Martin, G. K., & Lonsbury-Martin, B. L. (1991). Effects of the crossed acoustic reflex on distortion-product otoacoustic emissions in awake rabbits. *Hear Res*, *51*(1), 55-72. https://doi.org/10.1016/0378-5955(91)90007-v

Wicher, A., & Moore, B. C. (2014). Effect of broadband and narrowband contralateral noise on psychophysical tuning curves and otoacoustic emissions. *J Acoust Soc Am*, *135*(5), 2931-2941. https://doi.org/10.1121/1.4871358

Wier, C. C., Green, D. M., Hafter, E. R., & Burkhardt, S. (1977). Detection of a tone burst in continuous- and gated-noise maskers; defects of signal frequency, duration, masker level. *J Acoust Soc Am*, *61*(5), 1298-1300. https://doi.org/10.1121/1.381432

Wiley, T. L., Oviatt, D. L., & Block, M. G. (1987). Acoustic-immittance measures in normal ears. *J Speech Hear Res*, *30*(2), 161-170. https://doi.org/10.1044/jshr.3002.161

Wilson, R. H., & McBride, L. M. (1978). Threshold and growth of the acoustic reflex. *J Acoust Soc Am*, *63*(1), 147-154. https://doi.org/10.1121/1.381706

Wittekindt, A., Kaiser, J., & Abel, C. (2014). Attentional modulation of the inner ear: a combined otoacoustic emission and EEG study. *J Neurosci*, *34*(30), 9995-10002. https://doi.org/10.1523/JNEUROSCI.4861-13.2014

Wojtczak, M., Beim, J. A., & Oxenham, A. J. (2017). Weak Middle-Ear-Muscle Reflex in Humans with Noise-Induced Tinnitus and Normal Hearing May Reflect Cochlear Synaptopathy. *eNeuro*, *4*(6). https://doi.org/10.1523/ENEURO.0363-17.2017

Wojtczak, M., & Oxenham, A. J. (2010). Recovery from on- and off-frequency forward masking in listeners with normal and impaired hearing. *J Acoust Soc Am*, *128*(1), 247-256. https://doi.org/10.1121/1.3436566

Wong, E., & Cheesman, M. (2000). The overshoot effect in older versus young adults with normal hearing. *Canadian Acoustics*, *28*(3), 122-123.

Wong, N. F., & Xu-Friedman, M. A. (2022). Time course of activity-dependent changes in auditory nerve synapses reveals multiple underlying cellular mechanisms. *J Neurosci*. https://doi.org/10.1523/JNEUROSCI.1583-21.2022

Wong, S. J., Abrams, K. S., Amburgey, K. N., Wang, Y., & Henry, K. S. (2019). Effects of selective auditory-nerve damage on the behavioral audiogram and temporal integration in the budgerigar. *Hear Res*, *374*, 24-34. https://doi.org/10.1016/j.heares.2019.01.019

Wood, M. B., Nowak, N., Mull, K., Goldring, A., Lehar, M., & Fuchs, P. A. (2021). Acoustic Trauma Increases Ribbon Number and Size in Outer Hair Cells of the Mouse Cochlea. *J Assoc Res Otolaryngol*, *22*(1), 19-31. https://doi.org/10.1007/s10162-020-00777-w

Wright, B. A. (1994). Individual, sex, and ear differences in measures of overshoot and psychophysical two-tone suppression. *The Journal of the Acoustical Society of America*, *95*(5), 2942-2943. https://doi.org/10.1121/1.409145

Wright, B. A. (1997). Detectability of simultaneously masked signals as a function of masker bandwidth and configuration for different signal delays. *J Acoust Soc Am*, *101*(1), 420-429. https://doi.org/10.1121/1.417987

Wu, P. Z., Liberman, L. D., Bennett, K., de Gruttola, V., O'Malley, J. T., & Liberman, M. C. (2019). Primary Neural Degeneration in the Human Cochlea: Evidence for Hidden Hearing Loss in the Aging Ear. *Neuroscience*, *407*, 8-20. https://doi.org/10.1016/j.neuroscience.2018.07.053

Wu, P. Z., O'Malley, J. T., de Gruttola, V., & Liberman, M. C. (2020). Age-Related Hearing Loss Is Dominated by Damage to Inner Ear Sensory Cells, Not the Cellular Battery That Powers Them. *J Neurosci*, *40*(33), 6357-6366. https://doi.org/10.1523/JNEUROSCI.0937-20.2020

Wu, P. Z., O'Malley, J. T., de Gruttola, V., & Liberman, M. C. (2021). Primary Neural Degeneration in Noise-Exposed Human Cochleas: Correlations with Outer Hair Cell Loss and Word-Discrimination Scores. *J Neurosci*, *41*(20), 4439-4447. https://doi.org/10.1523/JNEUROSCI.3238-20.2021

Wynne, D. P., Zeng, F. G., Bhatt, S., Michalewski, H. J., Dimitrijevic, A., & Starr, A. (2013). Loudness adaptation accompanying ribbon synapse and auditory nerve disorders. *Brain*, *136*(Pt 5), 1626-1638. https://doi.org/10.1093/brain/awt056

Xu, Y., Cheatham, M. A., & Siegel, J. H. (2017). Identifying the Origin of Effects of Contralateral Noise on Transient Evoked Otoacoustic Emissions in Unanesthetized Mice. *J Assoc Res Otolaryngol*, *18*(4), 543-553. https://doi.org/10.1007/s10162-017-0616-x

Yasin, I., Drga, V., & Plack, C. J. (2014). Effect of human auditory efferent feedback on cochlear gain and compression. *J Neurosci*, *34*(46), 15319-15326. https://doi.org/10.1523/JNEUROSCI.1043-14.2014

Yin, D., Ren, L., Li, J., Shi, Y., Duan, Y., Xie, Y., Zhang, T., & Dai, P. (2020). Long-term moderate noise exposure enhances the medial olivocochlear reflex. *Auris Nasus Larynx*, *47*(5), 769-777. https://doi.org/10.1016/j.anl.2020.03.008

Zeng, F. G. (2015). Uncovering hidden hearing loss. *The Hearing Journal*, *68*(1), 6.

Zhang, K. D., & Coate, T. M. (2017). Recent advances in the development and function of type II spiral ganglion neurons in the mammalian inner ear. *Semin Cell Dev Biol*, *65*, 80-87. https://doi.org/10.1016/j.semcdb.2016.09.017

Zhao, F., & Stephens, D. (1996). Hearing complaints of patients with King-Kopetzky syndrome (obscure auditory dysfunction). *Br J Audiol*, *30*(6), 397-402. https://doi.org/10.3109/03005369609078427

Zhu, X., Vasilyeva, O. N., Kim, S., Jacobson, M., Romney, J., Waterman, M. S., Tuttle, D., & Frisina, R. D. (2007). Auditory efferent feedback system deficits precede age-related hearing loss: contralateral suppression of otoacoustic emissions in mice. *J Comp Neurol*, *503*(5), 593-604. https://doi.org/10.1002/cne.21402

Zwicker, E. (1965). Temporal Effects in Simultaneous Masking and Loudness. *J Acoust Soc Am*, *38*, 132-141. https://doi.org/10.1121/1.1909588